Etude du rôle des sucres, en interaction avec les hormones, dans la régulation du débourrement des bourgeons axillaires par l'intensité lumineuse. Une démarche aliiant expériences et modélisation.

Anne Schneider

DOCTORAT ECOLOGIE
BRETAGNE GEOSCIENCES
LOIRE AGRONOMIE ALIMENTATION

AGRO CAMPUS OUEST

THESE DE DOCTORAT DE

AGROCAMPUS OUEST

ECOLE DOCTORALE N° 600
Ecole doctorale Ecologie, Géosciences, Agronomie et Alimentation
Spécialité : « Biologie et Agronomie »

Par Anne SCHNEIDER

Etude du rôle des sucres, en interaction avec les hormones dans la régulation du débourrement des bourgeons axillaires par l'intensité lumineuse

Une démarche alliant expériences et modélisation

Thèse présentée et soutenue à Angers, le 17 juillet 2020
Unité de recherche : UMR IRHS, INRA, Agrocampus-Ouest, Université d'Angers, SFR 4207 QuaSaV, 49071 Beaucouzé, France

Rapporteurs avant soutenance :

Alexandra Jullien	Professeur, AgroParisTech
Christine Granier	Directrice de recherche, UMR AGAP, CIRAD

Composition du Jury :

Président :	Gerhard Buck-Sorlin	Professeur, AgroCampus Ouest
Examinateur :	Philippe Vivin	Chargé de recherches, INRAE
Dir. de thèse :	Soulaiman Sakr	Professeur, AgroCampus Ouest
Encadrante de thèse :	Jessica Bertheloot	Chargée de recherche, INRAE
Co-encadrant :	Christophe Godin	Directeur de recherche, INRIA
Invité :	Frédéric Boudon	Chargé de recherche, CIRAD

SOMMAIRE

INTRODUCTION GENERALE

ENJEUX ENVIRONNEMENTAUX, EXIGENCES SOCIETALES, ET PRODUCTIONS AGRICOLES ET HORTICOLES

Les productions agricoles et horticoles doivent s'adapter aux défis majeurs du 21ème siècle. Le réchauffement climatique, la diminution ou la difficulté d'accès à plusieurs ressources naturelles essentielles à l'agriculture (eau douce, phosphates pour les engrais, terres arables…) et l'augmentation exponentielle de la population mondiale qui devrait dépasser les 9 milliard d'habitants d'ici 2050 mettent les pratiques horticoles et agricoles face à de nouvelles contraintes (Atlas de l'agriculture ; La question agricole mondiale). Les productions agricoles doivent répondre aux exigences des consommateurs et des acteurs avals des filières en termes de qualité (capacité de stockage et de transformation, saveurs et aspects visuel des produits…) (Kyriacou , 2018), tout en maintenant la production globale (maintenir le rendement), et en s'adaptant aux attentes des consommateurs et des pouvoirs publics en termes de respect de l'environnement (réduction de l'utilisation des intrants et des produits phytosanitaires par exemple). Ces contraintes nombreuses, parfois difficiles à concilier, concernent aussi bien les cultures habituellement réalisées en extérieur (cultures de plein champ) que les cultures réalisées sous abris ou en conditions semi-contrôlées comme sous tunnels, serres, ou encore en fermes verticales. Dans le cas des productions couvertes semi-contrôlées, les enjeux sont alors d'optimiser les conditions de culture pour limiter les intrants (consommation d'énergie, d'engrais, d'eau, de produits phytosanitaires) et maximiser le rendement et la qualité des productions. Ces derniers s'élaborent au cours des différentes phases de développement et de croissance de la plante. Or la lumière, qui est facilement contrôlable dans les cultures en milieu contrôlé (fermes verticales) et semi-contrôlé (serre), est un facteur essentiel dans le fonctionnement et dans l'acquisition de la structure de la plante. Dans le contexte de production sous contraintes environnementales, la compréhension de la réponse du développement des plantes à la lumière pourrait permettre de mieux adapter les modes de productions en milieu contrôlé/semi-contrôlé aux exigences sociétales et environnementales.

ELABORATION DU RENDEMENT ET DE LA QUALITE DES PRODUCTIONS AU COURS DU DEVELOPPEMENT DE LA PLANTE

Le rendement et la qualité des productions agricoles et horticoles s'élaborent en partie au cours du développement de la plante et de la construction de son architecture. Le rendement d'une récolte (exprimé en masse de produits par unité de surface – q/ha), peut être décomposé en plusieurs variables qui permettent de mieux appréhender les étapes clés du développement de la plante impliquées dans l'acquisition du rendement final. Ainsi, chez les cultures annuelles dont on récolte uniquement les grains (céréales, pois, tournesol…), le rendement par unité de surface (Rdt/m²) s'exprime comme le produit du nombre de grains par unité de surface (NG/m²) et du poids moyen d'un grain (P1G) (Figure 1). Le

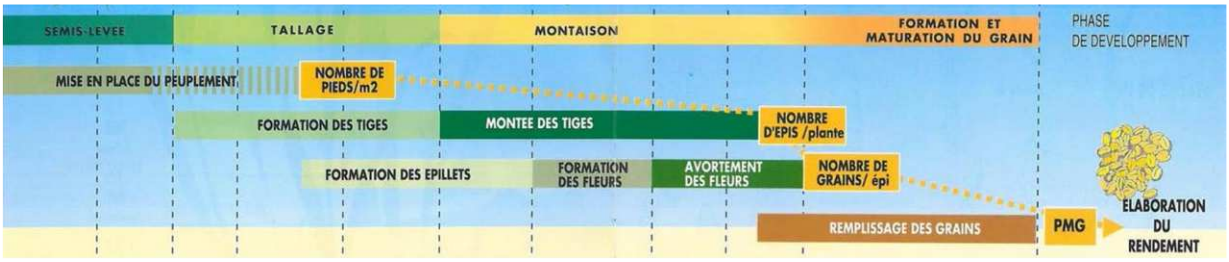

Figure 1 : Le rendement du blé tendre d'hiver s'élabore au cours des phases de développement de la culture. Le rendement final par unité de surface résulte du poids moyen d'un grain (PMG) et du nombre de grains par unité de surface (NG/m²). Cette variable s'élabore au cours des phases de levée et de tallage qui déterminent le nombre de pieds par unité de surface, et le nombre d'apis par plante. Enfin, le nombre de grains par épis est obtenu à l'issue de la montaison. D'après arvalis-infos.fr

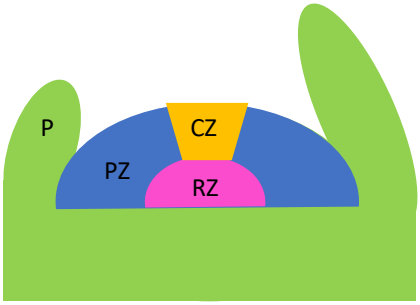

Figure 2 : Le meristème apical caulinaire se compose : de la zone centrale (CZ) contenant les cellules souches, d'une zone périphérique (PZ) où les primordia des organes latéraux comme les feuilles et les pièces florales sont initiées, et d'une zone de nervure (RZ) contenant le centre organisateur de la zone centrale et la zone de différenciation des cellules de la tige. (D'après Galvan-Ampudia et al., 2016)

nombre de grains par unité de surface chez les céréales est lui-même le produit du nombre de plantes par unité de surface (N pieds/m²), du nombre d'épis par plante (N épis/plante), et du nombre de grains par épis (N grains/épi). Parmi ces composantes, le nombre d'épis par plantes est déterminé par l'intensité du tallage (émission de nouvelles ramifications appelées talles chez les céréales) et le taux de maintien de ces nouvelles talles (senescence) (*arvalis-infos.fr*). Certaines variables de l'élaboration du rendement sont aussi acquises au cours de la ramification chez les plantes ligneuses. Chez la vigne, le nombre de raisins par unité de surface dépend du nombre de rameaux par pied, du nombre de grappes par rameau, et du nombre de raisins par grappe. Ces composantes du rendement s'établissent au cours de deux années consécutives et résultent des étapes d'initiation et de différenciation des inflorescences, de débourrement des bourgeons végétatifs et des taux de fructification des inflorescences (Guilpart, 2014). Chez les plantes pérennes comme la vigne ou les arbres fruitiers, des interventions techniques pour contrôler ces variables sont régulièrement réalisées.

Plusieurs critères de qualité des productions agricoles et horticoles s'acquièrent au cours du développement de la culture. Les critères de qualité retenus pour qualifier une production dépendent de l'acteur concerné (transformateur, consommateur final…) et sont variés : la capacité de transformation des produits, leur saveur, leur aspect visuel… Ces critères sont quantifiables à travers plusieurs variables. Par exemple, la capacité du blé à être panifié dépend de son taux protéique, la saveur d'un fruit dépend de ses teneurs en sucres et en polyphénols, etc. Plusieurs caractéristiques intervenant dans des critères de qualité dépendent de l'architecture acquise par la plante. Ainsi, l'architecture des plantes est impliquée dans la sensibilité des cultures aux ravageurs (Costes et al., 2013 ; Tivoli et al 2013), dans plusieurs critères de qualité gustative et d'apparence des fruits (Lescourret et al., 2011 ; Lal et al., 2017 ; Yarnes et al 2013), et dans l'acquisition de la qualité visuelle des plantes ornementales (Schreiner et al., 2013 ; Boumaza et al., 2010).

En conclusion, les phénomènes de développement de la plante et d'établissement de son architecture interviennent à la fois dans l'acquisition du rendement final et dans la qualité des productions. Une meilleure compréhension de ces processus de développement permettrait peut-être de concilier les différentes exigences des acteurs des filières et des consommateurs.

COMMENT S'ETABLIT L'ARCHITECTURE DES PLANTES CULTIVEES ?

L'élaboration du rendement des récoltes et de plusieurs critères de qualité sont liés au développement de la plante et à l'architecture acquise au cours de la culture. D'après Barthélémy et Caraglio (2007), l'architecture d'une plante se définit comme « la nature et la position relative de chacune de ses parties ». Elle repose entre autres sur la nature des ramifications (végétatives ou florifères), leurs dimensions, et leur agencement. L'acquisition de l'architecture de la plante est dynamique et relève de plusieurs processus liés au développement et à la croissance de la plante. Ci-

dessous, nous détaillons les processus de croissance de l'axe primaire et les processus de ramification qui mènent à l'acquisition de l'architecture végétative de la plante.

Développement et croissance de l'axe primaire

La mise en place des organes aériens de l'axe primaire, résulte du fonctionnement du méristème apical caulinaire. Le méristème est composé de plusieurs zones de cellules non différenciées (Clark, 1997). La zone centrale, composée de quelques cellules au centre du méristème, présente une faible activité mitotique, et permet le maintien du méristème (Figure 2). Autour, un anneau de cellules compose la zone périphérique (PZ), lieu d'une activité mitotique intense. En s'éloignant encore du centre du méristème, les cellules forment une zone d'organogenèse dans laquelle se fait la différenciation des primordia de feuilles ou de fleurs. Le fonctionnement du méristème apical caulinaire assure son propre maintien, ainsi que la formation et la différenciation des organes de l'axe primaire comme les entrenœuds et les feuilles (Bell et Bryan, 2008). L'organogenèse au niveau du méristème suit différents motifs spatiotemporels selon les espèces, les phases de développement, et les conditions environnementales (Galvan-Ampudia et al., 2016). La position des nouveaux organes par rapport à ceux déjà formés dessine la phyllotaxie de l'axe en développement. Avec le plastochrone (rythme d'émission de ces nouveaux organes), la phyllotaxie détermine le schéma de développement de l'axe primaire propre à chaque espèce. Le méristème apical végétatif peut ensuite, selon les espèces et variétés, évoluer en méristème floral, menant à la terminaison de l'axe par une fleur ou une inflorescence, ou bien continuer de produire des organes végétatifs.

Les organes de l'axe primaire une fois formés et différenciés augmentent en masse et en dimensions. Les feuilles se déplient, s'allongent et s'épaississent, alors que la longueur (et le diamètre, chez les dicotylédones) des entrenœuds augmente.

Le processus de ramification

Mise en place des bourgeons axillaires

Les méristèmes axillaires sont initiés à l'aisselle des feuilles de l'axe primaire, et sont donc positionnés les uns par rapports aux autres selon le schéma phyllotaxique de l'axe primaire. Le méristème axillaire, entouré de premières ébauches foliaires et d'écailles forment le bourgeon axillaire. La croissance de ce bourgeon pour donner un nouvel axe peut être immédiate (bourgeon sylleptique) ou différée par une ou plusieurs phases de dormances pendant lesquelles l'activité du méristème est très ralentie (bourgeon proleptique).

Etats de dormances des bourgeons axillaires

Une fois formés à l'aisselle des feuilles de l'axe primaire, l'organogenèse et la croissance des organes du bourgeon axillaires peuvent être arrêtés par plusieurs types de dormances (Shimizu-Sato et Mori 2001; Anderson et al., 2010 pour review). Tout d'abord, la croissance d'un bourgeon axillaire peut être empêchée par des processus d'inhibition dues aux autres organes, aussi appelée inhibition corrélative. Le bourgeon entre alors en **para-dormance**. Celle-ci peut être exercée par les organes en

croissance de l'axe primaire, on parle alors de dominance apicale, ou par d'autres bourgeons axillaires en croissance. Les rôles de plusieurs hormones (auxine, cytokinines, strigolactones) et des sucres ont été démontrés dans le processus de dominance apicale (Pour review : Rameau et al. 2015 ; Mason et al., 2014). Un deuxième type de dormance, **l'éco-dormance**, correspond à l'inhibition du débourrement des bourgeons axillaires lorsque les conditions environnementales de croissance de la plante sont défavorables : par exemple lors de stress hydriques, de carences en nutriments, ou de faibles températures (Allona et al., 2008 ; Horvath et al., 2003). Les processus impliqués dans le phénomène d'éco-dormance feraient aussi intervenir des hormones telles que les cytokinines (Roman et al., 2016 ; Corot et al. ; 2017), les strigolactones (Zhuang et al., 2017) et l'acide abscicique (Corot et al., 2017). En cela, des interactions entre les phénomènes de paradormance et d'écodormance sont susceptibles d'exister. L'écodormance est levée lorsque les conditions environnementales sont de nouveau favorables. Enfin, les bourgeons peuvent être soumis à une **endo-dormance**. Il s'agit d'une inhibition du débourrement intrinsèque au bourgeon axillaire. La perception de signaux environnementaux comme le raccourcissement de la photopériode, ou la nécessité d'une période de froid pour permettre le débourrement sont observés chez plusieurs espèces lors de la mise en place et pour la levée de cette dormance (Hauagge and Cummins, 1991; Arora et al., 2003).

Débourrement et émission d'un nouvel axe

Lorsque les différentes dormances d'un bourgeon axillaire sont levées par le rétablissement de conditions environnementales favorables et la réduction des inhibitions corrélatives, le bourgeon peut débourrer (Cline, 1997). L'activité méristématique reprend avec l'initiation et la différenciation de nouveaux organes au sein de bourgeon. De même la croissance des organes accélère, et le bourgeon est considéré comme débourré lorsqu'une feuille est visible entre les écailles (Girault et al., 2008).

Tous les bourgeons axillaires d'un même axe ne vont pas débourrer en même temps selon la levée des dormances, ce qui, avec leurs positions relatives le long de l'axe les portant va donner des motifs de ramification variés. Finalement, la combinaison des différentes modalités de développement de l'axe primaire et de ramifications mène à une diversité d'architectures aériennes des plantes, allant de la rosette chez les herbacées, au port arborescent ou buissonnant chez les ligneuses (Hallé et Oldeman, 1970).

DIVERSITE DANS LA RAMIFICATION DES PLANTES

Les processus de ramification jouant un rôle important dans l'acquisition de l'architecture des plantes, la diversité des architectures observées est en partie imputable aux modulations génétiques et environnementales de la ramification (Costes et al., 2012 ; Sultan 2000).

Diversité génétique de la ramification

La temporalité, l'intensité et la localisation le long de l'axe primaire de la ramification présentent une grande diversité génétique entre espèces éloignées ou variétés d'une même espèce. Ainsi, chez les céréales comme le blé ou l'orge cultivées en plein champ, l'émission de nouvelles ramifications

(talles) est coordonnée avec l'apparition des nouvelles feuilles du brin maître. Au sein des rosacées, des différences de motifs de débourrement ont été observés entre arbres fruitiers et entre espèces ou variétés de rosiers (Costes et al., 2014 ; Crespel et al., 2014), avec des schémas de ramifications acrotone, mésotone et basitone (ramification par le haut, le milieu et la base de l'axe primaire, respectivement) selon les génotypes.

Sensibilité de la ramification aux conditions environnementales

La sortie d'écodormance des bourgeons étant dépendante des conditions environnementales, les modulations des conditions de croissance des plantes entraînent une diversité de phénotypes de ramification pour un même génotype. Plusieurs facteurs environnementaux sont connus pour moduler la ramification des plantes.

Sensibilité de la ramification aux conditions lumineuses de croissance

Parmi les facteurs environnementaux modulant le développement et la croissance de la plante, les effets des conditions lumineuses sur la ramification ont été observés chez de nombreuses espèces (pour review : Kami et al., 2010 ; Demotes-Mainard et al., 2016). Au cours de la culture, la densité de semis ou de plantation et la fermeture du couvert impactent négativement la ramification des plantes : chez les céréales par exemple, le nombre de talles émises par plante diminue avec la densité de semis (Fioreze et al., 2014). La lumière intervient dans ce phénomène via deux variables : l'intensité lumineuse, et la qualité de la lumière, c'est-à-dire son spectre de longueurs d'ondes. Ces deux variables sont en effet modifiées par la présence proche de plantes voisines.

Les effets dissociés de l'intensité lumineuse et de la qualité de la lumière sur la ramification ont été étudiés. Globalement, une diminution de l'intensité lumineuse pendant la phase habituelle de ramification des plantes ligneuses et herbacées réduit le nombre de ramifications émises, diminue leurs dimensions (diamètre, longueur) et alonge le délai avant l'émission des ramifications (Bos and Neuteboom, 1998 ; Gautier et al., 2000 ; Evers et al., 2006). Les effets de variations temporelles de l'intensité lumineuse au cours de la croissance de la plante ont encore peu été étudiées - les études de la sensibilité de la ramification ou du débourrement aux conditions lumineuses en plein champ lissant ces variations à travers des moyennes de PAR perçu au cours de la culture. Récemment, une étude sur le rosier a mis en évidence un comportement non intuitif de réponse de la ramification suite à des variations d'intensité lumineuse au cours de la croissance de la plante : des plants de rosiers ayant été exposés à une diminution de l'intensité lumineuse lors de la mise en place de leur axe primaire, avant la période habituelle de ramification, puis réexposés à une intensité lumineuse favorable, présentent un plus grand nombre de ramifications que des rosiers ayant toujours cru sous une intensité lumineuse favorable (Demotes-Mainard et al., 2013).

Les effets de la modulation de la qualité de la lumière, c'est-à-dire la modulation du spectre lumineux par l'intensité plus ou moins élevée de certaines longueurs d'ondes, ont été étudiée chez plusieurs espèces et via la modulation de plusieurs longueurs d'onde. Globalement, une diminution du

ratio R :FR (rouge clair : rouge sombre) et/ou une augmentation de la lumière bleue inhibe le débourrement des bourgeons (Kebrom et al., 2010 ; Rameau et al., 2014 ; Demotes-Mainard et al., 2016 ; Huché-Thélier et al., 2016).

Sensibilité de la ramification aux autres conditions de culture

Plusieurs facteurs environnementaux, connus pour réguler la croissance et le développement des plantes, sont impliqués dans la modulation de la ramification et du débourrement. Ainsi, des conditions hydriques défavorables pendant la phase de débourrement sont connues pour diminuer le nombre de ramifications émises (Li-Marchetti et al., 2015 ; Demotes-Mainard et al., 2013). De même, des restrictions en nutrition minérale, et notamment en azote affectent négativement la fréquence de débourrement et modifient les motifs de ramification (Bouguyon et al., 2012 ; Huché-Thellier et al., 2011 ; Le Moigne et al., 2016). La ramification des plantes est aussi sensible à la température (Djennane et al., 2014), et aux stimulations mécaniques (Braam et al., 2017).

Face à cette diversité de phénotypes de ramifications, quels outils ont été mis en place pour la contrôler et maitriser cette variable importante dans l'acquisition du rendement des productions et de leur qualité ?

QUELS LEVIERS TECHNOLOGIQUES POUR MAITRISER LA RAMIFICATION DES PLANTES

Un levier pour contrôler la ramification des plantes cultivées passe par la sélection génétique des phénotypes désirés. Son efficacité dans la maîtrise de la ramification et de l'architecture des plantes a notamment été démontré chez le riz (Jin et al., 2008) : au cours de sa domestication, la ramification a été modifiée de façon importante via la sélection d'une mutation sur le gène PROG1, majoritairement exprimé dans méristèmes axillaires. Il en résulte des différences quant au nombre de talles et d'angles d'insertion des talles entre le riz sauvage et le riz domestiqué. Aujourd'hui, l'amélioration génétique est toujours utilisée pour sélectionner des plantes selon leur capacité de ramification et satisfaire les exigences des consommateurs en termes de plantes ornementales par exemple (Boumaza et al., 2010).

Les autres leviers de maîtrise de la ramification des plantes cultivées reposent sur le contrôle des itinéraires techniques. Une pratique très utilisée en arboriculture repose sur la contrainte mécanique et ou la taille des rameaux (Lescourret et al., 2010) qui permettent de modifier les inhibitions corrélatives entre bourgeons et de sélectionner les rameaux les plus forts ou ceux porteurs de fruits. Le contrôle de la ramification peut aussi passer par la modulation des conditions hydriques et de la nutrition minérale. Pour les cultures sous-abris, la température et les conditions lumineuses (photopériode, intensité lumineuse, qualité de la lumière) peuvent aussi être modulées. Dans un contexte de réduction des intrants et d'optimisation de l'énergie utilisée dans les productions sous-abris, l'utilisation des LEDs s'est répandue et permet le contrôle de la qualité et de l'intensité de la lumière au plus près des plantes cultivées (Kozai et al., 2013 ; Ramirez-Arias et al 2012).

Les effets de la lumière sur la ramification des plantes sont multiples et le débourrement des bourgeons axillaires est soumis à plusieurs régulations susceptibles d'interagir. La compréhension des mécanismes sous-jacents aux effets de la lumière sur la ramification permettrait de mieux prédire les phénotypes de ramifications selon les conditions lumineuses, et d'optimiser les traitements lumineux appliqués selon l'architecture souhaitée. Dans le chapitre 1, nous proposons un état des connaissances sur la régulation de la ramification par la lumière.

RÉFÉRENCES

Allona Alberich, I.M., Ramos, A., Ibáñez, C., Contreras Mogollón, Á., Casado García, R., and Aragoncillo Ballesteros, C. (2008). Molecular control of winter dormancy in establishment in trees. Spanish Journal of Agricultural Research 6, 201–210.

Anderson, J.V., Horvath, D.P., Chao, W.S., and Foley, M.E. (2010). Bud dormancy in perennial plants: a mechanism for survival. In Dormancy and Resistance in Harsh Environments, (Springer), pp. 69–90.

Arora, R., Rowland, L.J., and Tanino, K. (2003). Induction and release of bud dormancy in woody perennials: a science comes of age. HortScience 38, 911–921.

Barthélémy, D., and Caraglio, Y. (2007). Plant architecture: a dynamic, multilevel and comprehensive approach to plant form, structure and ontogeny. Annals of Botany 99, 375–407.

Bell, A.D., and Bryan, A. (2008). Plant form: an illustrated guide to flowering plant morphology (Timber Press).

BOS, H.J., and NEUTEBOOM, J.H. (1998). Morphological analysis of leaf and tiller number dynamics of wheat (Triticum aestivum L.): responses to temperature and light intensity. Annals of Botany 81, 131–139.

Boumaza, R., Huché-Thélier, L., Demotes-Mainard, S., Le Coz, E., Leduc, N., Pelleschi-Travier, S., Qannari, E.M., Sakr, S., Santagostini, P., and Symoneaux, R. (2010). Sensory profiles and preference analysis in ornamental horticulture: the case of the rosebush. Food Quality and Preference 21, 987–997.

Calonnec, A., Burie, J.B., Langlais, M., Guyader, S., Saint-Jean, S., Sache, I., and Tivoli, B. (2013). Impacts of plant growth and architecture on pathogen processes and their consequences for epidemic behaviour. European Journal of Plant Pathology 135, 479–497.

Charvet, J.-P. (2013). Atlas de l'agriculture. Comment nourrir le monde en 2050? (Autrement).

Clark, S.E. (1997). Organ formation at the vegetative shoot meristem. The Plant Cell 9, 1067.

Cline, M.G. (1997). Concepts and terminology of apical dominance. American Journal of Botany 84, 1064–1069.

Corot, A., Roman, H., Douillet, O., Autret, H., Perez-Garcia, M.-D., Citerne, S., Bertheloot, J., Sakr, S., Leduc, N., and Demotes-Mainard, S. (2017). Cytokinins and abscisic acid act antagonistically in the regulation of the bud outgrowth pattern by light intensity. Frontiers in Plant Science 8, 1724.

Costes, E., Lauri, P.-E., Simon, S., and Andrieu, B. (2013). Plant architecture, its diversity and manipulation in agronomic conditions, in relation with pest and pathogen attacks. European Journal of Plant Pathology 135, 455–470.

Costes, E., Crespel, L., Denoyes, B., Morel, P., Demene, M.-N., Lauri, P.-E., and Wenden, B. (2014). Bud structure, position and fate generate various branching patterns along shoots of closely related Rosaceae species: a review. Frontiers in Plant Science 5, 666.

Crespel, L., Le Bras, C., Relion, D., and Morel, P. (2014). Genotype$\times$ year interaction and broad-sense heritability of architectural characteristics in rose bush. Plant Breeding 133, 412–418.

Demotes-Mainard, S., Huché-Thélier, L., Morel, P., Boumaza, R., Guérin, V., and Sakr, S. (2013). Temporary water restriction or light intensity limitation promotes branching in rose bush. Scientia Horticulturae 150, 432–440.

Demotes-Mainard, S., Péron, T., Corot, A., Bertheloot, J., Le Gourrierec, J., Pelleschi-Travier, S., Crespel, L., Morel, P., Huché-Thélier, L., and Boumaza, R. (2016). Plant responses to red and far-red lights, applications in horticulture. Environmental and Experimental Botany 121, 4–21.

Djennane, S., Oyant, L.H.-S., Kawamura, K., Lalanne, D., Laffaire, M., Thouroude, T., Chalain, S., Sakr, S., Boumaza, R., Foucher, F., et al. (2014). Impacts of light and temperature on shoot branching gradient and expression of strigolactone synthesis and signalling genes in rose. Plant, Cell & Environment 37, 742–757.

Evers, J.B., and Vos, J. (2013). Modeling branching in cereals. Frontiers in Plant Science 4, 399.

Fioreze, S.L., and Rodrigues, J.D. (2014). Tillering affected by sowing density and growth regulators in wheat. Semina: Ciências Agrárias 35, 589–603.

Galvan-Ampudia, C.S., Chaumeret, A.M., Godin, C., and Vernoux, T. (2016). Phyllotaxis: from patterns of organogenesis at the meristem to shoot architecture. Wiley Interdisciplinary Reviews: Developmental Biology 5, 460–473.

Gautier, H., Měch, R., Prusinkiewicz, P., and Varlet-Grancher, C. (2000). 3D architectural modelling of aerial photomorphogenesis in white clover (Trifolium repens L.) using L-systems. Annals of Botany 85, 359–370.

Girault, T., Bergougnoux, V., Combes, D., VIEMONT, J.-D., and Leduc, N. (2008). Light controls shoot meristem organogenic activity and leaf primordia growth during bud burst in Rosa sp. Plant, Cell & Environment 31, 1534–1544.

Guilpart, N. (2014). Relations entre services écosystémiques dans un agroécosystème à base de plantes pérennes : compromis entre rendement de la vigne et régulation de l'oïdium. These de doctorat. Montpellier, SupAgro.

Hallé, F., and Oldeman, R. (1970). Essai sur l'architecture et la dynamique de croissance des arbres tropicaux.

Hauagge, R., and Cummins, J.N. (1991). Age, growing temperatures, and growth retardants influence induction and length of dormancy in Malus. Journal of the American Society for Horticultural Science 116, 116–120.

Horvath, D.P., Anderson, J.V., Chao, W.S., and Foley, M.E. (2003). Knowing when to grow: signals regulating bud dormancy. Trends in Plant Science 8, 534–540.

Jin, J., Huang, W., Gao, J.-P., Yang, J., Shi, M., Zhu, M.-Z., Luo, D., and Lin, H.-X. (2008). Genetic control of rice plant architecture under domestication. Nature Genetics 40, 1365–1369.

Kami, C., Lorrain, S., Hornitschek, P., and Fankhauser, C. (2010). Light-regulated plant growth and development. In Current Topics in Developmental Biology, (Elsevier), pp. 29–66.

Kebrom, T.H., Brutnell, T.P., and Finlayson, S.A. (2009). Suppression of sorghum axillary bud outgrowth by shade, phyB and defoliation signalling pathways. Plant, Cell & Environment.

Kozai, T. (2013). Resource use efficiency of closed plant production system with artificial light: Concept, estimation and application to plant factory. Proceedings of the Japan Academy, Series B 89, 447–461.

Kyriacou, M.C., and Rouphael, Y. (2018). Towards a new definition of quality for fresh fruits and vegetables. Scientia Horticulturae 234, 463–469.

Lal, S., Sharma, O.C., and Singh, D.B. (2017). Effect of tree architecture on fruit quality and yield attributes of nectarine (Prunus persica var. nectarina) cv.'Fantasia'under temperate condition. Indian Journal of Agricultural Sciences 87, 24–28.

Le Moigne, M.-A., Guérin, V., Furet, P.-M., Billard, V., Lebrec, A., Spíchal, L., Roman, H., Citerne, S., Morvan-Bertrand, A., Limami, A., et al. (2018). Asparagine and sugars are both required to sustain secondary axis elongation after bud outgrowth in Rosa hybrida. Journal of Plant Physiology 222, 17–27.

Lescourret, F., Moitrier, N., Valsesia, P., and Génard, M. (2011). QualiTree, a virtual fruit tree to study the management of fruit quality. I. Model development. Trees 25, 519–530.

Li-Marchetti, C., Le Bras, C., Relion, D., Citerne, S., HuchÃ©-ThÃ©lier, L., Sakr, S., Morel, P., and Crespel, L. (2015). Genotypic differences in architectural and physiological responses to water restriction in rose bush. Front. Plant Sci. 06.

Mason, M.G., Ross, J.J., Babst, B.A., Wienclaw, B.N., and Beveridge, C.A. (2014). Sugar demand, not auxin, is the initial regulator of apical dominance. Proceedings of the National Academy of Sciences 111, 6092–6097.

Rameau, C., Bertheloot, J., Leduc, N., Andrieu, B., Foucher, F., and Sakr, S. (2015). Multiple pathways regulate shoot branching. Frontiers in Plant Science 5, 741.

Ramírez-Arias, A., Rodríguez, F., Guzmán, J.L., and Berenguel, M. (2012). Multiobjective hierarchical control architecture for greenhouse crop growth. Automatica 48, 490–498.

Réchauchere, O., and Dore, T. (2010). La question agricole mondiale (Documentation française).

Roman, H., Girault, T., Barbier, F., Péron, T., Brouard, N., Pěnčík, A., Novák, O., Vian, A., Sakr, S., and Lothier, J. (2016). Cytokinins are initial targets of light in the control of bud outgrowth. Plant Physiology 172, 489–509.

Schreiner, M., Korn, M., Stenger, M., Holzgreve, L., and Altmann, M. (2013). Current understanding and use of quality characteristics of horticulture products. Scientia Horticulturae 163, 63–69.

Shimizu-Sato, S., and Mori, H. (2001). Control of outgrowth and dormancy in axillary buds. Plant Physiology 127, 1405–1413.

Sultan, S.E. (2000). Phenotypic plasticity for plant development, function and life history. Trends in Plant Science 5, 537–542.

Yarnes, S.C., Ashrafi, H., Reyes-Chin-Wo, S., Hill, T.A., Stoffel, K.M., and Van Deynze, A. (2013). Identification of QTLs for capsaicinoids, fruit quality, and plant architecture-related traits in an interspecific Capsicum RIL population. Genome 56, 61–74.

Zhuang, L., Wang, J., and Huang, B. (2017). Drought inhibition of tillering in Festuca arundinacea associated with axillary bud development and strigolactone signaling. Environmental and Experimental Botany 142, 15–23.

ARVALIS : Toute l’info pour gérer son exploitation agricole.

CHAPITRE 1 - ETAT DE L'ART ET PROBLEMATIQUE

ETAT DE L'ART

La modulation de la lumière (intensité et qualité) pour les cultures sous abris est un levier technique intéressant pour contrôler la croissance et le développement des plantes en limitant les intrants chimiques. Afin de mieux contrôler la ramification des plantes cultivées pour obtenir l'architecture souhaitée, il est utile de comprendre les effets de différents traitements lumineux sur la régulation de la ramification. Cependant, ces effets sont complexes. En effet, comme évoqué précédemment, la ramification est sensible à la fois l'intensité et à la qualité de la lumière, et il existe une interaction entre ces deux composantes (Su et al., 2011). De plus, la lumière est connue pour moduler d'autres phénomènes physiologiques de fonctionnement, de développement et de croissance de la plante qui pourraient interagir avec les processus de ramification. Enfin, plusieurs variables liées à la ramification sont modulées par les conditions lumineuses, comme le nombre de ramification émises, leur position le long de l'axe porteur, et le délai avant le débourrement des bourgeons. La réponse de la ramification aux conditions lumineuses n'est donc pas intuitive et la compréhension des mécanismes physiologiques sous-jacents est nécessaire pour améliorer les itinéraires lumineux.

Nous proposons dans la review Schneider et al. 2019 présentée ci-après un état de l'art des connaissances sur les mécanismes impliqués dans la régulation du débourrement des bourgeons axillaires, et de leur modulation par les conditions lumineuses (qualité et intensité de la lumière) expérimentées par la plante.

frontiers in Plant Science

REVIEW
published: 18 October 2019
doi: 10.3389/fpls.2019.01296

Light Regulation of Axillary Bud Outgrowth Along Plant Axes: An Overview of the Roles of Sugars and Hormones

*Anne Schneider[1], Christophe Godin[2], Frédéric Boudon[3], Sabine Demotes-Mainard[1], Soulaiman Sakr[1] and Jessica Bertheloot[1]**

[1] IRHS, INRA, Agrocampus-Ouest, Université d'Angers, SFR 4207 QuaSaV, Beaucouzé, France, [2] Laboratoire Reproduction et Développement des Plantes, Univ Lyon, ENS de Lyon, UCB Lyon 1, CNRS, INRA, INRIA, Lyon, France, [3] CIRAD, UMR AGAP & Univ. Montpellier, Montpellier, France

OPEN ACCESS

Edited by:
Benoit Schoefs,
Le Mans Université, France

Reviewed by:
Kosuke Fukui,
Okayama University of Science, Japan
Tibor Janda,
Centre for Agricultural Research (MTA), Hungary
Libo Xing,
Northwest A&F University, China

***Correspondence:**
Jessica Bertheloot
jessica.bertheloot@inra.fr

Specialty section:
This article was submitted to Plant Physiology, a section of the journal Frontiers in Plant Science

Received: 13 June 2019
Accepted: 18 September 2019
Published: 18 October 2019

Citation:
Schneider A, Godin C, Boudon F, Demotes-Mainard S, Sakr S and Bertheloot J (2019) Light Regulation of Axillary Bud Outgrowth Along Plant Axes: An Overview of the Roles of Sugars and Hormones. Front. Plant Sci. 10:1296. doi: 10.3389/fpls.2019.01296

Apical dominance, the process by which the growing apical zone of the shoot inhibits bud outgrowth, involves an intricate network of several signals in the shoot. Auxin originating from plant apical region inhibits bud outgrowth indirectly. This inhibition is in particular mediated by cytokinins and strigolactones, which move from the stem to the bud and that respectively stimulate and repress bud outgrowth. The action of this hormonal network is itself modulated by sugar levels as competition for sugars, caused by the growing apical sugar sink, may deprive buds from sugars and prevents bud outgrowth partly by their signaling role. In this review, we analyze recent findings on the interaction between light, in terms of quantity and quality, and apical dominance regulation. Depending on growth conditions, light may trigger different pathways of the apical dominance regulatory network. Studies pinpoint to the key role of shoot-located cytokinin synthesis for light intensity and abscisic acid synthesis in the bud for R:FR in the regulation of bud outgrowth by light. Our analysis provides three major research lines to get a more comprehensive understanding of light effects on bud outgrowth. This would undoubtedly benefit from the use of computer modeling associated with experimental observations to deal with a regulatory system that involves several interacting signals, feedbacks, and quantitative effects.

Keywords: light, hormones, sugar, bud outgrowth, branching, apical dominance, cytokinins, R:FR

INTRODUCTION

As sessile organisms, plants have to adapt to their growth environment. One important way is to adapt their branching architecture, above and below grounds, to accommodate endogenous (e.g., water and carbon status) and exogenous (light, space) constraints. In this process, branching regulation plays a crucial role as it defines strategies whereby plants colonize the underground and aerial spaces. Different environmental factors have been shown to impact this process, such as mineral or water supply to the roots, light, or temperature (Bouguyon et al., 2012; de Jong et al., 2014; Pierik and Testerink, 2014; Li-Marchetti et al., 2015). In the past two decades, due to spectacular advances in biotechnology, imaging, molecular biology, and computational modeling, major breakthroughs have been made in the understanding of the physiological regulation of branching of aerial axes.

In particular, the veil on the key mechanisms whereby light regulates aerial branching on plant axes has been partly lifted.

During growth, apical meristems of plant axes produce sequences of phytomers. One phytomer is composed of an internode with its axillary leaf and one or several axillary buds. Once initiated, axillary buds themselves may in turn enter growth immediately (sylleptic buds), or they can remain latent (proleptic buds) until some external event to the buds triggers their outgrowth (Lang et al., 1987; Kieffer et al., 1998; Barthelemy and Caraglio, 2007). This latter two-phase strategy is very frequent in both annual or perennial plants and has been shown to result from the dominance of the growing apex over its axillary meristems. This phenomenon, called apical dominance, offers plants the possibility to develop in a parsimonious way while preserving the possibility of branching to adapt their development to changing physiological or environmental contexts (Cline, 1994).

Light in particular has been recognized as a major modulator of the expression of apical dominance for decades. For example, increasing light intensity in photosynthetically active radiation (PAR) often results in an increase of the total number of lateral branches that develop on a given axis, thus reducing apical dominance (Mitchell, 1953; Su et al., 2011; Demotes-Mainard et al., 2013; Leduc et al., 2014). Likewise, a change in light quality, such as a high red-to-far-red wavelength ratio (R:FR) due to the use of red LEDs in a greenhouse or to gaps in a canopy, often leads to an increase of the number of outgrowing branches (Demotes-Mainard et al., 2016). In principle, these modulations may result from either an increase of the total number of primary nodes or from the probability for a bud to grow out. Light may affect both processes, resulting in significant modulations of branching intensity and plant architecture. Finally, light may also, in a more subtle way, affect the time taken by axillary buds to enter into growth (Bos and Neuteboom, 1998; Gautier et al., 1999; Evers et al., 2006; Demotes-Mainard et al., 2016).

The nature of the physiological or biophysical mechanisms whereby light interacts with the process of apical dominance and participates to releasing axillary bud latency is still largely elusive. A better understanding of these mechanisms requires identifying how light interacts with the physiological mechanisms regulating apical dominance. Two major putative mechanisms of apical dominance have been debated in the literature over the last decades. First, it has been experimentally shown on a variety of plant species that apical dominance is mediated by the plant hormone auxin, produced at the growing apex, and transported downward through the vascular tissues of the stem (Thimann and Skoog, 1933; Cline, 1996; Ongaro and Leyser, 2008). In this view, the leading apex continuously produces auxin, which reaches bud neighborhood through basipetal transport, and controls bud outgrowth indirectly. Two main signaling cascades have been identified (Domagalska and Leyser, 2011): (i) auxin in the stem controls the production of two other hormones, cytokinins and strigolactones, that move into the bud to control its outgrowth (second messenger theory); and (ii) auxin transport itself prevents auxin export out of the bud, a process necessary for bud outgrowth (canalization theory). These signaling cascades inhibit bud outgrowth as long as the main apex keeps producing auxin. This signaling hypothesis has long been challenged by a second hypothesis based on competition for resources (Luquet et al., 2006). This alternative view is based on the idea that during growth, plant organs compete for nutrients, and growing organs divert the nutrient resources from the freshly created buds. Deprived of resources, these buds remain latent as long as the main apex continues to grow. It was recently suggested that both hypotheses could be coupled in the regulation of bud outgrowth (Barbier et al., 2015; Barbier et al., 2019; Bertheloot et al., 2019).

In this review, we analyze how the effect of light on bud outgrowth has been interpreted in the context of the two main paradigms thought to be at the origin of apical dominance (which excludes the question of endodormancy in perennial plants). While previous review mainly focused on light effects in the vicinity of the bud (Leduc et al., 2014), this review aims to analyze how current knowledge from physiological and modeling studies helps to get a comprehensive understanding of light effects at the plant level. We start by a brief description of the main endogenous regulators of apical dominance, and their interaction and modulation at the plant scale. The hormonal regulation is described in a first section, while the regulation by the competition for nutrients is described in a second section. Then, we analyze the current knowledge about how light interacts with the previously identified endogenous network, including hormones and nutrients. We finally discuss the major gaps in the building of a comprehensive understanding of light-mediated bud outgrowth regulation and stress the potential complexity of the regulatory network, involving interactions between several regulators, dose-dependent effects, and feedback processes. We discuss why further detailed and quantitative analysis of this interaction will most probably require combining experimental and computational modeling approaches.

HORMONAL REGULATION OF BUD OUTGROWTH

Regulation of Apical Dominance in the Shoot

The Regulators of Apical Dominance: Auxin, Cytokinins, and Strigolactones

Auxin, a plant hormone produced in the apical region and transported downwards through the stem, has long been considered as the orchestrator of apical dominance in plants (Thimann and Skoog, 1933; Thimann and Skoog, 1934; Rinne et al., 1993; Ljung et al., 2001; Ongaro and Leyser, 2008; Teichmann and Muhr, 2015). While decapitation of the growing shoot tip promotes bud outgrowth, exogenous auxin applied to the decapitated shoot tip usually restores bud outgrowth inhibition (Thimann and Skoog, 1933; Thimann and Skoog, 1934; Cline, 1996). Furthermore, plants with reduced or increased auxin signaling/level display increased or reduced branching levels, respectively (Romano et al., 1991; Booker et al., 2003).

Auxin acts in an interconnected way with two other hormones, cytokinins (CKs) and strigolactones (SLs). CKs act as shoot-branching inducers that have an antagonistic effect to auxin on bud outgrowth (Wickson and Thimann, 1958; Sachs and Thimann, 1967; Shimizu-Sato et al., 2009; Mueller and Leyser, 2011). SLs act as shoot-branching repressors and enhance the inhibiting effect of auxin on branching (Beveridge,

2000; Beveridge, 2006 for reviews; Gomez-Roldan et al., 2008; Umehara et al., 2008; Crawford et al., 2010). While CKs and SLs are synthesized in both shoots and roots, only CKs can move through both the xylem sap (tZ-type) and the phloem sap (iP-type) (Bangerth, 1994; Mader et al., 2003; Kudo et al., 2010; Mueller and Leyser, 2011). SLs move primarily acropetally through the transpiration stream of the xylem sap, while their receptor—protein D14—is transported through the phloem to axillary buds in rice (Kohlen et al., 2011; Kameoka et al., 2016).

Auxin cannot enter buds (Prasad et al., 1993; Booker et al., 2003) and indirectly inhibits bud outgrowth. Several years of experiments have demonstrated that auxin acts through at least two non-exclusive mechanisms at the nodal segment and shoot scales, respectively (see Domagalska and Leyser, 2011; Rameau et al., 2015).

The Regulating System At the Scale of the Nodal Segment Adjacent to the Bud

In a theory known as "the second messenger theory," auxin in the nodal segment adjacent to the bud down-regulates CKs and up-regulates SLs, which are both supposed to migrate into the adjacent bud to control its outgrowth. The direct action of CKs and SLs in buds is supported by exogenous application of CKs and SLs on buds, which stimulated and inhibited their outgrowth, respectively (Sachs and Thimann, 1967; Gomez-Roldan et al., 2008; Dun et al., 2012). Furthermore, CK biosynthesis was rapidly enhanced in the nodal stem segment, and the CK content increased in the bud in response to auxin depletion, and these behaviors were prevented by exogenous auxin supply (Nordstrom et al., 2004; Tanaka et al., 2006; Liu et al., 2011; Li et al., 2018). By contrast, auxin depletion resulted in a rapid repression of SL biosynthesis-related genes in the stem, a behavior prevented by exogenous auxin application (Foo et al., 2005; Zou et al., 2006; Hayward et al., 2009).

The integration of the two antagonistic regulators CKs and SLs is at least partly mediated by the TCP transcriptional regulator TEOSINTE1/BRANCHED1 (*TB1*/*BRC1*) in the bud (for reviews Rameau et al., 2015; Wang et al., 2019). BRC1 locally inhibits bud outgrowth, and its transcript level can be downregulated by CKs and upregulated by SLs. However, the expression level of *OsTB1/FC1 (Oryza sativum Teosinte1/Fine Culm1)* in rice was insensitive to SLs (Minakuchi et al., 2010; Guan et al., 2012), and CKs promoted bud activation in pea *brc1* mutants (Braun et al., 2012). These results indicate that integration of CKs and SLs also involves a BRC1-independent pathway.

The Systemic Regulation System

In the "auxin canalization" theory, auxin transport in the stem is a systemic signal that prevents auxin export out of buds independently of any messengers relaying auxin signaling from the stem to the bud, and auxin export out of buds is necessary for their outgrowth. This theory relies on the observed tight correlation between bud outgrowth and auxin export out of the bud (Li and Bangerth, 1999; Bennett et al., 2006; Balla et al., 2011). As initially proposed by Sachs (1981) in the context of vascular strand differentiation, lateral auxin flow from the buds to the stem could be inhibited by the process of auxin canalization in the main stem, whereby the auxin flux upregulates and polarizes its own transport in one direction. From the 2000s, the identification of PIN auxin efflux carriers and visualization techniques based on PIN immunolocalization demonstrated the existence of a positive feedback between the auxin flow and its own transport. PIN polar targeting at the level of cell plasma membranes directs auxin flow, and this process is positively feedback-regulated by auxin itself (Sauer et al., 2006; Wisniewska et al., 2006). Introduction of such a feedback in a computer model confirmed the plausibility of the canalization theory. Prusinkiewicz et al. (2009) demonstrated through simulations that this feedback led to high auxin fluxes in the main stem, which may in turn prevent any lateral auxin flux from axillary buds. By stating that buds cannot enter sustained growth if they do not export their own auxin, auxin canalization in the main stem may thus explain bud inhibition during apical dominance. In this process, the directionality of canalization is determined by the auxin source that becomes active first (the apical one during apical dominance). Such a model also simulated several branching phenotypes observed in *Arabidopsis* mutants for auxin homeostasis or transport.

The discovery that SLs dampen polar auxin transport in the stem by down-regulating PIN accumulation in xylem parenchyma cells and triggering the rapid removal of PIN from the plasma membrane further confirmed the plausibility of the canalization theory (Bennett et al., 2006; Crawford et al., 2010; Xu et al., 2015; Li et al., 2018). A computational model in which the action of SLs is represented as an increase in the rate of removal of the auxin export protein—PIN—from the plasma membrane reproduced auxin transport and shoot branching phenotypes observed in various mutant combinations and SL treatments, including the counterintuitive ability of SLs to promote or inhibit shoot branching depending on the auxin transport status of the plant (Shinohara et al., 2013). Furthermore, exogenous supply of low doses of auxin transport inhibitors to the stem of SL mutants of *Arabidopsis* led to a phenotype close to that of wild-type plants, in accordance with a main role of auxin transport in determining the number of buds that grow out into branches (Bennett et al., 2006; Lazar and Goodman, 2006; Lin et al., 2009). However, even if several biological and modeling pieces of evidence support the canalization theory, the nature of the mechanism inducing export of axillary bud auxin into the stem is still relatively abstract (Prusinkiewicz et al., 2009).

Dynamic Regulation of Bud Outgrowth Along a Same Axis

The release of apical dominance leads to bud outgrowth at given positions on the plant depending on the plant species. Outgrowth of these buds then inhibits outgrowth of the other buds on the axis (Morris, 1977). In garden pea, the inhibition exerted by a growing bud on the buds below was related to auxin synthesized and exported by the growing bud and transported downward in the main stem (Balla et al., 2016). This mechanism limits excessive branching that may be detrimental for the plant.

SLs also appear as main components of this phenomenon and could act through a double feedback process (Dun et al., 2009b). In a first feedback, branching initiation increases SL biosynthesis through a branch-derived signal, probably auxin,

which could contribute to further inhibit bud outgrowth. This regulation scheme was identified from the experimental observation that the initiation of a new branch in garden pea correlated locally with the up-regulation of SL biosynthesis genes in the corresponding node, and this upregulation was prevented by branch removal (Dun et al., 2009b). Second, SL deficiency in the node, which contributes to promote bud outgrowth, activates a feedback signal that up-regulates SL biosynthesis and decreases CKs in the xylem sap, thus contributing to prevent bud outgrowth. At the origin of this hypothesis, SL mutants of different species (except pea *rms2*) were observed displaying reduced CKs in the xylem sap and higher expression of SL biosynthesis genes, while exogenous SL supply repressed SL biosynthesis (Foo et al., 2005; Snowden et al., 2005; Foo et al., 2007; Drummond et al., 2009; Hayward et al., 2009). Computer simulations support this double SL-based regulating system in pea branching regulation as they capture the overall experimental phenotypes of branching, SL biosynthesis gene expression, and xylem-sap CKs that are observed for different graft combinations between mutant and wild-type pea (Dun et al., 2009b).

In garden pea, the feedback signal derived from SL perception is dependent on *RMS2* and moves from shoots to roots (Beveridge, 2000; Foo et al., 2005; Foo et al., 2007). The chemical nature of the *RMS2*-dependent feedback has been extensively discussed (Ongaro and Leyser, 2008; Dun et al., 2009a). Ligerot et al. (2017) recently demonstrated that protein RMS2 functions as an auxin receptor. They also observed that SL root-feeding, as a disruption of auxin transport, repressed auxin biosynthesis in the shoot. This suggests the existence of a feedback loop in which auxin depletion in the stem stimulates SL biosynthesis in an RMS2-dependent manner in the roots, which in turn stimulates auxin biosynthesis in the shoot.

Contribution of Roots to Bud Outgrowth

As mentioned above, CK and SL biosynthesis in the shoot are main components of auxin-mediated apical dominance. But CKs and SLs are also synthesized in roots and root-derived CKs and SLs are transported in the shoots through the xylem and also contribute to stimulate and inhibit shoot branching, respectively (Beveridge, 2000; Young et al., 2014; Muller et al., 2015).

Root-derived CKs were long believed to contribute to the bud outgrowth response to decapitation because the xylem-sap CK content increases after decapitation and accumulates in buds, and this is prevented by exogenous auxin supply (Bangerth, 1994; Turnbull et al., 1997; Mader et al., 2003). However, the absence of a rapid response of CK-related biosynthesis genes in roots indicates that root-derived CKs may have a secondary role in this process (Tanaka et al., 2006). Recent experiments comparing root-bearing plants and root-depleted isolated nodal stem segments indicate that root-derived CKs may in fact antagonize the effect of auxin in apical dominance. Decapitated plants of garden pea SL mutants were indeed unresponsive to auxin supply, due to the antagonistic effect of root-derived CKs on the inhibitory effect of auxin, while the isolated nodal stem segments (without root-derived CKs) were auxin responsive (Young et al., 2014). In *Arabidopsis*, intact auxin-producing CK-synthesis/signaling mutants were accordingly less branched than wild-type plants, while the isolated nodal segment bud response to auxin was not impaired in CK mutants as compared to the wild-type (Muller et al., 2015). Since CK biosynthesis in the roots is promoted by high nitrogen nutrition (Takei et al., 2002; Xu et al., 2015), root-derived CKs could antagonize auxin-mediated apical dominance in case of a high soil nitrogen content by modulating the shoot CK levels. In line with this, CK mutants of *Arabidopsis* exhibited an altered positive branching response to an increase in the soil nitrogen conditions (Muller et al., 2015). On the opposite, root-derived SLs, sensitive to phosphate or nitrogen deficiency or water stress (Ha et al., 2014; Cochetel et al., 2018; Mostofa et al., 2018), could strengthen auxin-mediated apical dominance in case of a low soil nutrient status or water stress. Accordingly, root-derived SLs have been reported to mediate the effect of soil phosphate deficiency on shoot branching (Kohlen et al., 2011; Xi et al., 2015).

Regulation of Bud Outgrowth by Other Hormones

Abscisic acid (ABA) is well known for its role in plant adaptation to abiotic stresses (Vishwakarma et al., 2017), and gibberellins (GAs) modulate a range of processes such as cell elongation and fruit maturation (see Olszewski et al., 2002; Yamaguchi, 2008; Hartmann et al., 2011; Ragni et al., 2011). They both take part to bud outgrowth regulation, but their role has been less investigated than the roles of auxin, CKs, and SLs.

The effect of GAs on bud outgrowth varies strongly among species. GAs inhibit shoot branching in rice (Lo et al., 2008; Ito et al., 2018), bahiagrass (Agharkar et al., 2007), *Arabidopsis* (Silverstone et al., 1997), hybrid aspen (Mauriat et al., 2011), and tomato (Martinez-Bello et al., 2015). The exact mechanism behind their effect remains elusive and might be linked to the modification of SL biosynthesis (Ito et al., 2017) and an increase of sugar sink strength (see below) (Buskila et al., 2016). In perennial woody plants such as rose and *Jatropha curcas*, GAs are promoters of bud outgrowth (Choubane et al., 2012; Ni et al., 2017). In apple, exogenous application of GAs to axillary buds did not promote outgrowth (Tan et al., 2018).

The role of ABA as an inhibitor of bud outgrowth was long hypothesized based on the observations that exogenous ABA supply inhibits bud outgrowth (White and Mansfield, 1977; Chatfield et al., 2000; Cline and Oh, 2006; Corot et al., 2017; Yuan et al., 2018) and that the bud ABA content is negatively correlated to the bud ability to grow out. In particular, the bud ABA level decreases in response to decapitation and increases in response to exogenous auxin supply in annual plants (Eliasson, 1975; Everatbourbouloux and Charnay, 1982; Knox and Wareing, 1984; Gocal et al., 1991), and ABA accumulates during cold-induced bud dormancy in perennial plants (Rohde et al., 1999; Arora et al., 2003; Wang et al., 2016a). Mutants recently confirmed a role of ABA in bud outgrowth regulation. *Arabidopsis* mutants deficient in ABA biosynthesis (*nced3-2* and *aba2-1*) displayed higher bud outgrowth frequency (Reddy et al., 2013; Yao and

Finlayson, 2015). Similarly, genetically altered poplar with reduced sensitivity to ABA exhibited enhanced shoot branching (Arend et al., 2009).

ABA has been reported to act downstream of auxin signaling (AUXIN-RESISTANT 1 *AXR1*), MORE AXILLARY BRANCHED (MAX) signaling (*MAX2*), and BRANCHED1 (*BRC1*) gene (Gonzalez-Grandio et al., 2013; Yao and Finlayson, 2015; Gonzalez-Grandio et al., 2017). *AtBRC1* directly induces ABA synthesis in the bud by upregulating the expression of *9-CIS-EPOXICAROTENOID DIOXIGENASE 3* (*NCED3*), which encodes a key ABA-synthesis enzyme (Yao and Finlayson, 2015; Gonzalez-Grandio et al., 2017). ABA may partly inhibit bud outgrowth by reducing auxin biosynthesis and transport within the bud and also cell multiplication (Yao and Finlayson, 2015), which may impair bud capacity to export its own auxin and to grow out (Prusinkiewicz et al., 2009). ABA is also synthesized outside the bud and can access the buds (Everatbourbouloux, 1982; Lacombe and Achard, 2016). This raises the question of the role of such externally synthesized ABA in the control of bud outgrowth. ABA exogenously supplied to the stem below the bud inhibited bud outgrowth but did not do so when supplied above the bud, indicating a likely preferential role of upstream xylem-transported ABA (Cline and Oh, 2006). In barley, ABA was reported to suppress SL biosynthesis in the basal part of the plant and roots, which in this case promoted tiller emergence (Wang et al., 2018). These findings indicate the complexity of ABA-dependent bud outgrowth regulation and its interactions with other branching-related hormonal networks.

Summary

So far, many studies have focused on understanding how auxin, synthesized by growing apical organs and transported downwards through the stem in annual plants, acts to inhibit the outgrowth of a bud without entering the bud during apical dominance. They highlighted an intricate regulatory network described in **Figure 1** that displays two pathways. In the first pathway, auxin acts through a canalization mechanism that creates a main flux of auxin downwards and inhibits the initiation of auxin fluxes from lateral buds. In the second pathway, auxin acts more locally through its concentration in the node which modulates CK and SL biosynthesis, which in turn relay the auxin signal from the stem to the bud. CK and SL signals are integrated in the bud through BRC1-dependent and -independent pathways. *BRC1* acts at least partly by up-regulating ABA biosynthesis.

The relationship between both pathways is not fully understood. Both pathways probably interact because SLs also control auxin transport, and CKs were recently reported to control auxin efflux carrier proteins (PIN3, PIN4, PIN7) in *Arabidopsis* (Waldie and Leyser, 2018). From a temporal point of view, auxin transport regulation could come after local regulation, as indicated experimentally for garden pea (Chabikwa et al., 2019). Intriguingly, the role of CKs as a second messenger has recently been questioned for *Arabidopsis* because isolated nodal segments of mutants deficient in CK biosynthesis or signaling exhibited a normal response to exogenous auxin (Muller et al., 2015).

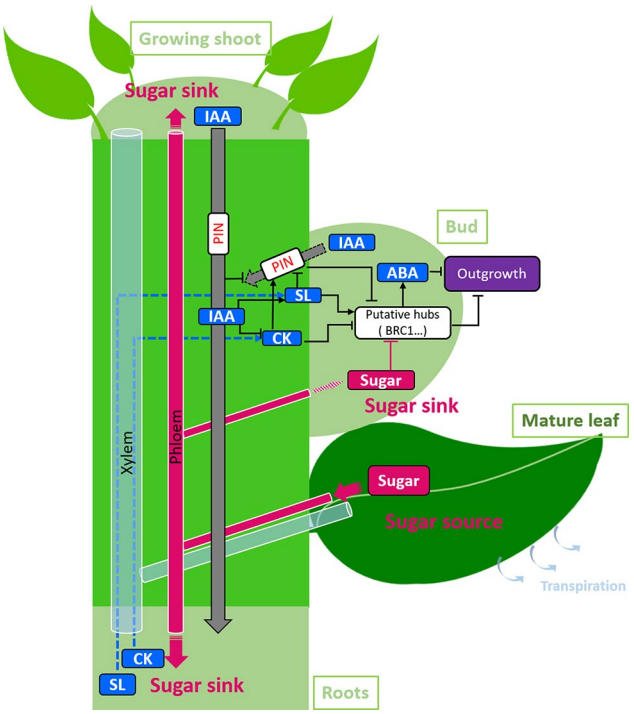

FIGURE 1 | Regulation of the outgrowth of one bud by sugars and hormones on a growing shoot. Sugars are produced by photosynthetic organs and transported by mass flow in the phloem to sugar sinks, *i.e.,* the growing organs (apical leaves and internodes, elongating branches, roots). Auxin (IAA) is produced by apical growing organs and is transported in the stem to the roots through PIN proteins (gray arrow). Auxin in the nodal stem down- and up-regulates the biosynthesis of cytokinins (CKs) and strigolactones (SLs), respectively and prevents auxin export out of the bud through the canalization process. Sugars, CKs, SLs, and auxin export are integrated in the bud by hubs, which include the gene *BRC1*, to control bud outgrowth. In addition, CK and SL syntheses in the roots and their transport upwards in the xylem by the transpiration stream may increase the CK and SL contents in the nodal stem (dotted arrows). ABA acts downstream of *BRC1* to inhibit bud outgrowth. The feedback loops between hormones are not represented. The hormonal regulators are represented in blue, and sugars in pink. Sugar sinks are represented in light green, sugar sources in dark green. Black arrows represent the effects of one regulator on a target. Large arrows represent active transport processes. The way sugars are transported to the bud is unknown and is represented by a large dashed arrow.

Besides these well-studied auxin-dependent pathways in the vicinity of the bud, some studies have also highlighted the important role of roots as a source of SLs and CKs. They indicate that auxin-related apical dominance in the shoot may be modulated by root-derived CKs and SLs, as a way to adjust apical dominance in the aerial part to soil nutrient status (Kohlen et al., 2011; Muller et al., 2015; Xi et al., 2015). Furthermore, evidences support a main role of root-derived CKs and SLs in regulating the outgrowth pattern along an axis through feedback loops between shoot and root, and SLs, CKs, and auxin (not represented on the figure; Dun et al., 2009b; Ligerot et al., 2017). However, research about the role of long-distant components from buds other than auxin is still scarce, and further work is definitely required to get a more integrated understanding of the hormonal regulation of apical dominance expression in plants.

BUD OUTGROWTH REGULATION THROUGH COMPETITION FOR NUTRIENTS

Relationships between the plant nutrient status and the number of new branches arising in a growth period have been suggested for decades. For example, for tree species, the number of new branches was found correlated to the vigor of the parent branch (Heuret et al., 2000). In wheat, the bud outgrowth probability at a given leaf rank on the main stem was correlated to the parent leaf mass *per* unit area (Bos, 1999; Evers et al., 2006). In ryegrass, the number of tillers that recovered after cutting was strongly correlated to the initial carbohydrate level before cutting (Davies, 1965). These observations led to the intuition that the degree of competition for nutrients within the plant regulates the investment into new branches.

The degree of competition within the plant is a complex variable that depends on nutrient supply to the plant, nutrient transport, storage, and use by the different organs and evolves dynamically with plant development. To address this complexity, different hypotheses related to competition for nutrients in shoot branching were first tested using computational models. The results of these simulations confirmed the plausibility of branching regulation by nutrient competition. These results have been corroborated in recent years by physiological experiments that brought evidence supporting the initial intuition and providing a better understanding of the mechanisms involved.

Computer Models of Branching Regulation by Competition for Nutrients

The first models were developed for trees and formalized that a limited amount of nutrients is assimilated by the plant and shared among tree branches according to given priority rules, and that the nutrient level in a branch determines the emergence of new branches. Based on the observations of weaker water flow in less vigorous branches as compared to the main trunk (Zimmermann, 1978), 25 years ago, Borchert and Honda implemented a model in which branches were in competition for nutrients coming from the roots through the transpiration stream (Borchert and Honda, 1984). Later, the model LIGNUM initially developed for young pine trees considered that branches were in competition for carbohydrates produced by photosynthesis in tree aerial parts (Perttunen et al., 1996; Perttunen et al., 1998). Competition for nutrients or carbohydrates among branches simulated qualitative observations made on real trees, such as a reduction of branch emergence with tree development or branching stimulation after branch removal by pruning (Borchert and Honda, 1984). Priority rules for nutrient or carbohydrate allocation among branches were essential to simulate observed tree forms (Perttunen et al., 1998; Palubicki et al., 2009). For example, in Borcher and Honda's model, preferential nutrient allocation to a given branch position and to the more vigorous branch (defined by the number of daughter transpirating branches) explained the morphological differentiation of branches into leaders and weaker lateral shoots observed in some species (Borchert and Honda, 1984).

Several years later, the concept emerged that competition for carbohydrates can be represented by the source-sink ratio (Warren-Wilson, 1972; Lacointe, 2000), which is the balance between the production rate of carbohydrates by photosynthesis and their utilization rate for growth. For grass species, this concept arises in particular from the observed correlations between the tillering level and the balance between (i) PAR intensity, that determines photosynthesis, and (ii) temperature, that determines the organ growth rate (Mitchell, 1953; Bos and Neuteboom, 1998). Based on findings that sugars act as signaling entities on meristematic activity (Sherson et al., 2003; Heyer et al., 2004), the authors of the rice model ecomeristem assumed that sugars also acted as signals in bud outgrowth regulation and that the source-sink ratio was a signal analogous to sugar signaling (Luquet et al., 2006). Supporting the concept, the source-sink ratio dynamics correlated with the dynamics of sugar reserves, an indicator of sugar availability. The authors argued that such a regulating system allowed for the plant to adjust the carbohydrate sinks to the sources: in case of a high source-sink ratio, plant development is stimulated, thus increasing the sink strength for carbohydrates, which in turn decreases the ratio. This concept has been taken up by other models, *e.g.,* for wheat (Evers et al., 2010) or trees (Letort et al., 2008; Mathieu et al., 2009). Simulations of plant development were validated against quantitative experimental observations for grasses, but the robustness of the models was not demonstrated (Luquet et al., 2006; Evers et al., 2010). For trees, the concept explained observed trends qualitatively, such as a low branch number under low light intensity, or branching rhythmicity as a result of the negative feedback between branch emergence and the source-sink ratio (Letort et al., 2008; Mathieu et al., 2009).

All these studies show that branching regulation by competition for nutrients explains some of the observed plant behaviors in different species. However, the concept was lacking more direct molecular experimental evidence. In the 2010s, several biological experiments, independent of modeling studies, confirmed bud outgrowth regulation by competition for carbohydrates and the involvement of sugar signaling in some species.

Experimental Evidence for Bud Outgrowth Regulation by Competition for Carbohydrates in Grasses and Garden Pea

A first series of experiments demonstrated that differences in tiller bud outgrowth induced by changes in the source-sink ratio in some grass species were correlated to differences in the bud sugar status. The *tin* mutant of wheat, which is characterized by earlier internode elongation as compared to the wild type, displayed a reduced number of tillers and over-expression of a sucrose-starvation gene, downregulation of a sucrose-inducible gene, and a reduced sucrose content in the inhibited buds (Kebrom et al., 2012). In sorghum, bud outgrowth inhibition by defoliation was correlated to up- and down-regulations of sucrose starvation and sucrose-inducible genes in buds, respectively (Kebrom and Mullet, 2015). In this case, defoliation of the subtending leaf blade or any other leaf blade inhibited bud outgrowth, indicating that outgrowth may be dependent on the overall plant sugar status, as implemented in models, rather than on sugar supply by the subtending leaf. No similar studies were made in tree species.

Definitive proof of a role of sugars in bud outgrowth regulation by the source/sink balance was given by Mason et al. (2014) in garden pea. Removal of the apical growing organs by decapitation of the shoot tip led to bud outgrowth and rapid sugar redistribution and accumulation in the outgrowing buds before auxin depletion in the nodal segment adjacent to the outgrowing bud. This phenomenon was abolished by defoliation which reduced sugar supply, while exogenous sucrose supply through the petioles of intact plants (not decapitated or defoliated) released the buds from apical dominance. These behaviors indicate that sugar accumulation in the buds of decapitated plants is both necessary and sufficient for bud outgrowth. Additional proof was given recently by the observation that the elevated sucrose and hexose levels of transgenic plants overexpressing fructose 1,6-bisphosphatase II in the cytosol increased the number of lateral shoots (Otori et al., 2017).

Role of Sugar in Bud Outgrowth Regulation

Using excised nodal stem segments *in vitro* to manipulate sugar availability for buds easily, evidence was brought about both the trophic and signaling roles of sugars in bud outgrowth, as demonstrated in other processes of plant development (Moore et al., 2003; Rolland et al., 2006; Lastdrager et al., 2014; Li and Sheen, 2016; Sakr et al., 2018). As compared to an osmotic control, sucrose supply or supply of its derivative hexoses (glucose and fructose) to isolated buds increased sugar levels in buds and stimulated their outgrowth in a dose-dependent manner in species such as rose and garden pea (Henry et al., 2011; Rabot et al., 2012; Barbier et al., 2015; Fichtner et al., 2017). In line with the trophic role of sugars, sugar-induced bud outgrowth in rose was characterized by a higher sugar metabolic activity of the bud linked to increased expression of the sugar transporter *RhSUC2* and in the expression and activity of vacuolar invertase *RhINV1*, an enzyme responsible for sucrose cleavage into hexoses and usually related to organ sink strength (Girault et al., 2010; Henry et al., 2011; Rabot et al., 2012). Interestingly, non-metabolizable sucrose or fructose analogs also induced bud outgrowth in rose (Rabot et al., 2012; Barbier et al., 2015; Wingler, 2018) and stimulated the expression and the activity of the vacuolar invertase *RhINV1* (Rabot et al., 2012). This observation supports a scenario in which sugar availability for the bud acts as a signaling entity regulating its outgrowth and its sink strength. This role may be mediated, at least partly, through trehalose-6-phosphate, an important indicator of the carbohydrate status in plants (Figueroa and Lunn, 2016). Sucrose supply to nodal stem segments of garden pea induced a rapid concentration-dependent increase of the trehalose-6-phosphate (Tre6P) content in the buds that was highly correlated with their outgrowth rate (Fichtner et al., 2017). Such a rapid Tre6P increase in outgrowing buds was also observed after removal of the main sink for sugars by decapitation of garden pea shoots. Sugar signal may regulate bud outgrowth through the sucrose non-fermenting kinase 1 (SnRK1) complex, which perceives cell energetic status and regulates growth activity accordingly (Tsai and Gazzarrini, 2014). This supports the concept implemented in models that the source-sink ratio controls a sugar signal that modulates bud outgrowth.

Sugar Interplays With Hormones

Interplays between sugar and hormonal pathways have been recently reported in bud outgrowth regulation in rose and pea (Barbier et al., 2015; Bertheloot et al., 2019). Bud outgrowth is under an antagonistic coupled control of sugar and auxin levels. While exogenous auxin supply to nodal segments *in vitro* inhibited bud outgrowth dose-dependently, sugar supply partially removed the inhibitory effect of auxin in a manner that was also dose-dependent. This supports the view that a high plant sugar status may attenuate auxin-mediated apical dominance, leading eventually to bushy phenotypes.

Sugar promoting effect on bud outgrowth was accompanied by a number of changes in the bud outgrowth hormonal network for rose nodal segments *in vitro* (Barbier et al., 2015). These changes include the simulation of CK biosynthesis and level in the stem and a down-regulation of a SL signaling gene (*MAX2*). However, CK level in the stem and auxin export from the bud to the stem are unlikely to be the main mediators of sugar promoting effect on bud outgrowth. Without sucrose, CK supply to rose nodal segments *in vitro* did not induce bud outgrowth, and sucrose could not antagonize the auxin-dependent repression of CK levels in the stem (Barbier et al., 2015; Bertheloot et al., 2019). Sugar-stimulated bud outgrowth was rather related to the impairment of SL response, because exogenously applied SL was inefficient in inhibiting bud outgrowth in the presence of high sugar concentration in rose and pea (Bertheloot et al., 2019). In addition, buds of pea mutants deficient in SL perception displayed a reduced response to changes in sugar supply *in vitro*. Finally, a computational model, in which auxin regulates bud outgrowth through regulation of the production of CKs and SLs (second messenger model) and sugar acts by suppressing SL response, captured the diversity of observed bud outgrowth responses to sugar and hormones in a quantitative manner. Further studies are required to decipher the exact targets of sugars, but the SL signaling-related gene *MAX2* and the integrator gene *BRC1* that are downstream of SLs and down-regulated under high sucrose conditions for different species may be involved (Kebrom et al., 2010; Kebrom et al., 2012; Mason et al., 2014; Barbier et al., 2015; Kebrom and Mullet, 2015; Otori et al., 2017).

Summary

These data highlight that competition for sugars within the plant, indicated by the source/sink ratio, is a key component of branching regulation at least in annual species. As depicted in **Figure 1**, sugars are produced by source organs, mainly photosynthetically leaves, and transported through the phloem to sink organs such as the shoot growing apical and root zones. High sugar availability in the vicinity of the bud, resulting from high ratio of source to sink activity, promotes bud outgrowth. The exact pathway by which sugar availability regulates bud outgrowth remains to be elucidated, but sugar signaling seems crucial (Rabot et al., 2012; Barbier et al., 2015; Fichtner et al., 2017). Such signaling role of sugar appears as an efficient way to adjust plant development to endogenous resources. New branches, which are highly demanding in resources, are created only if the resource status of the plant is sufficient to sustain their growth.

Recent studies highlight the existence of an interplay between sugar and the hormonal networks in bud outgrowth regulation; more particularly, high sugar availability antagonizes auxin inhibitory effect through inhibition of SL signaling (Bertheloot et al., 2019). A hormonal role has also been suggested by the simulations of previous nutrient-based models. Indeed, this kind of models could not fully explain branching phenotypes at the plant scale and should be coupled to other signaling processes. We report that Borchert and Honda's and LIGNUM models include priority rules for nutrient allocation among branches, essential to simulate tree branching habits (Borchert and Honda, 1984; Perttunen et al., 1996; Perttunen et al., 1998). Other models have to define which bud is sensitive to carbohydrates to simulate positions of branches on trees (Letort et al., 2008) or the observed coordination between tiller appearance and parent axis development in grasses (Letort et al., 2008; Evers et al., 2010). Sensitivity to carbohydrates also depends on mineral nutrition in grasses (Dingkuhn et al., 2007; Kim et al., 2010a; Kim et al., 2010b; Alam et al., 2014). All these effects may involve hormonal pathways, because hormones are regulated by both plant development and growth conditions. This raises the question of how sugar and hormonal signals are integrated to regulate bud outgrowth in spatial and temporal dynamics at the plant scale.

Contrary to sugars, the role of xylem-transported nutrients in bud outgrowth regulation has been the subject of very few studies. However, they could contribute to bud outgrowth regulation. Amino acids were required for bud outgrowth in nodal segments of rose *in vitro* (Le Moigne et al., 2018), transgenic lines deficient in amino acids displayed decreased tillering in rice (Funayama et al., 2013; Ohashi et al., 2017; Ohashi et al., 2018), and overexpression of a glutamine synthase gene promoted tillering in sorghum (Urriola and Rathore, 2015). Whether amino acids act as signaling entities in bud outgrowth remains to be investigated.

INTERACTION OF LIGHT WITH THE NETWORK OF ENDOGENOUS REGULATORS

Besides its role as an energy source for photosynthesis, light is also a powerful environmental signal that controls many developmental processes (de Wit et al., 2016; Gangappa and Botto, 2016; Lee et al., 2017). In particular, it is involved in the shade avoidance syndrome (SAS), characterized by typical morphological changes such as leaf hyponasty, an increase in hypocotyl and internode elongation, and extended petioles, which aim to maximize light interception by the plant for photosynthesis (Franklin, 2008). In bud outgrowth regulation, light also acts as a signal that may prevent a new branch from developing in low light conditions. In accordance with the signaling role of light, a very low light intensity on the bud was sufficient to trigger bud outgrowth in decapitated rose (Girault et al., 2008). Tillering can cease in grasses before the occurrence of a significant reduction in PAR intensity due to canopy closure, but concomitantly with a reduction of the R:FR ratio (Ballare et al., 1987). Simulation studies support a role of light in shaping plant branching architecture in different species. In trees, the global branching structure can be explained qualitatively by space colonization algorithms, which consider competition for space as the key factor determining the branching structure of the tree (Runions et al., 2007; Palubicki et al., 2009). In herbaceous species, the inhibiting effect of shading or high plant densities can be simulated by regulating bud outgrowth by the local light environment on the apical meristem at the time of bud formation (Gautier et al., 1999; Evers et al., 2007).

At the plant scale, light signaling interacts with hormonal and/or nutrient regulation by controlling the homeostasis, transport, and signaling of hormones and nutrients. Remarkably, light, hormones, and nutrients seem to converge to the same regulating hubs (Quail, 2002; Moore et al., 2003; Lau and Deng, 2012; Li et al., 2017; Mawphlang and Kharshiing, 2017; Sakuraba and Yanagisawa, 2018; Simon et al., 2018). Compared to the endogenous network responsible for apical dominance, relatively few studies have focused on the interaction of light with hormones and nutrients in the control of axillary bud outgrowth. Most studies have focused on the effect of the R:FR ratio, which is a signal of canopy closure. More recently, the effect of light intensity was also investigated.

Interaction of Light With the Hormonal Regulatory Network

R:FR Ratio

Studies were made by directly manipulating light quality or by using *phyB Arabidopsis* mutants, which are deficient in phytochrome B-mediated red light perception and display a low branching level as compared to the wild-type (Kebrom et al., 2006; Finlayson et al., 2010; Su et al., 2011). Those studies highlight that enhanced ABA biosynthesis in the bud has a main role in the effect of the R:FR ratio on bud outgrowth. The bud outgrowth response to R:FR is negatively correlated to the bud ABA level and to the expression of ABA biosynthesis- and signaling-related genes in different species (Tucker and Mansfield, 1972; Gonzalez-Grandio et al., 2013; Reddy et al., 2013; Yao and Finlayson, 2015; Kebrom and Mullet, 2016; Gonzalez-Grandio et al., 2017; Holalu and Finlayson, 2017; Tarancon et al., 2017; Yuan et al., 2018). The ABA response was even reported to precede the bud outgrowth response to an increase of the R:FR ratio in *Arabidopsis* (Holalu and Finlayson, 2017). Furthermore, *Arabidopsis* mutants deficient in ABA biosynthesis (*nced3-2* and *aba2-1*) exhibited lower suppression of bud outgrowth by low R:FR than the wild type (Reddy et al., 2013; Yao and Finlayson, 2015). The mechanisms leading to changes in the ABA level involve *BRC1*. *BRC1* induces ABA biosynthesis in buds, is up-regulated by low R:FR or following *phyB* mutation, and is involved in low R:FR-dependent branch suppression (Gonzalez-Grandio et al., 2013; Yuan et al., 2018). Low R:FR-induced ABA biosynthesis may repress bud outgrowth partly by reducing bud auxin biosynthesis, since both *phyB Arabidopsis* mutants and exogenous ABA supply to wild-type plants reduced the expression of an auxin biosynthesis gene within the bud (Finlayson et al., 2010; Yao and Finlayson, 2015).

Upstream of *BRC1*, several other regulators of bud outgrowth than ABA could contribute to bud inhibition by low R:FR. Auxin plays a key role in the shade-avoidance syndrome, including the promotion of hypocotyl and petiole growth, leaf hyponasty, and phototropism (Iglesias et al., 2018). In seedlings, low R:FR increases auxin level in the foliage by stimulating its biosynthesis; auxin then moves to the stem where it reaches epidermal tissues through lateral orientation of PIN proteins to drive the auxin flux to the epidermis to promote growth (Iglesias et al., 2018). Similarly, relationships have been observed between auxin and bud outgrowth inhibition in *Arabidopsis phyB* mutants, which cannot perceive red light. The branching inhibition reported in *phyB Arabidopsis* mutants was alleviated by disrupting auxin signaling (Finlayson et al., 2010). In this case, branching inhibition was related to elevated auxin sensitivity and signaling in the shoot segments proximal to axillary buds (Reddy and Finlayson, 2014). Low auxin level supply to isolated stem segments inhibited *phyB* buds more than wild-type, and *phyB* shoots displayed elevated auxin-responsive genes expression compared to the wild-type. This obviously raises the question of how auxin- and ABA-mediated pathways interact to regulate bud outgrowth in response to R:FR. Although ABA acts downstream of auxin signaling (Yao and Finlayson, 2015), Holalu and Finlayson (2017) reported that bud response to low R:FR involve changes in bud ABA signaling before any detectable alteration in stem auxin signaling, indicating that ABA and auxin signalings are part of different R:FR-induced pathways. ABA pathway may be responsible for a rapid response of the bud to R:FR, while auxin signaling in the stem may sustain this rapid response. Low auxin transport rate was also observed in the shoots of *phyB* mutants but its role in inhibiting bud outgrowth was not demonstrated (Reddy and Finlayson, 2014).

Besides auxin, SL biosynthesis- and signaling-related genes were also found to be up-regulated by low R:FR or by *phyB* mutation in chrysanthemum, sorghum, or petunia buds (Kebrom et al., 2010; Drummond et al., 2015; Yuan et al., 2018). Furthermore, bud outgrowth inhibition by *phyB* mutation was impaired in SL biosynthesis (*max4*) or signaling (*max2*) mutants as compared to wild-type *Arabidopsis* (Finlayson et al., 2010), indicating a potential role of these genes in low R:FR-dependent bud outgrowth regulation. This is in accordance with the main role of the SL signaling-related gene *MAX2* in light-regulated hypocotyl elongation in *Arabidopsis* seedlings (Shen et al., 2007; Shen et al., 2012; Jia et al., 2014). Future tasks would be to identify the role of *MAX2* and understand its relationship with ABA and auxin signaling pathways in bud response to R:FR.

Light Intensity

The interaction between light intensity and hormonal regulation of bud outgrowth has mainly been investigated in rose. First data indicate that GAs are not sufficient to mimic the promotive effect of light in dark-placed buds (Choubane et al., 2012). For decapitated plants, dark-repressed bud outgrowth correlated with a down-regulation of two GA biosynthesis genes, and light-induced bud outgrowth was inhibited by GA biosynthesis inhibitors, but GA supply to plants in the dark could not rescue bud outgrowth.

Recent experimental studies on rose support a model in which light intensity stimulates CK biosynthesis in the stem, which in turn stimulates bud outgrowth. As compared to darkness or low light intensity, a higher light intensity rapidly and significantly increased the CK content in the nodal segment bearing the light-stimulated bud (Roman et al., 2016; Corot et al., 2017). This was correlated with rapid up-regulation of genes encoding CK synthesis, transport and signaling, and down-regulation of genes encoding CK degradation (*RhCKX1*) (Roman et al., 2016). This is in line with the known effect of light on CK biosynthesis, metabolism, and transport in other biological processes (Zubo et al., 2008; Boonman et al., 2009; Zdarska et al., 2015; Janeckova et al., 2018). In addition, local exogenous CK application restored the bud outgrowth ability under non-permissive light conditions (Roman et al., 2016; Corot et al., 2017). Interestingly, studies on the shoot apical meristem in tomato and *Arabidopsis* also demonstrated the involvement of CKs in the light-induced activity of the apical meristem (Yoshida et al., 2011; Pfeiffer et al., 2016).

Light-induced bud outgrowth may involve the two CK-related processes controlling bud outgrowth: *BRC1* repression and PIN up-regulation (which would increase auxin canalization capacity) (Dun et al., 2012; Waldie and Leyser, 2018). Indeed, both light and CK exogenous supply down-regulated *BRC1* in the bud and up-regulated *PIN1* expression in the stem for rose decapitated plants (Roman et al., 2016). In line with this, light intensity was also reported to down-regulate *BRC1* in *Arabidopsis* (Su et al., 2011). In addition, both light and CKs supply to rose decapitated plants decreased the expression of the SL signaling-related gene *MAX2* and up-regulated sugar metabolism-related genes (Djennane et al., 2014; Roman et al., 2016), consistent with the well-known role of CKs on the strength of sink organs (Roitsch and Ehness, 2000; Wang et al., 2016b). For rose intact plants, high light intensity also decreased ABA level in the node adjacent to the bud compared to low light intensity, and ABA exogenous supply to the node could antagonize the promoting effect of CK supply under low light intensity (Corot et al., 2017). All these changes underline the complexity of the regulation, and further research is required to understand the basic mechanism behind the light effect on bud outgrowth.

Besides CKs located in bud vicinity, it is likely that root-derived CKs contribute to bud outgrowth stimulation in response to light intensity. Indeed, the concentration in root-derived CK forms (tZ, tZR, tZRMP) increases in stems and buds in these conditions (Roman et al., 2016; Corot et al., 2017); however, this remains to be demonstrated experimentally.

Interaction of Light With the Nutrient-Based Regulatory Network

Strong evidence is given about a main role of competition for carbohydrates, indicated by the source-sink ratio, in bud outgrowth regulation in garden pea and grasses (Kebrom et al., 2012; Kebrom and Mullet, 2015). The carbohydrate source-sink ratio may be affected by the plant light environment: a low R:FR ratio enhances stem growth (Demotes-Mainard et al., 2016), a strong sugar sink, and PAR intensity regulates photosynthesis as well as plant aerial morphogenesis and root growth (Granier and Tardieu, 1999; Chenu et al., 2005; Nagel et al., 2006). As proposed in some tillering models (Luquet et al., 2006; Evers et al., 2010) and by Kebrom (2017) and Bertheloot et al. (2019),

light regulation of source-sink relationships within the plant may modulate sugar availability for buds, leading in turn to reduced auxin-related apical dominance and induction of bud outgrowth. This is supported by studies reporting a negative impact of a low R:FR ratio on the sugar content or on genes related to sugar metabolism and signaling in the bud (Kebrom and Mullet, 2016; Yuan et al., 2018), as well as changes in stem sugar levels in response to light intensity, in ways correlated to bud outgrowth (Lafarge et al., 2010; Furet et al., 2014; Corot et al., 2017). However, the involvement of sugar in the effect of light has not been proved by physiological experiments yet.

Experimental data rather indicate that local sugar availability in the stem or in the bud may not be limiting for bud outgrowth in case of low PAR intensity. In decapitated and defoliated rose plants under white light, preventing light perception by the bud by masking it while leaving the photosynthetic stem under white light maintained the bud inhibited, while applying a photosynthesis inhibitor on the bud did not prevent its outgrowth (Girault et al., 2008; Roman et al., 2016). In addition, local exogenous sugar supply to decapitated shoot stumps under darkness, to the petioles of intact plants under low PAR intensity, or to rose nodal segments cultivated *in vitro* in darkness did not induce bud outgrowth (Henry et al., 2011; Rabot et al., 2012; Roman et al., 2016; Corot et al., 2017). The activity of isolated apical meristems of *Arabidopsis* was also prevented by darkness and was not restored by exogenous sugar supply (Yoshida et al., 2011; Pfeiffer et al., 2016; Li et al., 2017). For both apical meristem and axillary buds under limiting light conditions, CKs may be a limiting factor explaining the inability of sugars to promote bud outgrowth locally. CKs could act by limiting the bud sink strength for sugars (Albacete et al., 2014).

Summary

Experimental studies have revealed an interaction between light and hormonal regulators at the scale of the nodal stem segment and its bud. As illustrated in **Figure 2**, an increase in light intensity stimulates CK level in the stem, which promotes bud outgrowth, while a low R:FR ratio stimulates ABA synthesis in the bud, leading in turn to rapid bud inhibition, a process that could be reinforced by auxin signaling increase in stem. Besides these main pathways, several other endogenous regulators are impacted by light, such as the SL signaling-related genes or sugars, but their exact role has still to be understood. Evidence coming from rose under darkness or low PAR intensity indicates that stem sugars in the vicinity of the bud are not a locally limiting factor of bud outgrowth in these particular light conditions. Literature data on nodal stem segments *in vitro* rather indicate that light intensity and sugars may have a synergetic effect on bud outgrowth (Henry et al., 2011; Rabot et al., 2012; Rabot et al., 2014), as reported for the activity of the apical meristem (Li et al., 2017). This leads to the idea that the light lock should be lifted for a high sugar status of the shoot to stimulate bud outgrowth. Additional studies are also required to understand the role of elevated sugar levels in other plant parts than the stem segment bearing the bud in bud outgrowth. For example, sugars regulate nitrogen uptake by the roots (Lejay et al., 2003; Lejay et al., 2008) or hormone biosynthesis (Sakr et al., 2018), which may also indirectly impact bud outgrowth.

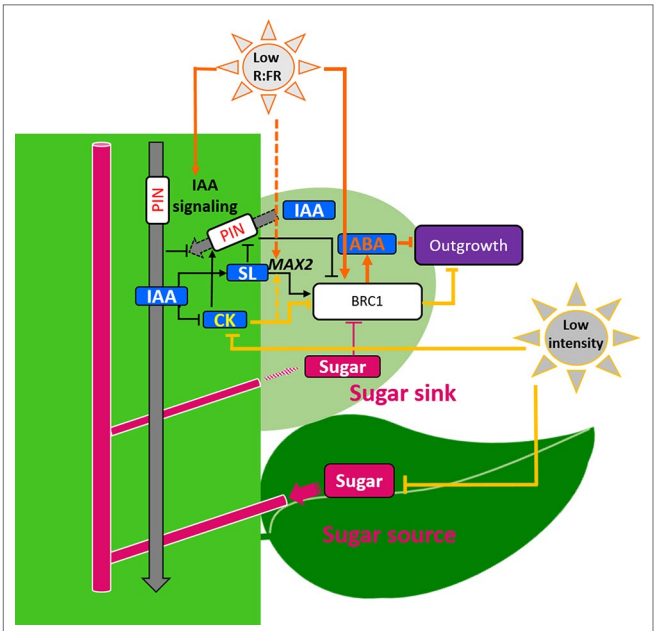

FIGURE 2 | Interaction of light intensity and the R:FR ratio with the endogenous regulators of bud outgrowth. A low R:FR ratio stimulates ABA production in the bud, which inhibits bud outgrowth, a phenomenon that is reinforced later on by auxin signaling stimulation through an unknown mechanism (solid dark orange arrows and text); low R:FR also up-regulates the SL signaling-related gene *MAX2* (dotted dark orange arrows), but the contribution of these changes to bud outgrowth regulation by the R:FR ratio is not known yet. Low light intensity reduces CK contents in the nodal stem by reducing the expression of CK synthesis genes and increasing that of CK degradation genes, which inhibits bud outgrowth (solid light orange arrows and text) and up-regulates *MAX2* but the contribution of this change to bud inhibition by low light intensity is not known yet (dotted light orange arrows and text); low light intensity also decreases the sugar content, but this is not a main limiting factor in the undertaken studies. For color and arrow significations, see also **Figure 1**.

DISCUSSION

Light signaling modulates plant involvement in lateral branching by controlling the release of axillary buds from apical dominance. So far, studies mainly conducted on annuals have provided an almost complete picture of the intricate hormonal regulatory network involved in apical dominance, regardless of environmental factors (**Figure 1**). In particular, great progress has been made since the 2000s with the discovery of SL mutants and of the role of PIN proteins. The development of simulation tools made it easier to investigate complex regulations like those related to the canalization theory or to the SL molecular network, both involving feedbacks (Domagalska and Leyser, 2011). The demonstration that the degree of competition for sugars within the plant regulates bud outgrowth is more recent (Mason et al., 2014) despite first assumptions supported by computer modeling (Luquet et al., 2006; Mathieu et al., 2009). Recent evidences of interplays between sugar and hormones further complicate bud outgrowth regulating network. In addition, the main branching-related hormones display dose-dependent effects on bud outgrowth (Chatfield et al., 2000; Dun et al., 2012; Barbier et al., 2015; Corot et al., 2017) and other compounds may

take a part in this mechanistic complexity, including reactive oxygen species (ROS) (Chen et al., 2016; Signorelli et al., 2018). For instance, H_20_2-dependent bud outgrowth inhibition may be linked to promotion of auxin biosynthesis in the apex which inhibits CK biosynthesis in the stem in tomato (Chen et al., 2016). The presence of different regulators quantitatively regulating bud outgrowth raises the question of their integration within the bud. *BRC1* plays certainly a key role, but some regulations also occur through BRC1-independent pathways (Minakuchi et al., 2010; Braun et al., 2012; Wang et al., 2019). Recently, studies indicate that integration could be done in the regulation of carbon metabolism of the bud (Tarancon et al., 2017; Martin-Fontecha et al., 2018).

Although the major role of light intensity and quality in branching regulation has been known for decades, knowledge about the interaction between light and the endogenous regulators of bud outgrowth emerged only recently. The current knowledge (**Figure 2**) indicates that (i) light intensity stimulates production of CKs (inducer of bud outgrowth) in the nodal stem segment and (ii) a low R:FR ratio stimulates production of ABA (inhibitor of bud outgrowth) in the bud, and this process seems to be later reinforced by an increase in auxin signaling in the stem. This knowledge remains however very fragmented and does not provide a comprehensive understanding of bud outgrowth regulation at the scale of the plant, as discussed below.

First, knowledge is missing about light interaction with other endogenous regulators close to the bud. Indeed, light impacts sugar level and SL signaling (Finlayson et al., 2010; Kebrom and Mullet, 2016; Roman et al., 2016; Corot et al., 2017), which raises the question whether these different regulators act or not in the same pathway. Second, no study has addressed the question of the role of light effects on organs located at distance from buds. Light induces changes in plant growth (Granier and Tardieu, 1999; Nagel et al., 2006; Kebrom, 2017) that may alter the competition for carbohydrates within the plant and the availability of sugar for bud outgrowth. Light modulation of plant growth may also induce changes in hormone metabolism, signaling, and transport, and thereby hormone distribution and quantities. Understanding all these changes is necessary for building a comprehensive picture of light effect on bud outgrowth. Third, light regulation of bud outgrowth pattern at the scale of an axis is unknown. Light was reported to influence the number of outgrowing buds and the time between successive outgrowths (Demotes-Mainard et al., 2013; Corot et al., 2017). Future tasks would be to investigate whether light effect could result from heterogeneous distribution of the different regulators along the axis and from a temporal feedback loop by which outgrowing buds modify the regulator levels in the vicinity of the remainder buds, maintaining them dormant. However, different sensitivities of the buds to their local regulators, due to bud age, light history for example, may obviously complicate bud outgrowth regulation at axis level.

All these elements highlight the complexity of light-mediated bud outgrowth regulation at the plant scale. In recent years, the use of modeling has become prevalent to gain insight into the complex regulation of developmental processes by both endogenous and exogenous processes. These models, combining biological process description with an explicit computational description of the plant biological structure, called functional–structural plant models (FSPM), have proved meaningful to address the complexity of developmental systems as a collection of interacting constituents (at molecular or cellular level for example). FSPMs make it possible to identify and test various hypotheses on the local interaction rules and to compare qualitatively and quantitatively, with the experiments, the result emerging from these simulated interactions at an integrated level. This approach has been successfully used in the last decade to study various aspects of plant development such as flowering and inflorescence architecture development (Prusinkiewicz et al., 2007; Wenden et al., 2009), phyllotaxis (de Reuille et al., 2006; Jonsson et al., 2006; Smith et al., 2006; Refahi et al., 2016), the role of mechanics in morphogenesis (Alim et al., 2012; Boudon et al., 2015; Bozorg et al., 2016). In the study of branching regulation as well, these models have been used to help deciphering the complexity of associated regulation networks and branching processes (Evers and Vos, 2013)—for example, in the analysis of the competition for sugars (Luquet et al., 2006), auxin regulation of bud outgrowth (Prusinkiewicz et al., 2009), auxin transport in mosses (Coudert et al., 2015), and sugar interplay with auxin (Bertheloot et al., 2019). Likewise, approaches combining quantitative experimental observations and computer simulations in FSPMs are thus expected to be instrumental in providing new insights into light interplay with sugar and hormones network in bud outgrowth regulation at the plant scale. In particular, to investigate bud outgrowth regulation with FSPM, carbon/sugar fluxes formalism will have to be coupled to a formalization of hormonal functioning, as well as with a representation of the root compartment.

AUTHOR CONTRIBUTIONS

AS, CG, FB, SD-M, SS, and JB searched for articles, synthetized them, and wrote parts of the review; SS gave the initial impetus for writing a review around light, bud outgrowth, and plant physiology; CG and JB structured the review; JB directed the work.

FUNDING

This review was conducted in the framework of a PhD thesis funded by the Environment and Agronomy department of the French National Institute for Agricultural Research (INRA), the French Region Pays de la Loire, and the program "Objectif Végétal, Research, Education and Innovation in Pays de la Loire" (supported by the Region Pays de la Loire, Angers Loire Métropole, and the European Regional Development Fund).

ACKNOWLEDGMENT

We thank PAIGE team (UMR IRHS) for the administrative work and Annie Buchwalter for reviewing the paper for English usage.

REFERENCES

Agharkar, M., Zhang, H., and Altpeter, F. (2007). Generation and characterization of bahiagrass (Paspalum notatum flugge) over-expressing a gibberellin-catabolizing enzyme. *In Vitro Cell. Dev. Biol.-Animal* 43, S56–S56.

Alam, M. M., Hammer, G. L., van Oosterom, E. J., Cruickshank, A. W., Hunt, C. H., and Jordan, D. R. (2014). A physiological framework to explain genetic and environmental regulation of tillering in sorghum. *New Phytol.* 203 (1), 155–167. doi: 10.1111/nph.12767

Albacete, A., Cantero-Navarro, E., Balibrea, M. E., Grosskinsky, D. K., Gonzalez, M. D., Martinez-Andujar, C., et al. (2014). Hormonal and metabolic regulation of tomato fruit sink activity and yield under salinity. *J. Exp. Bot.* 65 (20), 6081–6095. doi: 10.1093/jxb/eru347

Alim, K., Hamant, O., and Boudaoud, A. (2012). Regulatory role of cell division rules on tissue growth heterogeneity. *Front. Plant Sci.* 3, 174. doi: 10.3389/fpls.2012.00174

Arend, M., Schnitzler, J. P., Ehlting, B., Hansch, R., Lange, T., Rennenberg, H., et al. (2009). Expression of the *Arabidopsis* mutant abi1 gene alters abscisic acid sensitivity, stomatal development, and growth morphology in gray poplars. *Plant Physiol.* 151 (4), 2110–2119. doi: 10.1104/pp.109.144956

Arora, R., Rowland, L. J., and Tanino, K. (2003). Induction and release of bud dormancy in woody perennials: a science comes of age. *Hortscience* 38 (5), 911–921. doi: 10.21273/HORTSCI.38.5.911

Balla, J., Kalousek, P., Reinohl, V., Friml, J., and Prochazka, S. (2011). Competitive canalization of PIN-dependent auxin flow from axillary buds controls pea bud outgrowth. *Plant J.* 65 (4), 571–577. doi: 10.1111/j.1365-313X.2010.04443.x

Balla, J., Medved'ova, Z., Kalousek, P., Matijescukova, N., Friml, J., Reinohl, V., et al. (2016). Auxin flow-mediated competition between axillary buds to restore apical dominance. *Sci. Rep.* 6, 35955. doi: 10.1038/srep35955

Ballare, C. L., Sanchez, R. A., Scopel, A. L., Casal, J. J., and Ghersa, C. M. (1987). Early detection of neighbor plants by phytochrome perception of spectral changes in reflected sunlight. *Plant Cell Environ.* 10 (7), 551–557. doi: 10.1111/j.1365-3040.1987.tb01835.x

Bangerth, F. (1994). Response of cytokinin concentration in the xylem exudate of bean (phaseolus-vulgaris l) plants to decapitation and auxin treatment, and relationship to apical dominance. *Planta* 194 (3), 439–442. doi: 10.1007/BF00197546

Barbier, F., Peron, T., Lecerf, M., Perez-Garcia, M. D., Barriere, Q., Rolcik, J., et al. (2015). Sucrose is an early modulator of the key hormonal mechanisms controlling bud outgrowth in Rosa hybrida. *J. Exp. Bot.* 66 (9), 2569–2582. doi: 10.1093/jxb/erv047

Barbier, F. F., Dun, E. A., Kerr, S. C., Chabikwa, T. G., and Beveridge, C. A. (2019). An update on the signals controlling shoot branching. *Trends Plant Sci.* 24 (3), 220–236. doi: 10.1016/j.tplants.2018.12.001

Barthelemy, D., and Caraglio, Y. (2007). Plant architecture: a dynamic, multilevel and comprehensive approach to plant form, structure and ontogeny. *Ann. Bot.* 99 (3), 375–407. doi: 10.1093/aob/mcl260

Bennett, T., Sieberer, T., Willett, B., Booker, J., Luschnig, C., and Leyser, O. (2006). The *Arabidopsis* MAX pathway controls shoot branching by regulating auxin transport. *Curr. Biol.* 16 (6), 553–563. doi: 10.1016/j.cub.2006.01.058

Bertheloot, J., Barbier, F., Boudon, F., Perez-Garcia, M. D., Péron, T., Citerne, et al. (2019). Sugar availability suppresses the auxin-induced strigolactone pathway to promote bud outgrowth. *New Phytologist.* doi: 10.1111/nph.16201

Beveridge, C. A. (2000). Long-distance signalling and a mutational analysis of branching in pea. *Plant Growth Regul.* 32 (2-3), 193–203. doi: 10.1023/A:1010718020095

Beveridge, C. A. (2006). Axillary bud outgrowth: sending a message. *Curr. Opin. Plant Biol.* 9 (1), 35–40. doi: 10.1016/j.pbi.2005.11.006

Booker, J., Chatfield, S., and Leyser, O. (2003). Auxin acts in xylem-associated or medullary cells to mediate apical dominance. *Plant Cell* 15 (2), 495–507. doi: 10.1105/tpc.007542

Boonman, A., Prinsen, E., Voesenek, L., and Pons, T. L. (2009). Redundant roles of photoreceptors and cytokinins in regulating photosynthetic acclimation to canopy density. *J. Exp. Bot.* 60 (4), 1179–1190. doi: 10.1093/jxb/ern364

Borchert, R., and Honda, H. (1984). Control of development in the bifurcating branch system of tabebuia-rosea—a computer-simulation. *Bot. Gazette* 145 (2), 184–195. doi: 10.1086/337445

Bos, H. J. (1999). *Plant morphology, envrionment, and leaf area growth in wheat and maize*. Wageningen UR: PhD thesis.

Bos, H. J., and Neuteboom, J. H. (1998). Morphological analysis of leaf and tiller number dynamics of wheat (Triticum aestivum L.): responses to temperature and light intensity. *Ann. Bot.* 81 (1), 131–139. doi: 10.1006/anbo.1997.0531

Boudon, F., Chopard, J., Ali, O., Gilles, B., Hamant, O., Boudaoud, A., et al. (2015). A computational framework for 3d mechanical modeling of plant morphogenesis with cellular resolution. *PloS Comput. Biol.* 11 (1) , e1003950. doi: 10.1371/journal.pcbi.1003950

Bouguyon, E., Gojon, A., and Nacry, P. (2012). Nitrate sensing and signaling in plants. *Semin. Cell Dev. Biol.* 23 (6), 648–654. doi: 10.1016/j.semcdb.2012.01.004

Bozorg, B., Krupinski, P., and Jonsson, H. (2016). A continuous growth model for plant tissue. *Physical Biol.* 13 (6), 065,002. doi: 10.1088/1478-3975/13/6/065002

Braun, N., de Saint Germain, A., Pillot, J. P., Boutet-Mercey, S., Dalmais, M., Antoniadi, I., et al. (2012). The pea TCP transcription factor PsBRC1 acts downstream of strigolactones to control shoot branching. *Plant Physiol.* 158 (1), 225–238. doi: 10.1104/pp.111.182725

Buskila, Y., Sela, N., Teper-Bamnolker, P., Tal, I., Shani, E., Weinstain, R., et al. (2016). Stronger sink demand for metabolites supports dominance of the apical bud in etiolated growth. *J. Exp. Bot.* 67 (18), 5495–5508. doi: 10.1093/jxb/erw315

Chabikwa, T. G., Brewer, P. B., and Beveridge, C. (2019). Initial bud outgrowth occurs independent of auxin flow out of buds. *Plant Physiol.* 179 (1), 55–65 doi: 10.1104/pp.18.00519

Chatfield, S. P., Stirnberg, P., Forde, B. G., and Leyser, O. (2000). The hormonal regulation of axillary bud growth in *Arabidopsis*. *Plant J.* 24 (2), 159–169. doi: 10.1046/j.1365-313x.2000.00862.x

Chen, X. J., Xia, X. J., Guo, X., Zhou, Y. H., Shi, K., Zhou, J., et al. (2016). Apoplastic H2O2 plays a critical role in axillary bud outgrowth by altering auxin and cytokinin homeostasis in tomato plants. *New Phytol.* 211 (4), 1266–1278. doi: 10.1111/nph.14015

Chenu, K., Franck, N., Dauzat, J., Barczi, J. F., Rey, H., and Lecoeur, J. (2005). Integrated responses of rosette organogenesis, morphogenesis and architecture to reduced incident light in *Arabidopsis thaliana* results in higher efficiency of light interception. *Funct. Plant Biol.* 32 (12), 1123–1134. doi: 10.1071/FP05091

Choubane, D., Rabot, A., Mortreau, E., Legourrierec, J., Peron, T., Foucher, F., et al. (2012). Photocontrol of bud burst involves gibberellin biosynthesis in Rosa sp. *J. Plant Physiol.* 169 (13), 1271–1280. doi: 10.1016/j.jplph.2012.04.014

Cline, M. G. (1994). The role of hormones in apical dominance—new approaches to an old problem in plant development. *Physiol. Plant.* 90 (1), 230–237. doi: 10.1034/j.1399-3054.1994.900133.x

Cline, M. G. (1996). Exogenous auxin effects on lateral bud outgrowth in decapitated shoots. *Ann. Bot.* 78 (2), 255–266. doi: 10.1006/anbo.1996.0119

Cline, M. G., and Oh, C. (2006). A reappraisal of the role of abscisic acid and its interaction with auxin in apical dominance. *Ann. Bot.* 98 (4), 891–897. doi: 10.1093/aob/mcl173

Cochetel, N., Meteier, E., Merlin, I., Hevin, C., Pouvreau, J. B., Coutos-Thevenot, P., et al. (2018). Potential contribution of strigolactones in regulating scion growth and branching in grafted grapevine in response to nitrogen availability. *J. Exp. Bot.* 69 (16), 4099–4112. doi: 10.1093/jxb/ery206

Corot, A., Roman, H., Douillet, O., Autret, H., Perez-Garcia, M. D., Citerne, S., et al. (2017). Cytokinins and abscisic acid act antagonistically in the regulation of the bud outgrowth pattern by light intensity. *Front. Plant Sci.* 8, 1724. doi: 10.3389/fpls.2017.01724

Coudert, Y., Palubicki, W., Ljung, K., Novak, O., Leyser, O., and Harrison, C. J. (2015). Three ancient hormonal cues co-ordinate shoot branching in a moss. *ELife* 4, e06808. doi: 10.7554/eLife.06808

Crawford, S., Shinohara, N., Sieberer, T., Williamson, L., George, G., Hepworth, J., et al. (2010). Strigolactones enhance competition between shoot branches by dampening auxin transport. *Development* 137 (17), 2905–2913. doi: 10.1242/dev.051987

Davies, A. (1965). Carbohydrate levels and regrowth in perennial rye-grass. *J. Agricultural Sci.* 65, 213. doi: 10.1017/S0021859600083945

de Jong, M., George, G., Ongaro, V., Williamson, L., Willetts, B., Ljung, K., et al. (2014). Auxin and strigolactone signaling are required for modulation of *Arabidopsis* shoot branching by nitrogen supply. *Plant Physiol.* 166 (1), 384–U549. doi: 10.1104/pp.114.242388

de Reuille, P. B., Bohn-Courseau, I., Ljung, K., Morin, H., Carraro, N., Godin, C., et al. (2006). Computer simulations reveal properties of the cell-cell signaling network at the shoot apex in *Arabidopsis*. *Proc. Natl. Acad. Sci. U. S. A.* 103 (5), 1627–1632. doi: 10.1073/pnas.0510130103

de Wit, M., Keuskamp, D. H., Bongers, F. J., Hornitschek, P., Gommers, C. M. M., Reinen, E., et al. (2016). Integration of phytochrome and cryptochrome signals determines plant growth during competition for light. *Curr. Biol.* 26 (24), 3320–3326. doi: 10.1016/j.cub.2016.10.031

Demotes-Mainard, S., Huché-Thélier, L., Morel, P., Boumaza, R., Guérin, V., and Sakr, S. (2013). Temporary water restriction or light intensity limitation promotes branching in rosebush. *Sci. Hortic.* 150, 432–440. doi: 10.1016/j.scienta.2012.12.005

Demotes-Mainard, S., Peron, T., Corot, A., Bertheloot, J., Le Gourrierec, J., Pelleschi-Travier, S., et al. (2016). Plant responses to red and far-red lights, applications in horticulture. *Environ. Exp. Botany* 121, 4–21. doi: 10.1016/j.envexpbot.2015.05.010

Dingkuhn, M., Luquet, D., Clement-Vidal, A., Tambour, L., Kim, H. K., and Song, Y. H. (2007). "*Scale and Complexity in Plant Systems Research: Gene-Plant-Crop Relations*," in *Is plant growth driven by sink regulation?*. Eds. Spiertz, J. H. J., Struik, P. C., and VanLaar, H. H., Springer-Verlag GmbH 157–170. doi: 10.1007/1-4020-5906-X_13

Djennane, S., Hibrand-Saint Oyant, L., Kawamura, K., Lalanne, D., Laffaire, M., Thouroude, T., et al. (2014). Impacts of light and temperature on shoot branching gradient and expression of strigolactone synthesis and signalling genes in rose. *Plant Cell Environ.* 37 (3), 742–757. doi: 10.1111/pce.12191

Domagalska, M. A., and Leyser, O. (2011). Signal integration in the control of shoot branching. *Nat. Rev. Mol. Cell Biol.* 12 (4), 211–221. doi: 10.1038/nrm3088

Drummond, R. S. M., Janssen, B. J., Luo, Z. W., Oplaat, C., Ledger, S. E., Wohlers, M. W., et al. (2015). Environmental control of branching in petunia. *Plant Physiol.* 168 (2), 735–73+. doi: 10.1104/pp.15.00486

Drummond, R. S. M., Martinez-Sanchez, N. M., Janssen, B. J., Templeton, K. R., Simons, J. L., Quinn, B. D., et al. (2009). Petunia hybrida carotenoid cleavage dioxygenase7 is involved in the production of negative and positive branching signals in petunia. *Plant Physiol.* 151 (4), 1867–1877. doi: 10.1104/pp.109.146720

Dun, E. A., Brewer, P. B., and Beveridge, C. A. (2009a). Strigolactones: discovery of the elusive shoot branching hormone. *Trends Plant Sci.* 14 (7), 364–372. doi: 10.1016/j.tplants.2009.04.003

Dun, E. A., de Saint Germain, A., Rameau, C., and Beveridge, C. A. (2012). Antagonistic action of strigolactone and cytokinin in bud outgrowth control. *Plant Physiol.* 158 (1), 487–498. doi: 10.1104/pp.111.186783

Dun, E. A., Hanan, J., and Beveridge, C. A. (2009b). Computational modeling and molecular physiology experiments reveal new insights into shoot branching in pea. *Plant Cell* 21 (11), 3459–3472. doi: 10.1105/tpc.109.069013

Eliasson, L. (1975). Effect of indoleacetic-acid on abscisic-acid level in stem tissue. *Physiol. Plant.* 34 (2), 117–120. doi: 10.1111/j.1399-3054.1975.tb03803.x

Everatbourbouloux, A. (1982). Transport and metabolism of labeled abscisic-acid in broad-bean plants (VICIA-FABA L). *Physiol. Plant.* 54 (4), 431–439. doi: 10.1111/j.1399-3054.1982.tb00704.x

Everatbourbouloux, A., and Charnay, D. (1982). Endogenous abscisic-acid levels in stems and axillary buds of intact or decapitated broad-bean plants (VICIA-FABA L). *Physiol. Plant.* 54 (4), 440–445. doi: 10.1111/j.1399-3054.1982.tb00705.x

Evers, J. B., and Vos, J. (2013). Modeling branching in cereals. *Front. Plant Sci.* 4, 399. doi: 10.3389/fpls.2013.00399

Evers, J. B., Vos, J., Andrieu, B., and Struik, P. C. (2006). Cessation of tillering in spring wheat in relation to light interception and red: Far-red ratio. *Ann. Bot.* 97 (4), 649–658. doi: 10.1093/aob/mcl020

Evers, J. B., Vos, J., Chelle, M., Andrieu, B., Fournier, C., and Struik, P. C. (2007). Simulating the effects of localized red: far-red ratio on tillering in spring wheat (Triticum aestivum) using a three-dimensional virtual plant model. *New Phytol.* 176 (2), 325–336. doi: 10.1111/j.1469-8137.2007.02168.x

Evers, J. B., Vos, J., Yin, X., Romero, P., van der Putten, P. E. L., and Struik, P. C. (2010). Simulation of wheat growth and development based on organ-level photosynthesis and assimilate allocation. *J. Exp. Bot.* 61 (8), 2203–2216. doi: 10.1093/jxb/erq025

Fichtner, F., Barbier, F., Feil, R., Watanabe, M., Annunziata, M. G., Chabikwa, T. G., et al. (2017). Trehalose 6-phosphate is involved in triggering axillary bud outgrowth in garden pea (Pisum sativum L.). *Plant J.* 92 (4), 611–623. doi: 10.1111/tpj.13705

Figueroa, C. M., and Lunn, J. E. (2016). A Tale of Two Sugars: Trehalose 6-Phosphate and Sucrose(1 OPEN). *Plant Physiol.* 172 (1), 7–27. doi: 10.1104/pp.16.00417

Finlayson, S. A., Krishnareddy, S. R., Kebrom, T. H., and Casal, J. J. (2010). Phytochrome regulation of branching in *Arabidopsis*. *Plant Physiol.* 152 (4), 1914–1927. doi: 10.1104/pp.109.148833

Foo, E., Buillier, E., Goussot, M., Foucher, F., Rameau, C., and Beveridge, C. A. (2005). The branching gene RAMOSUS1 mediates interactions among two novel signals and auxin in pea. *Plant Cell* 17 (2), 464–474. doi: 10.1105/tpc.104.026716

Foo, E., Morris, S. E., Parmenter, K., Young, N., Wang, H. T., Jones, A., et al. (2007). Feedback regulation of xylem cytokinin content is conserved in pea and *Arabidopsis*. *Plant Physiol.* 143 (3), 1418–1428. doi: 10.1104/pp.106.093708

Franklin, K. A. (2008). Shade avoidance. *New Phytol.* 179 (4), 930–944. doi: 10.1111/j.1469-8137.2008.02507.x

Funayama, K., Kojima, S., Tabuchi-Kobayashi, M., Sawa, Y., Nakayama, Y., Hayakawa, T., et al. (2013). Cytosolic glutamine synthetase1;2 is responsible for the primary assimilation of ammonium in rice roots. *Plant Cell Physiol.* 54 (6), 934–943. doi: 10.1093/pcp/pct046

Furet, P. M., Lothier, J., Demotes-Mainard, S., Travier, S., Henry, C., Guerin, V., et al. (2014). Light and nitrogen nutrition regulate apical control in Rosa hybrida L. *J. Plant Physiol.* 171 (5), 7–13. doi: 10.1016/j.jplph.2013.10.008

Gangappa, S. N., and Botto, J. F. (2016). The multifaceted roles of HY5 in plant growth and development. *Mol. Plant* 9 (10), 1353–1365. doi: 10.1016/j.molp.2016.07.002

Gautier, H., Varlet-Grancher, C., and Hazard, L. (1999). Tillering responses to the light environment and to defoliation in populations of perennial ryegrass (Lolium perenne L.) selected for contrasting leaf length. *Ann. Bot.* 83 (4), 423–429. doi: 10.1006/anbo.1998.0840

Girault, T., Abidi, F., Sigogne, M., Pelleschi-Travier, S., Boumaza, R., Sakr, S., et al. (2010). Sugars are under light control during bud burst in Rosa sp. *Plant Cell Environ.* 33, 1339–1350. doi: 10.1111/j.1365-3040.2010.02152.x

Girault, T., Bergougnoux, V., Combes, D., Viemont, J., and Leduc, N. (2008). Light controls shoot meristem organogenic activity and leaf primordia growth during bud burst in Rosa sp. *Plant Cell Environ.* 31, 1534–1544. doi: 10.1111/j.1365-3040.2008.01856.x

Gocal, G. F. W., Pharis, R. P., Yeung, E. C., and Pearce, D. (1991). Changes after decapitation in concentrations of indole-3-acetic-acid and abscisic-acid in the larger axillary bud of Phaseolus vulgaris L. cv tender green. *Plant Physiol.* 95 (2), 344–350. doi: 10.1104/pp.95.2.344

Gomez-Roldan, V., Fermas, S., Brewer, P. B., Puech-Pages, V., Dun, E. A., Pillot, J. P., et al. (2008). Strigolactone inhibition of shoot branching. *Nature* 455 (7210), 189–U122. doi: 10.1038/nature07271

Gonzalez-Grandio, E., Pajoro, A., Franco-Zorrilla, J. M., Tarancon, C., Immink, R. G. H., and Cubas, P. (2017). Abscisic acid signaling is controlled by a BRANCHED1/HD-ZIP I cascade in *Arabidopsis* axillary buds. *Proc. Natl. Acad. Sci. U. S. A.* 114 (2), E245–E254. doi: 10.1073/pnas.1613199114

Gonzalez-Grandio, E., Poza-Carrion, C., Sorzano, C. O. S., and Cubas, P. (2013). BRANCHED1 Promotes axillary bud dormancy in response to shade in *Arabidopsis*. *Plant Cell* 25 (3), 834–850. doi: 10.1105/tpc.112.108480

Granier, C., and Tardieu, F. (1999). Leaf expansion and cell division are affected by reducing absorbed light before but not after the decline in cell division rate in the sunflower leaf. *Plant Cell Environ.* 22 (11), 1365–1376. doi: 10.1046/j.1365-3040.1999.00497.x

Guan, J. C., Koch, K. E., Suzuki, M., Wu, S., Latshaw, S., Petruff, T., et al. (2012). Diverse roles of strigolactone signaling in maize architecture and the uncoupling of a branching-specific subnetwork. *Plant Physiol.* 160 (3), 1303–1317. doi: 10.1104/pp.112.204503

Ha, C. V., Leyva-Gonzalez, M. A., Osakabe, Y., Tran, U. T., Nishiyama, R., Watanabe, Y., et al. (2014). Positive regulatory role of strigolactone in plant responses to drought and salt stress. *Proc. Natl. Acad. Sci. U. S. A.* 111 (2), 851–856. doi: 10.1073/pnas.1322135111

Hartmann, A., Senning, M., Hedden, P., Sonnewald, U., and Sonnewald, S. (2011). Reactivation of meristem activity and sprout growth in potato tubers require both cytokinin and gibberellin. *Plant Physiol.* 155 (2), 776–796. doi: 10.1104/pp.110.168252

Hayward, A., Stirnberg, P., Beveridge, C., and Leyser, O. (2009). Interactions between auxin and strigolactone in shoot branching control. *Plant Physiol.* 151 (1), 400–412. doi: 10.1104/pp.109.137646

Henry, C., Rabot, A., Laloi, M., Mortreau, E., Sigogne, M., Leduc, N., et al. (2011). Regulation of RhSUC2, a sucrose transporter, is correlated with the light

control of bud burst in Rosa sp. *Plant Cell Environ.* 34 (10), 1776–1789. doi: 10.1111/j.1365-3040.2011.02374.x

Heuret, P., BarthTlTmy, D., Nicolini, E., and Atger, C. (2000). Analysis of height growth factors and trunk development in the sessile oak, Quercus petraea (Matt.) Liebl. (Fagaceae) in dynamic sylviculture. *Can. J. Bot.-Revue Can. Bot.* 78 (3), 361–373. doi: 10.1139/b00-012

Heyer, A. G., Raap, M., Schroeer, B., Marty, B., and Willmitzer, L. (2004). Cell wall invertase expression at the apical meristem alters floral, architectural, and reproductive traits in *Arabidopsis thaliana*. *Plant J.* 39 (2), 161–169. doi: 10.1111/j.1365-313X.2004.02124.x

Holalu, S. V., and Finlayson, S. A. (2017). The ratio of red light to far red light alters *Arabidopsis* axillary bud growth and abscisic acid signalling before stem auxin changes. *J. Exp. Bot.* 68 (5), 943–952. doi: 10.1093/jxb/erw479

Iglesias, M. J., Sellaro, R., Zurbriggen, M. D., and Casal, J. J. (2018). Multiple links between shade avoidance and auxin networks. *J. Exp. Bot.* 69 (2), 213–228. doi: 10.1093/jxb/erx295

Ito, S., Yamagami, D., and Asami, T. (2018). Effects of gibberellin and strigolactone on rice tiller bud growth. *J. Pesticide Sci.* 43 (3-4), 220–223. doi: 10.1584/jpestics.D18-013

Ito, S., Yamagami, D., Umehara, M., Hanada, A., Yoshida, S., Sasaki, Y., et al. (2017). Regulation of strigolactone biosynthesis by gibberellin signaling. *Plant Physiol.* 174 (2), 1250–1259. doi: 10.1104/pp.17.00301

Janeckova, H., Husickova, A., Ferretti, U., Prcina, M., Pilarova, E., Plackova, L., et al. (2018). The interplay between cytokinins and light during senescence in detached *Arabidopsis* leaves. *Plant Cell Environ.* 41 (8), 1870–1885. doi: 10.1111/pce.13329

Jia, K. P., Luo, Q., He, S. B., Lu, X. D., and Yang, H. Q. (2014). Strigolactone-regulated hypocotyl elongation is dependent on cryptochrome and phytochrome signaling pathways in *Arabidopsis*. *Mol. Plant* 7 (3), 528–540. doi: 10.1093/mp/sst093

Jonsson, H., Heisler, M. G., Shapiro, B. E., Meyerowitz, E. M., and Mjolsness, E. (2006). An auxin-driven polarized transport model for phyllotaxis. *Proc. Natl. Acad. Sci. U. S. A.* 103 (5), 1633–1638. doi: 10.1073/pnas.0509839103

Kameoka, H., Dun, E. A., Lopez-Obando, M., Brewer, P. B., de Saint Germain, A., Rameau, C., et al. (2016). Phloem transport of the receptor DWARF14 protein is required for full function of strigolactones. *Plant Physiol.* 172 (3), 1844–1852. doi: 10.1104/pp.16.01212

Kebrom, T. H. (2017). A growing stem inhibits bud outgrowth—the overlooked theory of apical dominance. *Front. Plant Sci.* 8, 1874. doi: 10.3389/fpls.2017.01874

Kebrom, T. H., Brutnell, T. P., and Finlayson, S. A. (2010). Suppression of sorghum axillary bud outgrowth by shade, phyB and defoliation signalling pathways. *Plant Cell Environ.* 33 (1), 48–58. doi: 10.1111/j.1365-3040.2009.02050.x

Kebrom, T. H., Burson, B. L., and Finlayson, S. A. (2006). Phytochrome B represses teosinte branched1 expression and induces sorghum axillary bud outgrowth in response to light signals. *Plant Physiol.* 140 (3), 1109–1117. doi: 10.1104/pp.105.074856

Kebrom, T. H., Chandler, P. M., Swain, S. M., King, R. W., Richards, R. A., and Spielmeyer, W. (2012). Inhibition of tiller bud outgrowth in the tin mutant of wheat is associated with precocious internode development. *Plant Physiol.* 160 (1), 308–318. doi: 10.1104/pp.112.197954

Kebrom, T. H., and Mullet, J. E. (2015). Photosynthetic leaf area modulates tiller bud outgrowth in sorghum. *Plant Cell Environ.* 38 (8), 1471–1478. doi: 10.1111/pce.12500

Kebrom, T. H., and Mullet, J. E. (2016). Transcriptome profiling of tiller buds provides new insights into PhyB regulation of tillering and indeterminate growth in sorghum. *Plant Physiol.* 170 (4), 2232–2250. doi: 10.1104/pp.16.00014

Kieffer, M., Fuller, M. P., and Jellings, A. J. (1998). Explaining curd and spear geometry in broccoli, cauliflower and 'romanesco': quantitative variation in activity of primary meristems. *Planta* 206 (1), 34–43. doi: 10.1007/s004250050371

Kim, H. K., Luquet, D., van Oosterom, E., Dingkuhn, M., and Hammer, G. (2010a). Regulation of tillering in sorghum: genotypic effects. *Ann. Bot.* 106 (1), 69–78. doi: 10.1093/aob/mcq080

Kim, H. K., van Oosterom, E., Dingkuhn, M., Luquet, D., and Hammer, G. (2010b). Regulation of tillering in sorghum: environmental effects. *Ann. Bot.* 106 (1), 57–67. doi: 10.1093/aob/mcq079

Knox, J. P., and Wareing, P. F. (1984). Apical dominance in Phaseolus vulgaris l—the possible roles of abscisic and indole-3-acetic-acid. *J. Exp. Bot.* 35 (151), 239–244. doi: 10.1093/jxb/35.2.239

Kohlen, W., Charnikhova, T., Liu, Q., Bours, R., Domagalska, M. A., Beguerie, S., et al. (2011). Strigolactones are transported through the xylem and play a key role in shoot architectural response to phosphate deficiency in nonarbuscular mycorrhizal host *Arabidopsis*. *Plant Physiol.* 155 (2), 974–987. doi: 10.1104/pp.110.164640

Kudo, T., Kiba, T., and Sakakibara, H. (2010). Metabolism and long-distance translocation of cytokinins. *J. Integr. Plant Biol.* 52 (1), 53–60. doi: 10.1111/j.1744-7909.2010.00898.x

Lacointe, A. (2000). Carbon allocation among tree organs: a review of basic processes and representation in functional-structural tree models. *Ann. Forest Sci.* 57 (5-6), 521–533. doi: 10.1051/forest:2000139

Lacombe, B., and Achard, P. (2016). Long-distance transport of phytohormones through the plant vascular system. *Curr. Opin. Plant Biol.* 34, 1–8. doi: 10.1016/j.pbi.2016.06.007

Lafarge, T., Seassau, C., Martin, M., Bueno, C., Clement-Vidal, A., Schreck, E., et al. (2010). Regulation and recovery of sink strength in rice plants grown under changes in light intensity. *Funct. Plant Biol.* 37 (5), 413–428. doi: 10.1071/FP09137

Lang, G. A., Early, J. D., Martin, G. C., and Darnell, R. L. (1987). Endodormancy, paradormancy, and ecodormancy—physiological terminology and classification for dormancy research. *Hortscience* 22 (3), 371–377.

Lastdrager, J., Hanson, J., and Smeekens, S. (2014). Sugar signals and the control of plant growth and development. *J. Exp. Bot.* 65 (3), 799–807. doi: 10.1093/jxb/ert474

Lau, O. S., and Deng, X. W. (2012). The photomorphogenic repressors COP1 and DET1: 20 years later. *Trends Plant Sci.* 17 (10), 584–593. doi: 10.1016/j.tplants.2012.05.004

Lazar, G., and Goodman, H. M. (2006). MAX1, a regulator of the flavonoid pathway, controls vegetative axillary bud outgrowth in *Arabidopsis*. *Proc. Natl. Acad. Sci. U. S. A.* 103 (2), 472–476. doi: 10.1073/pnas.0509463102

Le Moigne, M.-A., Guérin, V., Furet, P. M., Billard, V., Lebrec, A., Spichal, L., et al. (2018). Asparagine and sugars are both required to sustain secondary axis elongation after bud outgrowth in *Rosa hybrida*. *J. Plant Physiol.* 222, 17–27. doi: 10.1016/j.jplph.2017.12.013

Leduc, N., Roman, H., Barbier, F., Péron, T., Huché-Thélier, L., Lothier, J., et al. (2014). Light signaling in bud outgrowth and branching in plants. *Plants* 3, 223–250. doi: 10.3390/plants3020223

Lee, H. J., Park, Y. J., Ha, J. H., Baldwin, I. T., and Park, C. M. (2017). Multiple routes of light signaling during root photomorphogenesis. *Trends Plant Sci.* 22 (9), 803–812. doi: 10.1016/j.tplants.2017.06.009

Lejay, L., Gansel, X., Cerezo, M., Tillard, P., Muller, C., Krapp, A., et al. (2003). Regulation of root ion transporters by photosynthesis: functional importance and relation with hexokinase. *Plant Cell* 15 (9), 2218–2232. doi: 10.1105/tpc.013516

Lejay, L., Wirth, J., Pervent, M., Cross, J. M. F., Tillard, P., and Gojon, A. (2008). Oxidative pentose phosphate pathway-dependent sugar sensing as a mechanism for regulation of root ion transporters by photosynthesis. *Plant Physiol.* 146 (4), 2036–2053. doi: 10.1104/pp.107.114710

Letort, V., Cournede, P. H., Mathieu, A., de Reffye, P., and Constant, T. (2008). Parametric identification of a functional-structural tree growth model and application to beech trees (Fagus sylvatica). *Funct. Plant Biol.* 35 (9-10), 951–963. doi: 10.1071/FP08065

Li-Marchetti, C., Le Bras, C., Relion, D., Citerne, S., Huche-Thelier, L., Sakr, S., et al. (2015). Genotypic differences in architectural and physiological responses to water restriction in rose bush. *Front. Plant Sci.* 6, 355. doi: 10.3389/fpls.2015.00355

Li, C. J., and Bangerth, F. (1999). Autoinhibition of indoleacetic acid transport in the shoots of two-branched pea (Pisum sativum) plants and its relationship to correlative dominance. *Physiol. Plant.* 106 (4), 415–420. doi: 10.1034/j.1399-3054.1999.106409.x

Li, L., and Sheen, J. (2016). Dynamic and diverse sugar signaling. *Curr. Opin. Plant Biol.* 33, 116–125. doi: 10.1016/j.pbi.2016.06.018

Li, M. J., Wei, Q. P., Xiao, Y. S., and Peng, F. T. (2018). The effect of auxin and strigolactone on ATP/ADP isopentenyltransferase expression and the regulation of apical dominance in peach. *Plant Cell Reports* 37 (12), 1693–1705. doi: 10.1007/s00299-018-2343-0

Li, X. J., Cai, W. G., Liu, Y. L., Li, H., Fu, L. W., Liu, Z. Y., et al. (2017). Differential TOR activation and cell proliferation in *Arabidopsis* root and shoot apexes. *Proc. Natl. Acad. Sci. U. S. A.* 114 (10), 2765–2770. doi: 10.1073/pnas.1618782114

Ligerot, Y., de Saint Germain, A., Waldie, T., Troadec, C., Citerne, S., Kadakia, N., et al. (2017). The pea branching RMS2 gene encodes the PsAFB4/5 auxin receptor and is involved in an auxin-strigolactone regulation loop. *PloS Genet.* 13 (12), e1007089. doi: 10.1371/journal.pgen.1007089

Lin, H., Wang, R. X., Qian, Q., Yan, M. X., Meng, X. B., Fu, Z. M., et al. (2009). DWARF27, an iron-containing protein required for the biosynthesis of strigolactones, regulates rice tiller bud outgrowth. *Plant Cell* 21 (5), 1512–1525. doi: 10.1105/tpc.109.065987

Liu, Y., Wang, Q. S., Ding, Y. F., Li, G. H., Xu, J. X., and Wang, S. H. (2011). Effects of external ABA, GA(3) and NAA on the tiller bud outgrowth of rice is related to changes in endogenous hormones. *Plant Growth Regul.* 65 (2), 247–254. doi: 10.1007/s10725-011-9594-x

Ljung, K., Bhalerao, R. P., and Sandberg, G. (2001). Sites and homeostatic control of auxin biosynthesis in *Arabidopsis* during vegetative growth. *Plant J.* 28 (4), 465–474. doi: 10.1046/j.1365-313X.2001.01173.x

Lo, S. F., Yang, S. Y., Chen, K. T., Hsing, Y. L., Zeevaart, J. A. D., Chen, L. J., et al. (2008). A novel class of gibberellin 2-oxidases control semidwarfism, tillering, and root development in rice. *Plant Cell* 20 (10), 2603–2618. doi: 10.1105/tpc.108.060913

Luquet, D., Dingkuhn, M., Kim, H., Tambour, L., and Clement-Vidal, A. (2006). EcoMeristem, a model of morphogenesis and competition among sinks in rice. 1. Concept, validation and sensitivity analysis. *Funct. Plant Biol.* 33 (4), 309–323. doi: 10.1071/FP05266

Mader, J. C., Emery, R. J. N., and Turnbull, C. G. N. (2003). Spatial and temporal changes in multiple hormone groups during lateral bud release shortly following apex decapitation of chickpea (Cicer arietinum) seedlings. *Physiol. Plant.* 119 (2), 295–308. doi: 10.1034/j.1399-3054.2003.00179.x

Martin-Fontecha, E. S., Tarancon, C., and Cubas, P. (2018). To grow or not to grow, a power-saving program induced in dormant buds. *Curr. Opin. Plant Biol.* 41, 102–109. doi: 10.1016/j.pbi.2017.10.001

Martinez-Bello, L., Moritz, T., and Lopez-Diaz, I. (2015). Silencing C-19-GA 2-oxidases induces parthenocarpic development and inhibits lateral branching in tomato plants. *J. Exp. Bot.* 66 (19), 5897–5910. doi: 10.1093/jxb/erv300

Mason, M. G., Ross, J. J., Babst, B. A., Wienclaw, B. N., and Beveridge, C. A. (2014). Sugar demand, not auxin, is the initial regulator of apical dominance. *Proc. Natl. Acad. Sci. U. S. A.* 111 (16), 6092–6097. doi: 10.1073/pnas.1322045111

Mathieu, A., Cournede, P. H., Letort, V., Barthelemy, D., and de Reffye, P. (2009). A dynamic model of plant growth with interactions between development and functional mechanisms to study plant structural plasticity related to trophic competition. *Ann. Bot.* 103 (8), 1173–1186. doi: 10.1093/aob/mcp054

Mauriat, M., Sandberg, L. G., and Moritz, T. (2011). Proper gibberellin localization in vascular tissue is required to control auxin-dependent leaf development and bud outgrowth in hybrid aspen. *Plant J.* 67 (5), 805–816. doi: 10.1111/j.1365-313X.2011.04635.x

Mawphlang, O. I. L., and Kharshiing, E. V. (2017). Photoreceptor mediated plant growth responses: implications for photoreceptor engineering toward improved performance in crops. *Front. Plant Sci.* 8, 1181. doi: 10.3389/fpls.2017.01181

Minakuchi, K., Kameoka, H., Yasuno, N., Umehara, M., Luo, L., Kobayashi, K., et al. (2010). FINE CULM1 (FC1) works downstream of strigolactones to inhibit the outgrowth of axillary buds in rice. *Plant Cell Physiol.* 51 (7), 1127–1135. doi: 10.1093/pcp/pcq083

Mitchell, K. J. (1953). Influence of light and temperature on the growth of ryegrass (Lolium spp.). II. The control of lateral bud development. *Physiol. Plant.* 6 (3), 425–443. doi: 10.1111/j.1399-3054.1953.tb08401.x

Moore, B., Zhou, L., Rolland, F., Hall, Q., Cheng, W. H., Liu, Y. X., et al. (2003). Role of the *Arabidopsis* glucose sensor HXK1 in nutrient, light, and hormonal signaling. *Science* 300 (5617), 332–336. doi: 10.1126/science.1080585

Morris, D. A. (1977). Transport of exogenous auxin in 2-branched dwarf pea-seedlings (Pisum sativum L.)—some implications for polarity and apical dominance. *Planta* 136 (1), 91–96. doi: 10.1007/BF00387930

Mostofa, M. G., Li, W. Q., Nguyen, K. H., Fujita, M., and Tran, L. S. P. (2018). Strigolactones in plant adaptation to abiotic stresses: an emerging avenue of plant research. *Plant Cell Environ.* 41 (10), 2227–2243. doi: 10.1111/pce.13364

Mueller, D., and Leyser, O. (2011). Auxin, cytokinin and the control of shoot branching. *Ann. Bot.* 107 (7), 1203–1212. doi: 10.1093/aob/mcr069

Muller, D., Waldie, T., Miyawaki, K., To, J. P. C., Melnyk, C. W., Kieber, J. J., et al. (2015). Cytokinin is required for escape but not release from auxin mediated apical dominance. *Plant J.* 82 (5), 874–886. doi: 10.1111/tpj.12862

Nagel, K. A., Schurr, U., and Walter, A. (2006). Dynamics of root growth stimulation in Nicotiana tabacum in increasing light intensity. *Plant Cell Environ.* 29 (10), 1936–1945. doi: 10.1111/j.1365-3040.2006.01569.x

Ni, J., Zhao, M. L., Chen, M. S., Pan, B. Z., Tao, Y. B., and Xu, Z. F. (2017). Comparative transcriptome analysis of axillary buds in response to the shoot branching regulators gibberellin A3 and 6-benzyladenine in Jatropha curcas. *Sci. Rep.* 7, 11417. doi: 10.1038/s41598-017-11588-0

Nordstrom, A., Tarkowski, P., Tarkowska, D., Norbaek, R., Astot, C., Dolezal, K., et al. (2004). Auxin regulation of cytokinin biosynthesis in *Arabidopsis thaliana*: a factor of potential importance for auxin-cytokinin-regulated development. *Proc. Natl. Acad. Sci. U. S. A.* 101 (21), 8039–8044. doi: 10.1073/pnas.0402504101

Ohashi, M., Ishiyama, K., Kojima, S., Kojima, M., Sakakibara, H., Yamaya, T., et al. (2017). Lack of Cytosolic glutamine synthetase1;2 activity reduces nitrogen-dependent biosynthesis of cytokinin required for axillary bud outgrowth in rice seedlings. *Plant Cell Physiol.* 58 (4), 679–690. doi: 10.1093/pcp/pcx022

Ohashi, M., Ishiyama, K., Kojima, S., Konishi, N., Sasaki, K., Miyao, M., et al. (2018). Outgrowth of rice tillers requires availability of glutamine in the basal portions of shoots. *Rice* 11, 31. doi: 10.1186/s12284-018-0225-2

Olszewski, N., Sun, T. P., and Gubler, F. (2002). Gibberellin signaling: biosynthesis, catabolism, and response pathways. *Plant Cell* 14, S61–S80. doi: 10.1105/tpc.010476

Ongaro, V., and Leyser, O. (2008). Hormonal control of shoot branching. *J. Exp. Bot.* 59 (1), 67–74. doi: 10.1093/jxb/erm134

Otori, K., Tamoi, M., Tanabe, N., and Shigeoka, S. (2017). Enhancements in sucrose biosynthesis capacity affect shoot branching in *Arabidopsis*. *Biosci. Biotechnol. Biochem.* 81 (8), 1470–1477. doi: 10.1080/09168451.2017.1321954

Palubicki, W., Horel, K., Longay, S., Runions, A., Lane, B., Mech, R., et al. (2009). Self-organizing tree models for image synthesis. *ACM Trans. Graphics* 28 (3), 58. doi: 10.1145/1531326.1531364

Perttunen, J., Sievanen, R., and Nikinmaa, E. (1998). LIGNUM: a model combining the structure and the functioning of trees. *Ecol. Model.* 108 (1-3), 189–198. doi: 10.1016/S0304-3800(98)00028-3

Perttunen, J., Sievanen, R., Nikinmaa, E., Salminen, H., Saarenmaa, H., and Vakeva, J. (1996). LIGNUM: A tree model based on simple structural units. *Ann. Bot.* 77 (1), 87–98. doi: 10.1006/anbo.1996.0011

Pfeiffer, A., Janocha, D., Dong, Y. H., Medzihradszky, A., Schone, S., Daum, G., et al. (2016). Integration of light and metabolic signals for stem cell activation at the shoot apical meristem. *ELife* 5, e17023. doi: 10.7554/eLife.17023

Pierik, R., and Testerink, C. (2014). The art of being flexible: how to escape from shade, salt, and drought. *Plant Physiol.* 166 (1), 5–22. doi: 10.1104/pp.114.239160

Prasad, T. K., Li, X., Abdelrahman, A. M., Hosokawa, Z., Cloud, N. P., Lamotte, C. E., et al. (1993). Does auxin play a role in the release of apical dominance by shoot inversion in ipomoea nil. *Ann. Bot.* 71 (3), 223–229. doi: 10.1006/anbo.1993.1028

Prusinkiewicz, P., Crawford, S., Smith, R. S., Ljung, K., Bennett, T., Ongaro, V., et al. (2009). Control of bud activation by an auxin transport switch. *Proc. Natl. Acad. Sci. U. S. A.* 106 (41), 17431–17436. doi: 10.1073/pnas.0906696106

Prusinkiewicz, P., Erasmus, Y., Lane, B., Harder, L. D., and Coen, E. (2007). Evolution and development of inflorescence architectures. *Science* 316 (5830), 1452–1456. doi: 10.1126/science.1140429

Quail, P. H. (2002). Phytochrome photosensory signalling networks. *Nat. Rev. Mol. Cell Biol.* 3 (2), 85–93. doi: 10.1038/nrm728

Rabot, A., Henry, C., Ben Baaziz, K., Mortreau, E., Azri, W., Lothier, J., et al. (2012). Insight into the role of sugars in bud burst under light in the rose. *Plant Cell Physiol.* 53 (6), 1068–1082. doi: 10.1093/pcp/pcs051

Rabot, A., Portemer, V., Peron, T., Mortreau, E., Leduc, N., Hamama, L., et al. (2014). Interplay of sugar, light and gibberellins in expression of rosa hybrida vacuolar invertase 1 regulation. *Plant Cell Physiol.* 55 (10), 1734–1748. doi: 10.1093/pcp/pcu106

Ragni, L., Nieminen, K., Pacheco-Villalobos, D., Sibout, R., Schwechheimer, C., and Hardtke, C. S. (2011). Mobile gibberellin directly stimulates *arabidopsis* hypocotyl xylem expansion. *Plant Cell* 23 (4), 1322–1336. doi: 10.1105/tpc.111.084020

Rameau, C., Bertheloot, J., Leduc, N., Andrieu, B., Foucher, F., and Sakr, S. (2015). Multiple pathways regulate shoot branching. *Front. Plant Sci.* 5 , 741. doi: 10.3389/fpls.2014.00741

Reddy, S. K., and Finlayson, S. A. (2014). Phytochrome B promotes branching in *Arabidopsis* by suppressing auxin signaling. *Plant Physiol.* 164 (3), 1542–1550. doi: 10.1104/pp.113.234021

Reddy, S. K., Holalu, S. V., Casal, J. J., and Finlayson, S. A. (2013). Abscisic acid regulates axillary bud outgrowth responses to the ratio of red to far-red light. *Plant Physiol.* 163 (2), 1047–1058. doi: 10.1104/pp.113.221895

Refahi, Y., Brunoud, G., Farcot, E., Jean-Marie, A., Pulkkinen, M., Vernoux, T., et al. (2016). A stochastic multicellular model identifies biological watermarks from disorders in self-organized patterns of phyllotaxis. *ELife* 5, e14093. doi: 10.7554/eLife.14093

Rinne, P., Tuominen, H., and Sundberg, B. (1993). Growth-patterns and endogenous indole-3-acetic-acid concentrations in current-year coppice shoots and seedlings of 2 betula species. *Physiol. Plant.* 88 (3), 403–412. doi: 10.1111/j.1399-3054.1993.tb01352.x

Rohde, A., Van Montagu, M., and Boerjan, W. (1999). The abscisic acid-insensitive 3 (ABI3) gene is expressed during vegetative quiescence processes in *Arabidopsis*. *Plant Cell Environ.* 22 (3), 261–270. doi: 10.1046/j.1365-3040.1999.00428.x

Roitsch, T., and Ehness, R. (2000). Regulation of source/sink relations by cytokinins. *Plant Growth Regul.* 32 (2-3), 359–367. doi: 10.1023/A:1010781500705

Rolland, F., Baena-Gonzalez, E., and Sheen, J. (2006). Annual Review of Plant Biology in Sugar sensing and signaling in plants: conserved and novel mechanisms. *Annu. Rev. Plant Biol.* 675–709. doi: 10.1146/annurev.arplant.57.032905.105441

Roman, H., Girault, T., Barbier, F., Peron, T., Brouard, N., Pencik, A., et al. (2016). Cytokinins are initial targets of light in the control of bud outgrowth(1 open). *Plant Physiol.* 172 (1), 489–509. doi: 10.1104/pp.16.00530

Romano, C. P., Hein, M. B., and Klee, H. J. (1991). Inactivation of auxin in tobacco transformed with the indoleacetic-acid lysine synthetase gene of pseudomonas-savastanoi. *Genes Dev.* 5 (3), 438–446. doi: 10.1101/gad.5.3.438

Runions, A., Lane, B., and Prusinkiewicz, P. (2007). "Modeling trees with a spacecolonization algorithm," in Proceedings of the 2007 Eurographics Workshop on Natural Phenomena, eds D. Ebert and S. Merillou (Geneva: The Eurographics Association), 63–70.

Sachs, T. (1981). The control of the patterned differentiation of vascular tissues. *Adv. Bot. Res. Incorp. Adv. Plant Pathol.* 9, 151–262. doi: 10.1016/S0065-2296(08)60351-1

Sachs, T., and Thimann, K. V. (1967). The role of auxins and cytokinins in the release of buds from dominance. *Am. J. Bot.* 54 (1), 136–144. doi: 10.1002/j.1537-2197.1967.tb06901.x

Sakr, S., Wang, M., Dedaldechamp, F., Perez-Garcia, M. D., Oge, L., Hamama, L., et al. (2018). The sugar-signaling hub: overview of regulators and interaction with the hormonal and metabolic network. *Int. J. Mol. Sci.* 19 (9), 2506. doi: 10.3390/ijms19092506

Sakuraba, Y., and Yanagisawa, S. (2018). Light signalling-induced regulation of nutrient acquisition and utilisation in plants. *Semin. Cell Dev. Biol.* 83, 123–132. doi: 10.1016/j.semcdb.2017.12.014

Sauer, M., Balla, J., Luschnig, C., Wisniewska, J., Reinohl, V., Friml, J., et al. (2006). Canalization of auxin flow by Aux/IAA-ARF-dependent feedback regulation of PIN polarity. *Genes Dev.* 20 (20), 2902–2911. doi: 10.1101/gad.390806

Shen, H., Luong, P., and Huq, E. (2007). The F-Box protein MAX2 functions as a positive regulator of photomorphogenesis in *Arabidopsis* (1 C W OA). *Plant Physiol.* 145 (4), 1471–1483. doi: 10.1104/pp.107.107227

Shen, H., Zhu, L., Bu, Q. Y., and Huq, E. (2012). MAX2 affects multiple hormones to promote photomorphogenesis. *Mol. Plant* 5 (3), 750–762. doi: 10.1093/mp/sss029

Sherson, S. M., Alford, H. L., Forbes, S. M., Wallace, G., and Smith, S. M. (2003). Roles of cell-wall invertases and monosaccharide transporters in the growth and development of *Arabidopsis*. *J. Exp. Bot.* 54 (382), 525–531. doi: 10.1093/jxb/erg055

Shimizu-Sato, S., Tanaka, M., and Mori, H. (2009). Auxin-cytokinin interactions in the control of shoot branching. *Plant Mol. Biol.* 69 (4), 429–435. doi: 10.1007/s11103-008-9416-3

Shinohara, N., Taylor, C., and Leyser, O. (2013). Strigolactone can promote or inhibit shoot branching by triggering rapid depletion of the auxin efflux protein PIN1 from the plasma membrane. *PloS Biol.* 11 (1), e1001474. doi: 10.1371/journal.pbio.1001474

Signorelli, S., Agudelo-Romero, P., Meitha, K., Foyer, C. H., and Considine, M. J. (2018). Roles for light, energy, and oxygen in the fate of quiescent axillary buds. *Plant Physiol.* 176 (2), 1171–1181. doi: 10.1104/pp.17.01479

Silverstone, A. L., Mak, P. Y. A., Martinez, E. C., and Sun, T. P. (1997). The new RGA locus encodes a negative regulator of gibberellin response in *Arabidopsis thaliana*. *Genetics* 146 (3), 1087–1099.

Simon, N. M. L., Sawkins, E., and Dodd, A. N. (2018). Involvement of the SnRK1 subunit KIN10 in sucrose-induced hypocotyl elongation. *Plant Signaling Behav.* 13 (6), e1457913. doi: 10.1080/15592324.2018.1457913

Smith, R. S., Guyomarc'h, S., Mandel, T., Reinhardt, D., Kuhlemeier, C., and Prusinkiewicz, P. (2006). A plausible model of phyllotaxis. *Proc. Natl. Acad. Sci. U. S. A.* 103 (5), 1301–1306. doi: 10.1073/pnas.0510457103

Snowden, K. C., Simkin, A. J., Janssen, B. J., Templeton, K. R., Loucas, H. M., Simons, J. L., et al. (2005). The decreased apical dominance 1/petunia hybrida carotenoid cleavage dioxygenase8 gene affects branch production and plays a role in leaf senescence, root growth, and flower development. *Plant Cell* 17 (3), 746–759. doi: 10.1105/tpc.104.027714

Su, H. W., Abernathy, S. D., White, R. H., and Finlayson, S. A. (2011). Photosynthetic photon flux density and phytochrome B interact to regulate branching in *Arabidopsis*. *Plant Cell Environ.* 34 (11), 1986–1998. doi: 10.1111/j.1365-3040.2011.02393.x

Takei, K., Takahashi, T., Sugiyama, T., Yamaya, T., and Sakakibara, H. (2002). Multiple routes communicating nitrogen availability from roots to shoots: a signal transduction pathway mediated by cytokinin. *J. Exp. Bot.* 53 (370), 971–977. doi: 10.1093/jexbot/53.370.971

Tan, M., Li, G. F., Liu, X. J., Cheng, F., Ma, J. J., Zhao, C. P., et al. (2018). Exogenous application of GA(3) inactively regulates axillary bud outgrowth by influencing of branching-inhibitors and bud-regulating hormones in apple (Malus domestica Borkh.). *Mol. Genet. Genomics* 293 (6), 1547–1563. doi: 10.1007/s00438-018-1481-y

Tanaka, M., Takei, K., Kojima, M., Sakakibara, H., and Mori, H. (2006). Auxin controls local cytokinin biosynthesis in the nodal stem in apical dominance. *Plant J.* 45 (6), 1028–1036. doi: 10.1111/j.1365-313X.2006.02656.x

Tarancon, C., Gonzalez-Grando, E., Oliveros, J. C., Nicolas, M., and Cubas, P. (2017). A conserved carbon starvation response underlies bud dormancy in woody and herbaceous species. *Front. Plant Sci.* 8 (788). doi: 10.3389/fpls.2017.00788

Teichmann, T., and Muhr, M. (2015). Shaping plant architecture. *Front. Plant Sci.* 6, 233. doi: 10.3389/fpls.2015.00233

Thimann, K. V., and Skoog, F. (1933). Studies on the growth hormone of plants. III. The inhibitory action of the growth substance on bud development. *Proc. Natl. Acad. Sci. U. S. A.* 19, 714–716. doi: 10.1073/pnas.19.7.714

Thimann, K. V., and Skoog, F. (1934). On the inhibition of bud development and other functions of growth substance in *Vicia Faba*. *Proc. R. Soc. Lond. B.* 114, 317–339. doi: 10.1098/rspb.1934.0010

Tsai, A. Y. L., and Gazzarrini, S. (2014). Trehalose-6-phosphate and SnRK1 kinases in plant development and signaling: the emerging picture. *Front. Plant Sci.* 5, 119. doi: 10.3389/fpls.2014.00119

Tucker, D. J., and Mansfield, T. A. (1972). Effects of light quality on apical dominance in xanthium-strumarium and associated changes in endogenous levels of abscisic acid and cytokinins. *Planta* 102 (2), 140–14+. doi: 10.1007/BF00384868

Turnbull, C. G. N., Raymond, M. A. A., Dodd, I. C., and Morris, S. E. (1997). Rapid increases in cytokinin concentration in lateral buds of chickpea (Cicer arietinum L) during release of apical dominance. *Planta* 202 (3), 271–276. doi: 10.1007/s004250050128

Umehara, M., Hanada, A., Yoshida, S., Akiyama, K., Arite, T., Takeda-Kamiya, N., et al. (2008). Inhibition of shoot branching by new terpenoid plant hormones. *Nature* 455 (7210), 195–U129. doi: 10.1038/nature07272

Urriola, J., and Rathore, K. S. (2015). Overexpression of a glutamine synthetase gene affects growth and development in sorghum. *Transgenic Res.* 24 (3), 397–407. doi: 10.1007/s11248-014-9852-6

Vishwakarma, K., Upadhyay, N., Kumar, N., Yadav, G., Singh, J., Mishra, R. K., et al. (2017). Abscisic acid signaling and abiotic stress tolerance in plants: a review on current knowledge and future prospects. *Front. Plant Sci.* 8, 161. doi: 10.3389/fpls.2017.00161

Waldie, T., and Leyser, O. (2018). Cytokinin targets auxin transport to promote shoot branching. *Plant Physiol.* 177 (2), 803–818. doi: 10.1104/pp.17.01691

Wang, D. L., Gao, Z. Z., Du, P. Y., Xiao, W., Tan, Q. P., Chen, X. D., et al. (2016a). Expression of ABA metabolism-related genes suggests similarities and differences between seed dormancy and bud dormancy of peach (Prunus persica). *Front. Plant Sci.* 6, 1248. doi: 10.3389/fpls.2015.01248

Wang, H. W., Chen, W. X., Eggert, K., Charnikhova, T., Bouwmeester, H., Schweizer, P., et al. (2018). Abscisic acid influences tillering by modulation of strigolactones in barley. *J. Exp. Bot.* 69 (16), 3883–3898. doi: 10.1093/jxb/ery200

Wang, M., Le Moigne, M. A., Bertheloot, J., Crespel, L., Perez-Garcia, M. D., Oge, L., et al. (2019). BRANCHED1: a key hub of shoot branching. *Front. Plant Sci.* 10, 76. doi: 10.3389/fpls.2019.00076

Wang, W., Hao, Q., Tian, F., Li, Q., and Wang, W. (2016b). Cytokinin-regulated sucrose metabolism in stay-green wheat phenotype. *PloS One* 11 (8), e0161351. doi: 10.1371/journal.pone.0161351

Warren-Wilson, J. (1972). "*Crop processes in Controlled Environments*.," in *Control of crop processes* (London: Academic Press), 7–30.

Wenden, B., Dun, E. A., Hanan, J., Andrieu, B., Weller, J. L., Beveridge, C. A., et al. (2009). Computational analysis of flowering in pea (Pisum sativum). *New Phytol.* 184 (1), 153–167. doi: 10.1111/j.1469-8137.2009.02952.x

White, J. C., and Mansfield, T. A. (1977). Correlative inhibition of lateral bud growth in Pisum sativum l and Phaseolus vulgaris l—studies of role of abscisic acid. *Ann. Bot.* 41 (176), 1163–1170. doi: 10.1093/oxfordjournals.aob.a085406

Wickson, M., and Thimann, K. (1958). The antagonism of auxin and kinetin in apical dominance. *Physiol. Plant.* 11, 62–74. doi: 10.1111/j.1399-3054.1958.tb08426.x

Wingler, A. (2018). Transitioning to the next phase: the role of sugar signaling throughout the plant life cycle. *Plant Physiol.* 176 (2), 1075–1084. doi: 10.1104/pp.17.01229

Wisniewska, J., Xu, J., Seifertova, D., Brewer, P. B., Ruzicka, K., Blilou, I., et al. (2006). Polar PIN localization directs auxin flow in plants. *Science* 312 (5775), 883–883. doi: 10.1126/science.1121356

Xi, L., Wen, C., Fang, S., Chen, X. L., Nie, J., Chu, J. F., et al. (2015). Impacts of strigolactone on shoot branching under phosphate starvation in chrysanthemum (Dendranthema grandiflorum cv. Jinba). *Front. Plant Sci.* 6 (694). doi: 10.3389/fpls.2015.00694

Xu, J. X., Zha, M. R., Li, Y., Ding, Y. F., Chen, L., Ding, C. Q., et al. (2015). The interaction between nitrogen availability and auxin, cytokinin, and strigolactone in the control of shoot branching in rice (Oryza sativa L.). *Plant Cell Reports* 34 (9), 1647–1662. doi: 10.1007/s00299-015-1815-8

Yamaguchi, S. (2008). Gibberellin metabolism and its regulation. *Annu. Rev. Plant Biol.* 59, 225–251. doi: 10.1146/annurev.arplant.59.032607.092804

Yao, C., and Finlayson, S. A. (2015). Abscisic acid is a general negative regulator of *arabidopsis* axillary bud growth. *Plant Physiol.* 169 (1), 611–626. doi: 10.1104/pp.15.00682

Yoshida, S., Mandel, T., and Kuhlemeier, C. (2011). Stem cell activation by light guides plant organogenesis. *Genes Dev.* 25 (13), 1439–1450. doi: 10.1101/gad.631211

Young, N. F., Ferguson, B. J., Antoniadi, I., Bennett, M. H., Beveridge, C. A., and Turnbull, C. G. N. (2014). Conditional auxin response and differential cytokinin profiles in shoot branching mutants. *Plant Physiol.* 165 (4), 1723–1736. doi: 10.1104/pp.114.239996

Yuan, C. Q., Ahmad, S., Cheng, T. R., Wang, J., Pan, H. T., Zhao, L. J., et al. (2018). Red to far-red light ratio modulates hormonal and genetic control of axillary bud outgrowth in chrysanthemum (Dendranthema grandiflorum "Jinba'). *Int. J. Mol. Sci.* 19 (6), 1590. doi: 10.3390/ijms19061590

Zdarska, M., Dobisova, T., Gelova, Z., Pernisova, M., Dabravolski, S., and Hejatko, J. (2015). Illuminating light, cytokinin, and ethylene signalling crosstalk in plant development. *J. Exp. Bot.* 66 (16), 4913–4931. doi: 10.1093/jxb/erv261

Zimmermann, M. H. (1978). Hydraulic architecture of some diffuse-porous trees. *Can. J. Bot.* 56, 2286–2295. doi: 10.1139/b78-274

Zou, J. H., Zhang, S. Y., Zhang, W. P., Li, G., Chen, Z. X., Zhai, W. X., et al. (2006). The rice HIGH-TILLERING DWARF1 encoding an ortholog of *Arabidopsis* MAX3 is required for negative regulation of the outgrowth of axillary buds. *Plant J.* 48 (5), 687–696. doi: 10.1111/j.1365-313X.2006.02916.x

Zubo, Y. O., Yamburenko, M. V., Selivankina, S. Y., Shakirova, F. M., Avalbaev, A. M., Kudryakova, N. V., et al. (2008). Cytokinin stimulates chloroplast transcription in detached barley leaves. *Plant Physiol.* 148 (2), 1082–1093. doi: 10.1104/pp.108.122275

Conflict of Interest: The authors declare that the research was conducted in the absence of any personal, professional, or financial relationships that could potentially be construed as a conflict of interest.

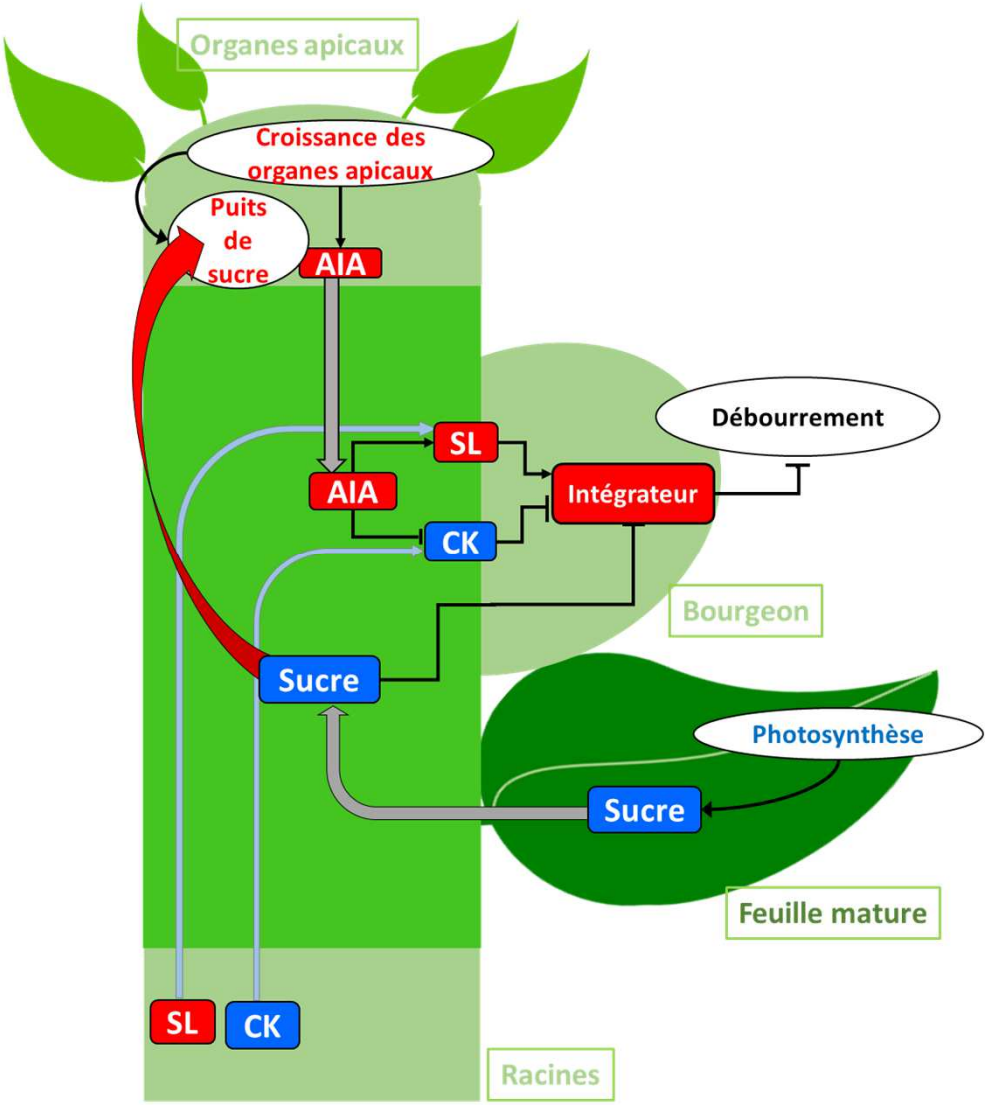

Figure 1 : Régulation du débourrement d'un bourgeon axillaire soumis à la dominance apicale.
Les organes en croissance de l'axe primaire inhibent le débourrement d'un bourgeon axillaire via (i) la voie hormonale, (ii) la compétition pour les sucres.

(i) L'auxine (AIA) apicale est produite par les organes en croissance de l'axe primaire. Elle est transportée de façon basipète le long de la tige et ne rentre pas dans le bourgeon. Son effet sur le débourrement passe par deux hormones relais : les strigolactones (SL) et les cytokinines (CK) qui inhibent et stimulent le débourrement, respectivement. Les SL et les CK sont aussi synthétisées dans les racines et transportées par le flux xylémien vers les parties aériennes

(ii) Les sucres du nœud stimulent le débourrement du bourgeon. Ils sont issus de la photosynthèse. Une partie des sucres est déviée par les organes en croissance de l'axe primaire.

Les signaux des SL, des CK et des sucres sont intégrés localement au niveau du nœud et du bourgeon. Un des intégrateurs est le gène BRC1, inhibiteur du débourrement. Les phénomènes physiologiques ou acteurs régulateurs du débourrement sont en bleu lorsqu'ils stimulent le débourrement, et en rouge lorsqu'ils l'inhibent. Les doubles flèches correspondent à des flux. Les flèches uniques à des signaux ou de l'information.

BILAN DE L'ETAT DE L'ART

La review Schneider et al. (2019) insérée ci-dessus fait état des connaissances liées aux régulations endogènes du débourrement, passant par les voies hormonales et les nutriments, et de celles liées aux effets de la qualité et de l'intensité lumineuse sur ces voies de régulations. Dans cette thèse nous nous concentrons sur la compréhension des effets de *l'intensité* lumineuse sur le débourrement des bourgeons axillaires. A partir de la review (Schneider et al., 2019), nous résumons ci-après la complexité des mécanismes physiologiques impliqués dans la régulation endogène du débourrement et dans sa réponse à l'intensité lumineuse, et faisons ressortir le caractère fragmenté de ces connaissances.

Nous avons vu dans l'état de l'art que le débourrement d'un bourgeon axillaire est soumis à des régulations endogènes liées à la croissance d'autres organes de la plante (aussi appelée inhibitions corrélatives). Parmi celles-ci, le phénomène de dominance apicale, exercé par les organes apicaux en croissance de l'axe primaire, a été mis en évidence par Skoog et Thimann dans les années 30 (Skoog and Thimann, 1934; Thimann and Skoog, 1933) grâce à des expériences de décapitations de pois. Chez les plantes dont l'apex avait été excisé, les bourgeons axillaires débourraient alors qu'ils restaient dormants chez les plantes intactes. La dominance apicale repose sur deux voies de régulation du débourrement des bourgeons axillaires qui coexistent et interagissent (Figure 1). Historiquement, la première voie démontrée est la voie hormonale. L'auxine, hormone inhibitrice du débourrement des bourgeons axillaires, est synthétisée dans les organes apicaux de l'axe primaire et est transportée de façon basipète le long de l'axe primaire. L'auxine apicale ne pouvant pas entrer dans les bourgeons axillaires (Prasad et al., 1993 ; Booker et al., 2003), les rôles de deux hormones relais de l'auxine (théorie du second messager) ont été démontrés. Les cytokinines (CK) et les strigolactones (SL) stimulent et inhibent, respectivement, le débourrement. Leurs teneurs dans le nœud portant le bourgeon sont, respectivement, négativement (CK) et positivement (SL) régulées par l'auxine (Dun et al., 2009).

La deuxième voie d'action démontrée dans le cadre de la dominance apicale, et détaillée dans l'état de l'art, est celle des sucres. Les rôles signal et trophique des sucres dans la stimulation du débourrement ont été mis en évidence chez plusieurs espèces par des expériences *in vitro* et *in planta* (Henry et al., 2011; Rabot et al., 2012; Barbier et al., 2015) et leur implication dans la levée de la dominance apicale a été démontrée chez le pois (Mason et al., 2014). Après décapitation de l'axe primaire, l'augmentation rapide des teneurs en sucres au voisinage du bourgeon axillaire est le premier signal de levée de la dominance apicale. Ainsi, le débourrement d'un bourgeon en position basale le long de la tige principale est déclenché avant même que la concentration en auxine, dont la vitesse de progression est plus faible que les sucres, soit modifiée dans le nœud. Le rôle de la compétition pour les sucres entre l'axe primaire et les bourgeons axillaires est de plus confirmé par des travaux sur des mutants *tin* de blé présentant une plus forte élongation des entrenœuds de l'axe primaire, accompagnée d'une réduction de la ramification (Kebrom et al., 2012).

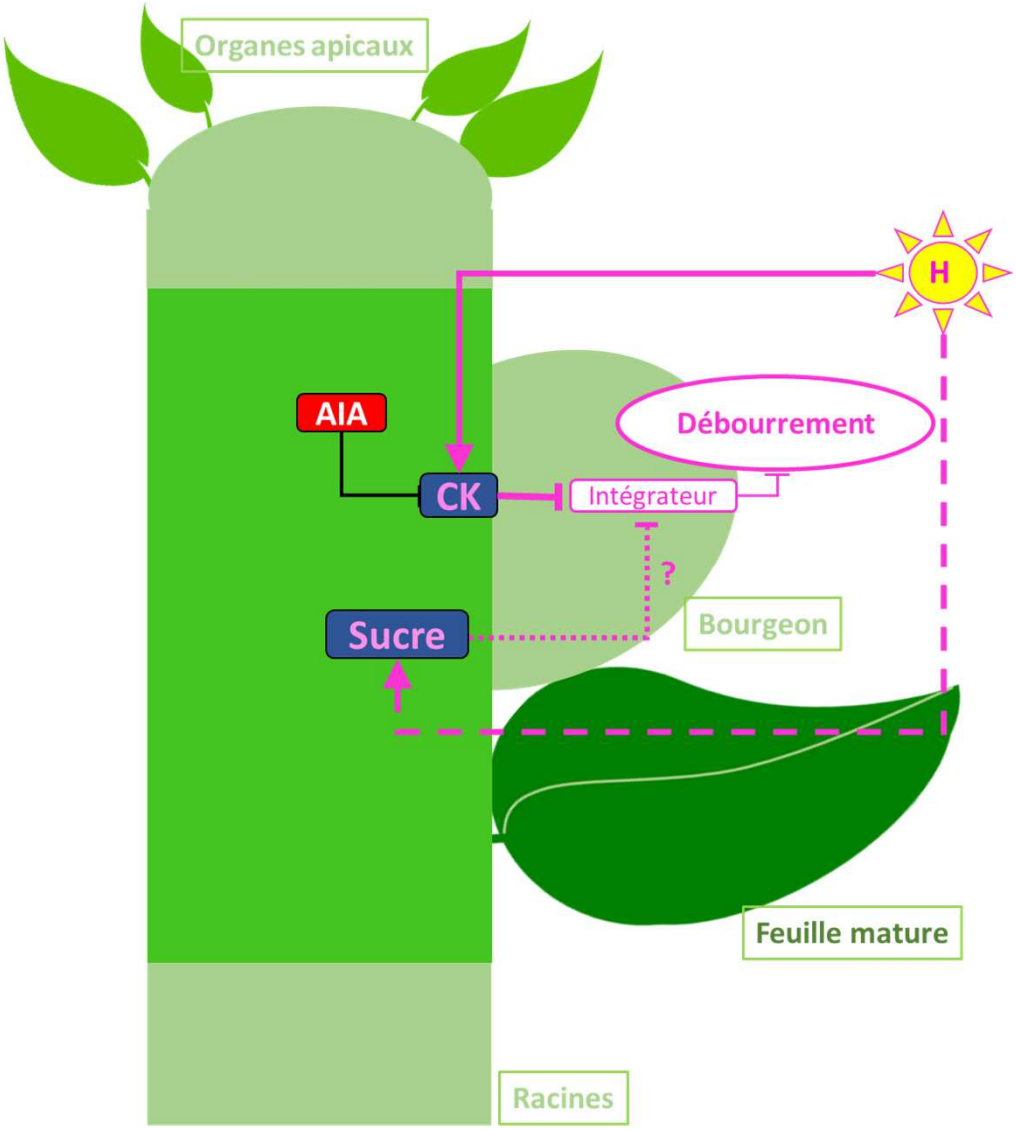

Figure 2 : Effets de l'intensité lumineuse sur la régulation du débourrement.
Comparé à des conditions lumineuses défavorables (faible intensité ou obscurité), une forte intensité lumineuse pendant la phase de ramification (H) stimule le débourrement des bourgeons axillaires. Les mécanismes démontrés à ce jour sont liés aux cytokinines (CK) (flèches pleines). H mène à l'augmentation des teneurs en CK au voisinage du bourgeon en stimulant leur synthèse et diminuant leur dégradation (Roman et al., 2016; Corot et al., 2017). Une augmentation des teneurs en sucres dans la tige comparé à une faible intensité lumineuse a aussi été observée, mais le lien entre cette augmentation des teneurs en sucres et la stimulation du débourrement par l'intensité lumineuse n'est pas établi (flèches pointillés).

Ces deux voies d'action de la dominance apicale, l'une passant par les hormones, l'autre par les sucres, ne sont pas indépendantes l'une de l'autre et sont liées de façon intriquée. En effet, comme détaillé précédemment dans l'état de l'art, la voie des hormones et celles des sucres sont connues pour interagir localement (au niveau du nœud portant le bourgeon). Les effets des sucres sur la signalisation des SL, la biosynthèse des CK dans le nœud, la production d'auxine par le bourgeon et l'expression du gène BRC1 ont été observés chez des nœuds isolés de rosiers cultivés *in vitro* (Barbier et al., 2015). L'interaction des sucres avec la signalisation des SL a été particulièrement mise en avant grâce à une approche de modélisation (Bertheloot et al., 2020).

Outre les interactions entre les hormones et les sucres au niveau du bourgeon et du nœud qui le porte, d'autres organes, comme les racines, sont impliquées dans la synthèse et l'export de CK et de SL vers les parties aériennes (Sakakibara et al., 2006 ; Gomez-Roldan et al., 2008). La régulation endogène du débourrement du bourgeon tient donc aux interactions entre plusieurs acteurs hormonaux et les sucres, et à l'implication de plusieurs organes de la plante, comme la zone apicale de l'axe primaire et les racines.

La compréhension des mécanismes impliqués dans la réponse du débourrement à l'intensité lumineuse reste partielle (Figure 2). Jusqu'à présent, seul le rôle des cytokinines (CK) dans la réponse du débourrement à l'intensité lumineuse appliquée *pendant* la période de ramification a été clairement démontré et identifié. Ainsi, sous une faible intensité lumineuse (ou obscurité), la synthèse et les teneurs en CK sont réduites au voisinage du bourgeon, et des apports exogènes de CK à des plantes sous faible intensité lumineuse permettent de reproduire le phénotype de débourrement observé dans des conditions lumineuses favorables (lumière ou forte intensité lumineuse) (Roman et al., 2016 ; Corot et al., 2017).

Bien que les sucres soient connus pour stimuler le débourrement des bourgeons, leur rôle dans la réponse du débourrement à l'intensité lumineuse n'est pour l'instant pas confirmé. En effet, malgré la diminution des teneurs en sucres au voisinage des bourgeons axillaires sous une faible intensité lumineuse (ou obscurité) appliquée *pendant* la période de ramification, des apports exogènes de sucres *in planta* ne permettent pas de lever l'inhibition du débourrement et de reproduire le phénotype observé sous forte intensité lumineuse (Roman et al., 2016 ; Corot et al., 2017). Ce résultat expérimental pourrait cependant s'expliquer par la déviation des sucres apportés *in planta* vers les organes apicaux en croissance, au détriment des bourgeons axillaires (Corot et al., 2017).

A ce jour, les connaissances liées à la réponse du débourrement à l'intensité lumineuse concernent surtout les effets d'une modification de l'intensité lumineuse *pendant* la phase de ramification (Figure 3). Peu d'études concernent les effets de variations de l'intensité lumineuse au cours de la culture sur la ramification. Un phénotype particulier a été observé chez le rosier buisson (Demotes-Mainard et al., 2013) : suite à une restriction temporaire de l'intensité lumineuse pendant la croissance de l'axe primaire, et au rétablissement d'une forte intensité lumineuse pendant la phase de ramification, la fréquence de débourrement des bourgeons axillaires chez ces plantes est augmentée, comparée à celle

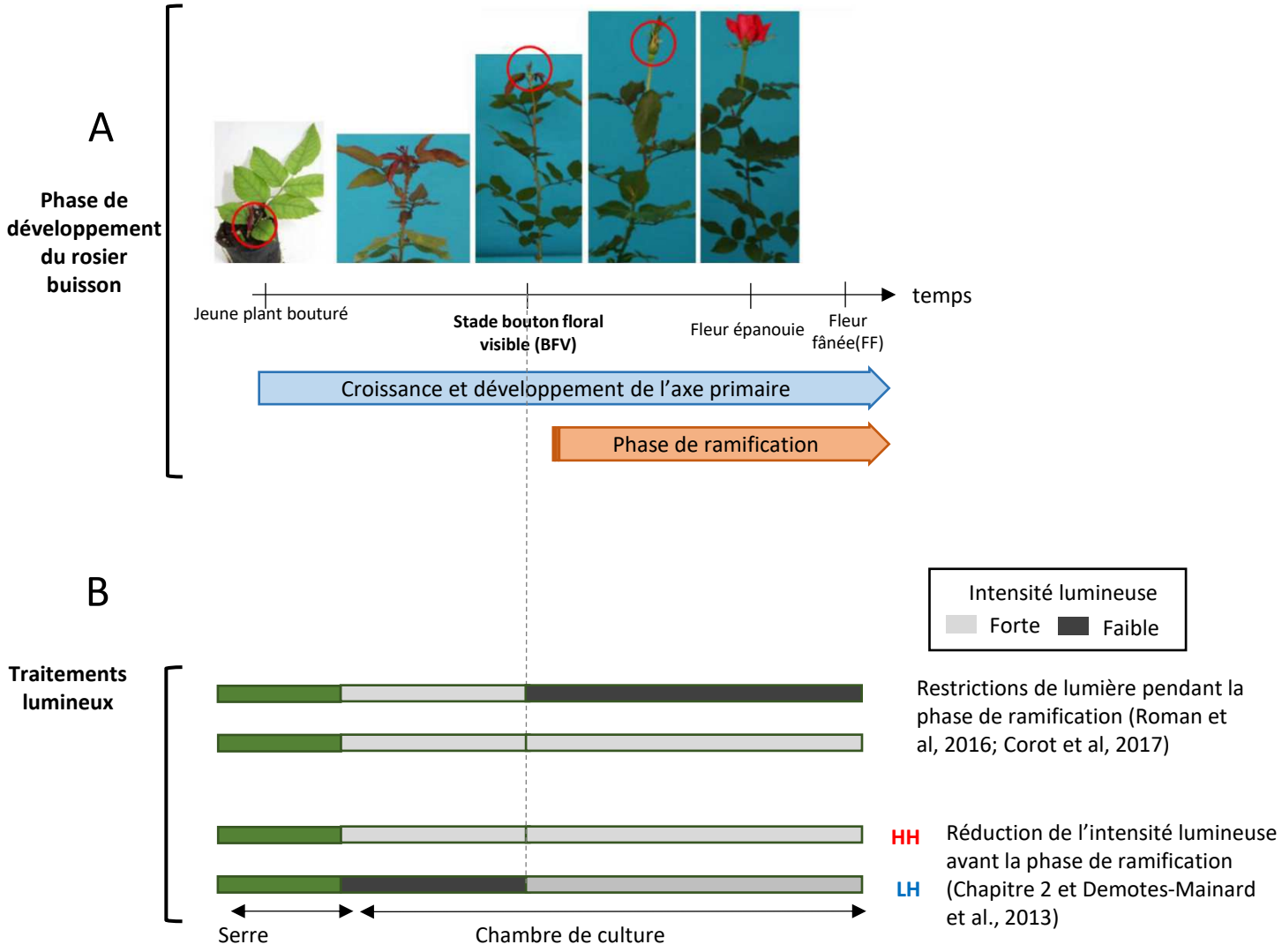

Figure 3 : Développement de R. hybrida "Radrazz" et périodes d'exposition aux traitements d'intensité lumineuse dans la littérature. (A) A partir d'une bouture, l'axe primaire se développe avec l'apparition successive de ses phytomères et suivie de leur élongation. Les phytomères sont constitués d'un entre-nœud, d'une feuille et d'un bourgeon à l'aisselle de la feuille. Les phytomères inférieurs ne présentent pas de feuille entière. Après l'apparition de tous les phytomères, le bouton floral et le pédoncule apparaissent (stade : bouton floral visible, BFV). Après le stade BFV, l'élongation des phytomères se poursuit, en même temps que le développement de la fleur (stades de la fleur ouverte et de la fleur fanée), le débourrement des bourgeons axillaires et la croissance des ramifications qui en sont issues. (B) Les traitements lumineux utilisés dans les publications de Roman et al. (2016) et Corot et al. (2017) correspondent à une réduction de l'intensité lumineuse (obscurité ou faible intensité, respectivement) pendant la phase de ramification comparé à un traitement avec une intensité lumineuse forte pendant toute la croissance de la plante. Dans la publication de Demotes-Mainard et al. (2013) et dans le chapitre 3, l'intensité lumineuse est modulée avant BFV et donc avant la phase de ramification (traitement LH versus traitement HH).

observée chez les plantes n'ayant pas subi de restriction temporaire de lumière. Les mécanismes sous-jacents à cette réponse du débourrement ne sont pour l'instant pas connus et le rôle des CK dans la réponse du débourrement à l'intensité lumineuse n'est pas démontré dans ce cas. L'hypothèse d'un rôle du sucre peut être émise car des variations de l'intensité lumineuse similaires exercées sur le riz mènent à une augmentation des teneurs en sucres dans la plante avant la reprise du débourrement (Lafarge et al., 2010).

Finalement, les rôles des sucres et des hormones dans l'obtention des phénotypes de débourrement observés en réponse à des modulations de l'intensité lumineuse avant ou pendant les phases de ramifications restent lacunaires.

NB : les références sont listées dans la review.

PROBLEMATIQUE ET PLAN DE LA THESE

Face à ces lacunes dans la compréhension des mécanismes impliqués dans la régulation du débourrement par l'intensité lumineuse, l'objectif de la thèse est **de mieux comprendre l'implication et le rôle des sucres, en relation avec les autres acteurs régulateurs, dans la réponse du débourrement à des modulations de l'intensité lumineuse**.

Pour cela, nous avons étudié l'effet de différents traitements lumineux sur le débourrement et ses régulateurs. Nous avons choisi le rosier buisson (Rosa hybrida KO) comme plante modèle car il a déjà fait l'objet d'études liées aux effets de la lumière sur le débourrement et, comme présenté ci-dessus, plusieurs phénotypes de réponse à la lumière ont été identifiés.

Nous avons traité la problématique en répondant à deux sous-questions. Tout d'abord nous avons (i) cherché à tester si les sucres pouvaient être impliqués dans la réponse du débourrement à l'intensité lumineuse (**Chapitre 2**). Nous nous sommes appuyés sur le cas particulier de la sur-stimulation du débourrement suite à une restriction temporaire de l'intensité lumineuse précédemment observée dans Demotes-Mainard et al. (2013). Pour ce traitement lumineux et un traitement de forte intensité lumineuse permanente (Figure3), nous avons quantifié puis modifié expérimentalement le statut carboné des plantes pour tester l'importance des sucres dans l'obtention du phénotype de débourrement observé. Nous avons également étudié l'origine des différences de sucre observé entre traitements en quantifiant les relations source-puits pour le carbone au sein de la plante.

Après avoir vérifié le rôle des sucres dans la réponse du débourrement à un traitement lumineux particulier, nous avons (ii) cherché à comprendre le rôle des sucres, en relation avec les autres hormones, dans la réponse du débourrement à l'intensité lumineuse. Plus précisément, nous avons cherché à déterminer si l'effet d'une modulation de l'intensité lumineuse sur le débourrement pouvait s'expliquer par des variations locales de l'équilibre entre les teneurs en hormones et en sucres (**Chapitre 3**). Pour cela, nous avons utilisé le modèle de Bertheloot et al. (2020) qui permet de simuler la réponse du

bourgeon au concentrations en sucre et aux hormones à son voisinage, nous l'avons calibré pour prendre en compte l'effet de l'intensité lumineuse, et avons vérifié sa capacité à reproduire des phénotypes de débourrement en réponse à l'intensité lumineuse en conditions *in vitro* et *in planta*. Nous avons ensuite simulé plusieurs traitements particuliers avec le modèle pour déterminer l'importance relatives de sucres et des CK dans la réponse du débourrement à l'intensité lumineuse.

Les résultats obtenus sont discutés dans chaque chapitre et en fin de manuscrit dans une **discussion générale**.

RESULTS - CHAPTER 2 - LOW COMPETITION FOR SUGARS STIMULATES BUD OUTGROWTH AFTER TEMPORARY LIGHT LIMITATION IN ROSE PLANTS

RESUME DU CHAPITRE 2

Contexte et objectifs

La ramification des plantes est une variable agronomique importante puisqu'elle intervient dans l'élaboration du rendement et de la qualité des productions, et est très sensible aux conditions environnementales. Des études récentes sur le rosier (Roman et al., 2016 ; Corot et al., 2017) ont mis en évidence l'effet stimulateur d'une forte intensité lumineuse *pendant* la phase de ramification sur le débourrement comparé à une faible intensité lumineuse. Cette stimulation du débourrement par l'intensité lumineuse est corrélée à de plus fortes teneurs en sucres et en CK au voisinage du bourgeon. Cependant, seul le rôle des CK dans la stimulation du débourrement par l'intensité lumineuse a été démontré expérimentalement dans ce cas.

Par ailleurs, un phénotype surprenant a été observé chez des plants de rosiers soumis à une restriction temporaire de lumière appliquée *avant* la phase de ramification, et replacés ensuite sous forte intensité lumineuse pendant la période de ramification (Demotes-Mainard et al., 2013). Suite à ce traitement lumineux, les plants de rosiers présentent un taux de débourrement dans la zone médiane de l'axe primaire plus important que chez des plantes ayant effectué toute leur croissance sous forte intensité lumineuse. Les mécanismes expliquant cette sur-stimulation du débourrement suite à une restriction temporaire de lumière restent cependant inconnus. Dans ce cas, les teneurs en CK ne constituent peut-être pas un élément limitant pour le débourrement, puisque celui-ci a lieu au moment où l'intensité lumineuse est forte. Des modulations similaires de l'intensité lumineuse au cours de la croissance du riz mènent à une accumulation de sucres dans la plante (Lafarge et al., 2010). Nous faisons l'hypothèse que la sur-stimulation du débourrement suite à une restriction temporaire de lumière résulte d'une diminution de la compétition pour les sucres entre l'axe primaire et les bourgeons axillaires.

Méthode

Pour vérifier cette hypothèse, nous avons mesuré le statut en sucre des plantes par des dosages juste avant le débourrement des bourgeons, en comparant deux traitements : d'une part, des plantes ayant subi une restriction temporaire de lumière (LH), d'autre part, des plantes ayant toujours été sous forte intensité lumineuse (HH). Nous avons ensuite testé l'implication des sucres dans la régulation du débourrement sous ces traitements lumineux en modifiant le statut en sucres des plantes par des apports de solutions sucrées, ou en affectant la photosynthèse grâce à des inhibiteurs. Enfin, nous avons caractérisé expérimentalement la croissance des organes de l'axe primaire et, par une approche de

modélisation, quantifié le bilan sources-puits en sucres de l'axe primaire pour les deux traitements lumineux.

Principaux résultats

Sous le traitement LH, la fréquence de débourrement en partie médiane de l'axe primaire est augmentée et le délai de débourrement raccourci, comparé aux plantes du traitement HH. Cette stimulation du débourrement est associée à de plus fortes teneurs en sucres solubles et en amidon pour les plantes LH juste avant le débourrement. L'implication des sucres dans l'obtention du phénotype de ramification est confirmée par la stimulation du débourrement observée après des apports de sucres chez des plantes sous traitement lumineux HH. Réciproquement, l'application d'inhibiteurs de photosynthèse chez des plantes sous traitement LH inhibe le débourrement. La plus forte accumulation de sucres peu de temps avant le débourrement sous le traitement LH comparé au traitement HH est expliquée par les différences de bilan sources-puits en sucres entre les traitements lumineux. Bien que la capacité photosynthétique surfacique soit diminuée pour les plantes sous LH comparé à HH, cela est compensée par une plus faible croissance, et donc une plus faible demande en sucres, des organes en croissance de l'axe primaire sous LH. Il en résulte en bilan sources-puits en sucres plus élevé sous LH comparé à HH.

Conclusion

La sur-stimulation du débourrement suite à une restriction temporaire de lumière avant la phase de ramification est expliquée par une diminution de la compétition pour les sucres entre l'axe primaire et les bourgeons axillaires. Cette étude démontre l'implication des sucres dans la réponse du débourrement à la lumière dans ce cas, mais n'exclut pas l'intervention d'autres régulateurs du débourrement.

INTRODUCTION

As sessile organisms, plants continually perceive and adjust their growth and development to environmental conditions they experience. Branching of the aerial part is a key process of this adaptation. It determines aerial space colonization and light interception by the plant, a major determinant of its fitness, and is also highly regulated by a variety of environmental inputs (Leduc et al., 2014, Rameau et al., 2015; Huché-Thélier et al., 2016; Demotes-Mainard et al., 2016, Schneider et al., 2019 for reviews). Branching environmental control concerns in particular axillary bud outgrowth, which is the motive force for initiation and elongation of new axes. On a plant axis, the existence of the fast-growing apical zone makes some axillary buds enter a latency phase, a phenomenon known as apical dominance. Bud outgrowth after apical dominance release is highly dependent on environmental conditions. Light intensity is in particular a strong regulator of bud outgrowth and the involved processes has started to be understood in the last years. Studies are however still required to grasp the entire complexity of light intensity impact on bud outgrowth.

In several studies and for different species, it was reported that a continuous high light intensity applied all over plant growth reduces the intensity of apical dominance along plant axes. The probability for a bud to grow out at a given position is increased (Mitchell, 1953; Su et al., 2011; Demotes-Mainard et al., 2013; Leduc et al. 2014 for a review), and in some studies the time-interval taken by buds to grow out is reduced (Bos and Neuteboom, 1998; Gautier et al., 1999; Mitchell, 1953). In this positive effect of light intensity, the current light environment of the bud at the time of its outgrowth plays a role. In rose, the number of outgrowing buds was reduced by transferring primary axes from high to low light intensity just before bud outgrowth period, compared to continuous high light intensity (Corot et al., 2017). Similarly, for the same species, the induction of bud outgrowth observed after apex region removal (decapitation) was repressed if plants were transferred to darkness (Roman et al., 2016). The regulation occurred at least locally to the bud, as demonstrated by localized covering of given organs (Roman et al., 2016; Djenanne et al., 2014). In addition to the current effect of light, plant light history has a strong impact on bud outgrowth. It was reported in intact rose plants that temporary exposure to low light intensity before the outgrowing bud period over-stimulated bud outgrowth compared to a continuous comfort light intensity (Demotes-Mainard et al., 2013). Similarly, a temporary and early shading over-stimulated the rate of tiller appearance in rice after the end of shading (Lafarge et al., 2010).

Two main paradigms co-exist so far to explain apical dominance-dependent bud outgrowth inhibition (for review: Rameau et al., 2015; Kebrom et al., 2017; Wang et al., 2019; Schneider et al., 2019). In a first mechanism, auxin from the fast-growing apical organs of the primary shoot is flowing downwards the stem and indirectly blocks axillary bud outgrowth, through the opposite action of two hormones, the cytokinins (CKs) and strigolactones (SLs). Auxin increases SL biosynthesis and decreases CK biosynthesis in the node, which are able to reach the bud where they act antagonistically

to control its outgrowth (Ferguson and Beveridge 2009; Domagalska and Leyser 2011; Barbier et al., 2019; Tan et al., 2019; Wang et al., 2019). Additional mechanisms exist by which CKs and SLs act outside the bud to regulate its outgrowth (Waldie and Leyser, 2018; Duan et al., 2019; van Rongen et al., 2019). In a second mechanism, high sugar importation by the fast-growing apical organs deprives axillary buds from sugars (Mason et al., 2014; Van den Ende, 2014). This lack of sugars inhibits bud outgrowth due to the positive signaling and trophic role of sugars (Rabot et al., 2012; Barbier et al., 2015; Fichtner et al., 2017, Bertheloot et al., 2019).

Investigations on the interaction between the current effect of light intensity limitation and the apical dominance-related regulating network revealed the role of CKs synthetized in the stem (Roman et al., 2016; Corot et al. 2017). Earlier studies reported a key role of CKs in dark-mediated inhibition of tomato meristematic activity (Yoshida et al., 2011). In rose, the transfer of plants to darkness after their decapitation led to a rapid decrease in CK content of both nodes and buds, and exogenous CK application on bud or stem restored partially bud outgrowth under darkness (Roman et al., 2016). In parallel with that, darkness resulted in downregulation of transcript levels of genes encoding CK biosynthesis (*RhIPT3,5*) and signaling (*RhARR3,5*) in both bud and node. Similar CK-based mechanisms come into play in bud outgrowth repression due to the shift of intact plants from high light intensity to low light intensity just before bud outgrowth period (Corot et al., 2017). Compared to plants maintained under high light, the transfer from high to low intensity dropped CK content in the nodes and exogenous vascular CK supply below the inhibited bud was sufficient to stimulate its outgrowth under low light intensity (Corot et al., 2017; Roman et al., 2016). Although photosynthetic activity and plant sugar content were lower for rose plants transferred to darkness or low light intensity, exogenous supply of soluble sugars were inefficient to restore bud outgrowth ability (Corot et al., 2017; Roman et al., 2016). Thus, repression of CKs in the stem, rather than a decrease in sugar availability, was limiting for bud outgrowth after intact rose plant transfer to low light intensity. This does not however explain how plant light history may impact bud outgrowth, and in particular how a temporary light limitation applied before bud outgrowth can promote it, compared to continuous light comfort regime.

In rice, the stimulation of tiller appearance rate observed after temporary light limitation compared to continuous high light was correlated to an increase in sugar (sucrose and starch) levels (Lafarge et al., 2010), indicating that sugar may be a key component of bud outgrowth regulation by plant light history. Sugar level in a plant depends on the balance between sugar production by photosynthesis and sugar demand for organ growth. Several studies have reported that light intensity induces an adaptation of organ growth and that this adaptation may be definitive, even after the return to high light intensity (Chenu et al. 2005; Tardieu et al., 1999; Sims and Pearcy, 1992; Oguchi et al., 2005). In particular, a transient reduction in light intensity applied only very early in the development of a given sunflower leaf considerably reduced its absolute expansion rate after the return to high light

intensity as well as final leaf area (Granier and Tardieu, 1999; Tardieu et al., 1999). Low light intensity reduced leaf expansion early during leaf development, and this initial lower size reduced leaf expansion rate thereafter. Besides leaf area, maximal leaf thickness and leaf mass per unit area were also reported to be reduced by a low light intensity during leaf development, and this could be hardly attenuated for a mature leaf returning to high light intensity because the number and size of cells determined by low light is limiting (Sims and Pearcy, 1992 ; Oguchi et al., 2005). Based on these findings, we made the assumption that light intensity regulates organ demand for sugars, and that it is permanently reduced after temporary light limitation leading to increase in sugar availability for buds and stimulation of bud outgrowth compared to continuous comfortable light.

The objective of the study is to test the hypothesis that the low sugar demand by the growing organs after temporary light limitation is involved in the stimulation of bud outgrowth compared to a situation of permanent light comfort for rose plants. In this species, the effect of plant light history on bud outgrowth can be easily studied because the outgrowth of axillary buds is inhibited during the entire first phase of growth of the primary axis, before the appearance of the flower bud. Two questions will be addressed: (1) is availability of sugars responsible for bud outgrowth stimulation observed after temporary light limitation? (2) how temporary light limitation modulates the dynamics of sugar production and demand, compared to a permanent comfort light regime? The first question was addressed by an experimental approach consisting in modulating light intensity and sugar contents in the plant. For the second question, we used a modelling approach to quantify sugar production and demand and test if temporary light limitation induced a lower sugar production/demand ratio.

MATERIALS & METHODS

Plant material, growth conditions and light treatments

Single-node cuttings of *R. hybrida* 'Radrazz' plants were obtained as described in Demotes-Mainard et al. (2013). They were grown in 500 ml pots containing a 50/40/10 mixture of neutral peat, coconut fibers and perlite, in a temperature-controlled greenhouse until the appearance of the third or fourth leaf of the primary axis. Then plants were transferred to a growth chamber (light/dark 16/8h photoperiod; 22/20°C at day/night; air humidity 60-70%). Plants were sub-irrigated every two or three days with a fertilized solution (5.0 mM KNO_3, 2.0 mM $Ca(NO_3)_2$, 2.0 mM NH_4NO_3, 2.0 mM KH_2PO_4, 2.0 mM $MgSO_4$, 0.25 mM NaOH. Additional trace elements: Kanieltra formula 6-Fe at 0.25 $ml.l^{-1}$ (Hydro Azote, Nanterre, France) to maintain optimal hydric and mineral nutrition. Bud outgrowth starts a few days after the floral bud becomes visible at the top of the primary axis (FBV stage) (Figure 1). As previously described in Demotes-Mainard et al. (2013), plants were either (i) exposed to a low light intensity (PPFD of 90 $\mu mol.m^{-2}.s^{-1}$ at the collar height, before plants installation) until FBV stage and then transferred to high light intensity (PPFD between 300 and 450 $\mu mol.m^{-2}.s^{-1}$depending on the experiment) (Low-High

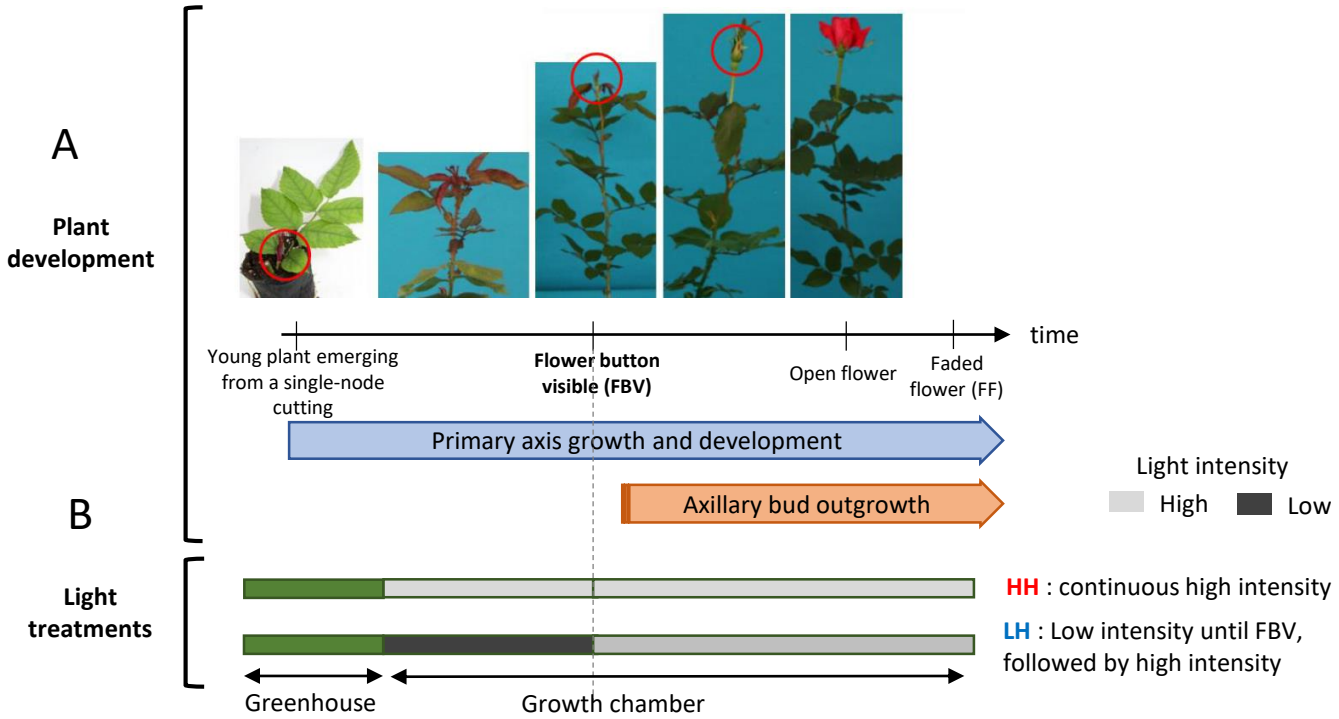

Figure 1 : Development of *R. hybrida* "Radrazz" and light intensity treatments. (A) From single-node cuttings, a primary axis develops, with the successive appearance of phytomers and their elongation. Phytomers consist of an internode, a leaf, and a bud in the axil of the leaf. The bottom leaves are non-foliated. After the appearance of a number of phytomers, the flower bud and the peduncle appear (stage: floral bud visible, FBV). After FBV, the elongation of the phytomers goes on, concomitantly with flower development (Open Flower and Faded Flower stages) and the outgrowth of axillary buds and the growth of their corresponding branches. **(B)** Light treatments were applied at given stages of primary axis development. After a short initial growth period in greenhouse, plants with three or four leaves emerged were transferred to a growth chamber under either a low (for LH treatment) or a high (for HH treatment) light intensity until FBV. From FBV, plants of both treatments LH and HH were grown under high light intensity. Experiments were conducted until faded flower stage of the primary axis (FF).

treatment, LH), or (ii) to a high light intensity throughout the duration of the experiments (High-High treatment, HH) (Figure 1). We conducted four experimental sessions on rosa plants obtained as just described. These experiments had different objectives: monitoring and describing the growth of the primary axis (Exp_PAG), modifying plant sugar status under different light regimes (Exp_Sug), quantifying nutrients and bud outgrowth related hormones (Exp_Dos), and fitting a carbon plant model (Exp_Mod). Different measurements are detailed below.

Primary axis description

Primary axis of intact rose plants was described as a succession of phytomers, each consisting of one internode, one leaf at the top, and an axillary bud at leaf axil (Supp Figure 2). The very basal phytomers bear non-foliated leaves (part called "base"), while other ones are foliated. The foliated phytomers were numbered from plant base, and their final number was definitive at FBV stage. The foliated part, where bud outgrowth pattern was studied, was divided into three zones, Z1, Z2, Z3 (Supp fig 2). These zones were defined as a function of the phytomer rank, expressed relatively to the total number of foliated phytomers to deal with the variable total number of phytomers existing a given light environment. Relative rank *r* was calculated as:

$$r = \frac{i-1}{n-1}$$

where *i* is the foliated phytomer rank and *n* the total number of foliated phytomers.

The relative ranks corresponding to each zone were: $0.7 \leq r \leq 1$ for Z1, $0.4 \leq r < 0.7$ for Z2, $0 \leq r < 0.4$.

Monitoring of axillary bud outgrowth (Exp_PAG, Exp_Sug, Exp_Dos and Exp_Mod)

The development stage (dormant or outgrowing) of each axillary bud along primary axes were scored three to four times a week from FBV stage. An axillary bud was considered to start its outgrowth when its first leaf was clearly visible between its scales (Supp. Fig 1; Girault et al., 2008; Henry et al., 2011). For intact plants, mean bud outgrowth frequency in each zone along the primary axis was calculated as the mean over all the plants of the ratio between the number of buds in a zone that had grown out at a given date and the total number of buds in this zone.

Monitoring of primary axis growth (Exp_PAG)

From primary axis emergence till faded flower stage, primary axis development was recorded three to four times a week. The number of appeared leaves on the primary axis was counted, the development stage of the flower button (FBV = flower button; visible; PCV = petal color visible; OF: open flower; FF: faded flower) was recorded, and, for each foliated phytomer, the length of each internode and each leaf terminal leaflet was measured with a ruler. In addition, thickness of the internode of the lowest foliated phytomer was measured every 4 days using a numeric slide caliper.

At faded flower (FF) stage, all plant organs including flower bud, individual internode and leaf of foliated phytomers, basal non-foliated phytomers ("base"), individual secondary axes, and roots were harvested 3h after the beginning of the light period, scanned, and then dried during 48h at 80°C before weighing. The length and diameter of each individual internode, and the area of each individual leaf were quantified on scanned images using ImageJ software. The mass per unit area (LMA) of each leaf was calculated as the ratio between its dry weight and its area.

Estimation of individual leaf and internode elongation kinetics (Exp_PAG)

Length of each terminal leaflet and internode (l_{lf} and l_{in} respectively, cm) of Exp_PAG were supposed to follow a sigmoidal function of time (*t*, d*)*, as previously demonstrated for rose in Demotes-Mainard et al. (2013). This function contains three parameters: the organ final length (L_{lf} and L_{in} respectively, cm), the relative maximal expansion rates (w_{lf} and w_{in}, d^{-1}) and the date of inflexion point (t^*_{lf} and t^*_{in}, d).

$$\forall(i,t) \quad l_{lf}(i,t) = \frac{L_{lf}(i)}{1 + exp\left(4 \cdot w_{lf}(i) \cdot \left(t^*_{lf}(i) - t\right)\right)} \qquad \text{[Eqn 1]}$$

$$\forall(i,t) \quad l_{in}(i,t) = \frac{L_{in}(i)}{1 + \exp\left(4 \cdot w_{in}(i) \cdot \left(t^*_{in}(i) - t\right)\right)} \qquad \text{[Eqn2]}$$

Thanks to experimental measurements (see above), parameters were estimated for each leaf and internode by optimization. The dates of beginning and end of each organ elongation were then estimated as the dates at which the length was at 10% and 90% of its final value, respectively.

For each leaf, leaf area (s_{lf}, cm^2) was calculated as a simple function of the terminal leaflet length, and of the number of leaflets per leaf (*N*) (Demotes-Mainard, et al., 2013):

$$\forall(i,t) \quad s_{lf}(i,t) = a \cdot l_{lf}(i,t) \cdot N(i)^b \qquad [Eqn\ 3]$$

Where parameters values of *a* and *b* were conserved from Demotes-Mainard et al. (2013).

Light intensity distribution and photosynthesis (Exp_PAG)

Light intensity distribution along the primary axis was measured every three days between FBV and 21 days after FBV using a quantum sensor (LI-190 Quantum Sensor, LI-COR, Lincoln, NE, United States). It was measured at four levels: at the axil of leaves 1, 3, and 4 (counted from plant base) against the stem, and at apex height. For its each leaf level, the sensor was positioned on the right of the leaf when its terminal leaflet was pointing towards the observer.

CO_2 net assimilation rate was measured every two or three days between FBV -1d to FBV+14d for the second basal most foliated leaf of the primary axis (Exp_PAG). Measurements were performed using an infrared gas analyzer, Li-Cor-6400 (Li-Cor Inc., Lincoln, NE, United States) with 22°C and a light

intensity of 400 µmol.m^{-2}.s^{-1} in the measurement chamber. In parallel, chlorophyll surfacic content (µg.cm^{-2}) of each foliated leaf of the primary axis was assessed three to four times a week during three weeks after FBV stage (Exp_PAG), using the Dualex 4 Scientific (Cerovic et al., 2012).

Exogenous sugar supply, leaf masking, and DCMU application (Exp_Sug)

Plant sugar level was manipulated for both intact and decapitated plants. Primary axes were decapitated at FBV 2 cm above the fourth foliated leaf (counted from base) and partly defoliated so as to maintain only one lateral leaflet per leaf (Supp. Figure 3A). Apical dominance was re-established by applying a NAA agar (composition: NAA 5 or 10 µM, 0.3% of agar, and 0.25% of preservative plant mixture) on the top of the stem. In a first experiment, either 25mM sucrose or 25mM mannitol for control (aqueous solutions, with 0.25% of PPM) was supplied through the petiole of each leaf. In a second experiment, all leaflets were masked from FBV stage using either a black opaque or a transparent plastic film. In a third experiment, a solution of photosynthetic inhibitor (composition: DCMU 50µM, 0.05% ethanol and 0.01% Tween) was applied on the half of leaflets.

In intact plants, the terminal leaflet of the higher foliated leaf of zone Z3 was removed and the corresponding petiole was immersed in a solution of either 100mM sucrose or 50mM mannitol, an osmotic control, as made in Bertheloot et al., 2019 and Lin et al., 2011 (Suppl. Figure 3B). In addition, to feed the growing apical organs of the primary stem, sucrose was vascularly supplied above Z3 (through the lowest internode of Z2), using the cotton wick-method described in Corot et al. (2017), for both sugar conditions (see Supp. Figure 3C).

Quantification of endogenous sugars and nitrogen compounds (Exp_Dos and Exp_Mod)

The content in endogenous sugars and nitrogen compounds was determined for organs in each zone of intact primary axes at FBV and several dates after FBV. For LH treatment, measurements at FBV stage were made while plants were still under low light intensity, just before plant transfer to high light intensity. Organs considered were leaves in both Exp_Dos and Exp_Mod, full-length internodes in Exp_Mod, and nodal segments with 5 mm of stem each side of the node in Exp_Dos. Roots, and the flower plus peduncle, were also considered in Exp_Mod. Organs were collected in the morning, were immediately frozen in liquid nitrogen and stored at -80°C. Samples were then lyophilized, crushed, and soluble sugars (sucrose, glucose, fructose), starch, nitrate, total amino-acids and soluble proteins were determined by colorimetry.

Estimation of the balance between carbon supply and demand (Exp_Mod)

To address the second question of our study, we compared the balance between carbon supply and demand of plants cultivated under LH and HH treatments. This was done preferentially using only Exp_Mod data, or combining other experimental data when necessary, as detailed below. Exp_Mod

provided for both light treatments, (i) non-destructive measurements of individual leaf appearance dates on primary axes and individual bud outgrowth stage (for further details, see above), as well as (ii) destructive measurements of dimensions, dry masses, and nutrient contents at several dates after FBV. From this experiment, structural mass was estimated as the difference between measured total carbon mass and carbon mass allocated to sucrose, hexoses, starch, soluble proteins, amino acids, and nitrates.

General principles of the carbon balance model

Carbon supply and demand was quantified each day (*t*) for LH and HH plants as the difference between (i) carbon acquisition by leaf photosynthesis and (ii) use for plant structural growth, which is carbon allocated to cell walls (Figure 8). Individual foliated leaves, corresponding internodes, the flower plus peduncle, and roots, were represented separately. Leaf and internode structural growth was decomposed into growth in dimension (area for leaves, length for internodes) and growth in thickness (structural dry mass per unit area for leaves; diameter and structural dry mass per unit volume for internodes). Both carbon acquisition and use were driven by light treatment, as detailed in the paragraphs below. The daily values of carbon acquisition and use was estimated for rose plants grown in Exp_Mod. From organ dimensions and structural masses at several dates measured in this experiment, the temporal patterns were estimated. Because some relations were first defined on Exp_PAG, all mathematical expressions related to the primary axis leaves and internodes mass growth and expansions are functions of the relative rank (*i*) of the leaf or internode. Simulations results were in contrast presented as a function of the absolute ranks, considering the observed number of phytomers on primary axis of Exp_Mod. All parameters values are summarized in Supp.Table 1.

Kinetics of leaf area, internode length and diameter

The area extension of each leaf *i* and elongation of each internode *i* of the primary axis through time were estimated using the function described in Eqn 1 and Eqn 2. For each internode and leaf *i* and each light treatment, the dates of inflexion points, $t^*_{in}(i)$ and $t^*_{lf}(i)$, respectively, were related to the date of leaf *i* appearance, $t_{app}(i)$, measured in Exp_Mod as described in Demotes-Mainard et al. (2013):

$$\forall i \quad t^*_{lf}(i) = a_{lf} \cdot t_{app}(i)^2 + b_{lf} \cdot t_{app}(i) + c_{lf} \qquad [Eqn\ 4]$$

$$\forall i \quad t^*_{in}(i) = a_{in} \cdot t_{app}(i) + b_{in} \qquad [Eqn\ 5]$$

Where values of the parameters a_{lf}, b_{lf}, c_{lf},, a_{in} and b_{in} are issued from Demotes-Mainard et al., (2013) (Supp. Table 1).

Final leaf areas and internode lengths were estimated from the values observed after FBV+16 days in Exp_Mod and, when values were missing, we estimated them assuming that the profiles of final leaf areas and internode lengths along the primary axis were similar in Exp_Mod and in Exp_PAG. First,

profiles observed in Exp_PAG were fitted as polynomial functions of leaf or internode rank and light treatment:

$$\forall i \quad S_{lf}(i) = d_{lf} \cdot i^3 + e_{lf} \cdot i^2 + f_{lf} \cdot i + g_{lf} \qquad \text{[Eqn 6]}$$

$$\forall i \quad L_{in}(i) = c_{in} \cdot i^3 + d_{in} \cdot i^2 + e_{in} \cdot i + f_{in} \qquad \text{[Eqn 7]}$$

where d_{lf},…,g_{lf} and c_{in},…f_{in} are parameters depending on light treatment (Supp. Table 1).

Then, a scaling factor was calculated as the ratio between measured final dimensions in Exp_PAG and those in Exp_Mod, and this factor was applied to estimate the missing dimensions in Exp_Mod (Supp Fig 4). From the measured and estimated final dimensions of Exp_Mod, estimated $t^*_{in}(i)$ and $t^*_{lf}(i)$, and the measurements of individual leaf area and internode length in Exp_Mod, w_{lf} and w_{in} were estimated. They were set as constant whatever the phytomer rank and the light treatment, as proposed by Demotes-Mainard et al. (2013). This led to a mean RMSE between simulated and measured leaf areas in Exp_Mod and between simulated and measured internode length of 15 cm², and 0.97cm respectively (Supp Fig 5 for illustration of fitting quality).

Each internode diameter kinetics was directly fitted on Exp_Mod measurements. It was ever-increasing from the time of leaf appearance and its increase rate was represented to decrease with time according to a monomolecular law (Paine et al., 2012) with a maximal value (V_Φ^{init}) at leaf appearance date (t_{app}), a relative decreasing rate r_Φ , and a minimum value V_Φ^{min}, as follows: :

$$\forall (i,t) \quad \frac{d\Phi(i,t)}{dt} = V_\Phi^{min} - \left(V_\Phi^{min} - V_\Phi^{init}\right) \times exp\left(-r_\Phi \cdot \left(t - t_{app}(i)\right)\right) \qquad [Eqn\ 8]$$

At each time t, the internode diameter at rank i was calculated by integrating the rate of diameter increase:

$$\forall (i,t) \quad \Phi(i,t) = \Phi_0 + V_\Phi^{min} \cdot \left(t - t_{app}(i)\right) + \frac{V_\Phi^{min} - V_\Phi^{init}}{r_\Phi} \times \left(exp\left(-r_\Phi \cdot \left(t - t_{app}(i)\right)\right) - 1\right) \qquad \text{[Eqn 9]}$$

where Φ_0 (cm) is the diameter of the internode at leaf appearance.

From fitting procedure, only the parameter V_Φ^{init} varied with light treatment. Mean RMSE was lesser 0.1 cm than for all internodes (Supp Fig 6 for illustration of fitting quality).

Kinetics of surfacic photosynthesis of each leaf

Carbon acquisition by photosynthesis (P, µmol C .m^{-2}.s^{-1}) of each leaf i in a light treatment at a time t was estimated as a saturating function of the ambient light intensity at the leaf level (I, µmol photons.m^{-2}.s^{-1}) and of the maximum value at saturating light intensity (P_{sat}, µmol C .m^{-2}.s^{-1}) (Thornley et al., 1998):

$$\forall (i,t) \quad P(i,t) = \frac{\alpha \cdot I(i,t) \cdot P_{sat}(i,t)}{\alpha \cdot I(i,t) + P_{sat}(i,t)} \qquad [Eqn\ 10]$$

Where α is the photosynthetic efficiency (µmol C. µmol^{-1} photons).

Photosynthetic capacity varies with leaf rank and age in link with the dynamics of leaf nitrogen contents (Lieth and Pasian, 1990; Hikosaka and Terashima, 1995; Kim and Lieth, 2003). We also observed an effect of light treatment on photosynthesis (Fig 7A). From this, we related P_{sat} to surfacic chlorophyll index (*chloro*, µg.cm^{-2}) which varied with leaf age, rank and light treatment in Exp_GAP (Supp. Fig. 13) and is known to limit photosynthesis (Buttery and Buzzell, 1976):

$$\forall(i,t) \quad P_{sat}(i,t) = P_1 + P_2 \cdot \frac{chloro(i,t)}{chloro(i,t) + K_{chloro}} \qquad [Eqn\ 11]$$

where P_1 (µmol C .m^{-2}.s^{-1}), P_2 (µmol C .m^{-2}.s^{-1}), K_{chloro} (µg.cm^{-2}) are parameters.

Chlorophyll contents were not measured in Exp_Mod, and measurements made in Exp_PAG were used to estimate parameter values. First, leaf surfacic chlorophyll index (*chloro*) was fitted on Exp_PAG measurements. It was a function of leaf age, and for each leaf, it increased with time from leaf appearance (t_{app}), with a relative rate r_{chloro}, till a maximal value ($chloro_{max}$):

[Eqn 12] : $\forall(i,t)$

$$chloro(i,t) = chloro_{max}(i) - \left(chloro_{max} - chloro_{app}\right) \cdot exp\left(-r_{chloro}(i) \cdot \left(t - t_{app}(i)\right)\right)$$

where r_{chloro} is expressed as a polynomial function of the relative rank *i*:

$$\forall i \quad r_{chloro}(i) = a_{chloro} \cdot i^2 + b_{chloro} \cdot i + c_{chloro} \qquad [Eqn\ 13]$$

Only $chloro_{max}$ differed between light treatments (see Supp Fig 7 for illustration of fitting quality). Once chlorophyll index obtained for Exp_PAG, a scaling factor was used to estimate surfacic chlorophyll content for Exp_Mod, thanks to a ratio of total protein compound between plants of Exp_Mod and Exp_PAG. Finally, α, P_1, P_2, K_{chloro} were estimated by minimizing the RMSE between simulated P and measured net photosynthesis (with LICOR, see above for further details) on the second leaf from the base (Supp fig 9).

Ambient light intensity at each leaf *i* level at each time step, *I*(*i*,*t*), was modelled assuming that light intensity attenuates towards plant base according to a Beer-Lambert like function (Thornley and France, 2007).

$$\forall(i,t) \quad I(i,t) = k_1 \cdot I_0(t) \cdot e^{k_2 \cdot A(i,t)} \qquad [Eqn\ 14]$$

where I_0 is light intensity at the top of the plants, $A(i,t)$ is the cumulative leaf area above the rank *i*, and k_1 and k_2 are two parameters.

To estimate *I*(*i*,*t*), k_1 and k_2 were first estimated using data of both light treatments in Exp_GAP (Supp Fig 8 for illustration of fitting quality), since light intensity measurements along the stem were missing in Exp_Mod. Then, *I*(*i*,*t*) was calculated using these values of k_1 and k_2, and $I_0(t)$ measured during Exp_Mod.

Kinetics of structural mass of individual leaves, individual internodes, roots, and flower plus peduncle

For each rank *i*, leaf structural mass (M_{lf}) at each time step was calculated as the product of its area and structural leaf mass per unit area (LMA):

$$\forall(i,t) \quad M_{lf}(i,t) = s_{lf}(i,t) \cdot LMA(i,t) \qquad [Eqn\ 15]$$

Structural LMA was fitted on Exp_Mod data. It increased with time for each leaf until a maximum. It was modelled as minimum at leaf appearance (LMA_{app}), to increase with leaf age with a relative rate r_{LMA} until it reached a maximum value LMA_{max} according to a monomolecular law of time (Paine et al., 2012):

$$\forall(i,t) \quad LMA(i,t) = LMA_{max} - \left(LMA_{max} - LMA_{app}\right) \cdot exp\left(-r_{LMA} \cdot \left(t - t_{app}(i)\right)\right) \qquad [Eqn\ 16]$$

Only LMA_{max} varied between light treatments.

Internode structural mass (M_{in}) was calculated as the product of its length, diameter Φ, and volumic structural mass ρ as follows:

$$\forall(i,t) \quad M_{in}(i,t) = \frac{\Pi}{4} \cdot l_{in}(i,t) \cdot \Phi(i,t)^2 \cdot \rho(i,t) \qquad [Eqn\ 17]$$

ρ was fitted using Exp_Mod measurements of internode structural mass and modelled as a positive linear function of internode age:

$$\forall(i,t) \quad \rho_{in}(i,t) = v_{\rho}\left(t - t_{app}(i)\right) + \rho_{app} \qquad [Eqn\ 18]$$

where ρ_{app} is the initial value of the internode volumic structural mass when the corresponding leaf appears, and v_{ρ} is the rate of internode volumic structural mass increasing.

Only v_{ρ} varied between light treatments (see Supp Fig 6 for illustration of fitting quality).

Following Exp_Mod observations, the structural mass of the flower bud plus the peduncle and of roots were correlated to the total leaf structural mass (Supp. Fig. 12):

$$\forall t \quad M_{flw}(t) = \sum_{i}^{n} M_{lf}(i,t) \cdot \left(a_{flw} \cdot t^2 + b_{flw} \cdot t + c_{flw}\right) \qquad [Eqn\ 19]$$

$$\forall t \quad M_{root}(t) = \sum_{i}^{n} M_{lf}(i,t) \cdot \left(a_{root} \cdot t + b_{root}\right) \qquad [Eqn\ 20]$$

where a_{flw}, b_{flw}, c_{flw} and a_{root} and b_{root} are parameters with similar values between LH and HH treatments.

Balance between carbon supply and demand

The balance between carbon supply and demand was calculated each day (*t*) as the difference between carbon acquisition by leaf photosynthesis and the use for the growth of the structural plant mass (M_{plant}, which is the sum of leaves, internodes, flower of the primary axis, and roots masses):

$$\frac{dC(t)}{dt} = \left(\sum_{i}^{n} P(i,t) - \gamma \cdot \frac{dM_{plant}(t)}{dt}\right) \qquad [Eqn\ 21]$$

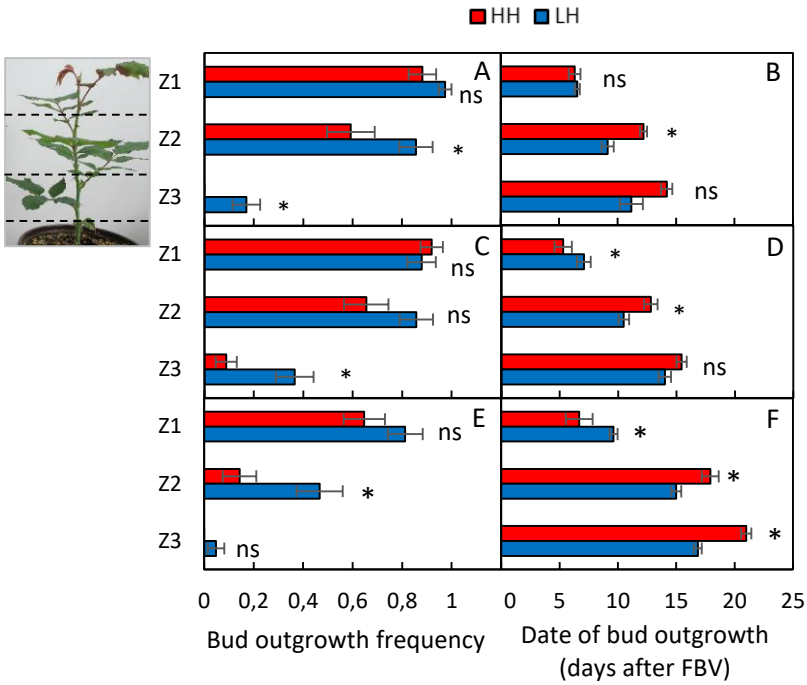

Figure 2 : Temporary light limitation stimulated bud outgrowth in primary axis median part. Impact of LH (blue) and HH (red) treatments on bud outgrowth frequency 14 days after FBV (A, C, E) and on the date of outgrowth (B, D) for different foliated zones along the primary axis, Z1, Z2, and Z3 (see Supp Figure 2 for details). Data from Exp_Dos in bright cabinets (A, B) and on racks (C, D), and Exp_PAG (E, F). Values are means of at least 14 plants per treatment ± SEM. Asterisks indicate significant differences between LH and HH treatments (exact Fisher test (A, C, E), or Wilcoxon test (B, D, F) : $P < 0.05$).

where γ is the mean carbon content in structural dry mass.

Statistics and estimation of fitting quality

Statistical analyses were performed using R software (R Core Team, 2014). Treatments were compared using non-parametric tests: Wilcoxon test for comparing mean values, and Exact Fisher test for bud outgrowth frequencies. The root mean square error (RMSE) of simulated variables related to organ mass growth, expansion and photosynthesis were calculated for each leaf or internode rank.

RESULTS

Bud outgrowth stimulation after a temporary light limitation was preceded by starch accumulation in all organs

First, we checked the assumption that a temporary light limitation stimulates bud outgrowth through higher sugar availability for axillary buds. To this end, we started by quantifying bud outgrowth and sugar contents along the primary axis of rose plants for the two different light regimes: (i) continuous high light intensity (High-High treatment, HH), or (ii) temporary light limitation till floral bud appearance at the top of primary axis, which is shortly before bud outgrowth (Low-High treatment, LH) (Figure 1). The primary axis corresponds to an assembly of phytomers, each consisting of an internode, a leaf and a bud at leaf axil. Since the basal phytomers bear non-foliated leaves without bud outgrowth, it was not considered for this study. These foliated phytomers were then separated into three zones according to their relative rank: Z1, the most apical one, Z2 the median one, and Z3 the most basal one (see material and methods for further details; Supp Figure 2).

In order to test the soundness of our hypothesis, bud outgrowth was followed for plants grown under LH and HH for three experimental devices. For all these devices and similarly to Demotes-Mainard et al. (2013), bud outgrowth was stimulated in the median parts of the primary axis in response to temporary light limitation compared to continuous high light intensity. The rate of bud outgrowth in LH was significantly higher in Z2 and/or Z3, depending on the experimental device (Fig. 2A, C, E). In addition, bud outgrowth started earlier for LH compared to HH (Fig. 2B, D, F). The date of outgrowth was significantly earlier for LH in Z2 for all experimental configurations, in Z3 for one experimental configuration, and values in Z3 were lower without being statistically significant for the other two experimental configurations. Contrary to the median parts of the primary axis, no significant difference between treatments was observed in bud outgrowth rate in the apical part of the axis (Z1) (Fig. 2A, C, E), but a delay in bud outgrowth was observed under LH for two experimental configurations (Fig. 2B, D, F).

Based on this, we tested whether bud outgrowth stimulation of zones Z2 and Z3 in LH was linked to a higher sugar availability in the corresponding nodes and leaves compared to HH. Soluble sugars

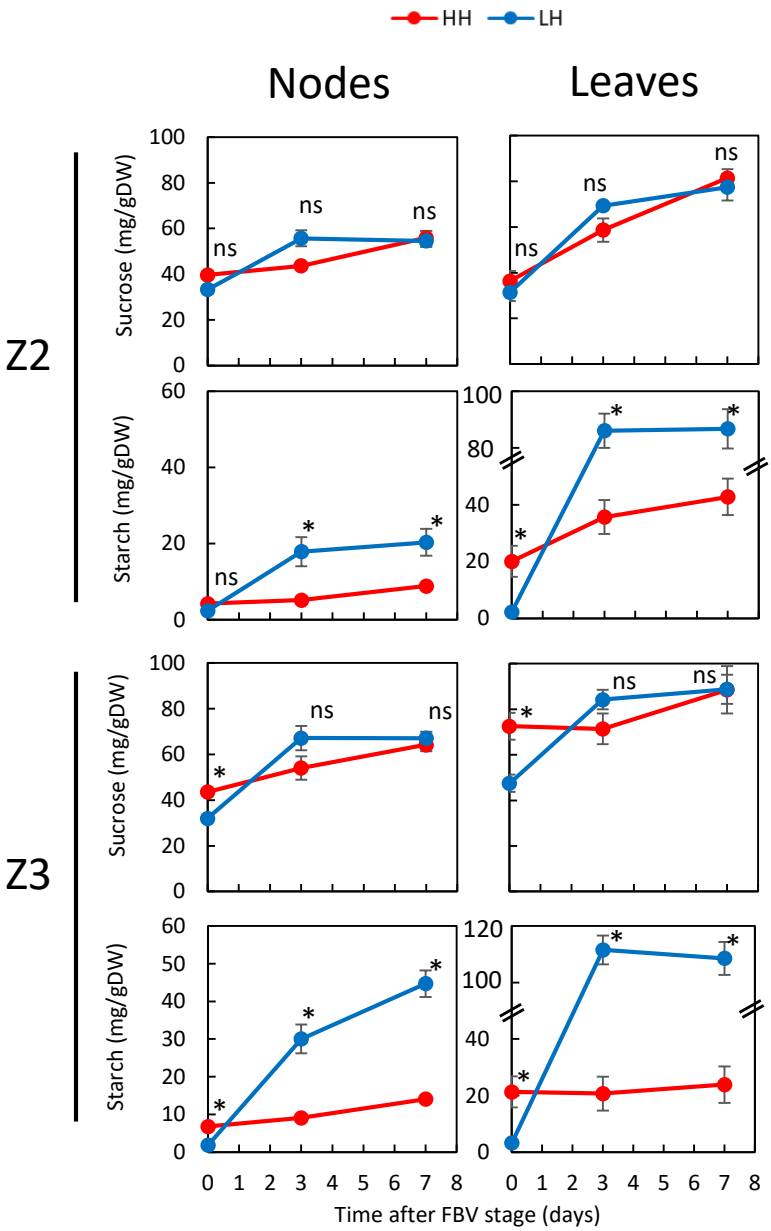

Figure 3 : Temporary light limitation stimulated sugar accumulation as starch in primary axis median part. Impact of the LH (blue) and HH (red) treatments on sucrose and starch contents in the nodes and leaves during the first 7 days following FBV for the median foliated zones along the primary axis, Z2 and Z3 (see Supp Figure 2 for details). Data are means ± SEM of 4 repetitions of at least four pooled plants each. Asterisks indicate significant differences between LH and HH treatments (Wilcoxon test : $P < 0.05$).

(sucrose, glucose and fructose) and starch (the main sugar reserve form in rose) contents were quantified in these organs for both treatments before bud outgrowth started (Fig. 3). At FBV, when LH plants were still under low light intensity, sugar content was either lower (sucrose and starch contents in Z3; leaf starch content in Z2) or similar compared to HH. The transfer of FBV stage-plants from low to high light intensity (LH) resulted in a rapid increase in sucrose and starch contents in nodes and leaves of Z2 and Z3, while HH treatment displayed no or a slower increase (leaves in Z2). As a result, at FBV + 3 days, sucrose contents were similar for both treatments, while starch contents were much higher in LH compared to HH. Relatively to HH, starch content is at least three times higher in nodes (Z2:18 and 5.2 mg/gDW), Z3 (30 and 9.1 mg/gDW for LH and HH respectively) and leaves (Z2: 132 and 36 mg/gDW; Z3: 169 and 21 mg/gDW for LH and HH respectively) in response to LH. This difference between LH and HH is still maintained until FBV+7 days. These results demonstrate that bud outgrowth stimulation under temporary light limitation (LH) was preceded by starch accumulation in nodes and leaves, which indicates a high plant sugar status under this condition.

Sucrose supply to HH plants stimulated bud outgrowth while photosynthesis inhibition of LH plants inhibited bud outgrowth

To determine whether sugar excess in LH may explain bud outgrowth promotion under this treatment compared to HH, we either supplied exogenous sugar to HH plants or decreased photosynthetic-derived sugars for LH plants and evaluated the impact on bud outgrowth. In intact plants, the effect of sugar manipulation treatments on bud outgrowth may be biased by the high ability of fast-growing apical zone to attract and use sugars. To avoid this possibility, we first used partially defoliated and decapitated plants that were supplied apically with exogenous auxin to mimic auxin-derived apical dominance of intact plants, as done previously in Bertheloot et al. (2019). They were grown either under low (LH treatment) or high light intensity (HH treatment) before decapitation, and then transferred to high light intensity. As in intact plants, bud outgrowth was stimulated for LH compared to HH in this experimental system. To reduce sugar supply for LH plants, the photosynthesis inhibitor DCMU was applied on leaves or an opaque plastic film was covered leaves. With the control solution (without DCMU), bud outgrowth percentage is of 52% along the axis that is dropped to 35% after DCMU treatment (Figure 4A). Leaf masking had a much stronger effect than DCMU application. Indeed, compared to leaf covering with a transparent plastic film, leaf covering with an opaque plastic film reduced bud outgrowth to ca. 6%. In order to increase sugar status of HH plants, 25 mM sucrose was supplied to the petioles of all leaves and compared to 25 mM mannitol, an osmotic control. While bud outgrowth percentage was 34% with mannitol supply, it almost doubled (61%) in response to sucrose supply. These results obtained on decapitated plants demonstrate that sugar supply is necessary for bud outgrowth stimulation for plants under LH, and sufficient to stimulate bud outgrowth for plants under HH.

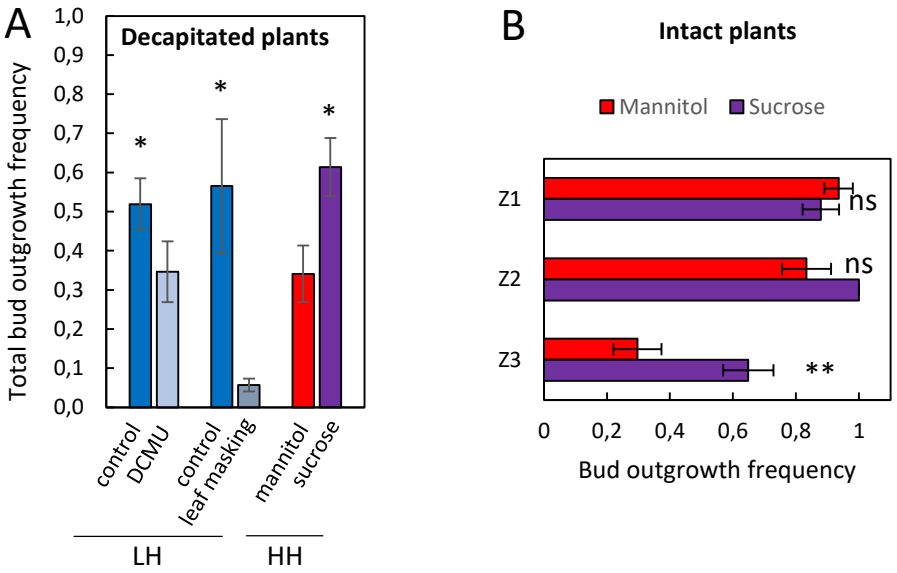

Figure 4 : Sucrose supply to HH plants stimulated bud outgrowth while photosynthesis inhibition of LH plants inhibited bud outgrowth. A/Impact of sucrose supply and photosynthesis inhibition on bud outgrowth frequency (at FBV+12d) for rose decapitated plants (with a 5µM auxin agar on their top) grown under HH and LH treatments, respectively. Plants were decapitated and partially defoliated at FBV stage. For plants grown under LH , leaflets were (i) treated with the photosynthesis inhibitor DCMU or a control solution, or (ii) masked with plastic opaque film or a control transparent plastic film. For plants grown under HH, 25mM sucrose or 25 mM mannitol were supplied through all the petioles. B/ Impact of sucrose supply on bud outgrowth frequency of plants under HH treatment. 100 mM sucrose or 50 mM mannitol was supplied through the petiole of the highest Z3 leaf. For both sugar treatments, plants were vascularly supplied with sucrose through the lowest internode of Z2. Measurements of bud outgrowth were made at 21 days after FBV. For A and B, data are means ± SEM of at least 12 plants. Asterisks indicate significant differences between treatments (Exact Fisher test : $P < 0.05$).

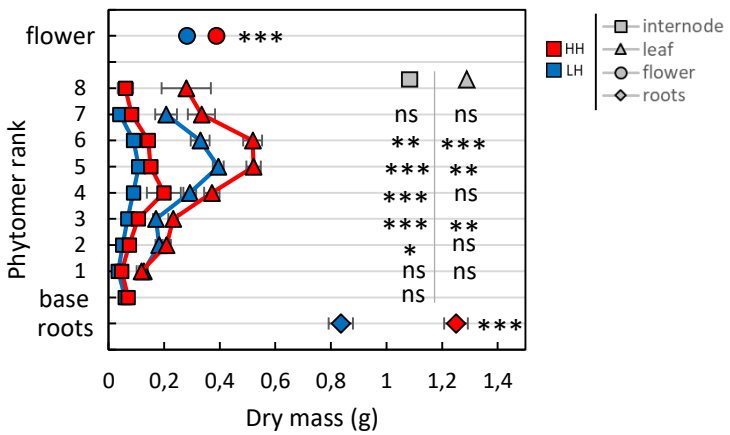

Figure 5 : A temporary light limitation reduced organs and root dry weights at a final development stage of the primary axis. Impact of LH and HH treatments on dry weights of the flower button, roots, individual internodes and individual leaves along the primary axis at faded flower stage. Data are means ± SEM of at least 14 plants per treatment. Asterisks indicate significant differences between LH and HH treatments (Wilcoxon: * $P < 0.05$; ** $P < 0,01$; ***$P < 0,001$).

We then wanted to test if the stimulation observed after sugar supply in HH for decapitated plants was conserved for intact plants. Intact plants were fed from FBV stage with 100 mM sucrose provided through the petiole of the highest leaf of the Z3, and the kinetic of bud outgrowth in this zone was measured and compared to 50 mM mannitol, osmotic control (osmotic control was kept at 50mM to prevent leaf necrosis observed with 100mM mannitol). 100 mM mannitol leads to leaf dehydration and senescence. To avoid that the supplied sugar solution was diverted by the growing apical organs from the axillary buds, sucrose was in addition supplied directly in the stem of Z2 with the cotton-wick method (through the lowest internode of Z2; for details see Corot et al., 2017 and Supp. Fig. 3). As for decapitated plants, exogenous sucrose supplies stimulated bud outgrowth compared to mannitol supply (65% and 30%, respectively) (figure 4B).

All these observations, together with the higher sugar level observed in intact plants under LH compared to those under HH, strongly support the hypothesis that bud outgrowth stimulation observed in LH is be sugars dependent.

Temporary light limitation before bud outgrowth period permanently reduced phytomer growth in length and thickness, and flower growth.

We then wanted to understand the origin of sugar accumulation observed for plants in LH compared to HH, after FBV. We hypothesized that plants under LH treatment displayed slower primary axis growth after FBV, thus leading to lower sugar demand and higher sugar accumulation compared to HH. To verify this hypothesis, we first assessed mass and dimensions of roots and organs of the primary axis at faded flower stage (FF), when all phytomers had ended their expansion. At this stage, the primary axis consists of non-foliated phytomers at the base (denoted “base”), topped with several foliated phytomers, a peduncle, and a flower (Supp. Figure 2). All plant parts, except the non-foliated basal phytomers, displayed lower final masses for LH compared to HH. The roots and the peduncle plus flower had a dry mass of 0.84 and 0.28 g, respectively for LH, against 1.25 and 0.39g for HH (Figure 5). The lower final mass of vegetative parts under LH resulted on the one hand from a lower number of foliated phytomers (6.9 and 7.4 for LH and HH, respectively; Wilcoxon test: $P < 0.05$), and on the other hand from lower individual internodes and leaves mass. Indeed, if we consider primary axis with 7 and 8 phytomers for LH and HH treatments, respectively, dry masses for ranks upper than 3 (counted from the base of the plant) were higher for LH compared to HH, even if differences were not significant for rank 7 (Figure 5). For lower ranks (<5 for leaves and <6 for internodes), leaf and internode lengths were similar between treatments and the lower masses in LH compared to HH resulted only from higher leaf mass per unit area and higher internode diameter and density (Figure 6 A,B,E,F,G). For upper ranks (≥5 for leaves and ≥6 for internodes), internode diameter was similar between LH and HH, and the lower masses observed in LH resulted from lower leaf area and leaf mass per unit area, as well as lower internode length and density.

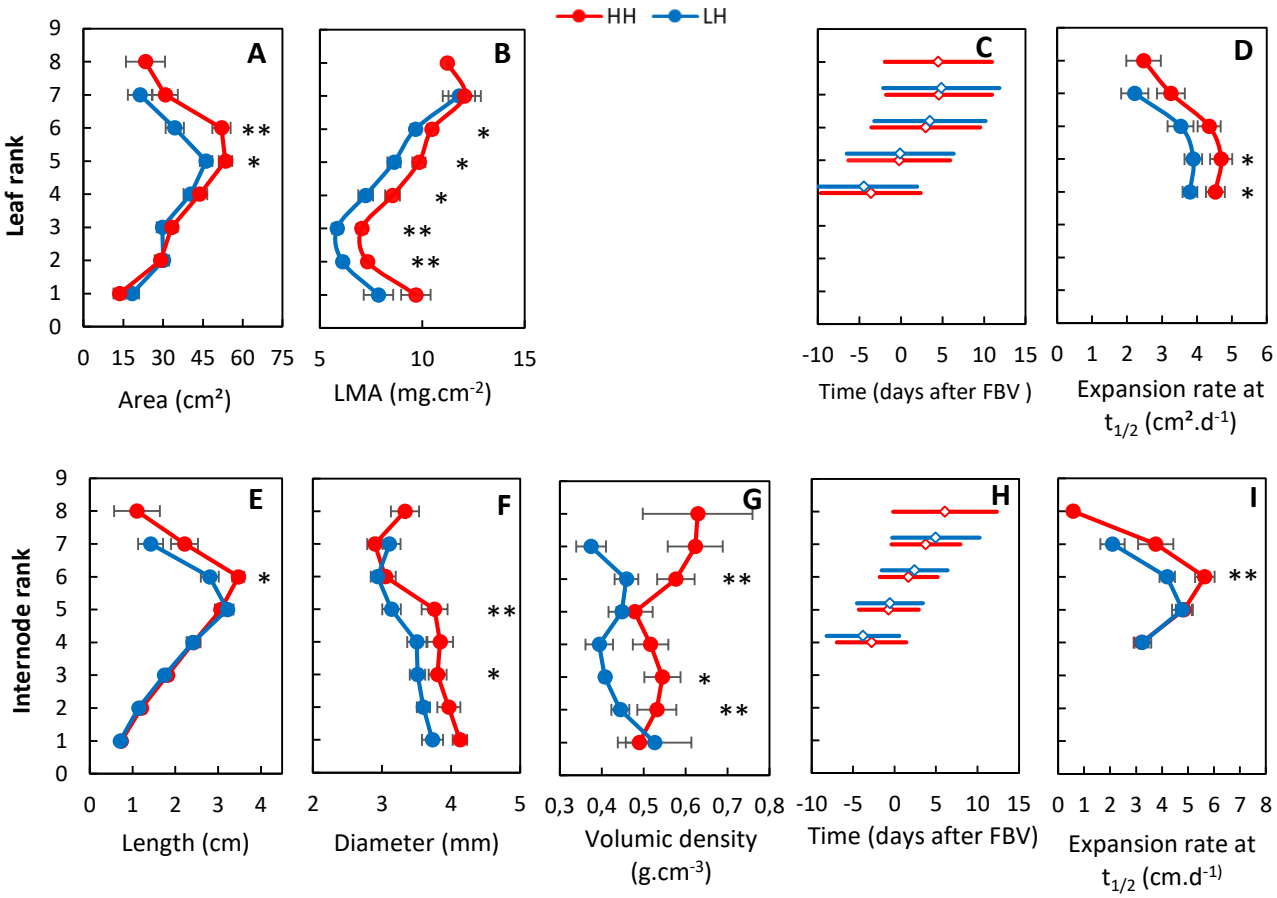

Figure 6 : Temporary light limitation reduced extension and thickening of individual leaves and internodes of the primary axis. A,B,E,F,G/ Impact of LH and HH treatments on individual leaf area (A), mass per unit area (B), individual internode length (E), diameter (F), and volumic density (G) at FF stage of the primary axis. C,H/ Expansion periods of individual leaves (C) and internodes (D) for foliated ranks ≥4 (counted from plant base) and dates the corresponding inflexion points (diamonds). Time is expressed relatively to FBV stage. D,I/ Maximal expansion rates of individual leaves and internodes for foliated ranks ≥4. Data are means ± SEM of at least 14 plants per treatment. Asterisks indicate significant differences between LH and HH treatments (Wilcoxon: * $P < 0.05$; ** $P < 0,01$; ***$P < 0,001$).

To determine if the difference in the final number of organs and their dimensions resulted from differences in the dynamics after FBV, we monitored at several times the appearance date and length of each internode and leaf above rank 4 (which had not finished their extension at FBV), as well as the diameter of internode 1 (*In1*). A sigmoidal function was fitted on the length measurements for each internode and leaf to estimate the beginning and end of extension, and extension rate at the inflexion point. The fitting showed that for each phytomer rank the dates of beginning and end of extension, relatively to FBV stage, were similar between LH and HH (Fig. 6 C, H). Treatment HH had one more phytomer (8 compared to 7 under LH treatment) after FBV, extending concomitantly with the previous one. For both treatments, phytomers of ranks ≥ 5 achieved at least half of their elongation after FBV, and all the corresponding leaves as well as internodes 6 and 7 presented reduced extension rates under LH compared to HH (Fig. 6 D, I). Similarly, the rate of the *In1* diameter increase was lower for LH compared to HH after FBV (data not shown; linear fitting: $R^2 > 0.84$; 0.047 mm/d compared to 0.053 mm/d). Thus, compared to continuous high light intensity, temporary light limitation before FBV reduced the number of organs that appear and their increase in dimension after FBV. Together with reduced LMA and internodes density at FF stage, it indicates that the demand in sugar for the vegetative part may be reduced after FBV for LH compared to HH.

Temporary light limitation reduced durably surfacic photosynthetic capacity of a basal mature leaf

We then wanted to assess if leaf photosynthesis after FBV was affected by temporary light limitation. A reduction of the light-saturated rate of photosynthesis per unit area was previously observed for leaves initiated under low light intensity and then transferred to high light intensity, in comparison to plants always grown under high light intensity (Oguchi et al., 2003). Such decreased photosynthesis was also observed for LH compared to HH in the present study. At a given light level (PAR =400 $\mu mol.m^{-2}.s^{-1}$), net photosynthesis of a basal leaf (leaf 2), that had already finished its extension after FBV, was significantly lower for LH compared to HH (Fig. 7A). In parallel, was found a lower surfacic chlorophyll content, estimated non-destructively with Dualex (Fig 7B). The lower photosynthesis observed for a mature leaf of plants submitted previously to light limitation indicates that sugar supply may be lower for this treatment compared to continuous high light regime.

A lower carbon demand after FBV for LH compared to HH likely explains their different sugar status

The above results demonstrate that plants grown under LH and HH have both different growth rates and photosynthetic capacity after FBV, and present different sugar contents. To answer our second question, we dynamically quantified the carbon balance during the 10 days after FBV for plants grown in an experiment made in 2011 (Exp_Mod). As described above, LH-treated plants in this experiment

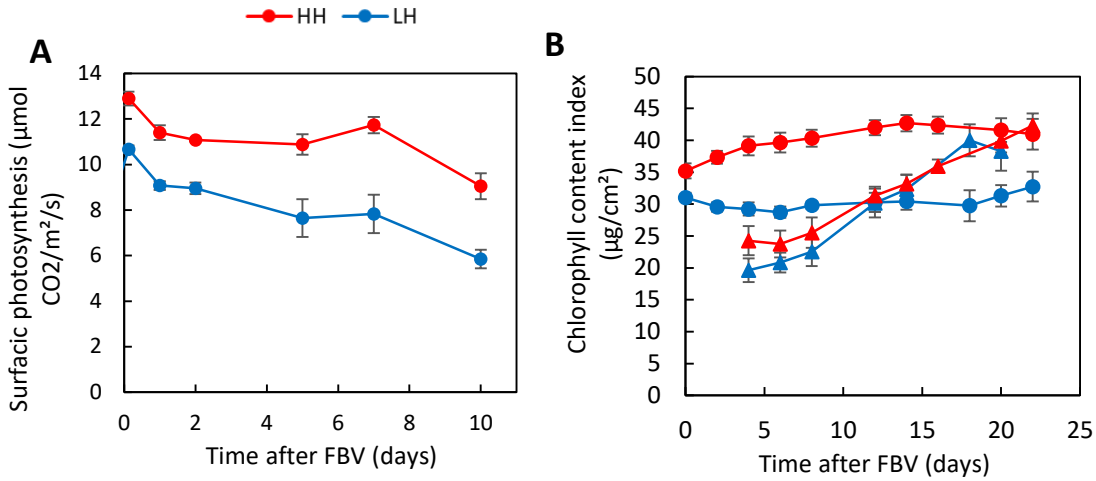

Figure 7 : A temporary light limitation reduced durably surfacic photosynthetic capacity of a basal mature leaf. Impact of LH and HH treatments on photosynthesis and chlorophyll. A/ Photosynthesis per unit leaf area measured for the foliated leaf 2 (counted from the base) at a light intensity of 400 µmol m^{-2} s^{-1} during the first 10 days after FBV. Values are means of at least 4 plants ± SEM. B/ Leaf surfacic chlorophyll index (measured with Dualex) for the foliated leaf 2 (circles) and 5 (triangles) (counted from the base) during 22 days after FBV . Values are means of at least 6 plants ± SEM.

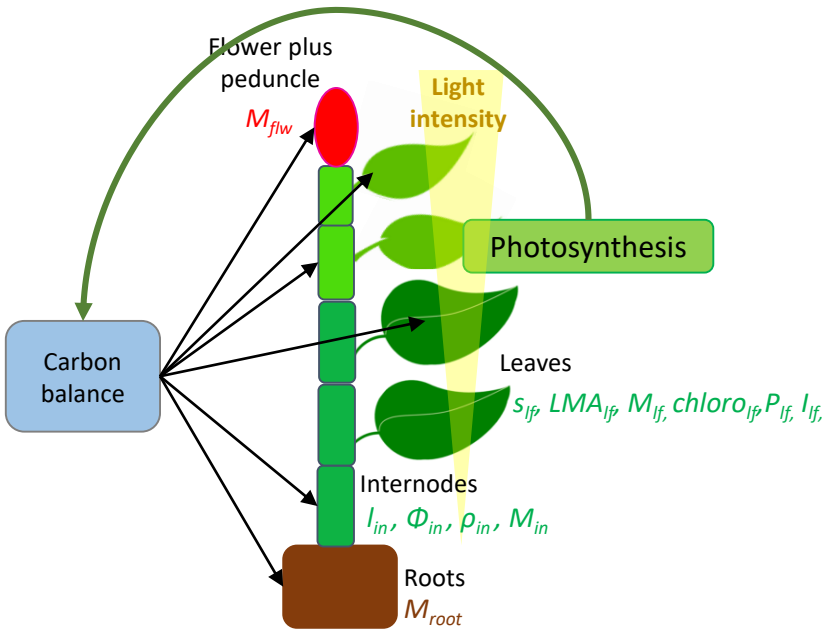

Figure 8 : Structure of the model estimating carbon balance within rose primary axes. The primary axis is described as a set of modules corresponding to the root compartment, individual foliated leaves, the corresponding internodes, and the flower plus peduncle. Roots, and the flower plus peduncle are characterized by their structural dry mass (M_{root}, M_{flw}, respectively). Each leaf is characterized its area (s_{lf}), structural mass per unit area (LMA_{lf}), structural mass (M_{lf}), surfacic chlorophyll index ($chloro_{lf}$), and surfacic photosynthesis (P_{lf}). Each internode is characterized by its length (l_{in}), diameter (Φ_{in}), structural mass per unit volume (ρ_{in}), and structural mass (M_{in}). Carbon balance each day is the difference between the rates of (i) carbon acquisition by leaf photosynthesis and (ii) carbon use for the increase in structural dry mass of the different modules. Leaf photosynthesis is a function of light ($I_{lf,}$), s_{lf}, and $chloro_{lf}$. The demand in structural dry mass for internodes dM_{in}/dt depends on l_{in}, Φ_{in} , ρ_{in}, and for leaves dM_{lf}/dt on s_{lf} and LMA_{lf}

displayed stimulated bud outgrowth and higher starch content in primary axis median part compared to HH-treated plants (Sup. Figures 10 and 11), which is in line with results of Exp_GAP presented above.
To quantify carbon balance, we developed a dynamic plant model fitted on discrete measurements made in Exp_Mod for both LH and HH treatments (see material and methods for details). The model explicitly represents each foliated leaf, its corresponding internode, the flower plus peduncle, and the root compartment (Fig. 8). Indeed, each displayed differential growth between treatments in the previous described experiments (Fig. 6). The fast outgrowing upper axillary buds are not represented since they did not display major differences in their size 10 days after FBV. Internode photosynthesis is neglected and carbon supply at each time step corresponds to leaf photosynthesis. Carbon demand at each time step corresponds to carbon required for organ structure building (cell wall material) as described by Luquet et al. (2006). It is subdivided into growth in dimension (leaf area and internode length) and thickness (LMA, internode diameter and volumic density), that each varies differentially with light treatment.
As in the experiment described above, primary axes had less foliated phytomers in LH (mean: 7.81 leaves) than HH (mean: 8.79 leaves) in Exp_Mod. We thus estimated carbon supply and demand for primary axis with 9 and 8 foliated phytomers for HH and LH, respectively. Estimated individual leaf and internode expansion displayed similar patterns than those in the experiment described above. For both light treatments, the first four phytomers had almost finished their growth at FBV, and only the upper phytomers undertook most of their extension after FBV (Fig. 9A, B,C,D). For LH, upper phytomer extension was lower compared to HH. Indeed, upper leaves displayed a lower increase rate in their area (≥ 5) and upper internodes a lower elongation rate (≥ 7) for LH compared to HH (Fig. 9A,B) and this led to lower final internode length and leaf area (Fig. 9C,D). However, on the contrary to observations in the experiment above, the expansion period of the last leaf of LH-treated plants was delayed compared to the corresponding leaf in HH-treated plants.
Except for the diameter of the most basal internode bearing a foliated leaf, thickening of leaves (LMA) and internodes (diameter and volumic density) was not followed in the experiment described above. Estimations made on Exp_Mod data showed that internode diameter increased for all phytomers, that the increase rates were stronger for upper than lower phytomers, and the rates were lower for LH compared to HH, which is in line with the observation on the first internode (Fig. 9F). Structural LMA and internode volumic density also increased with time with higher increase rates for upper phytomers (Fig. 9E,G). Values were globally lower for LH compared to HH, as described previously. But, increasing rates did not display much differences between light treatments on the contrary to diameter increase rate.
As a consequence of these patterns, the structural mass increase rates of leaves and internodes were lower for LH compared to HH (Fig. 10). The structural masses of the flower plus peduncle, and roots were correlated to leaf structural mass for each light treatment (Supp Fig 12), and the increase rate for

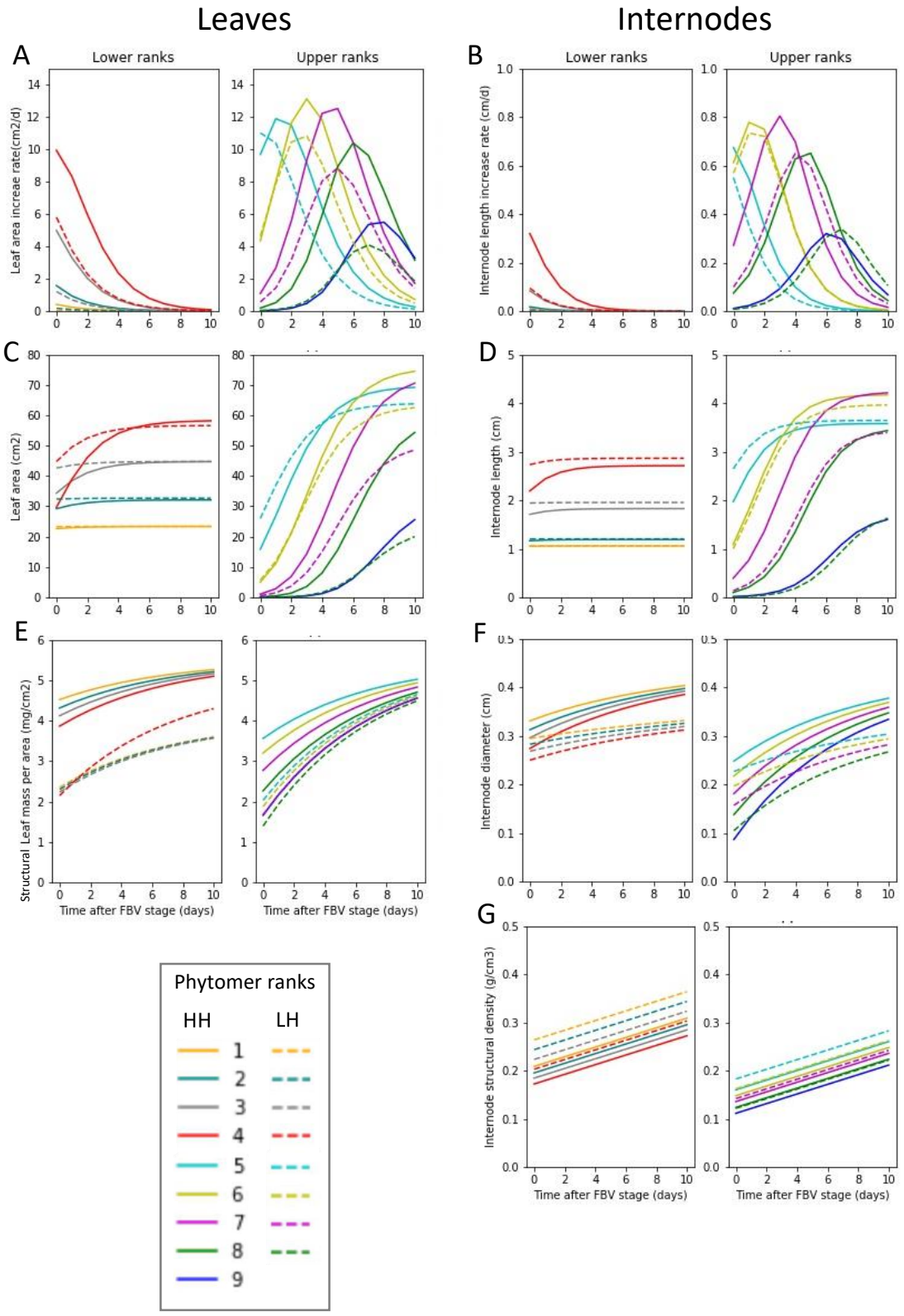

Figure 9 : Estimated leaf and internode expansions, and diameter growth of internodes were reduced for LH treatment in Exp_Mod. Estimations of the growth of individual leaves and internodes during the 10 days following FBV, for plants of LH (dotted lines) and HH treatments (continued lines). Kinetics of A/ leaf area increase rate, B/ internode elongation rate, C/ leaf area, D/ internode length, E/ structural leaf mass per unit area, F/ internode diameter, and G/ internode structural volumic mass for each foliated phytomer rank, counted from the base. “Lower ranks” refer to the 4 most basal foliated leaves and corresponding internodes. “Upper ranks” refer to organs with a rank ≥5. HH plants have 9 leaves, whereas LH plants have 8 leaves. Estimations were made on Exp_Mod data.

these compartments were thus also lower for LH compared to HH (Fig. 10). However, among leaves, internodes, flower plus peduncle, and roots, the largest fraction of the mass was represented by leaves. Altogether, these results indicate that structural growth and thus carbon demand is lower under LH compared to HH and that the lower leaf extension rate of the upper leaves could be the main determinant process.

LH-treated plants displayed higher estimated leaf surfacic photosynthesis, but lower total photosynthesis and lower carbon balance than HH-treated plants.

We modelled each leaf photosynthesis as a function of (i) its area, (ii) its photosynthetic capacity, and (ii) its ambient light intensity. Photosynthetic capacity, expressed as photosynthesis at saturating light intensity (Pmax), was estimated to increase with leaf maturity and leaf rank. LH treatment reduced Pmax increase with leaf maturity compared to HH, leading to lower photosynthetic capacity for all leaves after FBV (Figure 11A). This is consistent with the measured lower photosynthesis at 400 $\mu mol.m^{-2}.s^{-1}$ in LH for a basal foliated leaf 2 in Exp_GAP (Fig. 7A). The ambient light intensity of a given leaf depended on the cumulative leaf areas above the leaf. On the contrary to photosynthetic capacity, LH treatment increased leaf ambient light intensity compared to HH after FBV (Figure 11 B), due to the lower expansion of upper leaves (Figure 9C). This was observed only after FBV+3 days for basal leaves ($\leq$4), due to the estimated higher cumulative areas above (leaves 3, 4, 5) for LH compared to HH, between FBV and FBV+3 days (Fig. 9C). For upper leaves, which made most of their extension after FBV, ambient light intensity differences between treatments were gradually acquired with area development (Figure 11 B).

Leaf surfacic photosynthesis was calculated from Pmax and leaf ambient light intensity. For lower ranks corresponding to well-developed leaves (<4), the pattern through time and between light treatments followed that of ambient light intensity, and surfacic photosynthesis was higher for LH than HH plants after FBV+3 days (Figure 11C). For upper ranks, observed patterns were more complex and more impacted by Pmax patterns. From FBV, surfacic photosynthesis increased during the first stage of leaf development (until 2,4 and 5 days after FBV for leaves 5,6,7 respectively) and values were lower for LH compared to HH due to lower Pmax values for LH and quite similar light intensity values. Later during leaf development, surfacic photosynthesis of leaves 5,6,7 tended to drop due to ambient light intensity decrease and this was more pronounced for HH, leading to a higher surfacic photosynthesis for LH compared to HH. To sum up these results, except during the first days after FBV, leaf surfacic photosynthesis was higher for LH compared to HH for most leaves, mainly due to higher ambient light intensity. However, despite higher surfacic photosynthesis, estimated total leaf photosynthesis of the primary axis was lower for LH compared to HH after FBV+2 days (Figure 12A). Higher surfacic photosynthesis in LH was indeed not able to compensate for the lower leaf areas observed in this treatment.

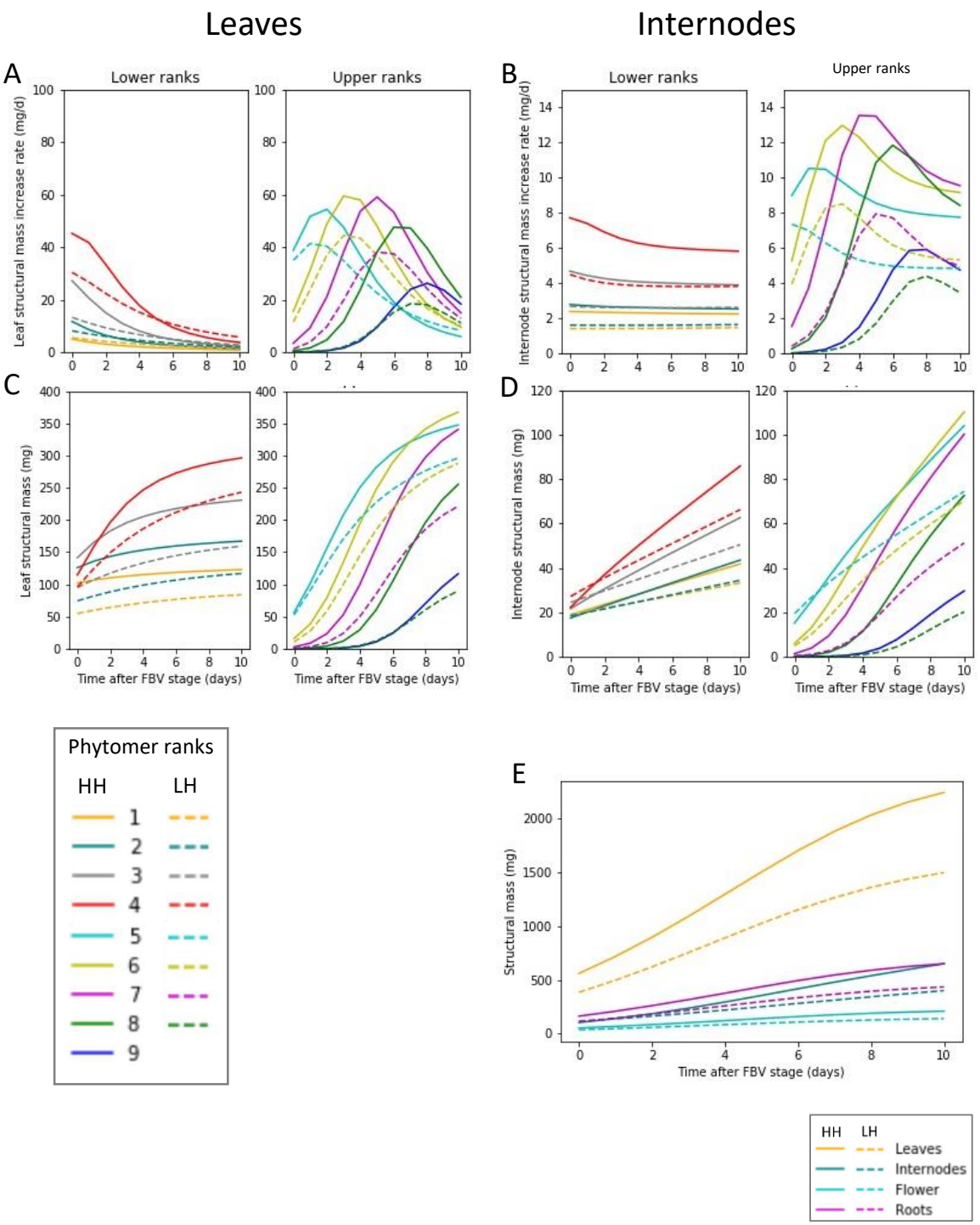

Figure 10 : Estimated structural mass growth of leaves, internodes, roots, and flower were reduced for LH treatment in Exp_Mod. Estimations of the growth of individual leaves and internodes during the 10 days following FBV, for plants of LH (dotted lines) and HH treatment (continued lines). Kinetics of A/ leaf structural mass increase rate, B/ internode structural mass increase rate, C/ leaf structural mass, D/internode structural mass, for each foliated phytomer counted from the base. E/ Kinetics of total structural masses of leaves, internodes, roots, and flower. “Lower ranks” refers to the 4 most basal foliated leaves and corresponding internodes. “Upper ranks” refers to organs with a rank ≥5. HH plants have 9 leaves, whereas LH plants have 8 leaves. Estimations were made on Exp_Mod data.

Altogether, dynamic estimations made on Exp_Mod demonstrate that LH-treated plants displayed both lower carbon supply and lower carbon demand after FBV. However, quantification of carbon supply and demand showed that the differences between LH and HH treatments in carbon supply was less pronounced that carbon demand, leading to a higher carbon balance for LH compared to HH-treated plants (Figure 12B). This estimation is in accordance with the higher sugar status of LH-treated plants compared to HH-treated plants (Fig.3).

DISCUSSION

Light is a major regulator of the outgrowth of axillary buds. Some studies assumed that light intensity, as a promoter of photosynthesis, induces bud outgrowth due to enhanced sugar availability for buds, and such process was included in some computer models (Luquet et al., 2006; Evers et al., 2010; Schneider et al., 2019 for review). However, such sugar involvement was speculative and non-yet validated by physiological experiments. In addition, recent data indicate a central role for cytokinins (CK) in bud outgrowth regulation by its ambient light intensity, while no involvement for sugars has been found (Roman et al., 2016; Corot et al., 2017). Based on an approach combining experiments and modelling, our study demonstrates that sugar plays a central role in bud outgrowth stimulation after rose primary axes were submitted to temporary light limitation. This light treatment induces a restriction of primary axis growth and thus of its sugar demand for growth, which stimulates sugar availability for buds.

A temporary light intensity limitation during the primary axis construction leads to irreversible effects on its organs growth

Light acts as a signal that regulates a number of plant morphological and architectural characteristics besides the number of buds that grow out to form new axes (*e.g.* Chenu et al., 2005; Lafarge et al., 2010; Pallas and Christophe, 2015). In addition, irreversible effects of early light limitation were reported on the subsequent growth of a leaf, in terms of expansion and mass per unit area (Granier and Tardieu, 1999; Sims and Pearcy, 1992; Oguchi et al., 2005). We highlight an irreversible effect of early light limitation during a rose axis development on the subsequent growth of all its organs, *i.e.* leaves, internodes, roots, and flower. All displayed reduced dry masses at the end of primary axis growth, including organs growing mainly under comfort light such as the flower, leaves and internodes.

For leaves and internodes, dry mass reduction was partly the result of a reduction of their expansion rate and final length at upper positions on rose primary axes. All these organs initiated their development under light limitation phase, but expanded mostly under light comfort, underlying the role of light applied at early leaf or internode developmental stage in setting out subsequent expansion rate. In contrast, expansion rate and final length of basal organs were not reduced. These organs were pre-formed in the initial bud of the cutting, from which rose plants emerged, and did not experience any light limitation at their early developmental stage. Such impact of early light limitation on subsequent

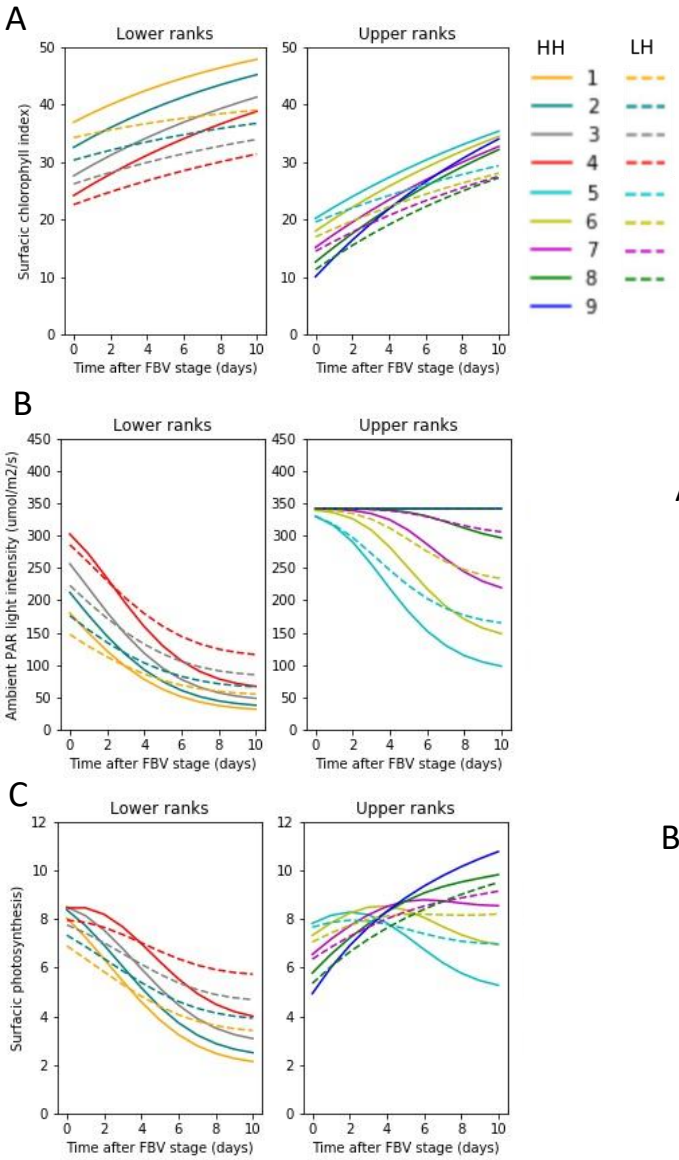

Figure 11 : Estimated leaf photosynthesis-related variables were complexly regulated by light treatments in Exp_Mod. Estimations of leaf photosynthesis-related variables during the 10 days following FBV, for plants of LH (dotted lines) and HH treatment (continued lines). Kinetics of A/ photosynthesis rate at saturatin light intensity, B/ ambient light intensity and C/ leaf surfacic photosynthesis. “Lower ranks” refers to the 4 most basal foliated leaves and corresponding internodes. “Upper ranks” refers to organs with a rank ≥5. HH plants have 9 leaves, whereas LH plants have 8 leaves. Estimations were made on Exp_Mod data.

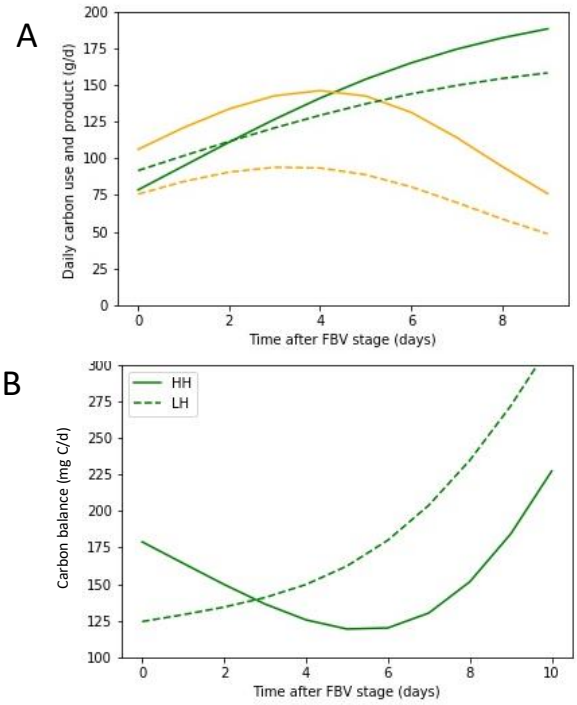

Figure 12 : Total structural mass growth was estimated to be more reduced by LH treatment than leaf photosynthesis, leading to a stimulated carbon balance. Simulations of the impact of the LH treatment on structural mass growth and daily total photosynthesis during the 10 days following FBV, for plants of LH (dotted lines) and HH treatment (continued lines). Kinetics of A/ the daily photosynthesis derived carbon (green), and of the daily use of carbon for structural mass synthesis (yellow). B/ Plant carbon balance. Estimations were made on Exp_Mod data.

expansion rate was reported for a sunflower leaf (Granier and Tardieu, 1999). It was mainly related to a reduction of the relative cell division rate, which takes place during the early stage of leaf development. The low cell pool to be expanded results in an overall low leaf expansion rate. Light-mediated cell division control could involve sugar and hormones (CKs), that are both the main regulators of cell division and are controlled by light (Van Dingenen, 2019; Wang and Ruan, 2013, for review; Skylar et al., 2011; Peng et al., 2014; Li et al., 2017). In line with a role of sugars, links were reported between photosynthesis and the cellular processes during early leaf growth (Andriankaja et al. 2012; Lastdrager et al. 2014; Van Dingenen et al. 2016). In Arabidopsis, Xiong et al. (2013) revealed that shoot photosynthesis-derived glucose drives target-of-rapamycin (TOR) signaling through glycolysis and mitochondrial bioenergetics to activate root meristematic activity.

Besides reduced expansion rate at upper positions, internodes and leaves except those at the most upper positions, displayed reduced diameter and leaf mass per unit area (LMA), respectively, after temporary light limitation. These organs achieved most of their growth under light limitation, indicating a light control of LMA and internode not restricted to the early development stage. An impact of light limitation during leaf growth on LMA once leaf is mature was previously reported (Sims and Pearcy, 1992; Oguchi et al., 2005). Light control of LMA could occur through modulation of the volume of the palisade parenchyma and leaf thickness. They are controlled by light (Poorter et al., 2009 for a review), and hardly increased after the transfer of mature leaves from light limitation to light comfort (Oguchi et al., 2005). Besides leaf thickness, the concentration in non-structural carbohydrates in leaves positively controls LMA and, in this way, LMA was reported to be controlled by plant carbon status (Poorter et al., 2009 for a review; Bertin and Gary, 1998; Bertin et al., 1999). Such control of LMA is not true in our case, since the lower LMA acquired after growth under light limitation was maintained despite high plant carbon status. A similar process of thickness adaptation occurred for rose internodes, which displayed diameter reduction when grown under temporary light limitation compared to continuous light comfort.

A temporary light intensity limitation during the primary axis development affects future leaves photosynthesis

During leaf development, light limitation-driven morphological changes results in a lower photosynthetic capacity, that can be hardly increased in response to plant transfer to comfort light conditions (Oguchi et al., 2015). Similarly, we reported lower leaf photosynthesis and chlorophyll content for rose leaves grown under temporary light limitation and then transferred to comfort light, compared to leaves grown permanently under comfort light. In addition, we assessed for the first time the impact of temporary light limitation on photosynthesis at the plant scale. Photosynthesis was lower after temporal light limitation, as expected from the lower photosynthetic capacities and lower leaf photosynthetic areas.

Reduced carbon (C) demand for the primary axis organs growth imbalances the source-sink ratio and leads to starch accumulation

Numerous studies have shown the impact of architectural and morphological modifications of the plant on its carbon status (e.g., Fanwoua et al., 2014; Cieslak et al., 2011). Here, we show that rose morphological changes caused by temporary light limitation were accompanied by starch accumulation in the plant. Starch accumulation in sink organs is the result of many processes responsible for the establishment of plant carbon status and including sink strength activity, starch remobilization and/or sugar export from source leaves (McNeill et al., 2017). To better understand the cause of starch accumulation observed after temporary light limitation in rose, we used a modelling approach that formalizes plant C status as the balance between C supply by photosynthesis and C demand for organ growth, as previously conducted in different biological contexts (*e.g.* Pallas et al., 2013; Jullien et al., 2011). In contrast with most models, which formalize C demand as a potential growth in dry mass irrespectively of the environmental conditions (*e.g.* Allen et al., 2005; Evers et al., 2010; Letort et al., 2009; Mathieu et al., 2009; Pallas et al., 2010; Lescourret et al., 2011), our model is based on a new concept for C demand formalization. Indeed, we need to account for a limitation of C demand by limited organ growth in response to low light exposure. Thus, we formalized C demand as carbon required for organ structure building, which is dependent on organ sizes (length and thickness), themselves controlled by light intensity. Supporting this new concept of demand formalization, we could simulate well starch accumulation after temporary light limitation in rose, compared to permanent comfort light. We demonstrate that this starch accumulation is the result of a lower negative effect of a light temporary limitation on the photosynthesis-mediated C supply compared to the C-demand related to the structural growth of the organs. This imbalance in favor of source leads to carbon excess that plant may convert into starch.

Bud outgrowth stimulation is correlated to higher starch contents in the vicinity of the bud

Sugar promoting effect on bud outgrowth was demonstrated till now by exogenous soluble sugar supply, and by close correlations with soluble sugars content in bud and its outgrowth (Henry et al., 2011; Mason et al., 2014; Barbier et al., 2015; Fichtner et al., 2017; Bertheloot et al., 2020). We demonstrated here a positive correlation between stem-located starch reserve and bud outgrowth promotion. Similarly, it was reported a close correlation between low starch reserves in rose stem and repressed bud outgrowth under low light intensity (Corot et al., 2017). The available data indicate that starch accumulates in bud shortly before the onset of its outgrowth (Maurel et al., 2004; Bonhomme et al., 2010; Girault et al., 2010). In contrast, the link between starch reserve in the stem and bud outgrowth ability remains unknown. Two non-exclusive hypotheses would be possible. Firstly, the high starch in stem might play a trophic role as “sugar source” when sugar is needed for sustaining organ growth. In perennial plant, the stem-stored starch is remobilized during unleafy period (at the end of ecodormancy) to sustain bud outgrowth (Bonhomme et al., 2010). The highly stored starch at the base of developing flowers as well as in

stamens, would be critical for reproductive development, by avoiding flower abortion under unfavorable environmental conditions (McNeil et al., 2015). Secondly, this starch accumulation could act as a marker of the whole-plant carbon status that mediates source-sink interaction. In this context, starch accumulation-governing processes would be sensed individually or collectively by plant to adjust its growth and development. For example, Arabidopsis mutants deficient in starch production (*adg1*, *pgi1*, *pgm1*) or degradation (*sex1*, *cam1*) all show late flowering phenotypes (Eimert et al., 1995; Corbesier et al., 1998), indicating that starch metabolism is sensed by the plant before the onset of the floral transition (MacNeil et al., 2017). In maize, loss-of-function id1– (INDETERMINATE), a nuclear-localized zinc finger protein, results in accumulation of leaf sucrose and starch, and an extreme delay in flowering (Colasanti et al., 1998; Coneva et al., 2007, 2012), pointing out that carbon export sensing is required for initiation of the reproductive state. Based on these findings, similar process cannot be excluded for bud outgrowth because rose stem-located starch accumulation is tightly linked to sugar supply (Barbier et al., 2005), which is able to antagonize the inhibitory effect of auxin on bud outgrowth through repression of strigolactone pathway (Bertheloot et al., 2020). All these findings open the avenue to address the exact role of the stem-stored starch metabolism in the regulatory network of shoot branching adjustment process.

Light effect on bud outgrowth is complex and involves cytokinins and sugars related pathways depending on light conditions

A recent study on rose demonstrated the main role of CK in bud outgrowth for rose plants transferred from comfort light to light limitation before bud outgrowth period (Roman et al., 2016; Corot et al., 2017). Here, many evidence support a central role of sugar in bud outgrowth promotion after plants were temporary exposed to light limitation. Firstly, compared to those continually placed under comfortable light condition, those experienced temporary light limitation exhibited concurrently more bud outgrowth and starch accumulation in vegetative organs (leaves and stem) of the primary axis. In consistence with this, a temporary shading period applied early during the growth of rice plants was followed by tillering stimulation and sugar accumulation at rates above those observed without temporal shading period (Lafarge et al., 2010). Secondly, decreasing sugar source by inhibiting photosynthesis prevented the stimulation of bud outgrowth observed for rose plants after temporal shading. Thirdly, increasing sugar availability by exogenous sucrose supply to plants under continuous comfortable light intensity stimulated bud outgrowth. These results, acquired in two different experimental situations, highlight the role of two distinct regulators in the effect of light intensity on bud outgrowth: CKs and sugars, that both act as inducers of bud outgrowth (Barbier et al., 2015 ; Bertheloot et al., 2019 ; Wang et al., 2019). This raises the question of the respective role of these two regulators in light intensity-dependent bud outgrowth regulation. In case of rose plants transfer from comfort light to light limitation, no stimulation

of bud outgrowth was observed in response to exogenous sucrose supply locally through the stem or through leaf petioles while exogenous CK supply locally to the bud or the stem did (Roman et al., 2016; Corot et al., 2017). It was hypothesized that the limiting amount of CKs prevents sugar to promote bud outgrowth by limiting bud sink strength for sugars (Roman et al., 2016; Schneider et al., 2019 for review). This supports the prevailing role of CK in sink strength establishment within plant (Roitsch and Ehneß, 2000). Alternatively to this hypothesis, which highlights a preferential role of CK compared to sugar, we can also suppose that the two regulators act in a complementary way, but the state of the plant is unfavorable after plants transfer from comfort light to light limitation which prevents any visible effect of localized exogenous sucrose supply. On the one hand, the low photosynthesis generated by light limitation compared to high sugar demand of organs initiated under comfort light could divert the exogenously and locally supplied sugar towards the high demand of growing organs (i.e. apical part of plant), and thus does not increase plant overall sugar status and sugar availability in bud neighborhood. On the other hand, these plants displayed low stem CK contents, which could imply a strong increase in the plant sugar status to compensate the low CK levels. On the contrary, plants permanently grown under comfort light have a favorable sugar and CK state, which could explain the ability of exogenous sucrose supply to promote bud outgrowth.

Conclusion

The outgrowth of axillary buds is a major process of plant adaptation to environment, and in particular to the amount of light energy the plant receives (Schneider et al., 2019). It is regulated by a complex physiological network, involving hormones and sugar, which act in a dose-dependent manner on the bud (Bertheloot et al., 2020). Recent data have highlighted a local pathway of light, which involves a modulation of the production of stem CKs, a stimulator of bud outgrowth (Roman et al., 2016; Corot et al., 2017). We demonstrate a systemic pathway which involves the regulation of the balance between sugar supply and use within the plant, and thus sugar availability for the buds. Further studies are needed to identify if such systemic regulation occurs whatever light treatment, its relationship with the CK-mediated regulation, and the way by which the overall plant sugar status is perceived by the bud. In addition, our results open the way for studying the role of sugars in the effect of other environmental factors, such as water supply or the quality of light, which also regulate plant development and thus plant sugar status.

CHAPTER 1- SUPPLEMENTARY DATA

Supplementary figure 1 : Bud development stages. A/Pointing axillary bud, before outgrowth. B/ Outgrown bud with the first leaf visible.

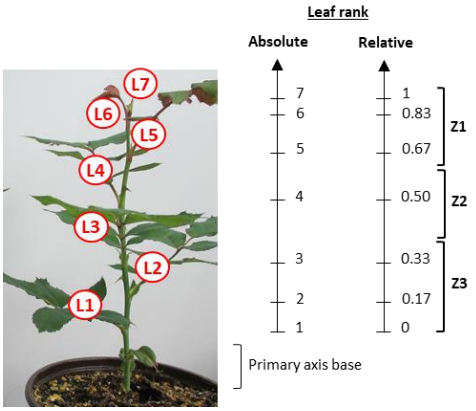

Supplementary figure 2 : Absolute and relative leaf ranks. Example with a 7 leaves plant.

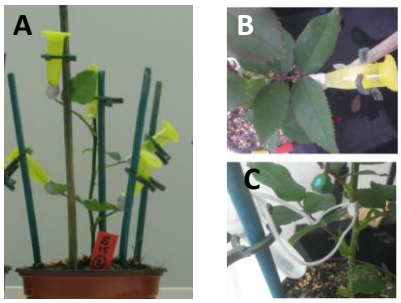

Supplementary figure 3 : Exogenous sugar supply. Sugar supply through the petiole of the A/ fourth most basal, partially defoliated, leaves of decapitated plants , or B/ highest Z3 leaf of intact plants. C/ Sugar supply directly to the stem of intact plants with the cotton-wick method.

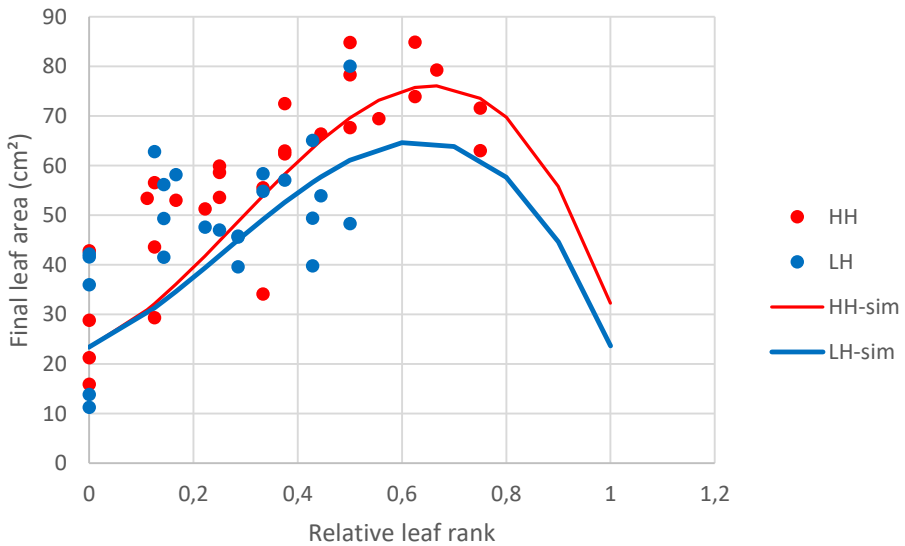

Supplementary figure 4 : Quality of fittings to leaf variables. Simulated (continued lines) versus experimental (points) final leaf areas depending on relative leaf rank, for HH (red) and LH (blue) treatments. Data are from Exp_Mod, and each point is a destructive measurement. Simulations with parameter values presented in Table 1.

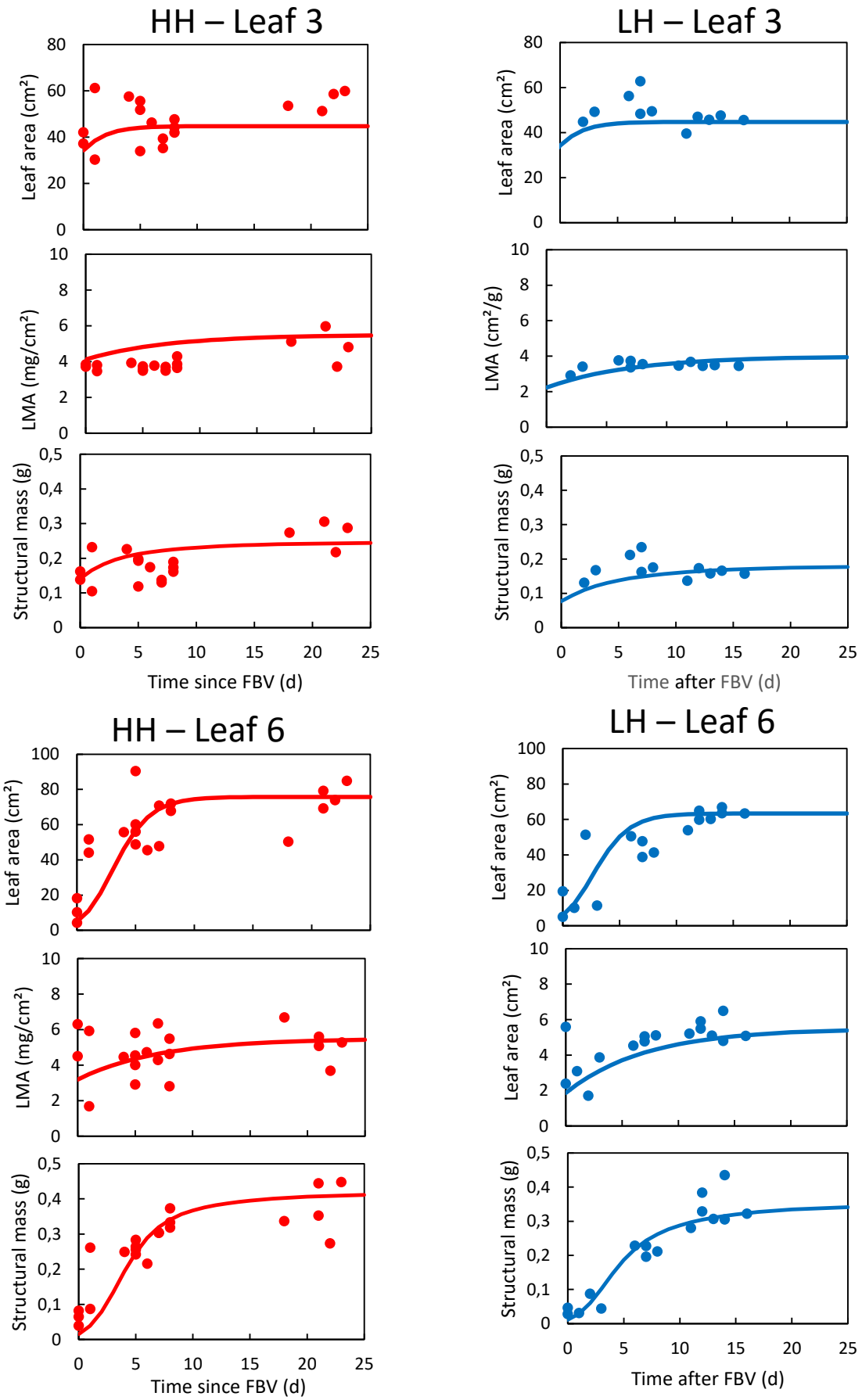

Supplementary figure 5 : Quality of fittings to leaf variables. Simulated (continued lines) versus experimental (points) leaf area, LMA and structural mass of ranks 3 and 6 leaves, for HH (red) and LH (blue) treatments. Data are from Exp_Mod, and each point is a destructive measurement. Simulations with parameter values presented in Table 1.

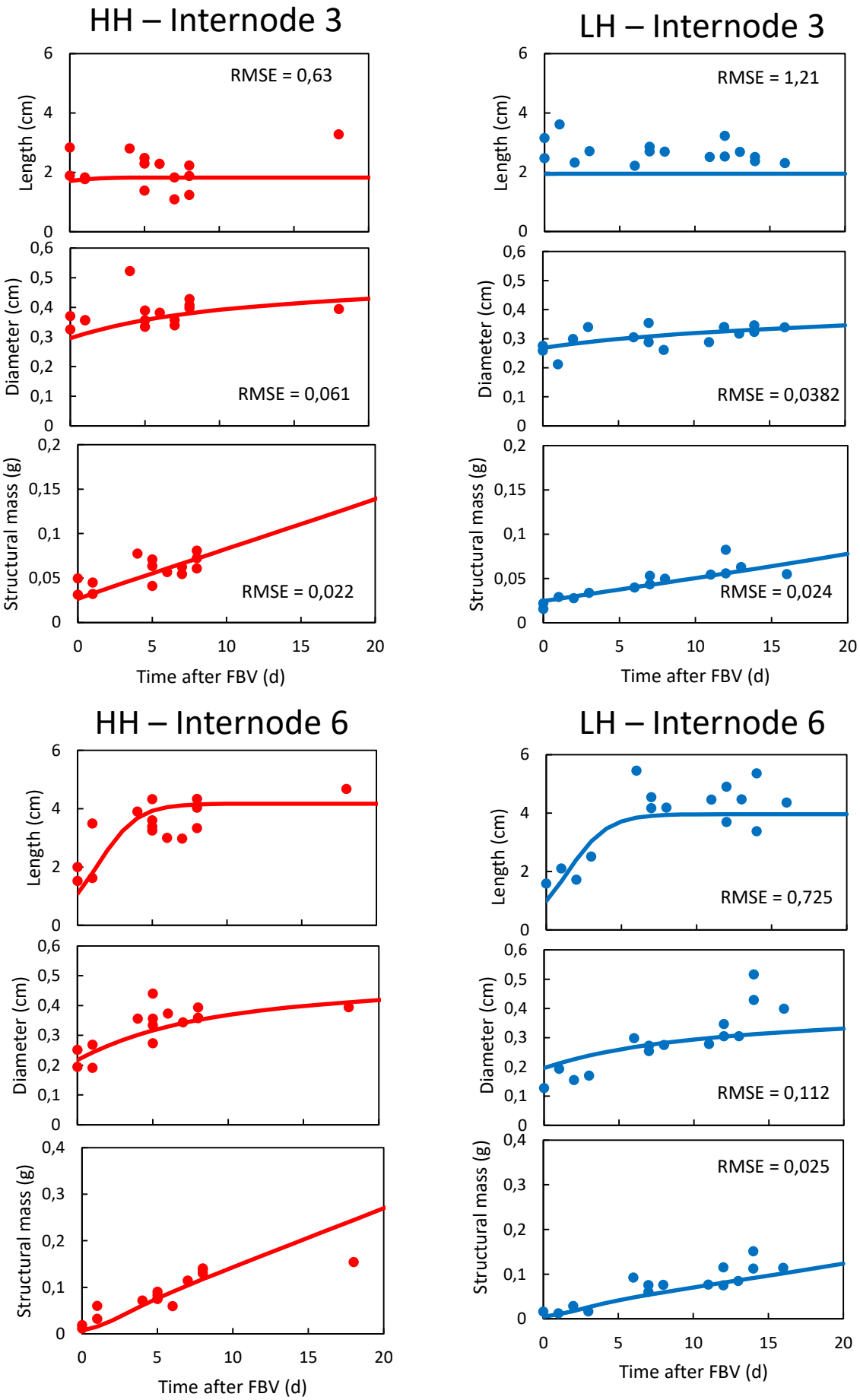

Supplementary figure 6 : Quality of fittings to internode variables. Simulated (continued lines) versus experimental (points) internode length, diameter and structural mass of ranks 2 and 6 internodes, for HH (red) and LH (blue) treatments. Data are from Exp_Mod, and each point is a destructive measurement. Simulations with parameter values presented in Table 1.

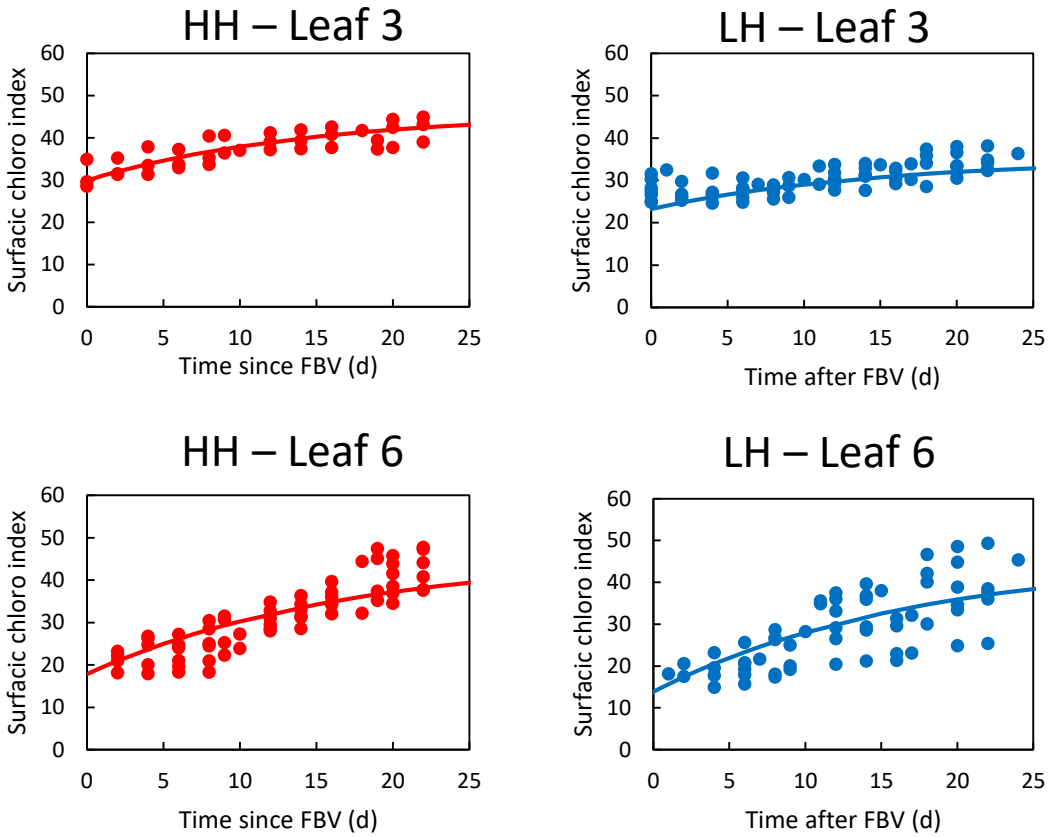

Supplementary figure 7 : Quality of fittings to surfacic chlorophyll contents. Simulated (continued lines) versus experimental (points) internode length, diameter and structural mass of ranks 2 and 6 internodes, for HH (red) and LH (blue) treatments. Data are from Exp_GAP (dualex). Simulations with parameter values presented in Table 1.

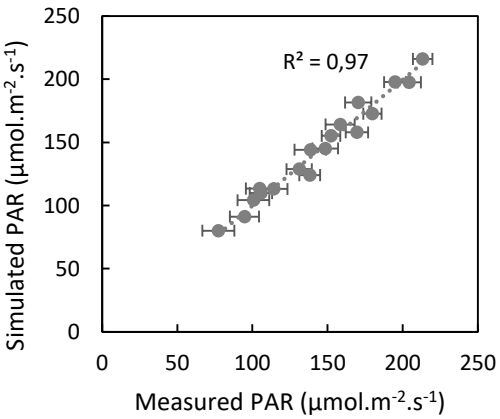

Supplementary figure 8 : Fitting quality of the PAR intensity simulations. Experimental values are means ± SEM of 14 plants) from Exp_GAP, for different positions along the stem and during the 10th days following FBV for HH and LH plants. Simulations with parameter values presented in Table 1.

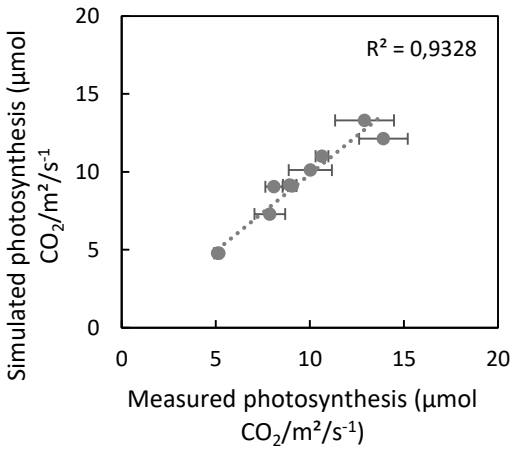

Supplementary figure 9 : Fitting quality of the surfacic photosynthesis simulations. Experimental values are means ± SEM of the second leaf of 4 plants from Exp_GAP, during the 10th days following FBV for HH and LH plants. Simulations with parameter values presented in Table 1.

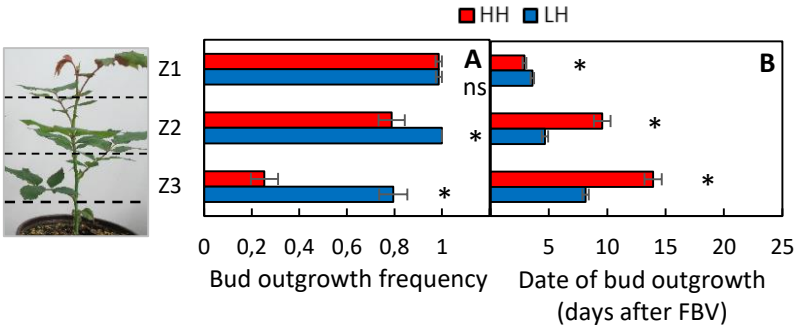

Supplementary figure 10 : Temporary PAR intensity restriction stimulates bud outgrowth in primary axis median parts. Impact of LH and HH treatments on the outgrowth frequency observed at FBV+14d (A, C) and on the date of outgrowth (B, D) of leaf-bearing buds belonging to different zones along the primary axis (zones Z1 : apical, Z2: medial, Z3: proximal). Values are means of at least ## plants (Exp_Mod) per treatment ± SEM. Asterisks indicate significant differences between LH and HH treatments (exact Fisher test : $P < 0.05$).

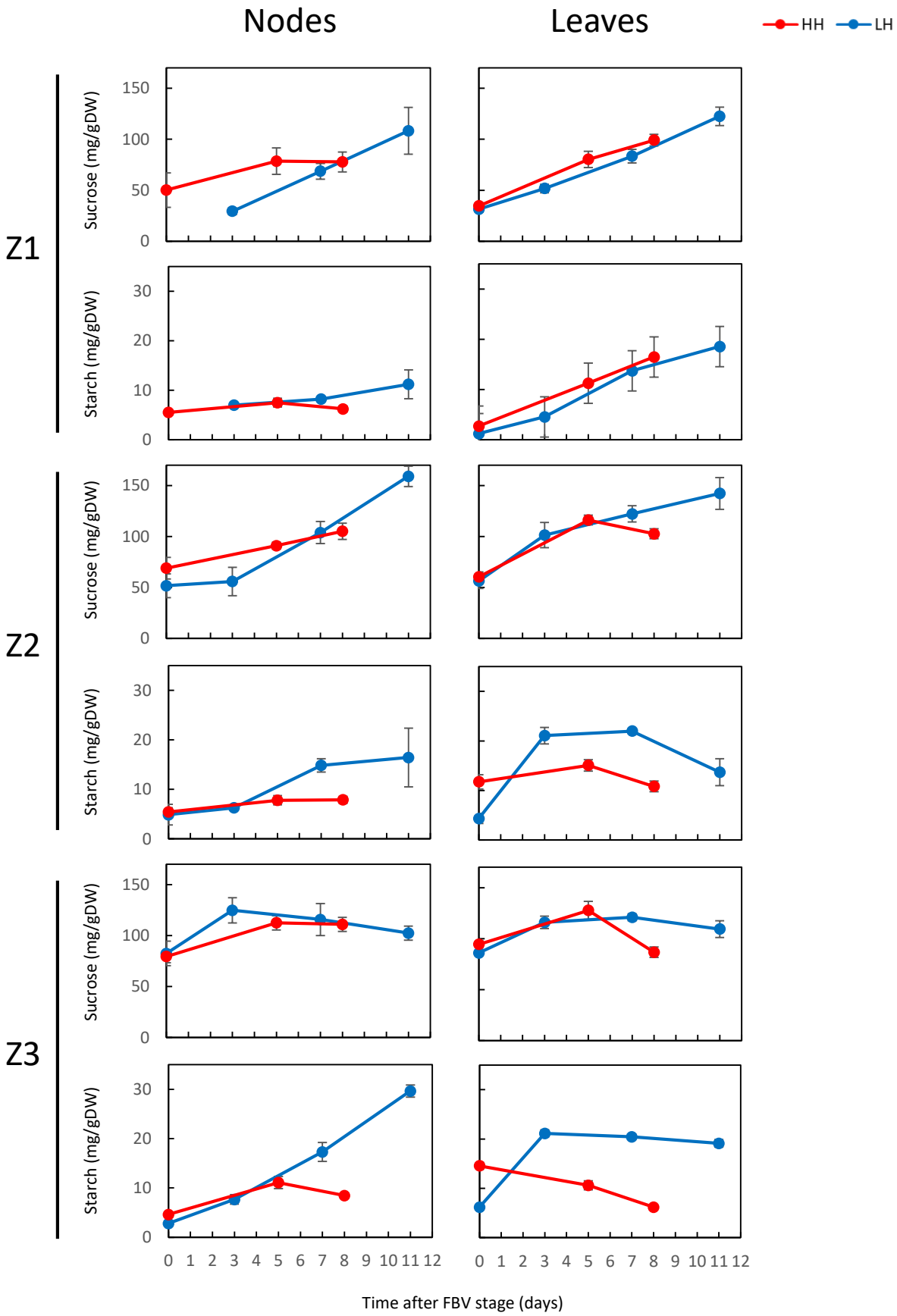

Supp Figure 11 : Temporary light intensity restriction stimulates sugar accumulation as starch in the median and basal zones of the primary axis. Impact of the LH and HH light treatments on sucrose and starch contents in the nodes and leaves after FBV. Three different zones (Z1, Z2 and Z3) along the primary axis were distinguished for leaves and nodes sampling. Data from Exp_Mod. Data are means of at least three plants ± SEM.

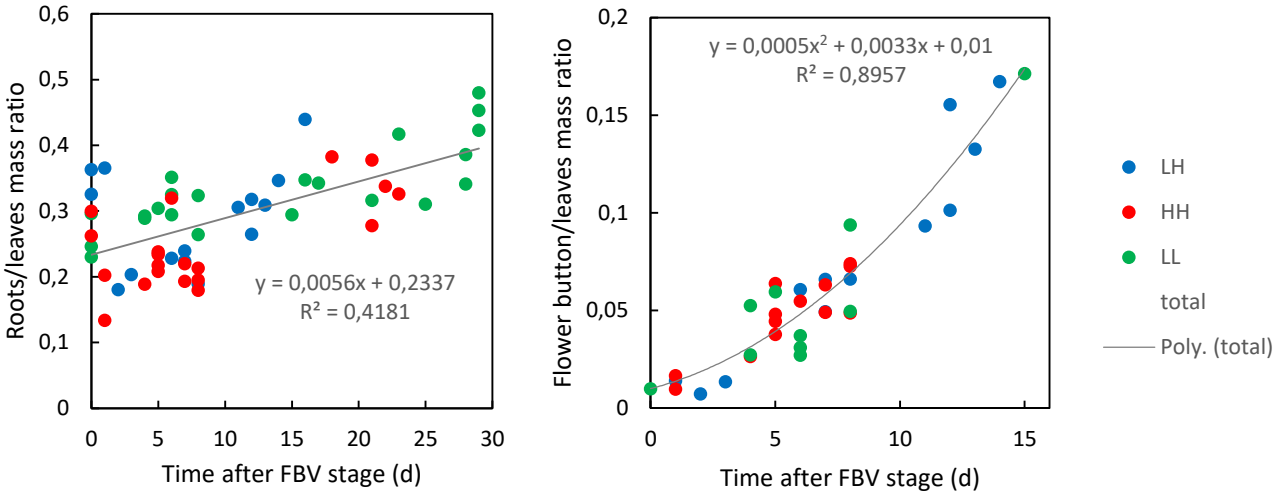

Supplementary figure 12 : Fitting quality of the roots/leaves and button flower/leaves mass ratio . Experimental values are from destructive measurements under LH, HH and LL (a continuous low light treatment) in Exp_Mod.

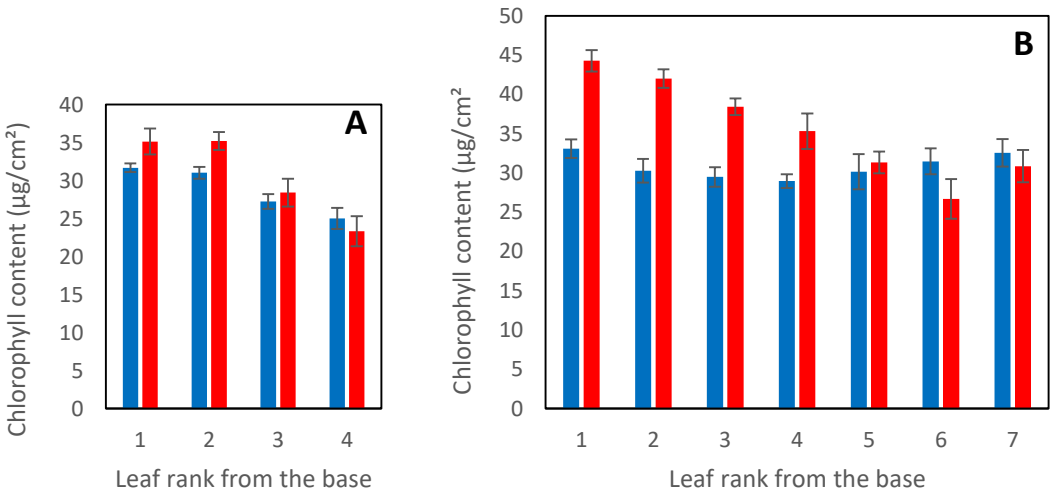

Supplementary figure 13: Impact of light intensity treament on leaf chlorophyll content of leaves of entire plants at FBV (A) and FBV+7d (B). Data are means of at least 5 plants +/- SEM (Exp_PAG).

Supp. Table 1: definitions, units and values of parameters

Dimensions of the primary axis organs						
Function	Equation	Description	Parameter	Value		Unit
				HH	LH	
Internode length (l_{in})	2	Maximal relative elongation rate	w_{in}	0.19		d^{-1}
Date of internode inflexion point (t^*_{in})	5		a_{in}	1.34		d^{-1}
			b_{in}	-7.75	-13.61	d
Maximal internode length (L_{in})	7		c_{in}	-14.42	-15.47	cm
			d_{in}	19.24	17.35	cm
			e_{in}	-1.32		cm
			f_{in}	0.83		cm
Internode diameter (Φ)	8-9	Initial diameter	Φ_0	0.03		cm
		Initial diameter increase rate	V_Φ^{init}	$5.4e-2$	$4.0e-2$	$cm.d^{-1}$
		Final diameter increase rate	V_Φ^{min}	$2e-3$		$cm.d^{-1}$
			r_Φ	0.15		d^{-1}
Leaf area (s_{lf})	1 ; 3	Maximal relative expansion rate	w_{lf}	0.146		d^{-1}
Date of leaf inflexion point (t^*_{lf})	4		a_{lf}	-2.08e-2		d^{-1}
			b_{lf}	1.62		Unitless
			c_{lf}	-8.25	-14.10	d
Maximal leaf area (S_{lf})	6		d_{lf}	-260.10	-208.91	cm^2
			e_{lf}	222.99	163.14	cm^2
			f_{lf}	46.01		cm^2
			g_{lf}	23.374		cm^2
		Corrective parameter between 2018 and 2011	$k_{S_{lf}}$	1.45		Unitless

Photosynthesis						
Function	Equation	Description	Parameter	Value		Unit
				HH	LH	
Surfacic photosynthesis (P)	10		α	7.35e-2		$m^2.s.\mu mol^{-1}$
Surfacic photosynthesis at saturation (P_{sat})	11		P_1	0.7867		$\mu mol.m^2.s^{-1}$
			P_2	3963.17		$\mu mol.m^2.s^{-1}$
			K_{chloro}	7419.83		$mmol.m^{-2}$
Chlorophyll ($chloro$)	12	Initial chlorophyll content at leaf appearance	$chloro_{app}$	5.0		$mmol.m^{-2}$
		Maximal chlorophyll content	$chloro_{max}$	46.0	35.1	$mmol.m^{-2}$
Rate of chlorophyll content increase r_{chloro}	13		a_{chloro}	9.99e-1		d^{-1}
			b_{chloro}	-0.1198		d^{-1}
			c_{chloro}	9.27e-2		d^{-1}
Light intensity gradient (I)	14		k_1	0.747		Unitless
			k_2	0.554		cm^{-2}

Structural mass of the primary axis organ						
Function	Equation	Description	Parameter	Value		Unit
				HH	LH	
Volumic structural mass (ρ)	18	Initial density	ρ_{app}	0.10		$g.cm^{-3}$
		Rate of density increasing	v_ρ	0.015	0.010	$g.cm^{-3}.d^{-1}$
Structural leaf mass per area (LMA)	16	Initial LMA	LMA_{app}	1.00		$mg.cm^{-2}$
		Maximal LMA	LMA_{max}	5.50	2.50	$mg.cm^{-2}$
		Rate of LMA increasing	r_{LMA}	0.14		d^{-1}
Flower button mass (M_{flw})	19		a_{flw}	5.0e-4		d^{-2}
			b_{flw}	3.3e-3		d^{-1}
			c_{flw}	1.0e-2		Unitless
Roots mass (M_{flw})	20		a_{root}	5.6e-3		d^{-1}
			b_{root}	2.337e-1		Unitless

REFERENCES

Allen, M.T., Prusinkiewicz, P., and DeJong, T.M. (2005). Using L-systems for modeling source–sink interactions, architecture and physiology of growing trees: The L-PEACH model. New Phytologist 166, 869–880.

Andriankaja, M., Dhondt, S., De Bodt, S., Vanhaeren, H., Coppens, F., De Milde, L., Mühlenbock, P., Skirycz, A., Gonzalez, N., and Beemster, G.T. (2012). Exit from proliferation during leaf development in Arabidopsis thaliana: a not-so-gradual process. Developmental Cell 22, 64–78.

Barbier, F., Péron, T., Lecerf, M., Perez-Garcia, M.-D., Barrière, Q., Rolčík, J., Boutet-Mercey, S., Citerne, S., Lemoine, R., Porcheron, B., et al. (2015). Sucrose is an early modulator of the key hormonal mechanisms controlling bud outgrowth in Rosa hybrida. J Exp Bot 66, 2569–2582.

Barbier, F.F., Dun, E.A., Kerr, S.C., Chabikwa, T.G., and Beveridge, C.A. (2019). An update on the signals controlling shoot branching. Trends in Plant Science 24, 220–236.

Bertheloot, J., Barbier, F., Boudon, F., Perez-Garcia, M.D., Péron, T., Citerne, S., Dun, E., Beveridge, C., Godin, C., and Sakr, S. (2020). Sugar availability suppresses the auxin-induced strigolactone pathway to promote bud outgrowth. New Phytologist 225, 866–879.

Bertin, N., and Gary, C. (1998). Short and long term fluctuations of the leaf mass per area of tomato plants—implications for growth models. Annals of Botany 82, 71–81.

Bertin, N., Tchamitchian, M., Baldet, P., Devaux, C., Brunel, B., and Gary, C. (1999). Contribution of carbohydrate pools to the variations in leaf mass per area within a tomato plant. The New Phytologist 143, 53–61.

Bonhomme, M., Peuch, M., Ameglio, T., Rageau, R., Guilliot, A., Decourteix, M., Alves, G., Sakr, S., and Lacointe, A. (2010). Carbohydrate uptake from xylem vessels and its distribution among stem tissues and buds in walnut (Juglans regia L.). Tree Physiology 30, 89–102.

BOS, H.J., and NEUTEBOOM, J.H. (1998). Morphological analysis of leaf and tiller number dynamics of wheat (Triticum aestivum L.): responses to temperature and light intensity. Annals of Botany 81, 131–139.

Buttery, B.R., and Buzzell, R.I. (1976). Flavonol glycoside genes and photosynthesis in soybeans. Crop Science 16, 547–550.

Cerovic, Z.G., Masdoumier, G., Ghozlen, N.B., and Latouche, G. (2012). A new optical leaf-clip meter for simultaneous non-destructive assessment of leaf chlorophyll and epidermal flavonoids. Physiologia Plantarum 146, 251–260.

Chenu, K., Franck, N., Dauzat, J., Barczi, J.-F., Rey, H., and Lecoeur, J. (2005). Integrated responses of rosette organogenesis, morphogenesis and architecture to reduced incident light in Arabidopsis thaliana results in higher efficiency of light interception. Functional Plant Biology 32, 1123–1134.

Cieslak, M., Seleznyova, A.N., Prusinkiewicz, P., and Hanan, J. (2011). Towards aspect-oriented functional–structural plant modelling. Annals of Botany 108, 1025–1041.

Colasanti, J., Yuan, Z., and Sundaresan, V. (1998). The indeterminate gene encodes a zinc finger protein and regulates a leaf-generated signal required for the transition to flowering in maize. Cell 93, 593–603.

Coneva, V., Zhu, T., and Colasanti, J. (2007). Expression differences between normal and indeterminate1 maize suggest downstream targets of ID1, a floral transition regulator in maize. Journal of Experimental Botany 58, 3679–3693.

Coneva, V., Guevara, D., Rothstein, S.J., and Colasanti, J. (2012). Transcript and metabolite signature of maize source leaves suggests a link between transitory starch to sucrose balance and the autonomous floral transition. Journal of Experimental Botany 63, 5079–5092.

Corbesier, L., Lejeune, P., and Bernier, G. (1998). The role of carbohydrates in the induction of flowering in Arabidopsis thaliana: comparison between the wild type and a starchless mutant. Planta 206, 131–137.

Corot, A., Roman, H., Douillet, O., Autret, H., Perez-Garcia, M.-D., Citerne, S., Bertheloot, J., Sakr, S., Leduc, N., and Demotes-Mainard, S. (2017). Cytokinins and abscisic acid act antagonistically in the regulation of the bud outgrowth pattern by light intensity. Frontiers in Plant Science 8, 1724.

Demotes-Mainard, S., Huché-Thélier, L., Morel, P., Boumaza, R., Guérin, V., and Sakr, S. (2013). Temporary water restriction or light intensity limitation promotes branching in rose bush. Scientia Horticulturae 150, 432–440.

Demotes-Mainard, S., Péron, T., Corot, A., Bertheloot, J., Le Gourrierec, J., Pelleschi-Travier, S., Crespel, L., Morel, P., Huché-Thélier, L., and Boumaza, R. (2016). Plant responses to red and far-red lights, applications in horticulture. Environmental and Experimental Botany 121, 4–21.

Dingenen, J.V., Milde, L.D., Vermeersch, M., Maleux, K., Rycke, R.D., Bruyne, M.D., Storme, V., Gonzalez, N., Dhondt, S., and Inzé, D. (2016). Chloroplasts Are Central Players in Sugar-Induced Leaf Growth. Plant Physiology 171, 590–605.

Djennane, S., HIBRAND-SAINT OYANT, L., Kawamura, K., Lalanne, D., Laffaire, M., Thouroude, T., Chalain, S., Sakr, S., Boumaza, R., and Foucher, F. (2014). Impacts of light and temperature on shoot branching gradient and expression of strigolactone synthesis and signalling genes in rose. Plant, Cell & Environment 37, 742–757.

Domagalska, M.A., and Leyser, O. (2011). Signal integration in the control of shoot branching. Nature Reviews Molecular Cell Biology 12, 211–221.

Duan, J., Yu, H., Yuan, K., Liao, Z., Meng, X., Jing, Y., Liu, G., Chu, J., and Li, J. (2019). Strigolactone promotes cytokinin degradation through transcriptional activation of CYTOKININ OXIDASE/DEHYDROGENASE 9 in rice. Proceedings of the National Academy of Sciences 116, 14319–14324.

Eimert, K., Wang, S.-M., Lue, W.I., and Chen, J. (1995). Monogenic recessive mutations causing both late floral initiation and excess starch accumulation in Arabidopsis. The Plant Cell 7, 1703–1712.

Evers, J.B., Vos, J., Yin, X., Romero, P., van der Putten, P.E.L., and Struik, P.C. (2010). Simulation of wheat growth and development based on organ-level photosynthesis and assimilate allocation. J Exp Bot 61, 2203–2216.

Fanwoua, J., Bairam, E., Delaire, M., and Buck-Sorlin, G. (2014). The role of branch architecture in assimilate production and partitioning: the example of apple (Malus domestica). Frontiers in Plant Science 5, 338.

Ferguson, B.J., and Beveridge, C.A. (2009). Roles for auxin, cytokinin, and strigolactone in regulating shoot branching. Plant Physiology 149, 1929–1944.

Fichtner, F., Barbier, F.F., Feil, R., Watanabe, M., Annunziata, M.G., Chabikwa, T.G., Höfgen, R., Stitt, M., Beveridge, C.A., and Lunn, J.E. (2017). Trehalose 6-phosphate is involved in triggering axillary bud outgrowth in garden pea (Pisum sativum L.). The Plant Journal 92, 611–623.

GAUTIER, H., Varlet-Grancher, C., and HAZARD, L. (1999). Tillering responses to the light environment and to defoliation in populations of perennial ryegrass (Lolium perenne L.) selected for contrasting leaf length. Annals of Botany 83, 423–429.

Girault, T., Bergougnoux, V., Combes, D., VIEMONT, J.-D., and Leduc, N. (2008). Light controls shoot meristem organogenic activity and leaf primordia growth during bud burst in Rosa sp. Plant, Cell & Environment 31, 1534–1544.

Girault, T., Abidi, F., Sigogne, M., PELLESCHI-TRAVIER, S., Boumaza, R., Sakr, S., and Leduc, N. (2010). Sugars are under light control during bud burst in Rosa sp. Plant, Cell & Environment 33, 1339–1350.

Granier, C., and Tardieu, F. (1999). Leaf expansion and cell division are affected by reducing absorbed light before but not after the decline in cell division rate in the sunflower leaf. Plant, Cell & Environment 22, 1365–1376.

Grashoff, C., and d'Antuono, L.F. (1997). Effect of shading and nitrogen application on yield, grain size distribution and concentrations of nitrogen and water soluble carbohydrates in malting spring barley (Hordeum vulgare L.). European Journal of Agronomy 6, 275–293.

Henry, C., Rabot, A., Laloi, M., Mortreau, E., Sigogne, M., Leduc, N., Lemoine, R., Sakr, S., Vian, A., and PELLESCHI-TRAVIER, S. (2011). Regulation of RhSUC2, a sucrose transporter, is correlated with the light control of bud burst in Rosa sp. Plant, Cell & Environment 34, 1776–1789.

Hikosaka, K., and Terashima, I. (1995). A model of the acclimation of photosynthesis in the leaves of C3 plants to sun and shade with respect to nitrogen use. Plant, Cell & Environment 18, 605–618.

Huché-Thélier, L., Crespel, L., Le Gourrierec, J., Morel, P., Sakr, S., and Leduc, N. (2016). Light signaling and plant responses to blue and UV radiations—Perspectives for applications in horticulture. Environmental and Experimental Botany 121, 22–38.

James, S.A., and Bell, D.T. (2000). Influence of light availability on leaf structure and growth of two Eucalyptus globulus ssp. globulus provenances. Tree Physiology 20, 1007–1018.

Kebrom, T.H. (2017). A growing stem inhibits bud outgrowth–the overlooked theory of apical dominance. Frontiers in Plant Science 8, 1874.

Kim, S.-H., and Lieth, J.H. (2003). A Coupled Model of Photosynthesis, Stomatal Conductance and Transpiration for a Rose Leaf (Rosa hybrida L.). Ann Bot 91, 771–781.

Lafarge, T., Seassau, C., Martin, M., Bueno, C., Clément-Vidal, A., Schreck, E., and Luquet, D. (2010). Regulation and recovery of sink strength in rice plants grown under changes in light intensity. Functional Plant Biology 37, 413–428.

Lastdrager, J., Hanson, J., and Smeekens, S. (2014). Sugar signals and the control of plant growth and development. Journal of Experimental Botany 65, 799–807.

Leduc, N., Roman, H., Barbier, F., Péron, T., Huché-Thélier, L., Lothier, J., Demotes-Mainard, S., and Sakr, S. (2014). Light signaling in bud outgrowth and branching in plants. Plants 3, 223–250.

Lescourret, F., Moitrier, N., Valsesia, P., and Génard, M. (2011). QualiTree, a virtual fruit tree to study the management of fruit quality. I. Model development. Trees 25, 519–530.

Letort, V., Cournède, P.-H., and de Reffye, P. (2009). Impact of Topology on Plant Functioning: A Theoretical Analysis Based on the GreenLab Model Equations. In 2009 Third International Symposium on Plant Growth Modeling, Simulation, Visualization and Applications, pp. 341–348.

Li, X., Cai, W., Liu, Y., Li, H., Fu, L., Liu, Z., Xu, L., Liu, H., Xu, T., and Xiong, Y. (2017). Differential TOR activation and cell proliferation in Arabidopsis root and shoot apexes. PNAS 114, 2765–2770.

Lieth, J.H., and Pasian, C.C. (1990). A Model for Net Photosynthesis of Rose Leaves as a Function of Photosynthetically Active Radiation, Leaf Temperature, and Leaf Age. Journal of the American Society for Horticultural Science 115, 486–491.

Luquet, D., Dingkuhn, M., Kim, H., Tambour, L., and Clement-Vidal, A. (2006). EcoMeristem, a model of morphogenesis and competition among sinks in rice. 1. Concept, validation and sensitivity analysis. Functional Plant Biology 33, 309–323.

MacNeill, G.J., Mehrpouyan, S., Minow, M.A.A., Patterson, J.A., Tetlow, I.J., and Emes, M.J. (2017). Starch as a source, starch as a sink: the bifunctional role of starch in carbon allocation. J Exp Bot 68, 4433–4453.

Mason, M.G., Ross, J.J., Babst, B.A., Wienclaw, B.N., and Beveridge, C.A. (2014). Sugar demand, not auxin, is the initial regulator of apical dominance. Proceedings of the National Academy of Sciences 111, 6092–6097.

Mathieu, A., Cournède, P.-H., Letort, V., Barthélémy, D., and De Reffye, P. (2009). A dynamic model of plant growth with interactions between development and functional mechanisms to study plant structural plasticity related to trophic competition. Annals of Botany 103, 1173–1186.

Maurel, K., Leite, G.B., Bonhomme, M., Guilliot, A., Rageau, R., Pétel, G., and Sakr, S. (2004). Trophic control of bud break in peach (Prunus persica) trees: a possible role of hexoses. Tree Physiology 24, 579–588.

Mitchell, K.J. (1953). Influence of Light and Temperature on the Growth of Ryegrass (Lolium spp.). Physiologia Plantarum 6, 21–46.

Müller, D., and Leyser, O. (2011). Auxin, cytokinin and the control of shoot branching. Ann Bot 107, 1203–1212.

Oguchi, R., Hikosaka, K., and Hirose, T. (2003). Does the photosynthetic light-acclimation need change in leaf anatomy? Plant, Cell & Environment 26, 505–512.

Oguchi, R., Hikosaka, K., and Hirose, T. (2005). Leaf anatomy as a constraint for photosynthetic acclimation: differential responses in leaf anatomy to increasing growth irradiance among three deciduous trees. Plant, Cell & Environment 28, 916–927.

Oguchi, R., Ozaki, H., Hanada, K., and Hikosaka, K. (2016). Which plant trait explains the variations in relative growth rate and its response to elevated carbon dioxide concentration among Arabidopsis thaliana ecotypes derived from a variety of habitats? Oecologia 180, 865–876.

Paine, C.T., Marthews, T.R., Vogt, D.R., Purves, D., Rees, M., Hector, A., and Turnbull, L.A. (2012). How to fit nonlinear plant growth models and calculate growth rates: an update for ecologists. Methods in Ecology and Evolution 3, 245–256.

Pallas, B., Clément-Vidal, A., Rebolledo, M.-C., Soulié, J.-C., and Luquet, D. (2013). Using plant growth modeling to analyze C source–sink relations under drought: inter-and intraspecific comparison. Frontiers in Plant Science 4, 437.

Peng, L., Skylar, A., Chang, P.L., Bisova, K., and Wu, X. (2014). CYCP2;1 integrates genetic and nutritional information to promote meristem cell division in Arabidopsis. Developmental Biology 393, 160–170.

Poorter, H., Niinemets, Ü., Poorter, L., Wright, I.J., and Villar, R. (2009). Causes and consequences of variation in leaf mass per area (LMA): a meta-analysis. New Phytologist 182, 565–588.

Rabot, A., Henry, C., Ben Baaziz, K., Mortreau, E., Azri, W., Lothier, J., Hamama, L., Boummaza, R., Leduc, N., and Pelleschi-Travier, S. (2012). Insight into the role of sugars in bud burst under light in the rose. Plant and Cell Physiology 53, 1068–1082.

Rabot, A., Portemer, V., Péron, T., Mortreau, E., Leduc, N., Hamama, L., Coutos-Thévenot, P., Atanassova, R., Sakr, S., and Le Gourrierec, J. (2014). Interplay of Sugar, Light and Gibberellins in Expression of Rosa hybrida Vacuolar Invertase 1 Regulation. Plant Cell Physiol 55, 1734–1748.

Rameau, C., Bertheloot, J., Leduc, N., Andrieu, B., Foucher, F., and Sakr, S. (2015). Multiple pathways regulate shoot branching. Frontiers in Plant Science 5, 741.

Roitsch, T., and Ehneß, R. (2000). Regulation of source/sink relations by cytokinins. Plant Growth Regulation 32, 359–367.

Roman, H., Girault, T., Barbier, F., Péron, T., Brouard, N., Pěnčík, A., Novák, O., Vian, A., Sakr, S., and Lothier, J. (2016). Cytokinins are initial targets of light in the control of bud outgrowth. Plant Physiology 172, 489–509.

Rongen, M. van, Bennett, T., Ticchiarelli, F., and Leyser, O. (2019). Connective auxin transport contributes to strigolactone-mediated shoot branching control independent of the transcription factor BRC1. PLOS Genetics 15, e1008023.

Schneider, A., Godin, C., Boudon, F., Demotes-Mainard, S., Sakr, S., and Bertheloot, J. (2019). Light regulation of axillary bud outgrowth along plant axes: an overview of the roles of sugars and hormones. Frontiers in Plant Science 10, 1296.

Sims, D.A., and Pearcy, R.W. (1992). Response of leaf anatomy and photosynthetic capacity in Alocasia macrorrhiza (Araceae) to a transfer from low to high light. American Journal of Botany 79, 449–455.

Skylar, A., Sung, F., Hong, F., Chory, J., and Wu, X. (2011). Metabolic sugar signal promotes Arabidopsis meristematic proliferation via G2. Developmental Biology 351, 82–89.

Su, H., Abernathy, S.D., White, R.H., and Finlayson, S.A. (2011). Photosynthetic photon flux density and phytochrome B interact to regulate branching in Arabidopsis. Plant, Cell & Environment 34, 1986–1998.

Tan, M., Li, G., Chen, X., Xing, L., Ma, J., Zhang, D., Ge, H., Han, M., Sha, G., and An, N. (2019). Role of Cytokinin, Strigolactone, and Auxin Export on Outgrowth of Axillary Buds in Apple. Front. Plant Sci. 10.

Tardieu, F., Granier, C., and Muller, B. (1999). Modelling leaf expansion in a fluctuating environment: are changes in specific leaf area a consequence of changes in expansion rate? The New Phytologist 143, 33–43.

Thornley, J.H.M. (1998). Dynamic Model of Leaf Photosynthesis with Acclimation to Light and Nitrogen. Annals of Botany 81, 421–430.

Thornley, J.H.M., and France, J. (2007). Mathematical Models in Agriculture: Quantitative Methods for the Plant, Animal and Ecological Sciences (CABI).

Van den Ende, W. (2014). Sugars take a central position in plant growth, development and, stress responses. A focus on apical dominance. Front. Plant Sci. 5.

Van Dingenen, J., Vermeersch, M., De Milde, L., Hulsmans, S., De Winne, N., Van Leene, J., Gonzalez, N., Dhondt, S., De Jaeger, G., Rolland, F., et al. (2019). The role of HEXOKINASE1 in Arabidopsis leaf growth. Plant Mol Biol 99, 79–93.

Waldie, T., and Leyser, O. (2018). Cytokinin Targets Auxin Transport to Promote Shoot Branching. Plant Physiology 177, 803–818.

Wang, L., and Ruan, Y.-L. (2013). Regulation of cell division and expansion by sugar and auxin signaling. Front. Plant Sci. 4.

Wang, M., Le Moigne, M.-A., Bertheloot, J., Crespel, L., Perez-Garcia, M.-D., Ogé, L., Demotes-Mainard, S., Hamama, L., Davière, J.-M., and Sakr, S. (2019). BRANCHED1: A Key Hub of Shoot Branching. Front Plant Sci 10.

Witkowski, E.T.F., and Lamont, B.B. (1991). Leaf specific mass confounds leaf density and thickness. Oecologia 88, 486–493.

Xiong, Y., McCormack, M., Li, L., Hall, Q., Xiang, C., and Sheen, J. (2013). Glucose–TOR signalling reprograms the transcriptome and activates meristems. Nature 496, 181–186.

Yoshida, S., Mandel, T., and Kuhlemeier, C. (2011). Stem cell activation by light guides plant organogenesis. Genes Dev. 25, 1439–1450.

RESULTS – CHAPTER 3 – SUGARS AND HORMONES CONTENTS EQUILIBRIUM IN THE VICINITY OF THE BUD QUANTITATIVELY DETERMINES BUD OUTGROWTH RESPONSE TO LIGHT INTENSITY

RESUME DU CHAPITRE 3

Contexte et objectifs

Pour le rosier, les conditions lumineuses passées et l'intensité lumineuse actuelle perçue pendant la période de phase de croissance du bourgeon ont un impact sur la précocité et la distribution spatiale du débourrement du bourgeon. Des études antérieures ont démontré que les cytokinines (CK) au voisinage du bourgeon ont un rôle majeur dans stimulation du débourrement par l'intensité lumineuse courante. Dans le chapitre 2, nous avons montré qu'une réduction temporaire de l'intensité lumineuse avant la période de débourrement augmentait de manière corrélée l'état de sucre de la plante et le débourrement des bourgeons. Cependant, il n'existe pas de vision claire et unifiée des mécanismes par lesquels l'intensité lumineuse perçue par la plante au cours de sa croissance peut réguler le débourrement des bourgeons axillaires. Ici, nous avons cherché à (i) établir un premier ensemble d'hypothèses mécanistes déterminant comment l'intensité lumineuse peut déclencher la croissance des bourgeons, en incluant les CK et les sucres comme deux acteurs principaux, et (ii) évaluer quantitativement les contributions respectives des CK et des sucres dans la réponse du débourrement des bourgeons à différents régimes d'intensité lumineuse.

Méthode

Pour formaliser nos hypothèses concernant la régulation du débourrement par les hormones, les sucres et l'intensité lumineuse, nous avons utilisé le modèle mécaniste de régulation du débourrement pour un bourgeon développé par Bertheloot et al. (2020). Ce modèle simule le délai avant le débourrement d'un bourgeon en fonction des teneurs locales en auxine, SL, CK et sucres. Nous y avons ajouté un effet de l'intensité lumineuse courante sur les teneurs en CK. Le modèle obtenu a été calibré *in vitro* sur une gamme de teneurs en sucres et en auxine, et sous différents traitements lumineux. Nous avons ensuite vérifié la capacité du modèle à reproduire des phénotypes de débourrement en réponse à des traitements lumineux *in planta*. Enfin, nous avons utilisé le modèle pour évaluer les contributions relatives des sucres et des CK dans la stimulation du débourrement par l'intensité lumineuse.

Principaux résultats

Notre approche de modélisation a permis de simuler la régulation du débourrement des bourgeons sous différents traitements de lumière pour des nœuds isolés ou *in planta* sans modifier les paramètres du modèle. En simulant des traitements virtuels spécifiques nous avons montré que les CK,

mais aussi les sucres jouent un rôle important dans la réponse du débourrement à plusieurs traitements d'intensité lumineuse, et que cet effet passe préférentiellement par la voie des SL.

Conclusions

Notre étude met en évidence les rôles importants des CK mais aussi des sucres dans la réponse du débourrement à différents niveaux d'intensité lumineuse perçu avant et/ou pendant la période de débourrement. Ces résultats issus de simulations numériques demandent à être confirmés par des mesures de variables physiologiques, mais ouvrent la voie à un modèle générique de régulation du débourrement par la lumière *in planta*.

INTRODUCTION

Shoot branching is an important agronomic trait that directly determines plant architecture and affects crop productivity (Rameau et al., 2015; Barbier et al., 2019; Shen et al., 2019). Shoot branching is among plant biological processes that is highly regulated and implies perception and integration of endogenous (hormones, sugars, nitrogen), developmental and environmental stimuli. Along the stem, axillary bud either remain dormant or grow out to form a branch (Greb et al., 2003; Schmitz et al., 2005, Shen et al., 2019). The light factor is one major environmental factor that tightly takes over the ability of an axillary bud to grow out, through both its quality and intensity components (Schneider et al., 2019). Several results underline a bud outgrowth stimulation by light intensity, in a way that depends on plant light history. After apical dominance release by decapitation, rose plant bud requires a local light perception to grow out because no bud outgrowth recorded when plant shifted into darkness condition (Girault et al., 2008; Roman et al., 2016). In intact plants of many species (ryegrass, grapevine and rose), low light intensity during the tillering or branching period decreases frequency, and increases the delay of bud outgrowth compared to high light intensity (Mitchell, 1953; Pallas and Christophe, 2015; Corot et al., 2017). Interestingly, bud outgrowth of intact rose plants is more stimulated (in terms of frequency and precocity) when plants grew under low light intensity during the primary axis organ establishment, before being transferred to high light intensity condition during the branching stage (light treatment referred as LH for Low-High), relatively to those placed constantly under high light intensity (referred as HH treatment) (see Chapter 2; Demotes-Mainard et al., 2013). Although these findings indicate a tight link between light intensity and bud outgrowth, the underlying mechanisms are a matter of debate and deserve to be further clarified.

Bud outgrowth regulation involves an interaction between several branching-related hormones (auxin, strigolactones (SL) and cytokinins (CK)) and nutrients (Domagalska, Leyser, 2011; Waldie et al., 2014; Martín-Fontecha et al., 2017; González-Grandío et al., 2018) including sugar which was demonstrated to act partly as a signaling entity for different species (Mason et al., 2014; Barbier et al., 2015; Fichtner et al., 2017). These different players tightly operate both outside and inside the bud to define its ability to grow out. In a very recent work, Bertheloot et al. (2020) quantitatively formalized the bud outgrowth response to the regulating network consisting of local hormones (auxin, CKs, SLs) and sugars, using isolated stem segments *in vitro*. They highlighted that bud outgrowth occurrence and start varied as a function of the quantitative balance between the levels of sugar and the different hormones in the node. However, this model does not account about how light interacts with the hormone and sugar regulating network.

Since light intensity modulates both bud outgrowth and photosynthesis, an early hypothesis was that branching or tillering regulation by light intensity was related to changes in plant sugar status (Luquet et al., 2006; Evers et al., 2010; for review: Schneider et al., 2019). This assumption was recently challenged when low CK levels were shown to play a key role in bud outgrowth repression for rose

plants under low light intensities (Roman et al., 2016; Corot et al., 2017). Compared to plants continuously grown under comfortable light intensity, the transfer of decapitated plants to darkness, or of intact plants to low light intensity repressed bud outgrowth and this was preceded by repression of CK-biosynthesis genes in the stem, and reduction of stem CK and sugar contents. The causal role of low CK level in bud outgrowth repression could be demonstrated by exogenous synthetic CK supply, which alleviated bud outgrowth repression (Roman et al., 2016; Corot et al., 2017). On the contrary, sugar role was questioned because exogenous sugar supply could not restore bud outgrowth under the same unfavorable conditions.

However, sugar role was demonstrated in the bud outgrowth promotion reported for rose plants submitted to temporary light limitation during the primary axis establishment and then transferred to comfortable light intensity conditions during the branching stage (LH treatment, Chapter 2). Compared to continuous comfortable light intensity (HH treatment, Chapter1), this light treatment resulted in a reduction of primary axis organ growth, which was maintained after the end of light limitation, leading to a high ratio source to sink and then to more sugar availability at the plant scale during bud outgrowth period. Such promoting effect of sugar in case of favorable current light environment, but not in darkness, have already been documented for rose stem segments *in vitro* (Henry et al., 2011; Rabot et al., 2012).

These experimental observations highlight a role of both CKs and sugar in bud outgrowth regulation, and indicate that CK and sugar may be the respective regulators of two different aspects of light: (i) bud ambient light intensity promotes its outgrowth through stimulating locally stem CK levels, (ii) plant light intensity regime all over its growth controls carbon source-sink relationships at the plant scale and plant sugar status, that impacts bud outgrowth if local light environment is favorable. However, this first vision emanates from a qualitative interpretation of a limited number of experimental observations (Roman et al., 2016; Corot et al., 2017), and the second one doesn't completely exclude a potential role of CKs. It emerges that there is no coherent vision of the relative roles of sugars and CKs in bud outgrowth response to the different light intensity regimes a plant can experiment during its development.

The objective of the present study is to better understand the relative roles of sugars and CKs in the light intensity effect on bud outgrowth of rose plants. We hypothesized that light intensity acts on bud outgrowth regulation at the plant scale through changes the sugar-hormone balance in the vicinity of the bud. To test this hypothesis and fulfill our objective, we used a quantitative approach combining biological experiments and modelling. First, we conceptualized a quantitative model of bud outgrowth regulation by light and local hormones and sugars contents and calibrated it on isolated buds experimental data. Second, we tested the capacity of the model to simulate observed CK contents and bud outgrowth phenotypes for plants cultivated under different light regimes. Third, we analyzed the

relative role of sugars and CKs in bud outgrowth response to light in planta thanks to specific experimental and virtual treatments.

MATERIALS AND METHODS

Plant material and growth conditions

Single-node cuttings of *R. hybrida* 'Radrazz' plants were obtained as described in Demotes-Mainard et al. (2013). They were grown in 500 ml pots containing a mixture (50/40/10) of neutral peat, coconut fibers and perlite, in a temperature-controlled greenhouse until the appearance of the third leaf of the primary axis. Then plants were transferred to growth chambers (light/dark 16/8h photoperiod; 22/20°C at day/night; air humidity 60-70%). Plants were sub-irrigated every two or three days with a fertilized solution (5.0 mM KNO3, 2.0 mM Ca(NO3)2, 2.0 mM NH4NO3, 2.0 mM KH2PO4, 2.0 mM MgSO4, 0.25 mM NaOH; additional trace elements: Kanieltra formula 6-Fe at 0.25 ml l^{-1} (Hydro Azote, Nanterre, France) to maintain optimal hydric and mineral nutrition.

Bud outgrowth starts a few days after the floral bud becomes visible at the top of the primary axis (FBV stage = 'flower button visible', see Figure 1 in Chapter 2 for definition of the plant development stages). Until FBV stage, plants were exposed to different light intensities: low (L; PPFD =90 $\mu mol.m^{-2}.s^{-1}$ when measured at pot height before the start of the culture) or high (PPFD between 300 and 400 $\mu mol.m^{-2}.s^{-1}$). At FBV, plants were either kept intact, beheaded, or a nodal stem segment in primary axis middle part was excised and cultivated i*n vitro*:

- Intact plants grown till FBV under low light intensity were, after FBV, either maintained under low light (LL treatment) or transferred to high light intensity (LH treatment). Plants grown till FBV under high light intensity were maintained after FBV to high light intensity (treatment HH).
- Plants grown under low light intensity till FBV were decapitated 2 cm above the fourth foliated leaf of the primary axis at FBV, and partly defoliated so as to maintain only one lateral leaflet per leaf Apical dominance was re-established by applying a NAA agar (composition: 5 µM NAA, 0.3% agar, 0.25% preservative plant mixture) on the top of the stem (see Supp. Figure 1A). Plants were maintained under low light intensity (treatment LL) and were supplied with an aqueous solution (with 0.25% of PPM) of sucrose (25mM), or an osmotic control, (mannitol 25mM), and/or BAP (a synthetic cytokinin. 10µM) through the petiole of each leaving leaflet (see Supp. Figure 1B).
- Stem segments of 1.5 cm-length were excised at FBV at the level of the third foliated leaf counting from plant base. They were cultivated *in vitro*, in the same growth chamber as intact plants, on classical solid MS medium (1% gelose), supplemented with different sucrose concentrations (50 or 100 mM) and auxin (synthetic auxin NAA: 0, 1 or 2.5 µM)

Biological model	Light treatment	Light intensity before FBV (µmol.m^{-2}.s^{-1})	Light intensity after FBV (µmol.m^{-2}.s^{-1})	Other treatments	
Intact plants	HH	High (340)	High (340)		
	LH	Low (90)	High (340)		
	LL	Low (90)	Low (90)		
Beheaded plants	LL	Low (90)	Low (90)	Mannitol (25mM) control vs exogenous sucrose (25 mM) and/or CK (BAP : 10µM) supply	
In vitro buds				Sucrose (mM)	Auxin (µM)
	HH	High (340)	High (340)	50	1
	LH	Low (90)	High (340)	50	0. 1. 2.5
				100	1
	LL	Low (90)	Low (90)	50	0. 1. 2.5
	HL	High (340)	Low (90)	50	1
				100	1

Table 1: Summary of treatments applied to intact or beheaded plants before and after FBV and excised bud bearing nodes cultivated *in vitro*.

(Supp. Figure 1C), and under different light intensities (low light, L: 90 µmol.m^{-2}.s^{-1}; high light, H: 350 µmol.m^{-2}.s^{-1}). As a result, there was four different light treatments for buds grown with 50mM sucrose and 1µM NAA in the medium. LL and HH treatments consisted in respectively continuous low or high light intensity before FBV and during the *in vitro* node culture. Under LH (and HL) treatment, plants were placed under low (respectively high) light intensity until nodes excision at FBV, which were then transferred to high (respectively low) light intensity for *in vitro* cultivation.

All treatments and experiment conditions are summarized in Supp.Table 1.

Primary axis description for intact plants

The foliated part of intact plants primary axis was divided into three zones, Z1, Z2, Z3 (see Supp. figure 2 in Chapter 2 for details) for bud outgrowth patterns and for organs pooling when dosing nutrients and hormones. The foliated phytomers were numbered from plant base. Zones Z1, Z2 and Z3 were defined as a function of the phytomer relative rank to deal with the variable total number of phytomers existing in a given light environment. For each intact plant, relative rank *r* was calculated as:

$$r = \frac{i-1}{n-1}$$

where *i* is the foliated phytomer rank from the plant base and *n* the total number of foliated phytomers. The relative ranks corresponding to each zone were: $0.7 \leq r \leq 1$ for Z1, $0.4 \leq r < 0.7$ for Z2, $0 \leq r < 0.4$ for Z3.

Monitoring of axillary bud outgrowth

For intact and beheaded plants, the length and development stage (dormant or outgrowing) of each axillary bud along the primary axis were scored three to four times a week. An axillary bud was considered to start its outgrowth when its first leaf was clearly visible between its scales (Girault et al., 2008; Henry et al., 2011). For intact plants, mean bud outgrowth frequency in each zone along the primary axis was calculated as the mean over all the plants of the ratio between the number of buds in a zone that had grown out at a given date and the total number of buds in this zone.

For stem segments *in vitro*, buds were daily photographed during 8 days and bud length was measured using ImageJ software, as described in Barbier et al. (2015). The date of bud outgrowth was estimated as the time at which buds enter a rapid elongation phase (as described in Barbier et al., (2015) and Bertheloot et al. (2020)).

Parameter	Unit	Definition	Value
CK			
c_1	$mol.s^{-1}$	Synthesis rate of CK without sucrose and auxin	0.79
b_1	mol^{-1}	Strength of CKsynthesis inhibition by auxin	0.96
a'_1	$mol.s^{-1}$	Maximum induction of CKsynthesis by sucrose and PARc	2
k_1	mol^2	Parameter of the Hill function relating sucrose and CK synthesis	0.19
k_4	$\mu mol.m^{-2}.s^{-1}$	Parameter of the Hill function relating PARc and CK synthesis	910
d_1	s^{-1}	CKdegradation rate	0.99
SL			
c_2	$mol.s^{-1}$	Base synthesis rate of SL without auxin	0.34
a_2	$mol.s^{-1}$	Maximum induction of SL synthesis by auxin	24.89
k_2	mol^2	Parameter of the Hill function relating auxin and SLsynthesis	294.58
d_2	s^{-1}	SL degradation rate	0.86
I			
c_3	$mol.s^{-1}$	Base production rate of I	0.33
a_3	$mol^{-1}.s^{-1}$	Parameter relating the production rate of Ito SLand sucrose	5.64
u_1	mol^{-2}	Minimum inhibiting effect of sucrose on SLresponse	4.8×10^{-13}
u_2	mol^{-4}	Strength of sucroseinhibiting effect on SLresponse	7.1
a_4	$mol.s^{-1}$	Parameter relating the production rate of Ito CK	287.53
k_3	mol^{-2}	Strength of CKeffect on Iproduction	1000
d_3	s^{-1}	Constant degradation rate of I	0.99
T			
m_0	day	Intercept of the linear relationship between Tand I	-2.2
m_1	$day.mol^{-1}$	Sensitivity of the time at which elongation starts to I	3.5
I_0	mol	Threshold of Iabove which bud elongation is completely prevented	3
S			
α	$mol.\mu mol^{-1}.m^2.s^1$	Sensitivity of S to PAR_p	1.50×10^{-3}
β	mol	Intercept of the linear relationship between S and PAR_p	-0.65

Table 2: Definition, units, and estimated values of the model parameters (adapted from Bertheloot et al., 2020).

Light intensity measurements

Photosynthetic active radiation (denoted PAR) light intensity was measured using a quantum sensor (LI-190 Quantum Sensor, LI-COR, Lincoln, NE, United States) for the different experimental devices and light treatments:

- For intact plants, it was measured at the axil of leaf 1 and 4 (counted from the basis of the primary axis; corresponding to a node in Z3 and Z2 respectively) against the stem at FBV +3 and FBV+7days. The sensor was positioned on the right of the leaf when its terminal leaflet was pointing towards the observer (see Chapter 2 for details). Values are means of at least 10 plants per light treatment (LL, LH and HH).
- For *in vitro* nodes cultivation, PAR intensity was measured at the plate height under low and high light intensities.

Quantification of endogenous sugars and hormones compounds

Sugars (starch, sucrose, glucose, and fructose) and hormones (auxin and different CK forms) contents in nodes were quantified for intact plants grown under LL, LH, and HH light treatments at 3 dates after FBV (FBV, FBV+3d, and FBV+7d). Content values resulted from the mean of four replicates (4 to 5 plants per treatment) per light treatment and per date. Nodal segments with 5 mm of stem each side of the node were collected in the morning, around three hours after the beginning of the light period, immediately frozen in liquid nitrogen and stored at -80°C. They were pooled in three groups depending on their position along the axis (Z1, Z2 and Z3, as described above). Samples were then lyophilized and crushed. Soluble sugars (sucrose, glucose, fructose) and starch were determined by colorimetry as described in Chapter1 whereas hormones contents were quantified as described in Corot et al. (2017).

Statistics

Statistical analyses were performed using R software (R Core Team, 2014). Treatments were compared using non parametric tests (Wilcoxon test for continuous variables, and Exact Fisher test for frequencies).

Bud outgrowth model

A node-scale model of bud outgrowth regulation by ambient light intensity (current PAR, noted PAR_c) was adapted from Bertheloot et al. (2020) (Figure 1). The initial model simulates if an *in vitro* cultivated bud grows out, and the time at which outgrowth starts, from auxin (A) and sucrose (S) levels in the medium. A and S control the level of cytokinins (CK) and strigolactones (SL) in the node, which are integrated by the bud to control quantitatively its outgrowth. We added an effect of the ambient light intensity of the bud (PAR_c) on CK synthesis in the node, as previously demonstrated in planta (Roman

et al., 2016; Corot et al., 2017) and observed in the present study (Fig. 6B and Supp. Fig4). As implemented in Bertheloot et al. (2020), the rate of change in CK level was negatively controlled by auxin (A) level. Since bud outgrowth stimulation by light requires the presence of sugars in the medium, and *vice versa* (Henry et al., 2011), we assumed a multiplicative positive effect of sugar (S) level and PARc on CK synthesis rate:

$$\frac{dCK}{dt} = \frac{c_1}{1 + b_1.A} + a'_1 \frac{S^2}{k_1 + S^2} \times \frac{PARc}{k_4 + PARc} - d_1 CK \quad \text{[Eqn 1]}$$

The rate of SL level change was implemented as in Bertheloot et al. (2020), assuming a positive regulation of SL synthesis by auxin (A) level, a base SL synthesis rate term and a SL-dependent degradation rate:

$$\frac{dSL}{dt} = c_2 + a_2 \frac{A^2}{k_2 + A^2} - d_2 SL \quad \text{[Eqn 2]}$$

Following the model of Bertheloot et al., (2020), both CK and SL control the level of an integrator (I). S represses I positive response to SL level, while CK level negatively regulates I change rate:

$$\frac{dI}{dt} = c_3 + a_3 \frac{SL^2}{1 + b_3(S)SL^2} + a_4 \frac{1}{1 + k_3 CK^2} - d_3 I \quad \text{[Eqn 3]}$$

with $b_3(S) = u_1 + u_2 S^2$ [Eqn 4]

I value positively controls bud outgrowth. If I is above a threshold ($I_{threshold}$ =3), bud outgrowth is completely inhibited, while below $I_{threshold}$, bud outgrowth occurs and the time (*T*) at which bud outgrowth starts is linearly related to I:

$T = m_0 + m_1 I$ if $I < I_0$ [Eqn 5]

$T = \infty$ otherwise

All parameters of Eqn1 to Eqn 5 are described in Table 2.

Model calibration

The above-described model was calibrated for stem segments originated from plants cultivated under different light intensities (noted PAR_p for "past PAR"), and then grown *in vitro* under different concentrations of sucrose and auxin in the growth medium and different ambient light intensities (PAR_c). These experiments (denoted "PAR" experiments in the results) were used for the model calibration on in vitro bud phenotypes and experimental conditions are summarized in Table 1. Experiments described in Bertheloot et al. (2020) (denoted "NP" experiments in the results) were also used to enlarge the range of calibration conditions (PAR_c= 130 µmol m^{-2} s^{-1}). Since PAR_p impacts node starch contents in nodes at the time of their excision (see starch dosages at FBV in Z2, Figure 3 in Chapter 2), we assumed a positive effect of PAR_p on S:

$S = \alpha + \beta . PAR_p$ [Eqn 6]

Model variables	Inputs			Outputs		
	PARc	A	S	CK	Bud outgrowth	
					I	T
Experimental observations for Z2 nodes at FBV+7d						
Units	*µmol/m²/s*	*ng/g*	*mg/g*	*ng/g*		*days after FBV+7d*
LL	44.7	145.49	1.91	41.86		None
LH	204	166.31	20.35	78.33		5.8
HH	158	143.44	8.85	65.91		3.5
Relative observed values (compared to HH treatment)						
LL		1.01	0.22	0.64		
LH		1.16	2.3	1.19		
HH		1	1	1		
Absolute values of simulations of Fig. 9 and 10						
LL	44.7	2.5	0.22	0.25	4.92	None
LL+sug	44.7	2.5	1	0.31	3.12	None
LL+sug//CK	44.7	2.5	1	0.25	5.48	None
LL+CK	44.7	2.5	0.22	0.49	5.81	None
HH	158	2.5	1	0.49	2.27	5.81
HH+sug	158	2.5	2.3	0.52	1.54	3.24
HH+sug//CK	158	2.5	2.3	0.49	1.71	3.84
LH	204	2.5	2.3	0.59	1.31	2.42
LH-sug	204	2.5	1	0.55	2.02	4.91

Table 3: Values of the model variables as (i) measured directly for nodes in Z2 at FBV+7d and (ii) expressed relatively to HH treatment; (iii) and implemented (absolute values of Fig9 and Fig 10) in the model for the different virtual treatments.

The values of k4, a'1, α and β were estimated in this work (Table 2). Other parameters kept identical values to those in Bertheloot et al. (2020). Expressions of CK synthesis genes were previously shown to be strongly increased (more than tripled) by light intensity when PAR values ranged between 0 and 470 µmol m^{-2} s^{-1} (Roman et al., 2016; Corot et al., 2017). We then assumed that CK synthesis response to PAR_c saturates at high light intensities and we fixed a high value for k_4 (=910). a'1 parameter value relative to the effect of PAR_c was first approached by assuming that the term of S and PAR_c effect on CK synthesis in Eqn 1 ($a'_1 \frac{S^2}{k_1+S^2} \times \frac{PARc}{k_4+PARc}$) should be equal to the term of S effect on CK ($a_1 \frac{S^2}{k_1+S^2}$) in Eqn1 of Bertheloot et al. (2020) where PARc =130 µmol m^{-2} s^{-1}. Then, the exact value of a'1, and values of α and β were determined by minimizing the differences between observed and simulated bud outgrowth values (occurrence and date). Parameters values are summarized in Table 2.

Simulations of bud outgrowth and relative CK contents for intact plants under LL, HH and LH treatments

Once the model of bud outgrowth regulation by light intensity was calibrated on *in vitro* experiments, we aimed to use it *in planta* to simulate CK contents and bud outgrowth (occurrence and delay) under LL, LH and HH treatments from experimental observations made at FBV+7d. PAR_c input values for LL, HH and LH treatments were equal to the respective light intensities measured for each treatment at FBV+7d (Table 3). One difficulty lay in the differences in sugars and auxin inputs values dimensions between *in vitro* and *in planta* conditions. For *in vitro* conditions, sugar (S) and auxin (A) inputs were expressed as sucrose and auxin contents in the medium (unit: 10^{-2} mmol.L^{-1} and 10^{-2} µmol.L^{-1} for sucrose and auxin, respectively), whereas hormones and sugars dosages of *in planta* nodes were expressed per to dry biomass unit (mg.gDW^{-1} or mmol.gDW^{-1}). Because we lacked some dosage data, we were not able to build a satisfying conversion function between metabolites contents in the *in vitro* culture medium, and metabolites contents of in nodes. Our work then consisted in establishing some (A,S) couples of input values to simulate bud outgrowth *in planta* under LL, LH and HH treatments. To respect observed differences of starch and auxin contents in Z2 nodes at FBV+7d between LL, LH and HH treatments (Fig. 6A and 7B, Table 3), we calculated relative contents of starch (S) and auxin (A) for LL and LH, in comparison to HH (Table 3). Four scenarii (A, B, C and D), differing in absolute A and S inputs values, but both respecting the observed relative contents between light treatments, were simulated (Fig.8).

Output variables for each light treatment were CK content, the value of the integrator I, and the delay before bud outgrowth (unit : days after FBV+7d). As for A and S variables, simulation of CK contents were expressed in a unit different from the experimental dosages made in Z2 nodes of LL, LH and HH plants. We then calculated relative simulated CK contents and relative observed CK contents (as made for starch and auxin, see above; Table 3) to allow a comparison between simulations and

experimental observations (by construction, relative simulated and observed CK contents were equal to 1 under HH). If applicable (I value < $I_{threshold}$), the delay before bud outgrowth was deducted from I value (Eqn 5) and expressed in days after FBV+7d.

Simulations of virtual sugar and CK changes for plants under LL, LH and HH treatments

Virtual sugar and/or CK changes under LL, LH and HH treatments *in planta* were simulated. For both virtual treatments, auxin input value was fixed (A=2.5) and PAR_c was kept identical to values used for LL, LH and HH respectively. We created 3 virtual treatments consisting in changing sugar input value (S). For two treatments S input value was increased compared to the initial light treatment: LL+sug, HH+sug corresponded to LL and HH treatments for PAR_c value, but S value was equal to that of HH and LH treatment respectively (Table 3). In a third one, S input value was decreased compared to the initial light treatment: LH-sug corresponded LH treatment for PAR_c value, but S value was equal to that observed in HH treatment.

Virtual CK changes were simulated for LL plants (treatment denoted LL+CK). To simulate an increase of CK contents, we added a constant term of CK synthesis in Eqn 1, so that simulated CK contents under LL+CK was similar to simulated CK content under HH treatment.

To explore the relative role of the CK synthesis pathway in bud outgrowth stimulation by sugar, we simulated two additional virtual treatments (LL+sug//CK and HH+sug//CK) consisting in freezing the effect of sugar content on CK synthesis for LL+sug and HH+sug virtual treatments respectively. More precisely, the value of the variable S in the CK synthesis equation (Eqn 1) was kept equal to the S input value of LL and HH treatments, whereas it was increased to the S input values of HH and LH treatments respectively for other equations.

RESULTS

A quantitative model integrating local interactions between hormones, sugars and current light intensity satisfyingly simulated observed bud outgrowth response to light intensity for isolated nodes

To test our hypothesis that light effect on bud outgrowth at the plant scale results from light-induced modulation of the levels of hormones, sugars, and the ambient light local to the node, we started by conceptualizing and calibrating a model of bud outgrowth regulation by sugars, hormones, and light intensity at the node scale. This model is based on the quantitative model of bud outgrowth response to sugar and hormone levels at the node scale developed by Bertheloot et al. (2020) and implemented as described in the Materials and Methods section. As schematized in Figure 1, Auxin (A) and sugars (S) are two inputs of the model. Both act indirectly through regulating the cytokinin (CK) and strigolactone (SL) pathways that are integrated by the bud. More precisely, auxin in the bud-bearing node suppresses

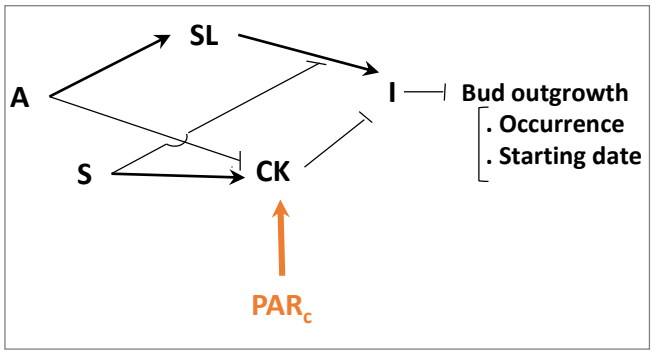

Figure 1: A node-scale model of bud outgrowth regulation by current ambient light intensity in interaction with local bud outgrowth regulators. Local contents in hormones (auxin: A. strigolactones: SL. cytokinins: CK) and sugar (S) determine a level of inhibitor (I) which inhibits bud outgrowth. I controls both bud outgrowth occurrence and the time at which bud outgrowth starts. Current ambient light intensity (PARc) positively regulates CK synthesis in the node (Roman et al.. 2016; Corot et al.. 2017). The model was calibrated on stem segments *in vitro* submitted to different level of S. A. PARc. Related equations are described in Material and Methods (adapted from Bertheloot et al.. 2020).

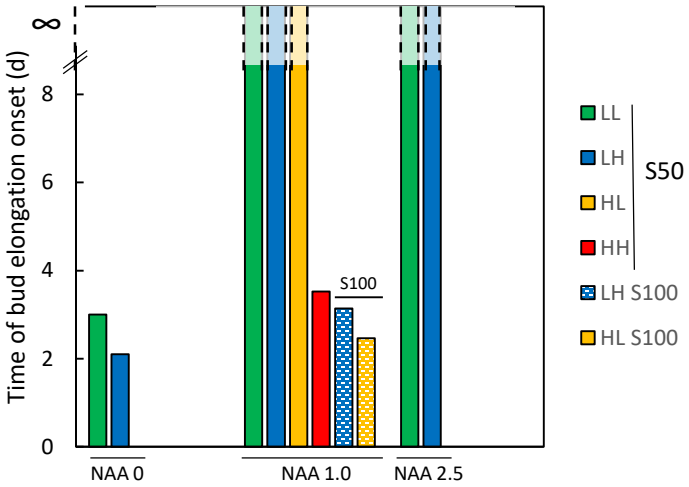

Figure 2: Current light intensity modulates bud outgrowth for stem segments *in vitro*. in interaction with past light intensity. auxin. and sucrose. Stem segments were excised from rose primary axis when floral bud was visible (FBV stage). Primary axes were grown either under low or high light intensity (PARp= L and H. respectively). Excised nodes were then grown *in vitro* under: (i) low or high light intensity. leading to four light intensity treatments: LL. LH. HH. HL; (ii) 0. 1 or 2.5µM NAA. a synthetic auxin; (iii) 50 or 100 mM sucrose (S50 and S100. respectively). Bud length measured every day. and time of bud elongation onset was determined as in Bertheloot et al.(2020).Data are means of at least 10 buds per treatment.

CK synthesis and stimulates SL synthesis. SL and CK induce responses that are antagonistically integrated within the bud, through an integrator denoted *I*. Sugar suppresses the SL response and slightly increases CK level, thus decreasing I level. Value of the integrator I determines bud outgrowth occurrence and date: for I above a given threshold ($I_{threshold}$ =3), bud outgrowth is completely inhibited; below this threshold, any decrease in I accelerates the time at which bud outgrowth starts. We introduced in this model a positive effect of bud ambient light intensity (named current PAR and denoted *PARc*) on CK synthesis. We assumed a multiplicative effect between light and sugar on Ck synthesis, to be able to account for the observations that sugar supply to rose nodal segments in vitro grown in darkness cannot stimulate bud outgrowth and, inversely, light supply cannot stimulate the outgrowth of buds not supplied with sugar (Henry et al., 2011).

For model calibration, we grew rose nodal segments *in vitro* under a range of experimental conditions which make ambient light varying in combination with sugars and auxin (see Table 1 and Materials and Methods section for details), the two inputs of Bertheloot et al. (2020)'s model. Nodes were grown under either low (noted L; 90 µmol m^{-2} s^{-1}) or higher light intensity (noted H; 350 µmol m^{-2} s^{-1}) with 1µM NAA (a synthetic auxin) and 50mM sucrose in the medium, a condition that results in a delayed bud outgrowth (ca. 5 days after excision) under low light intensity (130 µmol m^{-2} s^{-1}; Bertheloot et al., 2020). In addition, before nodal segments excision and transfer *in vitro,* plants received two different levels of incident light (named past PAR and denoted *PARp*), which result in different amount of sugar reserves in the nodal stem (Supp Figure 2). There were thus 4 light treatments: LL, LH, HH, HL, the first letter corresponding to *PARp* and second letter to ambient light (*PARc*). Moreover, for LL and LH treatments, NAA level in the medium was also changed to 0 or 2.5 µM, and sucrose level was increased to 100 mM for LH and HL treatment. With 1 µM auxin and 50 mM sucrose, increasing bud ambient light intensity stimulated its outgrowth only for plants previously submitted to high light level (Fig. 2). Bud outgrowth was completely inhibited for LL, LH, HL, but buds grew out at 3.1 days after excision for HH. The inhibition of bud outgrowth under LH and HL was overcome by increasing sucrose content in the medium to 100 mM. For nodes of plants submitted to low light level before node excision (LL and LH), bud outgrowth remained completely inhibited with a higher auxin level (2.5 µM), as expected due to the dose-dependent inhibiting effect of auxin on bud outgrowth. Bud outgrowth inhibition was on the contrary alleviated by removing auxin (NAA=0 µM), and increasing ambient light intensity decreased the delay before bud outgrowth started (3.0 and 2.1 days for LL and LH, respectively), while this was not visible with 1 µM auxin.

The model was calibrated under the range of experimental conditions (denoted "PAR" experiment) described just above, as well as on the experiments described in Bertheloot et al. (2020) (denoted "NP" experiments). To account for the effect of light history of the plant (*PARp*) on sugar reserves, the "S" variable of the model was the sum of sugar concentration in the growth medium and nodal stem reserve, expressed as a function of *PARp* (see Material and Methods for details and

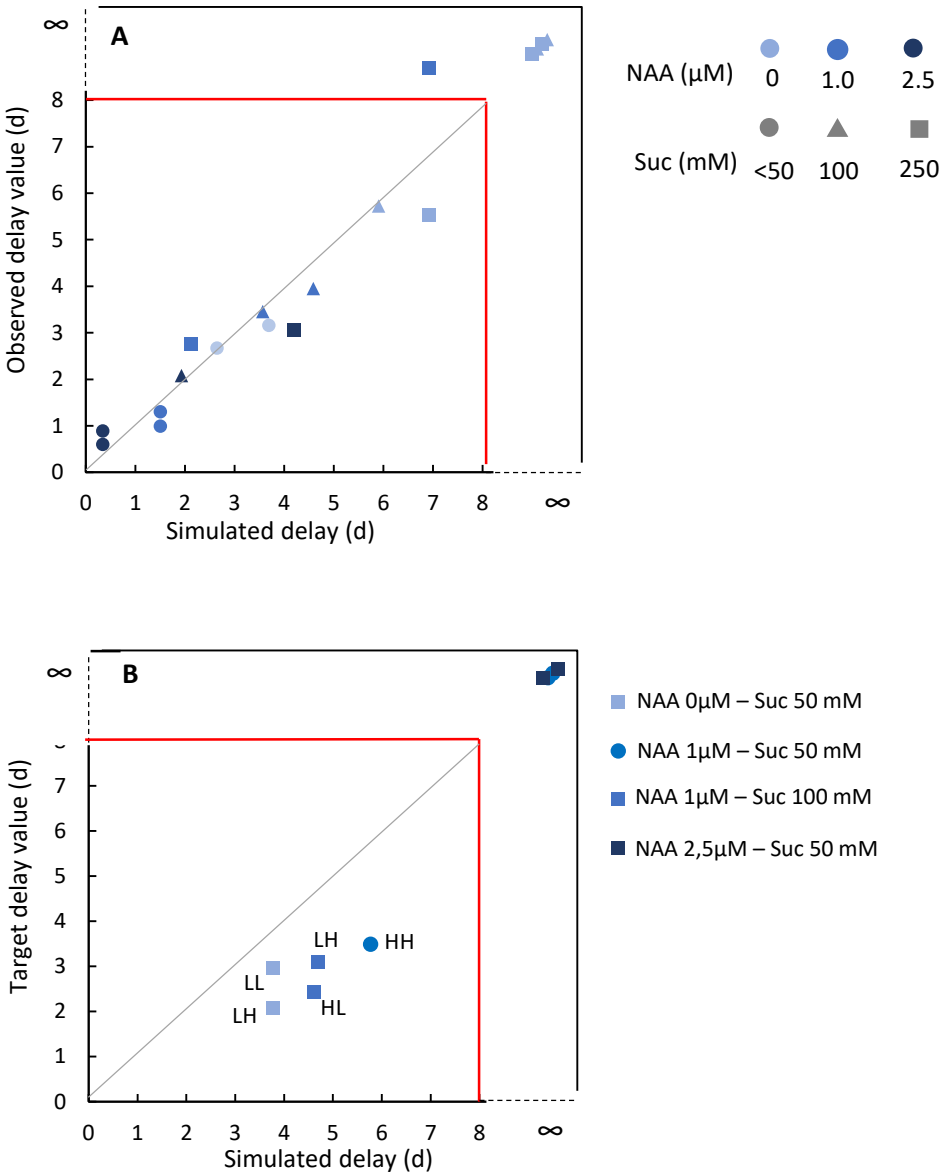

Figure 3: Quality of the node-scale model calibration on *in vitro* experiments. Observed vs. simulated starting date of bud outgrowth for two set of experiments: A/ « NP » . corresponding to experiments published in Bertheloot et al. (2020); stem segments were grown under a PARc of 130µmol/m2/s-1. and different sucrose (suc. 10-50-100-250 mM). NAA (0-1-2.5 µM). strigolactone (SL). and cytokinin (CK) levels. B/ « PAR » corresponding to the experiments presented Fig2. For both experiments. red lines corresponds to the threshold date after which bud outgrowth is completely inhibited. Ecah observed value of bud outgrowth starting date was calculated for a bud with a median final length.

equations). The calibration consisted in estimating parameters relating *PARp* to nodal stem reserve, and the effect of bud ambient light (*PARc*) on CK synthesis. The values of other parameters were kept similar to those in Bertheloot et al. (2020) (see Material and Methods section for details on the calibration process). Globally, parameter value estimation led to a good adequacy between simulated and observed values of bud outgrowth (Fig. 3). For "NP" experiment, the model simulated accurately the inhibition of bud outgrowth by increasing auxin level, and the reduction of auxin effect with an increase in sugar level. For "PAR" experiment, the model simulated the observed promoting effect of PARc on bud outgrowth, and its dependence to PARp and sugar and auxin levels in the medium.

Past and current light intensity modulated in planta bud outgrowth phenotypes for three light treatments (LL, LH and HH), in correlation with strong differences in local light intensity, starch and total CK contents in the stem between treatments.

Using the calibrated node-scale model, we aimed to test if bud outgrowth differences observed for whole plants grown under different light intensity regimes could also be explained by differences in bud ambient light intensity, and local sugar and auxin levels in the nodes. For that, we needed to quantify the differences in bud outgrowth along the primary axis, in hormones and sugar contents, and in local light intensity, for rose plants between different light intensity treatments. We grew rose plants under three different light regimes: two treatments consisted in a continuous low (LL) or high (HH) light intensity applied since plant transfers from greenhouses to growth chambers until the faded flower stage (noted "FF stage"; see Fig.1A in Chapter 2 for plant development stages), a third treatment, denoted LH, consisted in growing plants under low light intensity until the flower bud was visible on the primary axis (FBV stage, see Fig1A in Chapter 2), and then to switch to a high light intensity until FF stage. For each light regime, we measured if buds along the primary axis grew out and when they started their outgrowth, as well as sugar, auxin, and cytokinin concentrations in the bud-bearing nodes before bud outgrowth started. SL could not be quantified. Results of individual nodes and buds were pooled and presented according to three location zones (Z1, Z2 and Z3) along the primary axis. Only leaf bearing phytomers were integrated in these zones. Z1 refers to the most apical ones, while Z3 are the most basal leaf bearing phytomers of the primary axis (refer to Materials and Methods section for details, and Supp.Fig 2 in Chapter 2).

The three light intensity regimes presented contrasted axillary bud outgrowth phenotypes along the primary axis of intact plants (Figure 4). LH stimulated bud outgrowth in Z2 and Z3 compared to HH, both in terms of bud outgrowth frequency (86% *vs* 66% in Z2, and 36% *vs* 8.9% in Z3 for LH and HH, respectively) and precocity (10.5d *vs* 12.8d in Z2, and 14.0 *vs* 15.4d in Z3 for LH and HH, respectively) (Figure 4), as previously observed in Chapter1. On the opposite, LL repressed bud outgrowth compared to HH. On the one hand, bud outgrowth frequency was repressed in all zones: Z1, Z2 and Z3 buds grew out at less than 70%, 25% and near 0%, respectively, for LL, while they grew out

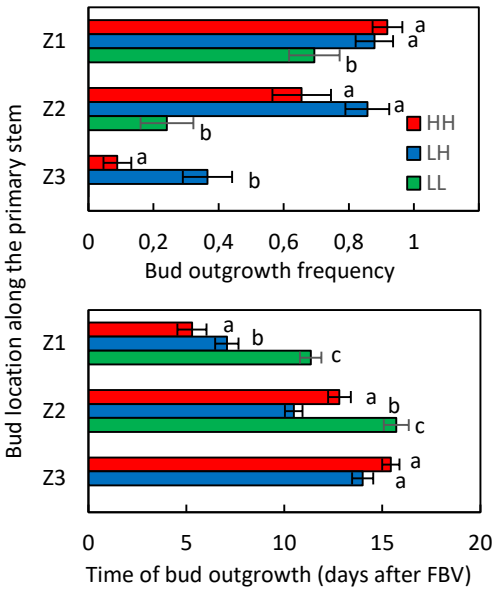

Figure 4: Past and current light intensity modulate frequency (A) and precocity (B) of axillary bud outgrowth along rose primary stems. Buds were pooled according to their belonging zone along the stem (Z1. Z2 and Z3; see chapter 1 Materials and Methods section for more details). Three light treatments were applied: LL refers to a continuous low light intensity (green bars). HH refers to a continuous high light intensity (red bars). and LH refers to a shift from low to high light when primary axis floral bud is visible (FBV stage; blue bars). Data are means ± SE of at least 14 plants per treatment.

at 92%, 66% and 8.9%, respectively, for HH. On the other hand, for Z1 and Z2, in which buds grew out at more than 20%, bud outgrowth was significantly delayed for LL compared to HH (bud outgrowth at 11.3d *vs* 5.3d in Z1 and 15.7d *vs* 12.8d in Z2 for LL and HH, respectively).

Bud outgrowth phenotypes differences between light treatments were associated to differences in ambient light intensity values in the vicinity of buds (Figure 5) and to contrasted levels in sugars and hormones in the primary axis stem (Figure 6). Ambient light intensity (PARc) was measured at the vicinity of the bud 4 (comprised in Z2; see materials and methods for details) at FBV+3d and FBV+7d for the three light treatments LL, HH and LH (Figure 5). Ambient light intensity measured at the node 4 level was slightly higher for LH plants compared to HH plants, and this difference was more marked at FBV+7d (204 and 158 $\mu mol.m^{-2}.s^{-1}$ at FBV+7d for LH and HH respectively), while light intensity was strongly lower for LL plants (45 $\mu mol.m^{-2}.s^{-1}$). Contents of sugars (sucrose, hexoses and starch) and hormones (auxin, cytokinins) were quantified in the nodes of Z2 and Z3, where differences of bud outgrowth between treatments were more marked, and at a few dates before bud outgrowth started: FBV, FBV+3 days, FBV+7days for LH and HH, and FBV and FBV+7 days for LL. The light treatments affected significantly the hormonal and sugar dynamics during the 7 days after FBV. Auxin contents were lower at FBV for plants grown before FBV under low light (LH and LL treatments) than under high light (HH) (1.81 and 3.03 nmol/g respectively for Z2) (Figure 6A). After FBV and in particular at FBV+7 days, differences between treatments became less marked due in particular to the higher rate of decrease for HH, compared to LL and LH. LL and HH displayed almost the same decreasing rate, however, auxin decrease was slightly slower for LH than LL, leading to slightly higher auxin contents (0.95 nmol/g in Z2 at FBV+7days) for LH compared to LL and HH (0.83 nmol/g in Z2 at FBV+7days).

For CK, active forms, iP and Z, were not detected. We thus compared between treatments the contents of intermediate forms, iPRMP, iPR, ZRMP and ZR. Similarly to auxin, total CK contents were higher at FBV for plants grown before FBV under high light (HH), compared to plants grown before FBV to low light (LL and LH) (Figure 6B). Between FBV and FBV+7 days, total CK contents increased for all treatments but with different extents. The increase was the smallest for LL. For LH, it was only visible between 3 and 7 days, while it was visible between 0 and 3 days for LH. This resulted, at FBV+7 days, in higher total CK contents for LH, compared to HH (78.3 vs 65.9 ng/g respectively) and for HH compared to LL (65.9 vs 41.9 ng/g respectively). Sucrose, starch, and hexoses contents at FBV were slightly lower for plants grown before FBV under low light (LH and LL) than high light (HH). After FBV, sucrose and starch displayed similar dynamics. While their contents were stable for LL, it increased slightly and continuously for HH, leading at FBV+7 days to higher values for HH compared to LL (sucrose: 55.9 and 36.5 mg/g; starch: 8.85 and 1.91 respectively in Z2). As for HH, sucrose and starch contents in LH increased but this increase was stronger and occurred mainly during the first three days. This was in particular strong for starch whose content at FBV+7 days in LH was more than twice

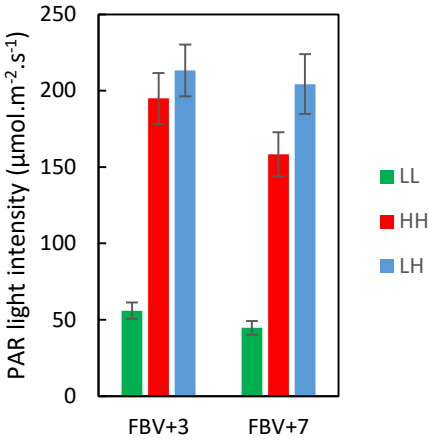

Figure 5: Effect of light intensity treatments (LL, LH and HH) on the ambient PAR light intensity at the level of node 4 (counted from the basis of the primary axis) at FBV+3 and FBV+7d. Data are means ± SE of at least 10 plant per treatment.

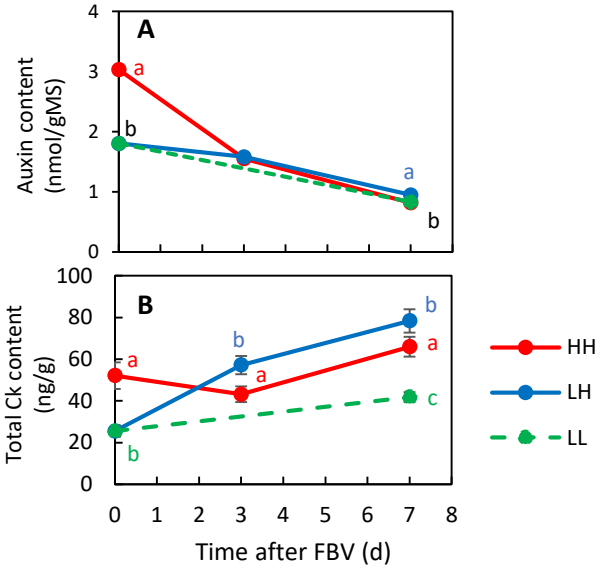

Figure 6: Effect of light intensity treatments (LL, LH and HH) on auxin (A) and total cytokinins (ZRMP. ZR. IPRMP and IPR) (B) contents for nodes taken from Z2 of rose primary axes. Nodes were taken when floral bud was visible on the primary axis (FBV). or 3 or 7 days later. Data are means ± SE of 4 repetitions of at least 4 pooled plants each.

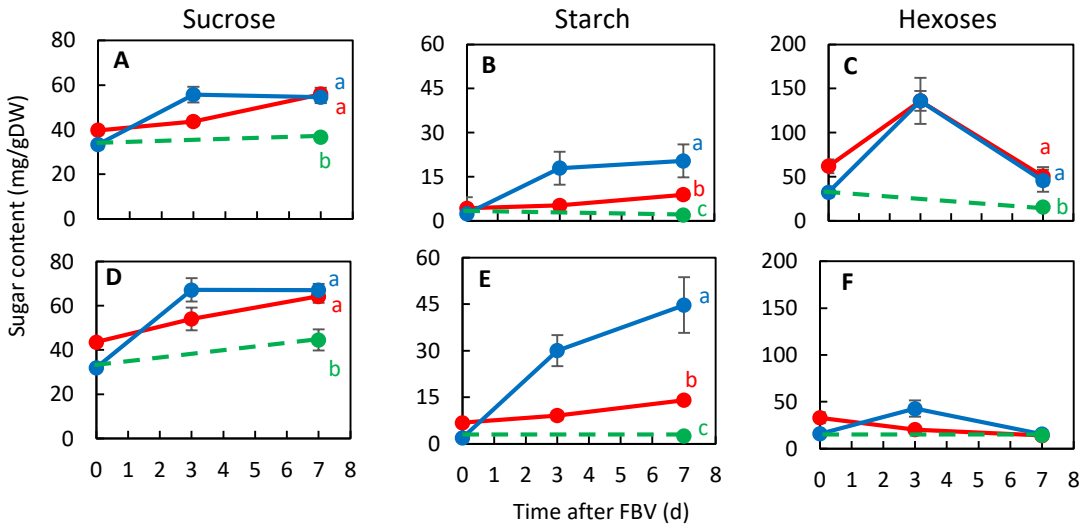

Figure 7: Effect of light intensity treatments (LL. LH and HH) on sugars (sucrose. starch and hexoses) contents of nodes taken from Z2 (A. B. C) and Z3 (D. E. F) of rose primary axes. Nodes were taken when floral bud was visible on the primary axis (FBV). or 3 or 7 days later. Data are means ± SE of 4 repetitions of at least 4 pooled plants each.

higher than HH starch contents (20.4 and 8.85mg/g for LH and HH, respectively in Z2). Sucrose content reached almost similar value in LH compared to HH at FBV+7 days (54.6 and 55.9mg/g respectively for Z2). Hexoses dynamics differed from sucrose and starch dynamics. For Z2, hexoses contents of LH and HH plants increased between FBV and FBV+3d (135.9 mg/g at FBV+3d for both LH and HH treatments) and then decreased to reach values at FBV+7d close to those observed at FBV (50.4 and 45.5 mg/g for HH and LH, respectively). For Z3, hexoses contents remained quite stable during the period for both LH and HH treatments. Despite these different dynamics compared to starch and sucrose, at FBV+7 days hexoses contents under LH and HH treatments were higher in Z2 compared to LL treatment, as found for sucrose contents (45.5, 32.2 and 15.6 mg/g in Z2 for LH, HH and LL respectively), and equal in Z3.

In summary, bud outgrowth phenotypes (occurrence frequency and delay before bud outgrowth) under LL, LH and HH treatments for intact plants were correlated to changes in sugars and hormones contents in the period before the bud outgrowth period. In particular, starch and total CK contents at FBV+7d were correlated to the intensity of bud outgrowth stimulation under the three light treatments.

Simulations of *in planta* bud outgrowth regulation by local light intensity, auxin, and starch levels explained observed differences in total CK contents and bud outgrowth dates between the different light treatments (LL, LH, HH).

We implemented observed differences of ambient PARc, and relative differences of auxin and sugar contents between light treatments as inputs of the node-scale model (schematized in Fig.1) to determine if they can quantitatively explain the observed cytokinin contents and the contrasted bud outgrowth phenotypes observed under LL, LH and HH treatments (see Materials and Methods for details). Values of PARc inputs were equal to the measured ambient PAR_c in Z2 at FBV+7d for each light treatment. Since the bud outgrowth model was calibrated for sugar and auxin contents brought in the medium of an *in vitro* cultivated bud, we could not directly use the absolute values of auxin and sugar concentrations observed *in planta* as model inputs. Instead, we used relative values with ratios between light treatments corresponding to observed ones. The idea was to test if, by conserving the observed ratios in sugar and auxin between light treatments, it was possible to simulate accurately the observed ratios of CK concentrations and dates of bud outgrowth between light treatments. These ratios were calculated from measurements in Z2 at FBV+7 days, and HH treatment was set as the reference treatment (value=1 for auxin, sugar and CK) (see Table 3 for ratio values). For sugar, we used starch whose content in the nodes of Z2 and Z3 was significantly different between LH and HH, and which was demonstrated to correlate well with bud outgrowth patterns observed in both treatments. The calculated starch contents ratio used for inputs reflected these observations since it was higher under LH (2.3) compared to HH (1) and LL (0.22). For CK, we calculated ratios of simulated CK contents to ratios of measured total CK contents (including iPR, iPRMP, tZR and ZRMP, as described above). We then

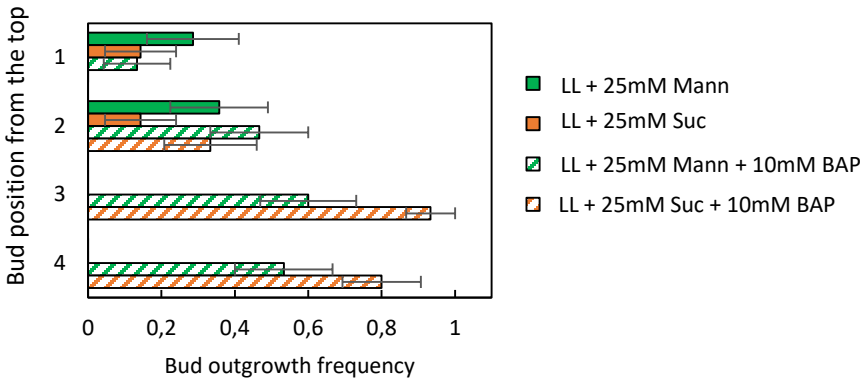

Figure 10: Impact of exogenous supply of cytokinins (CK) and/or sucrose (Suc) on bud outgrowth for decapitated rose stems grown under LL light treatment. Rose primary axes were decapitated above the fourth leaflet-bearing node when floral bud was visible (FBV) and supplied with 5 µM NAA at their top. and either 25 mM mannitol (Mann) or sucrose alone or together with 10 mM BAP a synthetic CK. Before and after decapitation plants were grown under low light intensity. Buds are numbered from decapitated plant top. Data are means ± SEM of at least 15 plants per treatment.

simulated CK contents and bud outgrowth occurrence and timing to a range of absolute auxin values (3.5, 2.5, 2, and 1 for HH), conserving calculated observed ratios between light treatments. Bud outgrowth occurrence and timing being dependent on auxin/sugar balance (Bertheloot et al., 2020), we adjusted sugar levels to fit well the observed absolute delay of bud outgrowth since FBV+7d for HH treatment for each input auxin level (Fig 8). This gave four simulation scenarios, A, B, C and D, for each of the three light treatments (Fig 8).

For all simulation scenarios, observed differences CK levels and bud outgrowth dates between light treatments were qualitatively well simulated (Fig. 8). Compared to HH (CK level=1 and bud outgrowth date =6 d after FBV+7d), LH simulations slightly increased CK levels and accelerated the start of bud outgrowth; LL strongly decreased CK level and completely repressed bud outgrowth. Simulations were quantitatively very close to observations for HH treatments by construction. Whatever the simulation scenario, LH ratios and delay before outgrowth were accurately simulated: the gap between observations and simulations was inferior to 10% for CK contents and to 1.1 day for bud outgrowth delay. In contrast, the accuracy of CK ratio between LL and HH was dependent on input values on auxin and sugar. Simulated CK in LL increased when auxin level decreased (and thus sugar level). As a consequence, simulated relative CK content was underestimated in scenarii A, B and C (0.47 *vs* 0.64 for simulated and observed ratios respectively), when auxin content was high ($A \geq 2$), while it was slightly overestimated in scenario D (0.72 *vs* 0.64 for simulated and observed ratios respectively), when auxin input value was lower (A=1) (Fig. 8). Interestingly, as observed for CK, the value of the integrator I under LL treatment was greatly variable between simulation scenarii (Fig.8): I value decreased with the decrease in auxin level (scenario A: A=3.5, I=11.2; B: A=2.5, I= 9.0; C: A=2, I=6.8) to reach values close to the bud outgrowth threshold ($I_{threshold} = 3$) for the lower auxin level tested (scenario D : A= 1, I=3.4).

In summary, by using observed differences between three light treatments (LL, HH and LH) in current light intensity, auxin and starch contents in the vicinity of the bud (Z2), the model satisfyingly simulated observed differences in total CK contents and bud outgrowth phenotypes between the light treatments for intact plants. This suggest that the model is valuable for in planta use, and that the used input variables are pertinent.

Sugar contribution in explaining bud outgrowth differences between LH and HH treatments is higher than CKs contribution: experimental results are confirmed by *in planta* simulations

The results above have highlighted that the over-stimulation of bud outgrowth in LH, compared to HH, was mainly correlated to sugar accumulation in the form of starch (Fig.7). In Chapter 2, experiments strongly support the hypothesis that sugar accumulation is responsible for bud outgrowth stimulation under LH (Chapter 2, Fig.4). On the one hand, bud outgrowth frequency was highly repressed for auxin-fed decapitated plants grown under LH and submitted to photosynthesis inhibitors on leaflets. On the

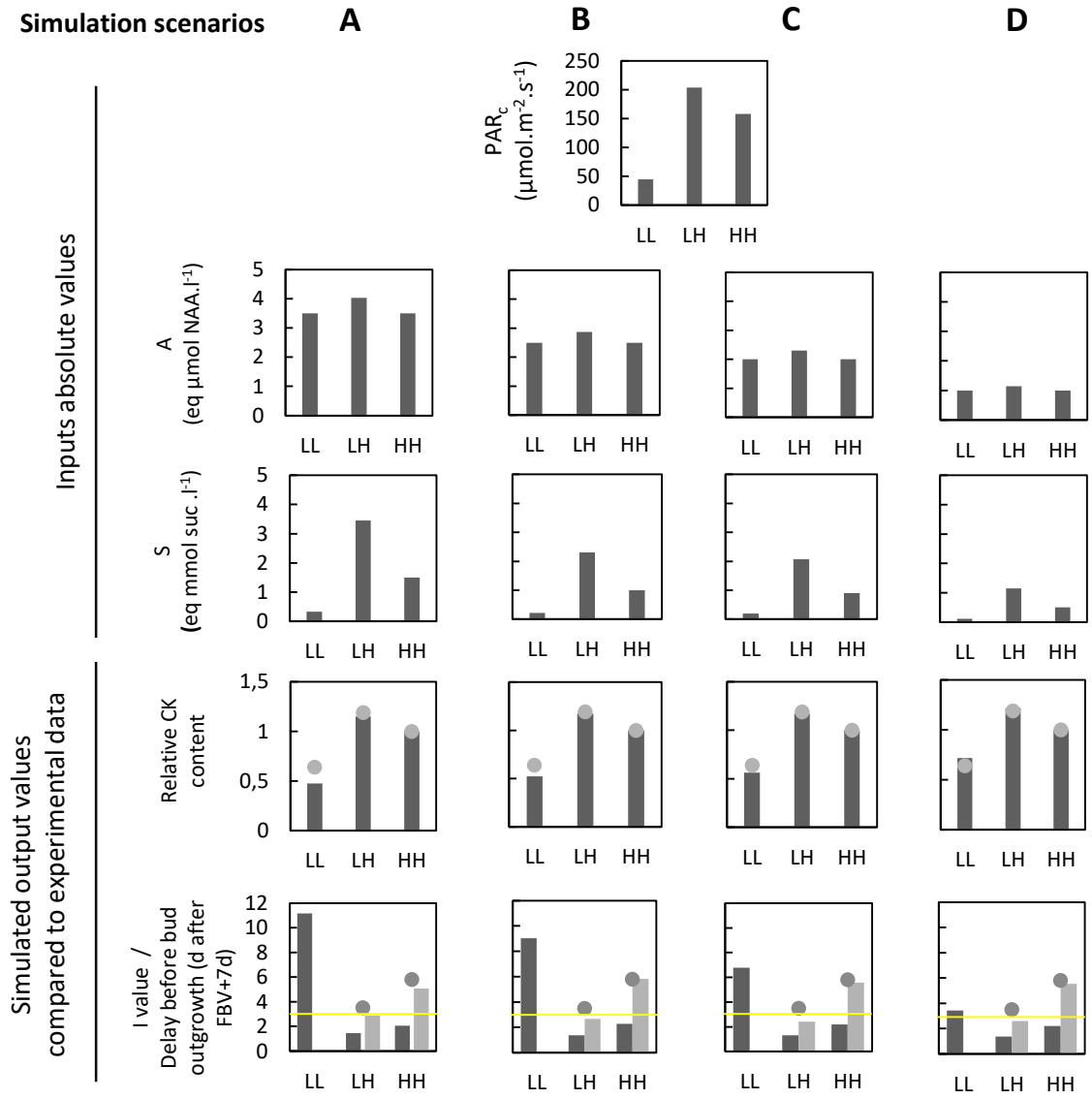

Figure 8: Simulated *vs*. observed stem CK contents and bud outgrowth for entire rose plants under LL, LH, and HH light treatments. Four simulation scenarios are represented: A, B, C and D. Inputs are: (i) PAR_c, equal to experimental measurements, (ii) auxin (A) and sugar (S), with different absolute value between simulation scenarii, but similar ratios between LL and HH, and LH and HH, compared to observed ones. Simulated outputs (vertical bars) and observations (symbols) are: (i) stem CK contents, expressed relatively to HH (black bar for simulation, symbol for observation); (ii) the value of the integrator I (black bar, simulation only), and bud outgrowth starting date (grey bar for simulation, symbol for observation). For the last line of graphs, the absence of a grey bar or of symbol represents a complete inhibition of bud outgrowth. Yellow horizontal lines indicate the I value threshold above which bud outgrowth is completely inhibited. All observations correspond to measurements in zone Z2 of the primary axis.

other hand, for both intact and auxin-fed decapitated plants under HH, sucrose exogenous supply stimulated bud outgrowth frequency to reach values close to those observed under LH.

However, stimulation of bud outgrowth under LH compared to HH was also accompanied by a stimulation of node CK contents (Fig 6B). To further test our assumption of sugar major role, we used the model to quantify the contribution of sugars and CKs in bud outgrowth stimulation under LH compared to HH. We simulated LH and HH treatments under the simulation scenario B (with A=2.5), and created two other virtual treatments: (i) HH+sugar, where sugar level was increased to that of LH, (ii) LH-sugar where sugar level was decreased to that of HH (in each case, PARc was kept identical as in HH and LH, respectively) (Fig.9A). The simulated start of bud outgrowth occurred earlier for HH+sugar compared to HH (3.24 versus 5.81 days, respectively), in line with the stimulation of bud outgrowth frequency observed experimentally after exogenous sucrose supply to HH. However, the simulated bud outgrowth delay remained higher than LH one (delay =2.42 days under LH). This indicates that sugar contribution has a main contribution (76%) in bud outgrowth stimulation under LH compared to HH, but that CKs, which are the only metabolite varying between LH and HH+sugar, also played a role. Similar conclusions were found by comparing simulated bud outgrowth start between LH-sugar and HH. Bud outgrowth was delayed under LH-sugar compared to LH (4.92d and 2.42 respectively), in line with our previous experimental observations. However, bud outgrowth delay remained lower than HH one (delay = 5.81 days under HH)), and sugar contributes to 74% to bud outgrowth stimulation under LH compared to HH.

Simulations of in planta bud outgrowth highlighted the strong contribution of sugars in bud outgrowth differences between LL and HH treatments, and confirmed the requirement of high CK content for buds to grow out

The results above have highlighted that bud outgrowth inhibition observed for intact rose plants grown under LL compared to HH was accompanied by much lower node CK and sugar (starch and sucrose) contents (Fig. 6B and Fig 7A,B). To test experimentally the role of low sugar and CK levels in bud outgrowth inhibition under LL, we exogenously supplied sucrose and CKs to plants under LL. We used auxin-fed decapitated plants with 4 remaining leaves (Supp Fig. 1A,B), instead of intact plants, to avoid interactions with plant growing organs other than buds. As for intact plants, bud outgrowth was strongly inhibited under LL compared to HH for auxin-fed decapitated plants (Supp Fig. 6). Bud outgrowth frequency was lower under LL compared to HH: for the 2nd and 3rd buds bud outgrowth frequency was reduced from 50% under HH to less than 30% under LL. Similarly, bud outgrowth of the 1rst and the 4th buds was strongly inhibited under LL (frequency of bud outgrowth lower than 10%) compared to HH plants (frequency around 30%; Supp. Fig 6). Exogenous sucrose supply under LL did not stimulate bud outgrowth when supplied alone, on the contrary to exogenous CK supply, but sucrose supply promoted bud outgrowth after CK supply (Fig. 10). Indeed, whatever 25

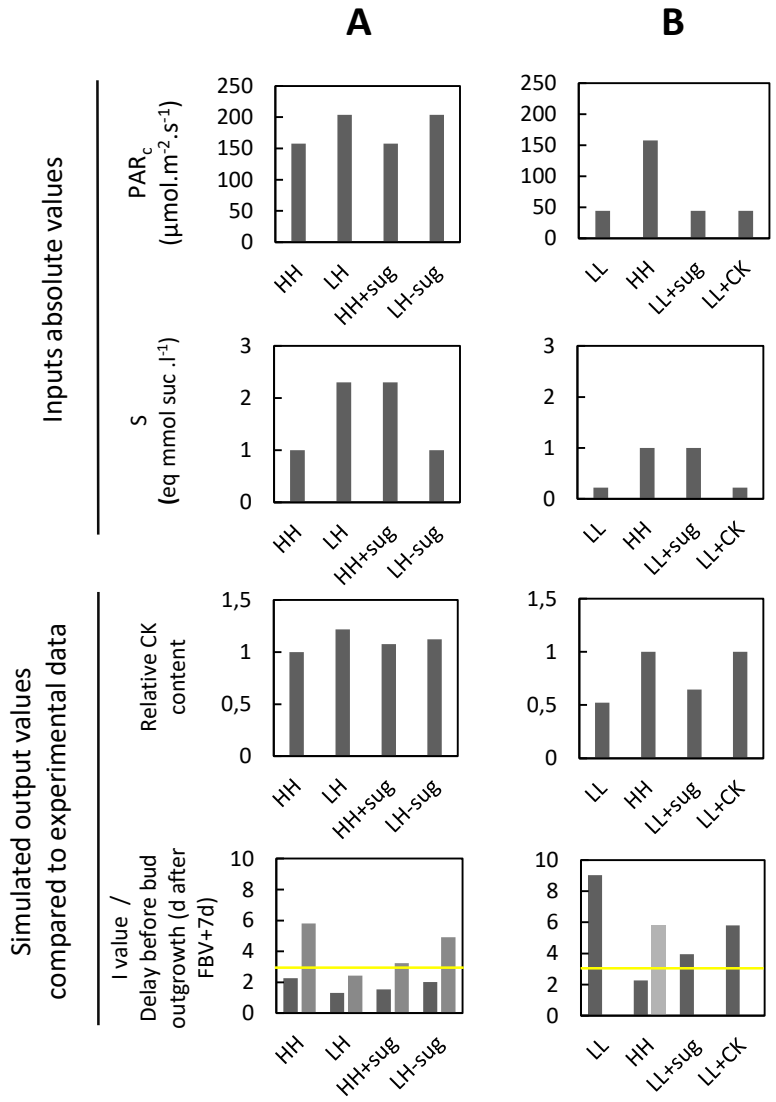

Figure 9: Effects of virtual changes in cytokinin (CK) and sugar (sug) levels on simulated stem CK contents and bud outgrowth for entire rose plants under different light intensities. A/ HH and LH treatments were simulated as in scenario B of Fig 8. In HH+sug and LH-sug treatments, S values were increased and decreased to values similar to LH and HH, respectively. B/ LL and HH treatments were simulated as in scenario B of Fig 8. In LL+sug, S value was increased to the value of HH treatment; in LL+CK, CK was increased to the level of HH. For A/ and B/, and each treatment, relative CK content (except for LL+CK), I value (dark grey bars), and the date of bud outgrowth start (light grey bars) were simulated. The absence of light grey bar represents a complete inhibition of bud outgrowth. Yellow horizontal lines correspond to the I value threshold above which bud outgrowth is completely inhibited.

mM sucrose or 25 mM mannitol, an osmotic control, was supplied through the petioles of all leaves, bud outgrowth was completely inhibited for the third and fourth position from the top, while bud outgrowth frequencies of the first and second position were inferior to 40%. On the contrary, the petiole supply of 10 µM BAP, a synthetic cytokinin, together with 25 mM mannitol, triggered bud outgrowth of the 3rd and 4th buds (frequency between 50% and 60%), and bud outgrowth frequency was over increased when CK supply was coupled with 25 mM sucrose supply instead of 25 mM mannitol (95% and 80% for the 3rd and 4th buds, respectively). These results indicate a potential role of both low CK and low sugar in nodes in bud outgrowth inhibition in LL treatment compared to HH.

To quantify the contributions of sugar and CK, we used our node-scale model. We simulated LL and HH treatments under the simulation scenario B (with A=2.5; Fig. 8B), and created two other virtual treatments: (i) LL+sugar, where sugar level was increased to that of HH, (ii) LL+CK where CK level was increased to that of HH (in each case, PARc was kept identical as in LL) (Fig 9B). For LL, bud outgrowth was inhibited and the integrator I value was around 9.0. LL+sugar and LL+CK treatments could not trigger bud outgrowth but did reduce the value of the integrator I (from 9.0 under LL, to 4.0 under LL+sugar, and 4.57 under LL+CK). However, I reduction was not sufficient to drop below the threshold for bud outgrowth triggering ($I_{threshold}$=3). By comparing I values between LL, LL+sugar, and HH, we calculated a contribution of sugar of 75% in I differences between LL and HH. Interestingly, the simulated behavior for LL+sugar was similar to those observed experimentally after exogenous sucrose and CK supply, while this was not the case for LL+CK (Fig. 9 and 10).

All together, these experimental and simulation results have highlighted a high contribution of sugars (75%) in the observed bud outgrowth differences between HH and LH on the one hand, and LL and HH on the other hand.

Simulations indicate that sugars would act preferentially via SL, rather than CK pathway, to stimulate bud outgrowth

According to our node-scale model (Fig. 1), sugar acts via two distinct ways on bud outgrowth: on the one hand, sugar stimulates CK synthesis, and on the other hand, sugar represses bud outgrowth response to SLs. To determine in the model by which way sugar acts in bud outgrowth promotion between LL and HH, we removed the effect of sugar on CK synthesis in LL+sugar treatment (treatment “LL+sugar//CK”; see Material and Methods for details), and quantified if that abolished or not the effect of sugar supply to LL on the integrator I value (Fig. 10A). I value of LL+sug//CK was slightly higher than I value of LL+sugar (5.48 versus 4, respectively) but remained much lower than I value of LL (9). Removing the effect of sugar on CK synthesis only explained 30% of I value variation between LL and LL+sugar, indicating that SL contributed to 70% of the variation and was a main contributor of the effect of sugar supply under LL on I.

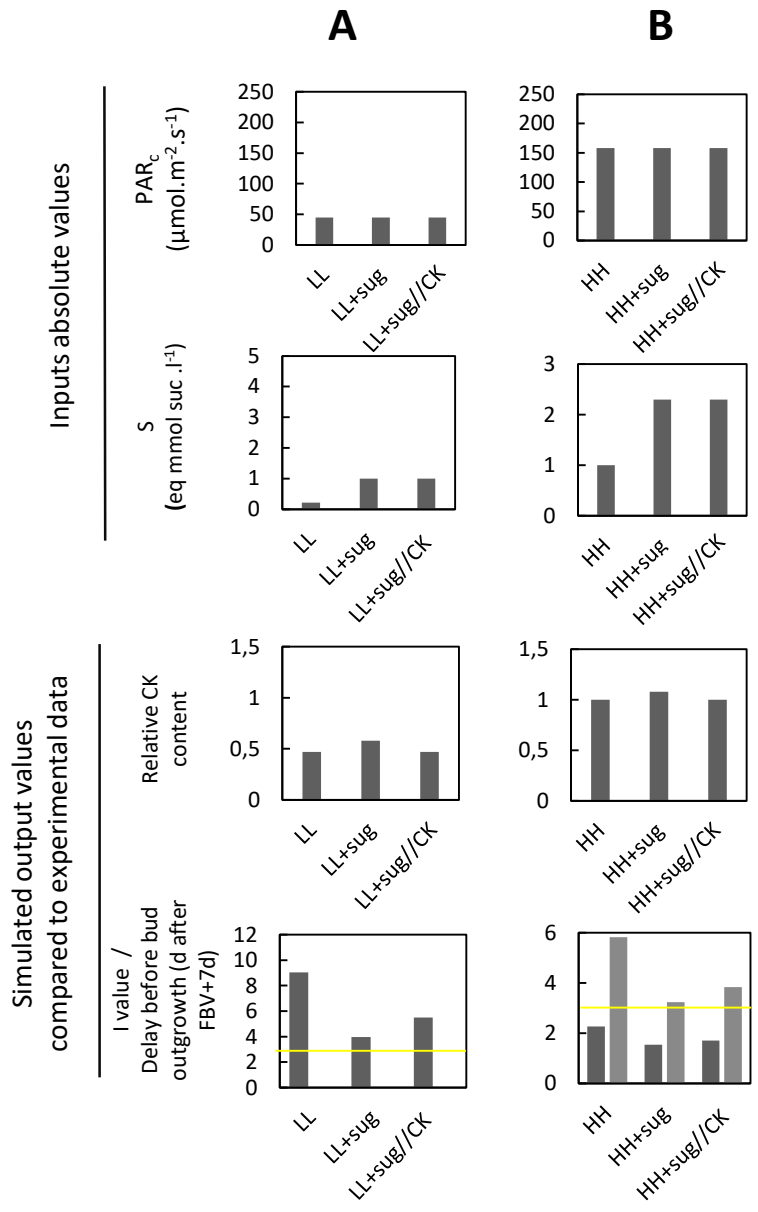

Figure 10: Cytokinins (CK) play a minor role in bud outgrowth stimulation by sugar supply under LL (A) and HH (B). Simulations of LL, LL+sug HH and HH+sug treatments were conducted as done Fig.9. LL+sug//Ck and HH+sug//CK refers to simulations similar to LL+sug and HH+sug, except that the promoting effect of sugars on CK synthesis was frozen. For each treatment, relative CK content, I value (dark grey bars), and the date of bud outgrowth start (light grey bars) were simulated. The absence of light grey bar represents a complete inhibition of bud outgrowth. Yellow horizontal lines correspond to the I value threshold above which bud outgrowth is completely inhibited.

Similarly, we simulated HH and HH+sug treatments as previously done above (Fig 9A, A=2.5), and created another virtual treatment HH+sugar//CK (Fig. 10B), where sugar level was increased to that of LH and the effect of sugar on CK synthesis was removed (see Materials and Methods for details; in each case PARc was kept identical as in HH). In contrast to simulations made under low light intensity (LL ; Fig10B), the three virtual treatments under HH presented simulated I values inferior to the $I_{threshold}$, leading to bud outgrowth in delays inferior to 6 days. Delay value of HH+sug//CK was slightly higher than delay value of HH+sugar (3.84 versus 3.24, respectively) but remained much lower than I value of HH (5.81 days). Removing the effect of sugar on CK synthesis only explained 23% of I value variation between HH and HH+sugar, indicating that SL contributed to 77% of the variation and also was a main contributor of the effect of sugar supply under HH on bud outgrowth phenotype.

DISCUSSION

The current knowledge relative to the basic mechanisms behind light effect on bud outgrowth remains fragmentary and qualitative. The so-far available results bring out the role of two major regulatory pathways (i) sugar-based mechanisms when light drives a modification in the source / sink relationship of the primary axis, (ii) CKs-based mechanisms, when light acts locally on bud outgrowth. Using a quantitative model and experiments, we demonstrate that each of these two pathways contributes to the differences in bud outgrowth observed along the primary axis for rose plants grown under different light intensity regimes.

At the node scale, local light and sugar availability act synergistically and through two different pathways on bud outgrowth

In rose, light is perceived as a local signal promoting bud outgrowth (Girault et al., 2008). As observed for isolated apical meristematic activity (Li et al., 2017), light acts synergistically with sugars since both are required to trigger bud outgrowth for isolated stem segments in vitro (Rabot et al., 2012; 2014). We have highlighted a dose-dependent synergic effect of local light intensity and sugar. Increasing light intensity of *in vitro*-cultured rose stem segments stimulated bud outgrowth and this effect was amplified by raising stem carbohydrate status, either by taking stem segments from plants grown under higher light intensity or by supplying more sugar to the in vitro growth medium. This synergic effect between sugar and light for isolated stem segments could be related to the action of each regulator on two different pathways of bud outgrowth regulation, CK and SL, as we demonstrated by computer modelling. CK and SL are two opposite regulators of bud outgrowth (repressor for SL, inducer for CK), whose balance is integrated dose-dependently by the bud (Dun et al., 2012, Wang et al., 2019). Changes in levels of both CK and SL mediate auxin action on bud outgrowth, while sugar operates through suppressing SL pathway rather than through enhancing CK level (Barbier et al., 2015; 2019; Bertheloot et al., 2020). Using a computer implementation of this network and assuming a local light on

stem CK contents as observed *in planta* (Fig. 1, Roman et al., 2016; Corot et al., 2017), we demonstrated that this network quantitatively explained the wide –range of observed interactions between local light environment, sugar, and hormones on bud outgrowth. More interestingly, it takes into account of sugar and light synergic effect. Experimental measurements of light effect on sugar, and hormones (auxin, ABA, SL) would be necessary to bring additional evidence for this regulatory network. However, early results showed clearly a low photosynthetic activity of rose stems, supporting our assumption of non-effect of light on sugar (J. Lothier, personal communication). As a complementary mechanism, the synergic effect of light and sugar on bud outgrowth may also involve a positive feedback of CK on the sink strength of node and buds, which would increase sugar availability and thus stimulate sugar-related regulatory pathway (Barbier et al., 2019). The role of CK in sink strength has been reported in many biological contexts (for review: Roitsch and Ehness, 2000), including bud outgrowth in rose (Roman et al., 2016). These authors showed that CK upregulates the expression of *RhVI1*, Rosa hybrida Vacuolar Invertase, a well-known marker of both sink strength and bud outgrowth (Girault et al., 2010; Rabot et al. 2012; 2014). In addition, and even though under light condition, CK fails to promote the outgrowth of in-vitro cultured bud fed with mannitol (non metabolizable sugars) in contrast to those placed on sucrose (metabolizable sugars), indicating that CK effect depends on sugar availability for bud (M. Wang, personal communication). Taken together, further investigation are needed to dismantle the role of this putative mechanism in the light and sugar synergic effect observed.

At the plant scale, light regime acts on bud outgrowth by modulating both bud local light environment and plant source-sink relationship for carbohydrates.

Plant light regime has multiple impacts on the plant, including its physiology and morphology, which should influence bud outgrowth. In chapter 2, we reported for rose that, compared to continuous high light (treatment HH), temporary light limitation before bud outgrowth period (treatment LH) reduced primary axis growth including during bud outgrowth period, which increased sugar availability for buds. Other studies in rose reported lower sugar and CK levels in bud neighborhood for decapitated plants transferred to darkness compared to those maintained under light, and for intact plants transferred from high to low light intensity compared to those maintained under high light intensity (Roman et al., 2016; Corot et al., 2017). More importantly, we provide here, for the first time, a quantification of light regime impact simultaneously on auxin, CKs, sugar, and bud ambient light intensity. We demonstrate that CKs, sugar and ambient light levels were all stimulated in the median leafy zone of rose primary axes under continuous high light (HH) compared to continuous low light (LL), and under LH compared to HH. CK variations between light treatments were correlated to changes in local light levels, in line with previous results and our node-scale model described above (Roman et al., 2016; Corot et al., 2017). The origin of sugar variation was not investigated in the present

study, but as demonstrated for LH in Chapter 2, it should be related to changes in light-induced changes in plant morphology and photosynthesis, that modifies source-sink relationship within the plant.

These local light-triggered variations in CK levels and global light-induced variations in sugar levels both explained the different bud outgrowth intensities between LL, LH, and HH. Indeed, including these differences in CK and sugar as input of the node-scale model described above was sufficient to simulate the observed differences in bud outgrowth in the median leafy zone of the primary axis between light treatments. We bring here that both light-induced changes in CK and sugar levels contributed to bud outgrowth differences between light treatments. On the contrary, early results showed only that the limited CK level, and not the limited sugar level, was responsible for bud outgrowth repression in both experimental model (decapitated rose plants under darkness and intact plants transferred from high to low light intensity) (Roman et al., 2016; Corot et al., 2017). In this case, only exogenous CK supply and not exogenous sugar supply was sufficient to restore bud outgrowth under unfavorable conditions. However, CK could not restore completely bud outgrowth activity, indicating that additional components of branching regulatory network would take part in this mechanism. One possible actor would be sugar because the sugar level under these restrictive conditions remains lower, and for stem segment in vitro, CK requires sugar to promote bud outgrowth (M. Wang, personnel communication).

On the other hand, we cannot exclude that in the studied light conditions, local bud conditions (sugar, light-induced CK) may be too unfavorable so that exogenous sugar supply alone was not sufficient to induce any visible effect on its outgrowth. We simulated this behavior in response to virtually increasing sugar levels for LL plants. Interestingly, this artificial situation modified the balance between the different signals controlling bud outgrowth, reflected through the value of the model-related signal integrator, but still not sufficient to reach the threshold required for bud outgrowth. However, such behavior was also simulated after virtual increase in CK for LL plants. Indeed, the model did not predict any positive effect of exogenous CK supply *in planta* which differs from experimental data (Ramon et al., 2016; Corot et al., 2017). One explanation lies in that CK supply results in an increase in sugar locally in the node and bud, due to CK effect on carbon sink strength (Roitsch and Gonzalez, 2004), a not-yet considered behavior in our model yet. Tackling these questions would require a deeper confrontation between simulations and observations in other light conditions (darkness vs light). Monitoring bud expression of *BRC1*, a dormancy-related gene that integrates both CK and sugar (Wang et al., 2019) or the consequences of sugar and CK exogenous supply in planta to CK and sugar contents in nodes would also be of a great interest.

Both iP- et Z- types CK in stems are involved in the local bud outgrowth stimulation by light.

Several CK forms are present in plants (Hirose et al., 2008, Kamada-Nobusada and Sakakibara, 2009). Two main groups are distinguished, iP-types and Z-types, the first one being mostly synthetized in shoots, the second one mostly synthetized in roots (for review Daviere and Achard, 2017).

Our simulation results for rose plants under different light regimes indicate that the total pool of these two types of CKs, is involved in bud outgrowth stimulation by local light environment. Indeed, measured total CK (iP types and Z-types) contents in stem matched with the local-light driven CK simulations (Fig.8; data not shown). Previous studies on rose also reported the involvement of both CK-types in bud outgrowth regulation by light (Roman et al., 2016, Corot et al., 2017). Submitting decapitated plants to darkness or intact plants to low light intensity during bud outgrowth period repressed bud outgrowth as well as both iP- and Z-types CK in stems, and exogenous supply of both CK types to decapitated plants under darkness could trigger bud outgrowth. The respective role of both CK types in bud outgrowth is unknown yet. For rose decapitated plants under light, iP-types preferentially accumulated in node and tZ-types in bud (Roman et al., 2017), indicating that only tZ-types may be transferred to buds and control bud outgrowth (Osugi et al., 2017). In this case, iP-types accumulation in node was related to light-upregulation of the CK biosynthesis genes (IPT3 and IPT5). However, the origin of Z-types accumulation was not studied. The adequacy between measured iP- and Z-types and local light-driven CK simulation indicate that synthesis of these two types of CK may also be stimulated by local light environment in stem. In line with this, the presence of both iP- and Z- forms was observed for rose stem segments in vitro (Bertheloot et al., 2020), and we also recently showed an alteration of the expression of CYP735A gene, responsible for Z-type CK synthesis from iP-type CK, in rose stem in response to different light treatments (data not shown). In literature, plant light regime was reported to control root-derived CK (Boonman et al., 2007) and their systemic transport was recently shown to regulate leaf expansion and meristem activity (Osugi et al., 2017; Poitout et al., 2018). Further studies are required to decipher the roles of root-derived CK (Z-types) compared to shoot-synthetized CK (iP-types) in bud outgrowth regulation by plant light regime, and the involvement of Z-type CK in the control of bud outgrowth by root-to-shoot signaling.

Conclusion

Our results support the hypothesis that light intensity-driven bud outgrowth regulation at the plant scale relies on two concomitant pathways: (i) CKs, whose synthesis is controlled by local light intensity at node scale, and (ii) the availability of sugars, through light-driven changes in morphogenesis and photosynthesis at plant scale. Both are branching inducers that operate through two independent pathways contributing to their synergistic effect on bud outgrowth. This was demonstrated by using (i) a quantitative computer node-scale model of bud outgrowth regulation by the local balance in sugar, hormones, and light, and (ii) measurements of the effect of three light treatment at plant scale on this local balance. To further support our regulation hypothesis at plant scale, it would be necessary to include measurements of more physiological variables in more experimental conditions. In addition, coupling the node-scale model in a virtual plant integrating sugar and hormones fluxes between

compartments could be helpful for understanding the contribution of other organs (root, leaves…) on bud outgrowth.

CHAPTER 2 - SUPPLEMENTARY DATA

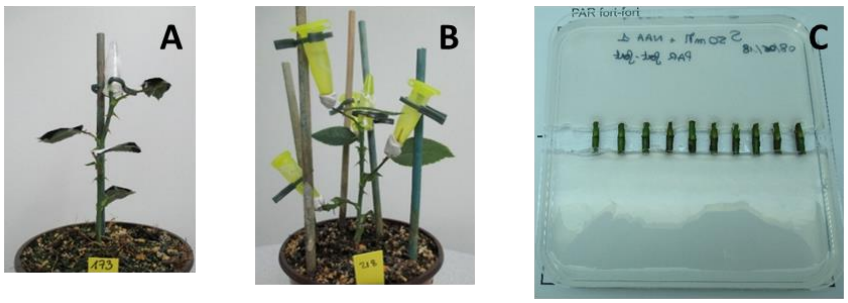

Supp. Figure 1: Modified biological models used after FBV stage. A/Plant decapitated 2cm above the fourth leaf of the primary axis at FBV. and partly defoliated keeping only one lateral leaflet per leaf. An auxin agar (NAA 5µM) is places at the tope of the cut stem. B/ Exogenous sucrose or cytokinin supplu to beheaded plants through the petiole of each kept leaf. C/Single bud berring nodes cultivated *in vitro*.

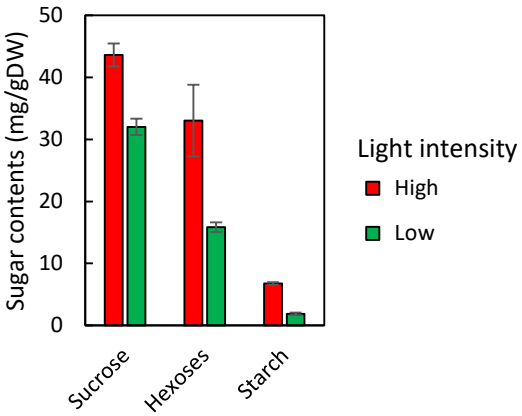

Supp Figure 2: Light intensity of rose primary axes positively controls stem sugar contents. Plants were grown either under low light intensity (green bars) or high light intensity (red bars) before floral bud was visible on the primary axis (FBV stage). Sucrose. hexoses (Glucrose + Fructose). and starch were measured in nodes collected in the most leaf-bearing basal part of the primary axis (Z3. for more details: see Chapter 1). where stem segments were excised for *in vitro* cultivation. Data are means ± SEM of 4 repetitions (4 to 5 plants per repetition).

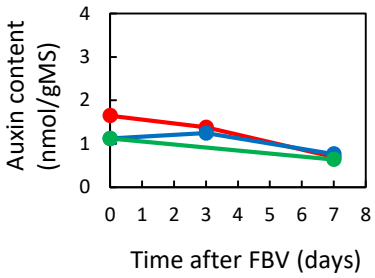

Supp. Figure 3: Effect of light intensity treatments (LL. LH and HH) on auxin contents for nodes taken from Z3 of rose primary axes. Nodes were taken when floral bud was visible on the primary axis (FBV) and at 3 and 7 days later. Data are means SE of 4 repetitions of at least 4 pooled plants each.

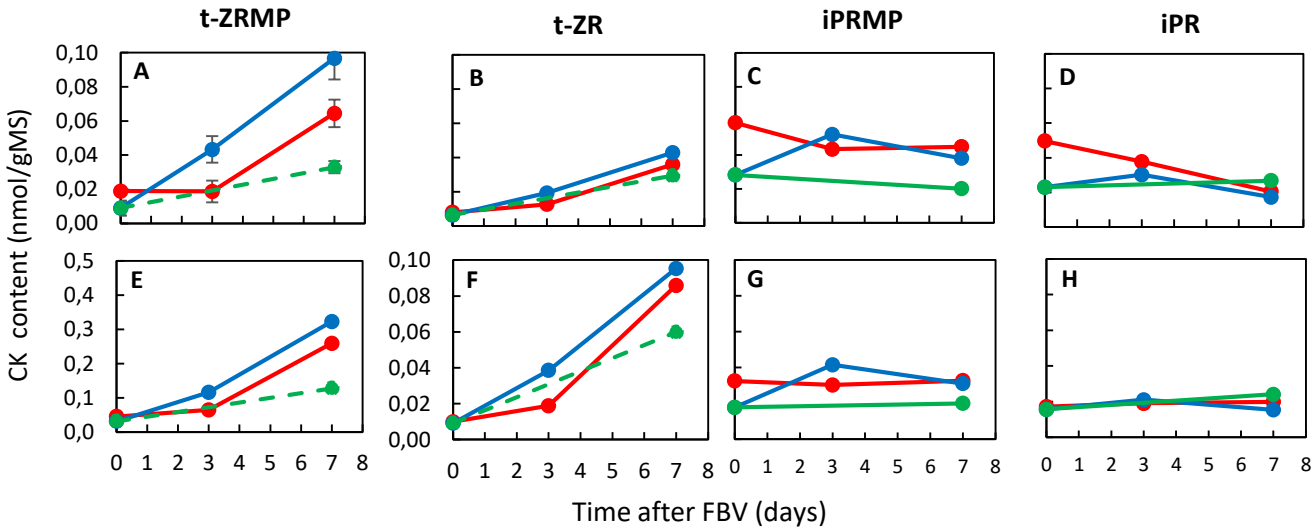

Supp. Figure 4: Effect of light intensity treatments (LL. LH and HH) on cytokinins (t-ZRMP, t-ZR, IPRMP and IPR) contents for nodes taken from Z2 and Z3 of rose primary axes. Nodes were taken when floral bud was visible on the primary axis (FBV) and at 3 and 7 days later. Data are means of 4 repetitions of at least 4 pooled plants each.

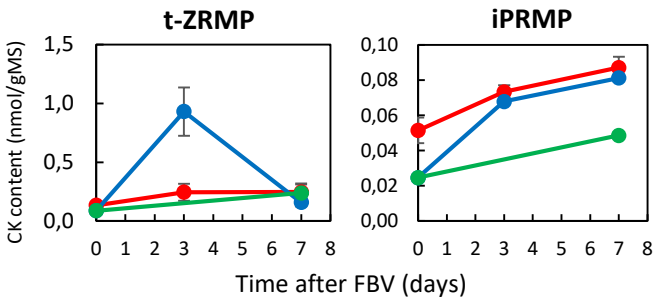

Supp. Figure 5: Effect of light intensity treatments (LL. LH and HH) on cytokinins (t-ZRMP, IPRMP) contentsin roots. Roots were taken when floral bud was visible on the primary axis (FBV) and at 3 and 7 days later. Data are means of 4 repetitions of at least 4 pooled plants each.

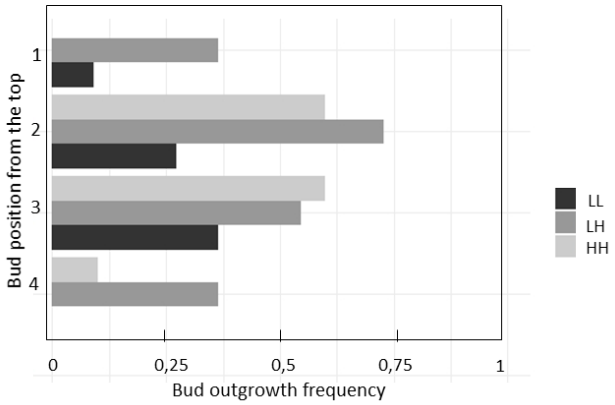

Supp. Figure 6: Impact of light intensity treatments (LL, LH and HH) on bud outgrowth for decapitated rose stems. Rose primary axes were decapitated above the fourth leaflet-bearing node when floral bud was visible (FBV). and supplied with 5 µM NAA at their top. and either 25 mM mannitol. Buds are numbered from decapitated plant top. Data are means of at least 11 plants per treatment at FBV+17d.

REFERENCES

Barbier, F., Péron, T., Lecerf, M., Perez-Garcia, M.-D., Barrière, Q., Rolčík, J., Boutet-Mercey, S., Citerne, S., Lemoine, R., Porcheron, B., et al. (2015). Sucrose is an early modulator of the key hormonal mechanisms controlling bud outgrowth in Rosa hybrida. J Exp Bot 66, 2569–2582.

Barbier, F.F., Dun, E.A., Kerr, S.C., Chabikwa, T.G., and Beveridge, C.A. (2019). An update on the signals controlling shoot branching. Trends in Plant Science 24, 220–236.

Bertheloot, J., Barbier, F., Boudon, F., Perez-Garcia, M.D., Péron, T., Citerne, S., Dun, E., Beveridge, C., Godin, C., and Sakr, S. (2020). Sugar availability suppresses the auxin-induced strigolactone pathway to promote bud outgrowth. New Phytologist 225, 866–879.

Boonman, A., Prinsen, E., Gilmer, F., Schurr, U., Peeters, A.J.M., Voesenek, L.A.C.J., and Pons, T.L. (2007). Cytokinin Import Rate as a Signal for Photosynthetic Acclimation to Canopy Light Gradients. Plant Physiology 143, 1841–1852.

Corot, A., Roman, H., Douillet, O., Autret, H., Perez-Garcia, M.-D., Citerne, S., Bertheloot, J., Sakr, S., Leduc, N., and Demotes-Mainard, S. (2017). Cytokinins and abscisic acid act antagonistically in the regulation of the bud outgrowth pattern by light intensity. Frontiers in Plant Science 8, 1724.

Davière, J.-M., and Achard, P. (2017). Organ communication: Cytokinins on the move. Nature Plants 3, 1–2.

Demotes-Mainard, S., Huché-Thélier, L., Morel, P., Boumaza, R., Guérin, V., and Sakr, S. (2013). Temporary water restriction or light intensity limitation promotes branching in rose bush. Scientia Horticulturae 150, 432–440.

Domagalska, M.A., and Leyser, O. (2011). Signal integration in the control of shoot branching. Nature Reviews Molecular Cell Biology 12, 211–221.

Dun, E.A., Germain, A. de S., Rameau, C., and Beveridge, C.A. (2012). Antagonistic Action of Strigolactone and Cytokinin in Bud Outgrowth Control. Plant Physiology 158, 487–498.

Evers, J.B., Vos, J., Yin, X., Romero, P., van der Putten, P.E.L., and Struik, P.C. (2010). Simulation of wheat growth and development based on organ-level photosynthesis and assimilate allocation. J Exp Bot 61, 2203–2216.

Fichtner, F., Barbier, F.F., Feil, R., Watanabe, M., Annunziata, M.G., Chabikwa, T.G., Höfgen, R., Stitt, M., Beveridge, C.A., and Lunn, J.E. (2017). Trehalose 6-phosphate is involved in triggering axillary bud outgrowth in garden pea (Pisum sativum L.). The Plant Journal 92, 611–623.

Girault, T., Bergougnoux, V., Combes, D., VIEMONT, J.-D., and Leduc, N. (2008). Light controls shoot meristem organogenic activity and leaf primordia growth during bud burst in Rosa sp. Plant, Cell & Environment 31, 1534–1544.

Girault, T., Abidi, F., Sigogne, M., PELLESCHI-TRAVIER, S., Boumaza, R., Sakr, S., and Leduc, N. (2010). Sugars are under light control during bud burst in Rosa sp. Plant, Cell & Environment 33, 1339–1350.

González-Grandío, E., Pajoro, A., Franco-Zorrilla, J.M., Tarancón, C., Immink, R.G.H., and Cubas, P. (2017). Abscisic acid signaling is controlled by a BRANCHED1/HD-ZIP I cascade in Arabidopsis axillary buds. PNAS 114, E245–E254.

Greb, T., Clarenz, O., Schäfer, E., Müller, D., Herrero, R., Schmitz, G., and Theres, K. (2003). Molecular analysis of the LATERAL SUPPRESSOR gene in Arabidopsis reveals a conserved control mechanism for axillary meristem formation. Genes Dev. 17, 1175–1187.

Henry, C., Rabot, A., Laloi, M., Mortreau, E., Sigogne, M., Leduc, N., Lemoine, R., Sakr, S., Vian, A., and PELLESCHI-TRAVIER, S. (2011). Regulation of RhSUC2, a sucrose transporter, is correlated with the light control of bud burst in Rosa sp. Plant, Cell & Environment 34, 1776–1789.

Hirose, T., Scofield, G.N., and Terao, T. (2008). An expression analysis profile for the entire sucrose synthase gene family in rice. Plant Science 174, 534–543.

Kamada-Nobusada, T., and Sakakibara, H. (2009). Molecular basis for cytokinin biosynthesis. Phytochemistry 70, 444–449.

Luquet, D., Dingkuhn, M., Kim, H., Tambour, L., and Clement-Vidal, A. (2006). EcoMeristem, a model of morphogenesis and competition among sinks in rice. 1. Concept, validation and sensitivity analysis. Functional Plant Biology 33, 309–323.

Martín-Fontecha, E.S., Tarancón, C., and Cubas, P. (2018). To grow or not to grow, a power-saving program induced in dormant buds. Current Opinion in Plant Biology 41, 102–109.

Mason, M.G., Ross, J.J., Babst, B.A., Wienclaw, B.N., and Beveridge, C.A. (2014). Sugar demand, not auxin, is the initial regulator of apical dominance. PNAS 111, 6092–6097.

Mitchell, K.J. (1953). Influence of Light and Temperature on the Growth of Ryegrass (Lolium spp.). Physiologia Plantarum 6, 21–46.

Pallas, B., and Christophe, A. (2015). Relationships between biomass allocation, axis organogenesis and organ expansion under shading and water deficit conditions in grapevine. Functional Plant Biol. 42, 1116–1128.

Poitout, A., Crabos, A., Petřík, I., Novák, O., Krouk, G., Lacombe, B., and Ruffel, S. (2018). Responses to Systemic Nitrogen Signaling in Arabidopsis Roots Involve trans-Zeatin in Shoots. The Plant Cell 30, 1243–1257.

Rabot, A., Henry, C., Ben Baaziz, K., Mortreau, E., Azri, W., Lothier, J., Hamama, L., Boummaza, R., Leduc, N., and Pelleschi-Travier, S. (2012). Insight into the role of sugars in bud burst under light in the rose. Plant and Cell Physiology 53, 1068–1082.

Rameau, C., Bertheloot, J., Leduc, N., Andrieu, B., Foucher, F., and Sakr, S. (2015). Multiple pathways regulate shoot branching. Frontiers in Plant Science 5, 741.

Roitsch, T., and Ehneß, R. (2000). Regulation of source/sink relations by cytokinins. Plant Growth Regulation 32, 359–367.

Roitsch, T., and González, M.-C. (2004). Function and regulation of plant invertases: sweet sensations. Trends in Plant Science 9, 606–613.

Roman, H., Girault, T., Barbier, F., Péron, T., Brouard, N., Pěnčík, A., Novák, O., Vian, A., Sakr, S., and Lothier, J. (2016). Cytokinins are initial targets of light in the control of bud outgrowth. Plant Physiology 172, 489–509.

Roman, H., Girault, T., Gourrierec, J.L., and Leduc, N. (2017). In silico analysis of 3 expansin gene promoters reveals 2 hubs controlling light and cytokinins response during bud outgrowth. Plant Signaling & Behavior 12, e1284725.

Schmitz, G., and Theres, K. (2005). Shoot and inflorescence branching. Current Opinion in Plant Biology 8, 506–511.

Schneider, A., Godin, C., Boudon, F., Demotes-Mainard, S., Sakr, S., and Bertheloot, J. (2019). Light regulation of axillary bud outgrowth along plant axes: an overview of the roles of sugars and hormones. Frontiers in Plant Science 10, 1296.

Shen, J., Zhang, Y., Ge, D., Wang, Z., Song, W., Gu, R., Che, G., Cheng, Z., Liu, R., and Zhang, X. (2019). CsBRC1 inhibits axillary bud outgrowth by directly repressing the auxin efflux carrier CsPIN3 in cucumber. PNAS 116, 17105–17114.

Waldie, T., McCulloch, H., and Leyser, O. (2014). Strigolactones and the control of plant development: lessons from shoot branching. The Plant Journal 79, 607–622.

Wang, M., Le Moigne, M.-A., Bertheloot, J., Crespel, L., Perez-Garcia, M.-D., Ogé, L., Demotes-Mainard, S., Hamama, L., Davière, J.-M., and Sakr, S. (2019). BRANCHED1: A Key Hub of Shoot Branching. Front Plant Sci 10.

DISCUSSION GENERALE, CONCLUSION ET PERSPECTIVES

RAPPEL DU CONTEXTE ET DES OBJECTIFS

L'analyse de la littérature scientifique présentée en introduction (review : Schneider et al., 2019) soulignait le caractère fragmenté des connaissances actuelles sur la régulation du débourrement des bourgeons axillaires par l'intensité lumineuse. L'effet positif d'une forte intensité lumineuse pendant la phase de ramification sur le débourrement (fréquence et précocité) des bourgeons axillaires est connu chez plusieurs espèces herbacées et ligneuses (Mitchell, 1953 ; Su et al, 2011 ; Leduc et al., 2014). Durant la dernière décennie, il a aussi été observé pour le rosier que l'historique des conditions lumineuses expérimentées par la plante au cours de sa croissance pouvait moduler la réponse du débourrement à l'intensité lumineuse. Ainsi, des plants de rosiers ayant subi une restriction temporaire de lumière pendant la croissance de l'axe primaire, présentent une stimulation du débourrement des bourgeons axillaires plus importante que des plantes ayant toujours été sous de bonnes conditions lumineuses (Demotes-Mainard et al., 2013). Par ailleurs, la compréhension des mécanismes physiologiques impliqués dans la régulation du débourrement et de la dominance apicale a fortement progressé ces dernières années, avec la découverte du rôle de messagers intermédiaires des SL et des CKs, relais de l'auxine apicale (Domagalska and Leyser, 2011), et de l'effet stimulateur des sucres (Mason et al., 2014 ; Barbier et al., 2015, Bertheloot et al., 2020). Plus récemment, des études expérimentales sur le rosier ont montré l'importance de la synthèse *de novo* de CKs de type iP dans le nœud porteur du bourgeon lors de la stimulation du débourrement par l'intensité lumineuse courante (Roman et al., 2016 ; Corot et al., 2017). Parallèlement, plusieurs modèles de croissance des plantes faisaient l'hypothèse d'un contrôle de la ramification ou du tallage des plantes par l'intensité lumineuse, via le statut carboné global de la plante (Luquet et al., 2006). Malgré la modification observée des teneurs en sucres (saccharose et amidon) dans la tige lors de traitements lumineux pendant la phase de débourrement, le rôle des sucres dans la réponse de la ramification à l'intensité lumineuse a été écarté expérimentalement. Des apports exogènes de sucres ne compensaient pas l'inhibition du débourrement observée dans des conditions lumineuses défavorables (faible intensité ou obscurité), comparé au débourrement observé sous forte intensité lumineuse (Roman et al., 2016 ; Corot et al., 2017). Les acteurs régulateurs du débourrement et les mécanismes physiologiques mis en jeu pour expliquer l'effet à long terme d'une restriction temporaire de lumière restaient cependant inconnus. Sachant qu'une modulation de l'intensité lumineuse pendant le développement des organes de l'axe primaire pourrait modifier leur croissance et donc la compétition exercée par l'axe primaire sur les bourgeons axillaires pendant la période de débourrement, l'hypothèse d'un rôle des sucres n'étaient pas à écarter dans ce cas. Notre objectif était de comprendre le rôle que jouaient les sucres, en interaction avec les autres hormones régulatrices du débourrement, dans la régulation du débourrement par la lumière.

Pour y répondre, nous avons orienté nos recherches sur la compréhension de trois principaux phénotypes *in planta*, consistant à moduler l'intensité lumineuse avant et pendant la période de débourrement. Les

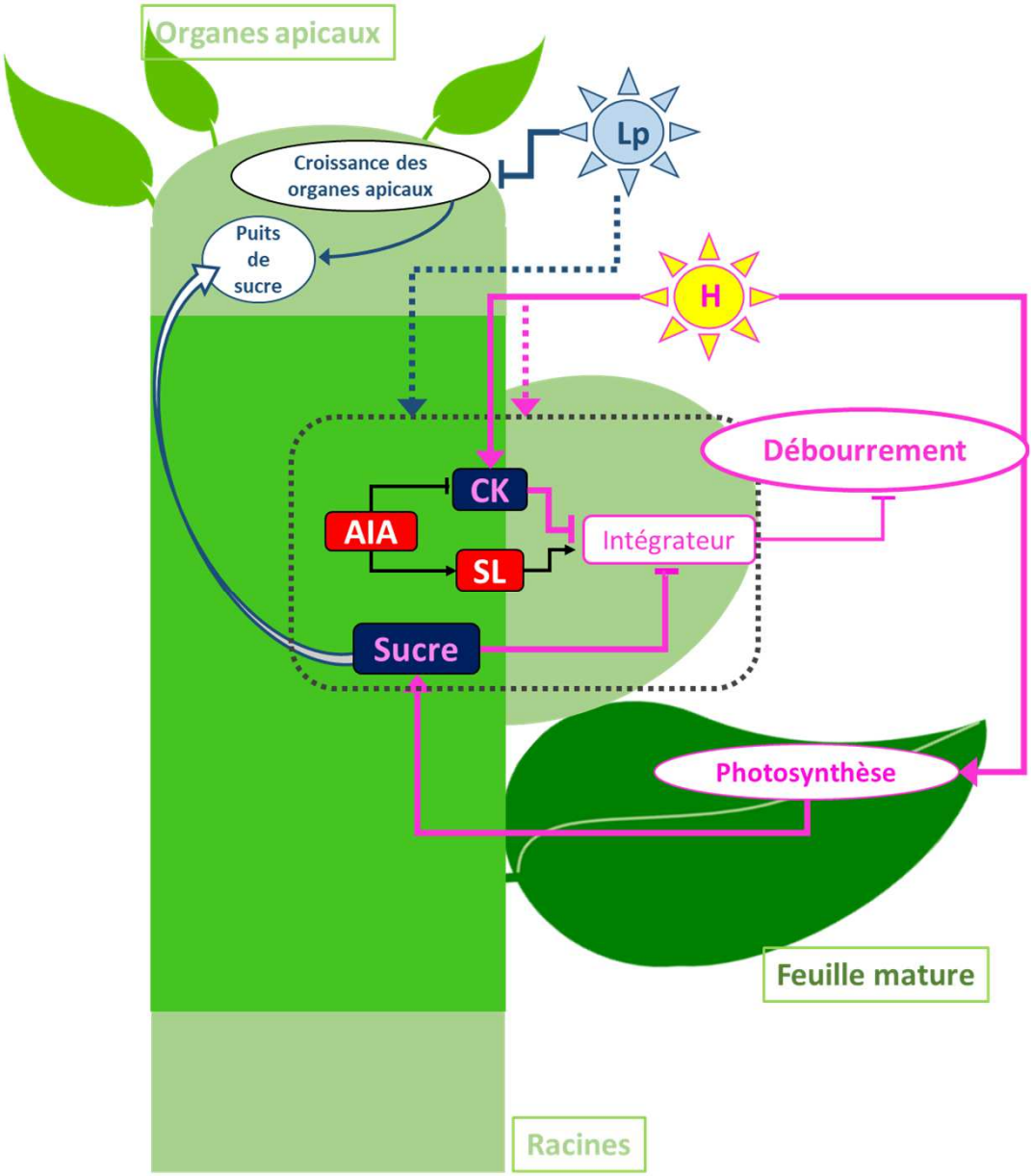

Figure Bilan : Effets de l'intensité lumineuse sur la régulation du débourrement mis en évidence à la fin de cette thèse.
Le débourrement des bourgeons axillaires est stimulé par une forte intensité lumineuse pendant la phase de ramification (H) - comparé à une faible intensité lumineuse-, et cette stimulation est accentuée par une faible intensité lumineuse passée (Lp). Nous montrons que les effets de H et Lp sur le débourrement peuvent être expliqués par une modification de l'équilibre quantitatif entre les teneurs d'hormones et sucres au voisinage du bourgeon (Chapitre 3; flèches en pointillés). Dans les deux cas, la lumière agit en augmentant les CK et le sucre au voisinage du bourgeon, ce qui contrecarre l'effet négatif de l'auxine sur le débourrement et ainsi le stimule. Pour Hc, nous démontrons qu'en plus du rôle promoteur des CK, stimulées localement par la lumière (Corot et al., 2017; Roman et al., 2016), le sucre, stimulé par une augmentation de la photosynthèse, contribue également à la stimulation du débourrement. Pour Lp, la croissance des organes apicaux est réduite, y compris après la fin de a restriction lumineuse, ce qui diminue leur force puits et augmente le sucre au voisinage du bourgeon (chapitre 2). En plus, cela augmente la lumière arrivant au niveau des organes sous-jacents et leur teneur en CK (chapitres 2 et 3).

expériences biologiques (phénotypages, apports pharmacologiques, dosages) ont été couplées avec une démarche de modélisation pour mieux appréhender le bilan en sucres des plantes par exemple, et pouvoir quantifier les rôles de chaque acteur dans la réponse du bourgeon à l'intensité lumineuse.

Ci-dessous, nous résumons les principaux résultats établis dans ce travail de thèse, en regard des connaissances de la littérature, et complétons le schéma de compréhension global de régulation du débourrement par l'intensité lumineuse (Figure bilan). Je détaillerai les avantages et limites de la démarche couplant expériences et modélisation. Enfin, nous évoquerons plusieurs perspectives de recherche dans la prolongation de ce travail de thèse.

PRINCIPAUX RESULTATS ET APPORTS A LA COMPREHENSION DE LA REGULATION DU DEBOURREMENT AXILLAIRE PAR L'INTENSITE LUMINEUSE

La réponse du débourrement des bourgeons axillaires à l'intensité lumineuse implique des régulations systémiques à l'échelle de la plante.

Le rôle de la synthèse de novo de CKs de type iP dans le nœud portant le bourgeon a été démontré chez des plants de rosiers soumis à des conditions lumineuses défavorables pendant la période attendue de débourrement (Roman et al., 2016 ; Corot et al., 2017). En étudiant la réponse de la plante lors de variations de l'intensité lumineuse avant et pendant la phase de débourrement, nous avons montré que d'autres mécanismes de régulation, à l'échelle de la plante, interviennent dans la réponse du débourrement à l'intensité lumineuse perçue pendant la croissance de la plante et impliquent plusieurs organes.

L'effet de l'intensité lumineuse passe en partie par une modulation de la compétition pour les sucres entre les organes préexistants et les bourgeons axillaires

Grâce à la quantification du statut en sucres des plantes, et à des expériences de modulation des teneurs en sucres dans la plante sous différents traitements lumineux, nous avons démontré le rôle important de la compétition pour le sucre entre les bourgeons axillaires et l'axe primaire dans la régulation de la dominance apicale par l'intensité lumineuse (Chapitre 2). Jusqu'alors, plusieurs modèles de croissance des plantes avaient implémenté une régulation du débourrement par l'intensité lumineuse via la compétition avec les autres organes et le statut carboné global de la plante (Luquet et al., 2006). L'effet inhibiteur de la compétition pour les sucres de l'axe primaire sur le débourrement des bourgeons avait été montré expérimentalement (Kebrom et al., 2012 ; Mason et al., 2014 ; Kebrom, 2017). Cependant, aucun résultat expérimental ne confirmait l'implication de la compétition pour les sucres entre l'axe primaire et les bourgeons dans la régulation du débourrement par l'intensité lumineuse. Nous avons ici démontré son rôle dans le cas particulier d'une restriction temporaire de lumière avant la période habituelle de débourrement, suivie d'une forte intensité lumineuse pendant la phase de débourrement (LH versus HH dans Chapitre 2). Dans ce cas particulier, les teneurs en CKs n'étaient pas

limitantes dans la tige (Fig. 6B Chapitre 3), et les différences de disponibilité en sucres pour le débourrement menaient donc à des phénotypes différents entre les traitements lumineux.

Au contraire, lors d'une restriction de lumière pendant la phase de débourrement (HL versus HH dans Corot et al., 2017), le rôle des sucres dans la régulation du débourrement par l'intensité lumineuse perçue pendant la phase de débourrement avait été jugé négligeable par rapport au rôle des CKs qui étaient en concentrations limitantes sous faible intensité lumineuse (HL) (Corot et al., 2017). En effet, des apports exogènes de sucres ne permettaient pas de lever la dominance apicale sous faible intensité lumineuse (HL). Nous avons aussi observé expérimentalement l'incapacité d'apports exogènes de saccharose à stimuler le débourrement chez des plantes placées sous faible intensité lumineuse (LL chap2). Cependant, l'intervention d'une compétition pour les sucres dans le maintien de la dominance apicale sous faible intensité lumineuse n'est pas à exclure totalement. En effet, les techniques expérimentales d'apports de sucres sur des plantes placées sous faible intensité lumineuse (HL ou LL) n'excluent pas une diversion des sucres initialement apportés pour le bourgeon par les organes de l'axe primaire. Des apports exogènes de sucres *in planta* inefficaces pour stimuler le débourrement n'excluent donc pas totalement un possible rôle des sucres. Une quantification du statut global en sucres de la plante lors d'une restriction de la lumière pendant la phase de débourrement, comme réalisé dans le chapitre 2 pour les traitements LH et HH, permettrait de préciser le niveau de compétition entre l'axe primaire et les bourgeons axillaires dans ce contexte lumineux. De plus, les simulations de débourrement menées dans le Chapitre 3 suggèrent que les sucres joueraient un rôle important pour expliquer la différence de débourrement entre des plantes placées sous une faible intensité lumineuse continue comparé à des plantes sous forte intensité lumineuse continue, même si apportés seuls, les sucres ne mènent pas un phénotype visible de débourrement. Suite à ces simulations numériques, l'implication des sucres dans la différence de débourrement entre une forte et une faible intensité lumineuse courante (HL versus HH) mérite d'être validée expérimentalement. La quantification par exemple d'expression d'un des gènes marqueurs du débourrement, comme l'intégrateur TEOSINTE/BRANCHED1, suite à l'apports de sucres sous HL ou LL permettraient de quantifier la réponse du bourgeon aux sucres, même si le débourrement *stricto-sensu* n'est pas observé.

Les CKs d'origine racinaire sont impliquées dans la réponse du débourrement à des variations d'intensité lumineuse passée ou courante.

De façon inattendue, les teneurs totales en CKs (formes iP et tZ) permettaient de mieux discriminer les 3 traitements lumineux (LL, LH et HH) consistant à moduler l'intensité lumineuse avant et/ou pendant la phase de débourrement (Chapitre 3), alors que les teneurs CKs de type iP prises seules ne permettaient pas de distinguer une restriction temporaire de lumière (LH) du traitement consistant à appliquer une forte intensité lumineuse continue (HH). Nous avons tout d'abord observé dans le Chapitre 3 une corrélation positive entre l'intensité du débourrement (fréquence et précocité) et les teneurs totales en CKs dans les nœuds portant les bourgeons sous trois traitements lumineux. De plus,

lors des simulations numériques du débourrement à partir des valeurs observées *in planta* de teneurs en sucres et auxine au voisinage du bourgeon, et des valeurs locales d'intensité lumineuse, les simulations des teneurs en CKs sont cohérentes avec les teneurs totales de CKs observées expérimentalement. Ces éléments suggèrent donc un rôle des CKs de type tZ, en plus des CKs de type iP, dans l'obtention des phénotypes de débourrement sous différents traitements lumineux. Ces résultats sont cohérents avec ceux de Roman et al. (2016) et Corot et al. (2017) sur le rosier : la stimulation du débourrement sous forte intensité lumineuse est corrélée à des teneurs en CKs de type tZ dans la tige plus importantes, comparé à des conditions lumineuses défavorables. De plus, l'application de CKs de type tZ sur la blessure de plants de rosiers décapités placés à l'obscurité permet de lever l'inhibition du débourrement, de la même façon que l'application de CKs de type iP (Roman et al., 2016). Cela démontre le caractère suffisant des CKs de type tZ pour stimuler le débourrement des bourgeons dans des conditions lumineuses défavorables.

Les mécanismes expliquant la modulation des teneurs en CKs de type tZ dans la tige selon les traitements lumineux restent flous. Contrairement aux CKs de type iP, celles de type tZ sont majoritairement synthétisées dans la racine (Sakakibara, 2006 ; Hirose et al., 2007). Toutefois, des premiers résultats de dosages des transcrits du gène codant l'enzyme CYP735A, responsable de la transformation des formes iP en tZ ont montré une expression dans les nœuds (comm. pers. J. Bertheloot). De plus, les résultats de simulation montrent une relation étroite entre la teneur en CKs totales (iP+tZ) au niveau du nœud et la lumière ambiante. L'ensemble de ces résultats suggèrent que la lumière locale pourrait agir sur la production de CK de forme tZ au niveau des nœuds. D'autre part, les dosages de CK réalisés dans les racines (Chapitre 3, Supp. Fig.5) montraient une modulation des teneurs en CKs de forme iPRMP et tZRMP entre les trois traitements lumineux (LL, LH et HH), suggérant une modulation par la lumière des CKs dans les racines. Un message de type « tige vers racines » pourrait exister avec une modification des teneurs en sucres par les traitements lumineux qui constituerait un signal pour la modulation de synthèse de CKs dans les racines (Foo et al., 2007). Un tel mécanisme a déjà été observé dans le cadre de la floraison chez *Sinapsis alba* (Havelange et al., 2000). Cette hypothèse serait cohérente avec la corrélation observée entres les teneurs en amidon et les teneurs en CKs dans les racines sous les trois traitements lumineux (Chapitre 3, Supp.Fig. 5). Plus récemment, l'importance des sucres d'origine photosynthétique dans la stimulation des gènes de synthèse des CK de type iP et tZ, ainsi que du transporteur de CKs tZ (ABCG14) dans les racines a été démontrée chez Arabidopsis (Kiba et al., 2019). Des plantes placées sous fortes concentrations de CO_2 atmosphérique, ou supplémentées en sucres présentent des expressions de gènes de synthèses des CKs (AtIPT3 et CYP735A2 pour la synthèse des formes iPRMP et leur transformation en formes tZRMP, respectivement) plus importantes dans les racines. Réciproquement, cette stimulation de l'expression de ces gènes sous forte [CO_2] est inhibée par l'application d'un inhibiteur de photosynthèse (DCMU) sur la plante. Cette étude révèle aussi que la stimulation de l'expression des gènes de synthèse des CKs par

les sucres est indépendante de la nutrition azotée apportée à la plante, suggérant que les sucres agissent par une voie indépendante des nitrates sur la stimulation de la synthèse des CKs dans les racines.

Pour résumer, les organes de l'axe primaire (phytomères et fleur) ainsi que le compartiment racinaire viennent enrichir le schéma de compréhension de la régulation du débourrement par l'intensité lumineuse. Une restriction de l'intensité lumineuse perçue pendant le développement de l'axe primaire affecte de façon irréversible la croissance des organes aériens et racinaires, et ainsi diminue la compétition exercée par l'axe primaire pour les sucres sur les bourgeons axillaires. D'autre part, le compartiment racinaire pourrait avoir un rôle positif sur le débourrement via la synthèse de cytokinines de type tZ, qui serait sous le contrôle du statut carboné de la plante. Cette hypothèse mérite cependant d'être évaluée.

La régulation du débourrement par la lumière résulte d'une modification de l'équilibre quantitatif entre les teneurs des différents acteurs régulateurs du débourrement dans le nœud

Dans le troisième chapitre, nous avons simulé le débourrement de bourgeons *in planta* sous différents traitements lumineux, en prenant comme variables d'entrée et intermédiaires les teneurs locales en auxine, amidon, CKs totales et les valeurs locales de l'intensité lumineuse ambiante du bourgeon.

La bonne adéquation entre d'une part les valeurs de débourrement et de teneurs en CK simulées, et d'autre part les valeurs observées expérimentalement, suggère que les variables et les mécanismes choisis et implémentés dans le modèle sont suffisants pour expliquer la réponse du débourrement des bourgeons à des variations d'intensité lumineuse (Chapitre 3). Plus particulièrement, nos résultats suggèrent un rôle important de l'amidon pour expliquer les phénotypes de débourrement observés, au lieu du saccharose initialement utilisé comme entrée du modèle *in vitro* (Bertheloot et al., 2020). En effet, les dosages des teneurs en amidon dans les nœuds *in planta* (Chapitre 3) permettaient de discriminer les trois traitements lumineux étudiés (LL, LH et HH), alors que les teneurs en saccharose étaient similaires lorsque l'intensité lumineuse était forte pendant la période de ramification, indépendamment de l'historique lumineux (LH et HH). Une corrélation entre les teneurs en amidon et le débourrement avait aussi été observée par Corot et al. (2017) lors de la variation de l'intensité lumineuse pendant la phase attendue de débourrement. En tant que molécule de stockage, l'amidon sert tour à tour de puits et de sources de sucres (McNeill, 2017) et les teneurs en amidon peuvent alors rendre compte du statut en carbone global de la plante. L'utilisation de l'amidon comme variable d'entrée du modèle *in planta* est donc cohérente avec les modèles de plantes existants, et basés sur le carbone, dans lesquels la ramification est contrôlée par le statut carboné de la plante (Luquet et al.,2006 ; Evers et al., 2010).

D'autre part, la modélisation de la réponse du débourrement par les teneurs locales en hormones et en sucres, a permis de quantifier les rôles relatifs des sucres et des CKs dans la stimulation du débourrement sous différentes intensités lumineuses (Chapitre 3) et de dépasser l'opposition entre les

sucres et les CKs pour leur rôle majeur dans la réponse du débourrement à l'intensité lumineuse. Nous avons montré que les sucres locaux jouaient un rôle dans la stimulation du débourrement par l'intensité lumineuse courante (LL versus HH) ce qui avait été écarté lors de précédentes publications expérimentales (Roman et al., 2016 ; Corot et al., 2017). De plus, la comparaison de simulations du débourrement avec apports de sucres sous différents traitements lumineux, nous a permis de montrer que les sucres et les CKs stimulent le débourrement par des voies en partie distinctes. Selon les simulations, l'effet des sucres dans la stimulation du débourrement par l'intensité lumineuse passerait majoritairement par la voie des SLs. Ce résultat vient dans la continuité des études sur la levée de l'inhibition du débourrement par l'effet des sures sur le signal des SLs (Barbier et al., 2015 ; Bertheloot et al., 2020). Cependant, le modèle construit ne permet pas de prendre en compte l'effet que pourraient avoir localement la présence de CKs dans la tige sur la force puits du bourgeon, et donc l'effet positif des teneurs en CK dans la tige sur les teneurs en sucres (Roitsch and Ehneß, 2000).

Les acteurs et mécanismes mis en avant dans la régulation du débourrement par l'intensité lumineuse dans les simulations du Chapitre 3 méritent d'être vérifiés expérimentalement. La validation du modèle sur les données *in vitro* et *in planta* des teneurs en CKs et des phénotypes de débourrement ne permettent pas d'affirmer que les mécanismes et les acteurs implémentés sont exacts. Des expériences de dosages des SL et des transcrits des gènes impliqués dans leur signalisation (MAX2) permettraient de confirmer leur forte implication dans la réponse du débourrement à l'intensité lumineuse. Par ailleurs, l'utilisation du modèle *in planta* n'exclue pas que certaines fonctions du modèle, comme la synthèse des CKs et des SLs, confondent des mécanismes ayant lieu dans le nœud et dans les racines. On peut enfin s'interroger sur l'absence de prise en compte de l'ABA dans la régulation du débourrement par la lumière dans ce modèle. L'augmentation des teneurs en ABA dans le nœud est en effet corrélée à l'inhibition du débourrement sous faible intensité lumineuse chez le rosier (Corot et al., 2017), cependant la compréhension des mécanismes sous-jacents est encore floue.

AVANTAGES ET LIMITES D'UNE DEMARCHE COUPLANT EXPERIMENTATIONS BIOLOGIQUES ET MODELISATION

L'objectif principal de la thèse était de mieux comprendre les rôles relatifs des sucres et des hormones dans la réponse du débourrement à différentes variations de l'intensité lumineuse. Pour ce faire, je me suis concentrée sur la compréhension des mécanismes sous-jacents aux phénotypes observés en plante entière sous trois traitements lumineux (LL, LH et HH) consistant à moduler l'intensité lumineuse avant et pendant la période de débourrement. J'ai dans un premier temps travaillé à comprendre les mécanismes expliquant les différences de débourrement suite à une restriction temporaire de lumière (LH versus HH) (Chapitre 2), puis j'ai travaillé sur une vision harmonisée de la régulation du débourrement par des variations d'intensité lumineuse (Chapitre 3).

La démarche et les résultats de modélisation permettent d'orienter les expériences et les mesures conduites pour répondre à la problématique

La réflexion de ma thèse s'est faite par des allers-retours successifs entre la démarche de modélisation et la vérification d'hypothèses par des expériences biologiques. Les premiers résultats de dosages effectués en 2011 révélaient des différences de statut en sucres entre les plantes du traitement LH et du traitement HH. Deux questions se sont alors posées : (i) à quoi était due l'accumulation de sucres sous LH par rapport à HH, et (ii) quel était le rôle des sucres dans la stimulation du débourrement observée ? La première question supposait de comparer les sources et les puits de sucres dans la plante. De nombreux modèles de croissances des plantes sont basés sur le bilan sources-puits en carbone (Letort et al., 2008 ; Mathieu et al., 2009). C'est en me positionnant dans une démarche de conceptualisation de modèle sources-puits en carbone pour comparer les traitements LH et HH, que j'ai décidé de plusieurs mesures à réaliser. La création du modèle nécessitait des données pour quantifier les sources et les puits de façon dynamique et à chaque étage foliaire de la plante. Nous avons donc suivi de façon fine les cinétiques de croissance des organes en masse et en dimensions pour pouvoir calculer des vitesses de croissance et donc la demande en carbone des organes. D'autre part, nous avons réalisé des mesures de taux de chlorophylle pour toutes les feuilles, et des mesures d'intensité lumineuse à différentes hauteurs le long de la plante. Sans la perspective de construire un modèle architecturé et dynamique de la plante, nous n'aurions sûrement pas suivi le développement et la photosynthèse de la plante de manière aussi fine, et nous n'aurions pas pu trancher sur la modulation du statut carboné entre les traitements LH et HH.

Par ailleurs, les simulations de débourrement en réponse à des teneurs en sucres et en hormones obtenues dans le Chapitre 3 ouvrent des perspectives de recherche qui avaient jusqu'alors été fermées. Alors que les résultats expérimentaux d'apports de sucres sous faible intensité lumineuse n'étaient pas concluants, la quantification de la réponse du bourgeon par les simulations incite à explorer expérimentalement le rôle des sucres dans ce contexte, en quantifiant les expressions de gènes liés au débourrement par exemple.

La modélisation permet de s'affranchir en partie des conditions expérimentales spécifiques et de proposer une vision générique de la réponse du débourrement à la lumière

Le modèle de débourrement utilisé dans le chapitre 3 a permis de simuler le débourrement de bourgeons cultivés in vitro ou sur la plante sous différentes intensités lumineuses. Cela suggère qu'une compréhension du système de régulation du débourrement, commune aux différentes conditions expérimentales, existe. Cependant, le passage d'un système étudié in vitro au système in planta n'était pas évident et demandait de modifier les variables d'entrées (amidon à la place du saccharose pour la variable de sucres) et leurs dimensions. La difficulté du passage de résultats obtenus sur des systèmes in vitro à des résultats obtenus in planta est aussi perçue dans les études de manipulations des apports d'auxine et/ou de CK exogènes au nœud ou à la plante (Barbier et al., 2015 ; Roman et al., 2016 ; Corot

et al., 2017). Les concentrations de ces composés apportés dans les solutions sont difficilement comparables aux concentrations qui peuvent être expérimentées par un bourgeon dans la plante, d'une part parce qu'elles sont exprimées dans des unités différentes (mM pour les apports exogènes, et mol/gMS pour les concentrations dans la plante), et d'autre part car il est difficile de déterminer la part de l'apport en auxine ou CKs qui va être absorbé par la plante. La réalisation de courbes de « conversion » entre les apports exogènes d'hormones et les concentrations retrouvées dans le nœud in vitro ou in planta permettrait d'une part de mieux adapter le modèle de débourrement proposé dans le Chapitre 3 à différents modèles biologiques, et d'autre part de recentrer les études de réponse du débourrement sur des valeurs d'hormones apportées cohérentes avec ce qui est naturellement expérimenté par la plante. Ainsi, les simulations de débourrement faites dans le Chapitre 3 pour des bourgeons in planta avec une forte valeur d'auxine en entrée (correspondant à une valeur absolue supérieure à 2µM dans une gélose) suggère que ce qui est expérimentée par le bourgeon in planta correspond au haut de la gamme de teneurs en auxine apportées dans les expériences in vitro (Barbier et al., 2015 ; Bertheloot et al., 2020).

Le modèle de bilan sources-puits en carbone construit dans le chapitre 2 pour estimer le statut en sucre des plantes sous LH et HH pourrait être généralisé à d'autres traitements lumineux consistant à faire varier l'intensité lumineuse au cours de la croissance de la plante. En effet, ce modèle prend en compte les différences de croissance et de photosynthèse établies par des variations d'intensité lumineuse précoces. Cependant, pour être aisément généralisable à d'autres traitements lumineux (comme les traitements LL et HL par exemple), l'effet de l'intensité lumineuse sur la variation du LMA et de la vitesse d'expansion des feuilles devrait être implémenté de façon mécaniste, et non à travers des valeurs de paramètres différentes entre les traitements lumineux. Cela demande un travail important de modélisation et de validation des mécanismes, notamment pour implémenter l'effet de variations de la lumière sur le LMA (Bertin and Gary, 1998). Dans cette thèse, nous avons choisi un modèle moins générique mais qui permettait de répondre aux questions directes liées à la compréhension des trois traitements lumineux étudiés.

PERSPECTIVES

Vers un modèle dynamique et intégré de réponse du débourrement à l'intensité lumineuse

A l'issue de cette thèse, nous disposons d'un modèle de quantification du bilan source-puits en carbone établi sur des plantes entières pour deux traitements lumineux (HH et LH ; chapitre 2), et d'un modèle de réponse du débourrement aux conditions locales en hormones, sucres et intensité lumineuse (Chapitre 3). Dans l'optique de créer un modèle de réponse du débourrement à l'intensité lumineuse générique pour différents traitements lumineux, deux enjeux sont à considérer.

Le premier est de proposer un modèle de réponse du bourgeon aux conditions locales en hormones, sucres et intensité lumineuse qui puisse intégrer dans le temps des variations des valeurs d'entrée. En effet, le modèle utilisé dans le Chapitre 3 prend comme entrées des variables constantes dans le temps, et sa conception ne permet pas de rendre compte d'un phénotype de débourrement si ces valeurs varient. Pour intégrer dans le temps la réponse du bourgeon aux conditions fluctuantes expérimentées *in planta*, on peut choisir de modéliser non pas directement l'occurrence et la date de débourrement s'il y a lieu, mais plutôt la croissance du bourgeon. En effet, la taille du bourgeon (en masse ou volume) serait une variable de sortie continue, et la vitesse de croissance du bourgeon pourrait rendre compte des variations des régulateurs du débourrement dans le nœud. Au-delà d'un volume seuil atteint, le bourgeon pourrait être considéré comme débourré et la date de débourrement déduite. Pour conceptualiser un tel modèle, le bourgeon pourrait être assimilé à une grosse cellule végétale dont le volume augmente selon le ratio entre la pression exercée par le volume d'eau accumulé dans la vacuole et la pression de paroi, suivant la loi de Lockhart pour l'accroissement cellulaire (Lockhart, 1965 ; Cosgrove, 1986). L'invertase vacuolaire et les expansines sont deux gènes dont l'expression est corrélée au débourrement (Rabot et al., 2012 ; Roman et al., 2016). Le taux d'invertase vacuolaire pourrait réguler l'entrée d'eau dans la cellule par osmose après une entrée de sucres, et ainsi augmenter la pression osmotique dans la cellule. Les expansines réduiraient quant à elles la pression de paroi de la cellule-bourgeon (Cosgrove, 1993 ; 2000). Etant sensibles aux hormones, au sucre, et à la lumière, ces deux gènes pourraient agir en amont d'un ou de plusieurs gènes clé de l'activité du bourgeon.

Un autre défi est d'intégrer dans un modèle à l'échelle de la plante les effets de l'intensité lumineuse sur la synthèse et les flux des hormones dans la plante (Rameau et al., 2015). Trois types d'hormones pourront être considérées dans un premier temps, l'auxine, les cytokinines, et les strigolactones, qui jouent un rôle majeur dans la dominance apicale et qui est elle-même modulée par l'intensité lumineuse. Des connaissances physiologiques ciblées existent quant à la biosynthèse et au transport de ces hormones dans la plante (Schneider et al., 2019). Les enjeux seront de rassembler et d'intégrer ces connaissances au sein d'un modèle à l'échelle de la plante, de caractériser l'effet de l'intensité lumineuse sur les différents paramètres du modèle, et de tester la robustesse de ce modèle. Dans ce modèle, les organes apicaux en croissance, source d'auxine, ainsi que les racines, sources de cytokinines et strigolactones seront représentés. Nos résultats du chapitre 2 ont montré que l'intensité lumineuse modifie la croissance aérienne et racinaire. Nous pouvons donc nous attendre à une modification de la synthèse et ainsi des flux hormonaux au sein de la plante en réponse à l'intensité lumineuse. Ceci pourrait impacter indirectement le débourrement.

REFERENCES

Barbier, F., Péron, T., Lecerf, M., Perez-Garcia, M.-D., Barrière, Q., Rolčík, J., Boutet-Mercey, S., Citerne, S., Lemoine, R., Porcheron, B., et al. (2015). Sucrose is an early modulator of the key hormonal mechanisms controlling bud outgrowth in Rosa hybrida. J Exp Bot 66, 2569–2582.

Bertheloot, J., Barbier, F., Boudon, F., Perez-Garcia, M.D., Péron, T., Citerne, S., Dun, E., Beveridge, C., Godin, C., and Sakr, S. (2020). Sugar availability suppresses the auxin-induced strigolactone pathway to promote bud outgrowth. New Phytologist 225, 866–879.

Bertin, N., and Gary, C. (1998). Short and long term fluctuations of the leaf mass per area of tomato plants—implications for growth models. Annals of Botany 82, 71–81.

Corot, A., Roman, H., Douillet, O., Autret, H., Perez-Garcia, M.-D., Citerne, S., Bertheloot, J., Sakr, S., Leduc, N., and Demotes-Mainard, S. (2017). Cytokinins and abscisic acid act antagonistically in the regulation of the bud outgrowth pattern by light intensity. Frontiers in Plant Science 8, 1724.

Cosgrove, D. (1986). Biophysical Control of Plant Cell Growth. Annual Review of Plant Physiology 37, 377–405.

Cosgrove, D.J. (1993). Wall extensibility: its nature, measurement and relationship to plant cell growth. New Phytologist 124, 1–23.

Cosgrove, D.J. (2000). Loosening of plant cell walls by expansins. Nature 407, 321–326.

Demotes-Mainard, S., Huché-Thélier, L., Morel, P., Boumaza, R., Guérin, V., and Sakr, S. (2013). Temporary water restriction or light intensity limitation promotes branching in rose bush. Scientia Horticulturae 150, 432–440.

Domagalska, M.A., and Leyser, O. (2011). Signal integration in the control of shoot branching. Nature Reviews Molecular Cell Biology 12, 211–221.

Evers, J.B., Vos, J., Yin, X., Romero, P., van der Putten, P.E.L., and Struik, P.C. (2010). Simulation of wheat growth and development based on organ-level photosynthesis and assimilate allocation. J Exp Bot 61, 2203–2216.

Foo, E., Morris, S.E., Parmenter, K., Young, N., Wang, H., Jones, A., Rameau, C., Turnbull, C.G.N., and Beveridge, C.A. (2007). Feedback Regulation of Xylem Cytokinin Content Is Conserved in Pea and Arabidopsis. Plant Physiology 143, 1418–1428.

Havelange, A., Lejeune, P., and Bernier, G. (2000). Sucrose/cytokinin interaction in Sinapis alba at floral induction: a shoot-to-root-to-shoot physiological loop. Physiologia Plantarum 109, 343–350.

Hirose, N., Takei, K., Kuroha, T., Kamada-Nobusada, T., Hayashi, H., and Sakakibara, H. (2008). Regulation of cytokinin biosynthesis, compartmentalization and translocation. J Exp Bot 59, 75–83.

Kebrom, T.H. (2017). A growing stem inhibits bud outgrowth–the overlooked theory of apical dominance. Frontiers in Plant Science 8, 1874.

Kebrom, T.H., Chandler, P.M., Swain, S.M., King, R.W., Richards, R.A., and Spielmeyer, W. (2012). Inhibition of Tiller Bud Outgrowth in the tin Mutant of Wheat Is Associated with Precocious Internode Development. Plant Physiology 160, 308–318.

Kiba, T., Takebayashi, Y., Kojima, M., and Sakakibara, H. (2019). Sugar-induced de novo cytokinin biosynthesis contributes to Arabidopsis growth under elevated CO 2. Sci Rep 9, 1–15.

Leduc, N., Roman, H., Barbier, F., Péron, T., Huché-Thélier, L., Lothier, J., Demotes-Mainard, S., and Sakr, S. (2014). Light signaling in bud outgrowth and branching in plants. Plants 3, 223–250.

Letort, V., Cournède, P.-H., and de Reffye, P. (2009). Impact of Topology on Plant Functioning: A Theoretical Analysis Based on the GreenLab Model Equations. In 2009 Third International Symposium on Plant Growth Modeling, Simulation, Visualization and Applications, pp. 341–348.

Lockhart, J.A. (1965). An analysis of irreversible plant cell elongation. Journal of Theoretical Biology 8, 264–275.

Luquet, D., Dingkuhn, M., Kim, H., Tambour, L., and Clement-Vidal, A. (2006). EcoMeristem, a model of morphogenesis and competition among sinks in rice. 1. Concept, validation and sensitivity analysis. Functional Plant Biology 33, 309–323.

MacNeill, G.J., Mehrpouyan, S., Minow, M.A.A., Patterson, J.A., Tetlow, I.J., and Emes, M.J. (2017). Starch as a source, starch as a sink: the bifunctional role of starch in carbon allocation. J Exp Bot 68, 4433–4453.

Mason, M.G., Ross, J.J., Babst, B.A., Wienclaw, B.N., and Beveridge, C.A. (2014). Sugar demand, not auxin, is the initial regulator of apical dominance. Proceedings of the National Academy of Sciences 111, 6092–6097.

Mathieu, A., Cournède, P.-H., Letort, V., Barthélémy, D., and De Reffye, P. (2009). A dynamic model of plant growth with interactions between development and functional mechanisms to study plant structural plasticity related to trophic competition. Annals of Botany 103, 1173–1186.

Mitchell, K.J. (1953). Influence of Light and Temperature on the Growth of Ryegrass (Lolium spp.). Physiologia Plantarum 6, 21–46.

Rameau, C., Bertheloot, J., Leduc, N., Andrieu, B., Foucher, F., and Sakr, S. (2015). Multiple pathways regulate shoot branching. Frontiers in Plant Science 5, 741.

Roitsch, T., and Ehneß, R. (2000). Regulation of source/sink relations by cytokinins. Plant Growth Regulation 32, 359–367.

Roman, H., Girault, T., Barbier, F., Péron, T., Brouard, N., Pěnčík, A., Novák, O., Vian, A., Sakr, S., and Lothier, J. (2016). Cytokinins are initial targets of light in the control of bud outgrowth. Plant Physiology 172, 489–509.

Sakakibara, H. (2006). CYTOKININS: Activity, Biosynthesis, and Translocation. Annual Review of Plant Biology 57, 431–449.

Schneider, A., Godin, C., Boudon, F., Demotes-Mainard, S., Sakr, S., and Bertheloot, J. (2019). Light regulation of axillary bud outgrowth along plant axes: an overview of the roles of sugars and hormones. Frontiers in Plant Science 10, 1296.

Su, H., Abernathy, S.D., White, R.H., and Finlayson, S.A. (2011). Photosynthetic photon flux density and phytochrome B interact to regulate branching in Arabidopsis. Plant, Cell &s Environment 34, 1986–1998.

APPENDIX 1 – ACTA HORTICULTURAE GREENSYS 2019 – ACCEPTED VERSION

Sugar availability is involved in rose bud outgrowth stimulation following a temporary light intensity restriction during the vegetative development of the main stem

A. Schneider[1], F. Boudon[2], S. Demotes-Mainard[1], L. Ledroit[1], MD. Perez-Garcia[1], N. Brouard[1], C. Godin[3], S. Sakr[1], J. Bertheloot[1]

[1]IRHS, INRA, Agrocampus-Ouest, Université d'Angers, SFR 4207 QuaSaV, 49071 Beaucouzé, France ; [2]CIRAD, UMR AGAP & Univ. Montpellier, Avenue Agropolis, TA A-108/01, F-34398 Montpellier, France ; [3]Laboratoire Reproduction et Développement des Plantes, Univ Lyon, ENS de Lyon, UCB Lyon 1, CNRS, INRA, Inria, F-69342, Lyon, France

Abstract

Branching is a major agronomic variable determining yield and quality, and is very sensitive to environmental conditions. Previous studies on rose showed that a continuous high light intensity perceived during the bud outgrowth period stimulated bud outgrowth compared to a continuous low light intensity. This effect was related to higher cytokinin contents in the nodes. Interestingly, a temporary light intensity restriction applied before the bud outgrowth period over-stimulated bud outgrowth, but the mechanisms involved remain unknown. In this case, we assume a non-limitation in cytokinins because of the current high light intensity during the bud outgrowth period, but an increase in sugars that would explain bud outgrowth stimulation. To test sugar involvement, we quantified bud outgrowth, sugar contents, and the balance between sources and sinks for sugars in the bud outgrowth period of plants grown under either continuous high light intensity or under a temporary light restriction followed by a high light intensity. In addition, we quantified the effect of exogenous sugar supply on bud outgrowth for plants under continuous high light intensity, and the effect of leaf masking under the non-continuous treatment. Our results showed that after a temporary light intensity restriction and return to high light intensity, sugars accumulated compared to a continuous high light intensity. Furthermore, the growth of apical organs was reduced indicating that sugar accumulation might be due to a higher balance between sources and sinks for sugars. Exogenous sucrose supply through the petiole of intact plants grown under high light intensity stimulated bud outgrowth. Conversely, leaf masking after a temporary light intensity restriction inhibited bud outgrowth. This supports that sugar accumulation is an important trigger of bud outgrowth after a temporary light intensity restriction. Together these results indicate that an anterior low light intensity applied during the main stem development reduces growth of apical organs while higher sugar availability afterward favors lateral bud outgrowth.

Keywords: bud outgrowth, light intensity, branching, sugar, source-sink

INTRODUCTION

Plant branching is an important agronomic trait as it determines final yield (Whiting et al., 2005), and is involved in sanitary (Simon et al., 2012) and visual quality (Boumaza et al., 2010) of productions. Branching is highly responsive to environmental factors such as nitrogen fertilization, water supply, temperature, or light (Lafarge et al., 2010; Djennane et al., 2014; Furet et al., 2014; Li-Marchetti et al., 2015; Corot et al., 2017;). Thus, understanding and predicting branching response to environmental conditions is essential to improve technical itineraries and culture ideotypes. We focus our study on the impact of light intensity on bud outgrowth, which determines early steps of branching.

Bud outgrowth is inhibited by low (versus high) light intensity imposed during bud outgrowth period, as observed for rose (Roman et al., 2016; Corot et al., 2017). This inhibition was correlated to low cytokinin biosynthesis and level, and to low sugar level in the stem. However, only cytokinins were shown to be involved in bud outgrowth regulation in response to low light intensity, since exogenous sugar supplies did not restore any bud growth under this non-permissive light condition (Roman et al., 2016; Corot et al., 2017).

Bud outgrowth is also sensitive to anterior light intensity. Demotes-Mainard et al. (2013) reported for rose an overstimulation of bud outgrowth under high light intensity after a temporary restriction of light intensity (LH treatment), compared to continuous high light intensity (HH treatment). The limiting role of cytokinins, demonstrated for low light intensity during bud outgrowth, is unlikely true in this case, since plants under both light treatments are under high light intensity during bud outgrowth period. We will thus look for the possible role of sugars in bud outgrowth stimulation under LH treatment. Under this treatment, apical leaves and internodes of the primary stem, which are still growing during bud outgrowth period, are initiated under low light intensity. Granier and Tardieu (1999) demonstrated for sunflower that low light intensity during leaf initiation reduced leaf elongation rate persistently, even after restoration of high light intensity. This indicates that growing organs of the primary stem may represent lower sugar sinks during bud outgrowth period under LH treatment compared to HH, and that subsequent primary axis competition for sugars is reduced under LH treatment. Recent studies also support a possible role of sugars, since their signal role in bud outgrowth stimulation has been demonstrated for rose and pea (Mason et al., 2014; Barbier et al., 2015)

The objective of this paper is to determine whether sugars are involved in bud outgrowth stimulation after a temporary light intensity restriction (LH treatment), and whether this can result from primary axis growth reduction, leading to an increase of available sugars for bud growth.

MATERIALS AND METHODS

Plant material and growth conditions

Plants were obtained from cuttings of *Rosa hybrida* 'Radrazz' as described in Demotes-Mainard et al. (2013). Well-rooted cuttings were grown in 500 ml pots containing a 50/40/10 mixture of neutral peat, coconut fibers, and perlite. After a short growth in a heated greenhouse (until three leaves were visible), plants were transferred to a growth chamber (light/dark 16/8h photoperiod; 22/20°C at day/night; humidity was maintained between 60 and 70%). Water and mineral nutrition (5,0 mM KNO_3, 2,0 mM $Ca(NO_3)_2$, 2,0 mM NH_4NO_3, 2,0 mM KH_2PO_4, 2,0 mM $MgSO_4$, 0,25 mM NaOH) were provided by sub-irrigation to maintain the plants in comfortable water and mineral conditions.

Light treatments

Plants in growth chamber were submitted to two different regimes of light intensity in the Photosynthetically Active Radiation (PAR) : (1) a continuous high PAR intensity (300-320 µmol/m^2/s) (referred to as HH), (2) a low PAR intensity (80-100 µmol/m^2/s) until the appearance of the flower bud (FBV : flower bud visible on the main stem), and a high PAR intensity from FBV onwards (treatment LH).

Morphological measurements

For all experiments, the state (dormant or outgrown) and length of each bud were monitored three to four times a week since FBV + 4 days. A bud was considered has grown out when the first leaf was clearly visible above the bud scales (Girault et al., 2008; Corot et al., 2017). As soon as the third leaf of the primary axis appeared, length of the final leaflet of each leaf of the primary axis was measured every two days until wilted flower bud stage. At wilted flower stage, leaves were excised and scanned. Images were treated using ImageJ software to estimate final area of each leaf of the primary axis.

Photosynthesis measurements

Under both light treatments, CO_2 net assimilation rate per leaf surface unit per second was performed 4 times between FBV and FBV + 7 days on the second most basal leaf on the primary axis on entire plants, at a temperature of 20°C, and an ambient CO_2 concentration of 400 mmol mol^{-1} (Li-Cor Inc., Lincoln, NE, United States).

Quantification of endogenous sugars

Roots, stem, leaves and flower button of the primary axis were collected at 7 days after FBV stage on entire plants grown under LH and HH regimes. Sampling were started 3h after the beginning of the light period, frozen in liquid nitrogen, and stored at -80°C before lyophilization and grounding. Sucrose and starch were determined by colorimetry.

Manipulating plant sugar contents

To avoid any interaction with the apical part of the plant, which is a strong sink for sugars, experiments of sugar manipulation were undertaken on plants decapitated at FBV. These plants were obtained by removing all the plant parts 2 cm above the fourth node bearing a true leaf (counting from plant base). Regarding the remaining leaves, all leaflets except a most basal one, were removed to limit photosynthetic sugar content. To maintain auxin-mediated apical dominance, a 2 ml-tube containing a basic medium (1% agar, 2,5 $ml.l^{-1}$ PPM), supplemented with a synthetic auxin (10µM 1-naphthaleneacetic acid, NAA), was applied at the cut end of the decapitated stump.

Decapitated plants grown under HH treatment were supplied with sucrose (25 or 50 mM) or mannitol (50 mM), an osmotic control, through the 4th petiole as described in Lin *et al.*, (2011). The petiole was rapidly immersed in a sugar-containing liquid solution in a 1.5 ml reservoir. After 1 week the petiole was cut 0,5 cm lower.

The four leaflets of decapitated plants grown under LH treatment were half covered with black plastic sheets or transparent plastic (control).

Statistical analysis

Statistical analyses were performed using R software (R Core Team, 2014). Groups were compared using Student's or Fisher's test. Significant differences (p-value <0.05) are indicated with the symbol *.

RESULTS

A temporary restriction in PAR intensity before bud outgrowth stimulated bud outgrowth and plant sugar status

In accordance with previous results of Demotes-Mainard et al. (2013), a temporary period of low PAR intensity (treatment LH) stimulated significantly bud outgrowth on rose primary axis, compared to continuous high PAR intensity (treatment HH). The total percentage of axillary buds that grew out was 12 % higher for LH than for HH treatment 10 days after the flower bud was visible on the primary axis (FBV stage) (Table 1). We showed that plant starch content was also multiplied by 1.64 for LH compared to HH at FBV + 8 days, while stem sucrose contents was similar between both treatments. This demonstrates an excess of sugars in LH compared to HH, and indicates that this excess may explain in part the stimulation of bud outgrowth in LH compared to HH.

Sugar stimulates bud outgrowth under high light intensity

To test whether the sugars excess in LH compared to HH is involved in bud outgrowth stimulation, we either (i) brought exogenous sucrose to plants in HH through petiole, or (ii) masked leaves of plants in LH to decrease sugar supply by photosynthesis. In HH, exogenous sucrose supply increased by 25% total bud outgrowth frequency compared to the osmotic control (figure 1A). Conversely, in LH, masking leaves reduced by almost 70% bud outgrowth percentage (figure 1B). Thus, this indicates that sugar excess in LH has a role in bud outgrowth stimulation.

The sources/sinks balance of sugars is higher under LH treatment compared to HH treatment

To understand the sugar excess under LH compared to HH, we estimated the source and sink strengths for sugars for both treatments. At FBV, just before the onset of bud outgrowth, the four most basal phytomers had finished their elongation, whereas upper phytomers were still elongated (data not shown). We therefore considered the four most basal leaves as the main sources of sugar, and the upper organs as the main sinks of sugars. The photosynthetic area of the main source leaves was similar in HH and LH (118 cm^2) at FBV, and photosynthesis per unit area was 26% lower for LH compared to HH (Table 2) during 7 days after FBV. Thus, source strength

of sugars was lower in LH than in HH and does not explain the excess of sugars observed in LH compared to HH. The final mass of the main sinks was 39% lower in LH compared to HH, indicating a lower sink strength for sugars in LH compared to HH. Sugar excess in LH condition may be thus explained by a favorable sources-sinks ratio due to lower growth of the upper organs during the period of bud outgrowth.

Table 1. Effect of light treatments on intact plant bud outgrowth frequency at FBV +10 days, and on total plant sugars content at FBV + 8 days. Plant bud outgrowth frequencies are means of at least 14 plants per treatment ± SE. Plant sucrose and starch content are means of at least 3 plants per treatment ± SE.

Bud outgrowth and sugars contents	**LH**		**HH**	
% of outgrown buds per plants at FBV + 10d	4 8,9	,3	3 6,9	,0
Plant sucrose content (µmol gluc/gDW)	5 27,7	2,9	5 37,2	1,7
Plant starch content (µmol gluc/gDW)	5 27,7	,1	5 8,2	,1

Table 2. Effect of light treatments on sources and sinks of sugars. (i)Surfacic photosynthetic capacity during 7 days after FBV. Values are means ± SE of 4 plants measured at 4 dates between FBV and FBV +7 days . (ii)Total surface of photosynthetic leaves at FBV (leaves 1 to 4 from the base of the plant). Values are means of at least 14 plants per treatment ± SE. (iii) Final dry mass of still growing apical organs after FBV (leaves and internodes upper the fifth phytomer). Values are means of at least 14 plants per treatment ± SE.

Sources and sinks of sugars	**LH**		**HH**	
Surfacic photosynthetic capacity ($\mu mol/m^2/s$)	8,4	,5	1 1,3	0 ,3
Total surface of photosynthetic leaves at FBV (cm^2)	118 ,4	,2	1 18,7	5 ,4
Total dry mass of aerial growing organs on the primary axis after FBV (g)	1,4	,1	2 ,3	0 ,2

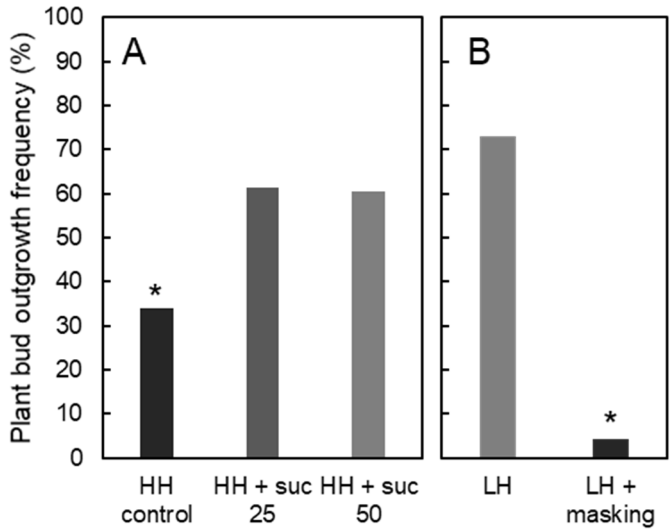

Figure 1. Effect of global sugar content manipulation under HH and LH treatments on total bud outgrowth frequency. For both experiments, plants were decapitated at FBV above the fourth leaf, and NAA agar (10µM) was applied on the top of the stem. A/ Effect of exogenous input of sucrose (25 and 50mM) under HH treatment compared to mannitol

control (50mM). At least, 11 plants per treatment. B/ Effect of masking leaves under LH treatment. n = 12 plants per treatment.

DISCUSSION

Unfavorable environmental conditions are known to modulate bud outgrowth via hormonal and nutrient regulators (Roman et al., 2016; Corot et al., 2017). We aimed to validate the impact of a temporal unfavorable light intensity, applied before the branching period, on bud outgrowth, and to determine the role of sugars in this regulation. As observed previously by Demotes-Mainard et al. (2013), rose bud outgrowth frequency was significantly increased by a temporary light intensity restriction applied before the branching period (table 1), compared to a continuous high light intensity. Interestingly, bud outgrowth stimulation following a temporary light intensity restriction was correlated to sugar accumulation as starch, compared to the continuous high light treatment (table 1).

Because sugars are known to stimulate bud outgrowth (Mason et al., 2014; Barbier et al., 2015), we tested if sugars might be involved in the phenotype observed under high light intensity following a temporary light intensity restriction (LH treatment). To do so, we manipulated sugar supply in plants under the two light treatments (figure 1). The results support that sugars are involved in bud outgrowth stimulation under high light intensity after a temporary light intensity restriction.

Quantification of sugar sources and sinks revealed that starch accumulation may be due to lower sugar demand of the growing organs of the main axis following a restriction in light intensity (table 2). Such sugar accumulation after the recovery of comfortable conditions was previously observed for rice after a temporary shading during the development of the main stem (Lafarge et al., 2010).

Therefore, bud outgrowth stimulation by a temporary light intensity restriction might result of a lesser competition for sugars between main axis and lateral buds compared to plants grown under continuous high light intensity. Such modulation of bud outgrowth by the growth of the main axis was previously observed for wheat plants of different internode lengths (Kebrom et al., 2012).

A branching stimulation for rose was similarly observed after a temporary water restriction before the branching period compared to continuous comfortable hydric conditions (Demotes-Mainard et al., 2013), questioning the possibility of common mechanisms of bud outgrowth stimulation by temporary unfavorable environmental conditions before the branching period.

CONCLUSION

A temporary light intensity restriction applied before the bud outgrowth period, during the development of the main axis, leads to a bud outgrowth stimulation. Our results indicate that smaller apical sinks of sugars after the high light intensity recovery can explain this phenotype.

ACKNOWLEDGMENTS

We thank Chloé Mouchès and Lisa Billaud (trainees UMR IRHS) for technical assistance during the experiments and for first data analysis.

Literature cited

Barbier, F., Péron, T., Lecerf, M., Perez-Garcia, M.-D., Barrière, Q., Rolčík, J., Boutet-Mercey, S., Citerne, S., Lemoine, R., Porcheron, B., et al. (2015). Sucrose is an early modulator of the key hormonal mechanisms controlling bud outgrowth in Rosa hybrida. J. Exp. Bot. *66*, 2569–2582.

Boumaza, R., Huché-Thélier, L., Demotes-Mainard, S., Le Coz, E., Leduc, N., Pelleschi-Travier, S., Qannari, E.M., Sakr, S., Santagostini, P., Symoneaux, R., et al. (2010). Sensory profiles and preference analysis in ornamental horticulture: the case of the rosebush. Food Qual. Prefer. *21*, 987–997.

Corot, A., Roman, H., Douillet, O., Autret, H., Perez-Garcia, M.-D., Citerne, S., Bertheloot, J., Sakr, S., Leduc, N., and Demotes-Mainard, S. (2017). Cytokinins and abscisic acid act antagonistically in the regulation of the bud outgrowth pattern by light intensity. Front. Plant Sci. *8*, 1724.

Demotes-Mainard, S., Huché-Thélier, L., Morel, P., Boumaza, R., Guérin, V., and Sakr, S. (2013). Temporary water restriction or light intensity limitation promotes branching in rose bush. Sci. Hortic. *150*, 432–440.

Djennane, S., HIBRAND-SAINT OYANT, L., Kawamura, K., Lalanne, D., Laffaire, M., Thouroude, T., Chalain, S., Sakr, S., Boumaza, R., Foucher, F., et al. (2014). Impacts of light and temperature on shoot branching gradient and expression of strigolactone synthesis and signalling genes in rose. Plant Cell Environ. *37*, 742–757.

Furet, P.-M., Lothier, J., Demotes-Mainard, S., Travier, S., Henry, C., Guérin, V., and Vian, A. (2014). Light and nitrogen nutrition regulate apical control in Rosa hybrida L. J. Plant Physiol. *171*, 7–13.

Girault, T., Bergougnoux, V., Combes, D., VIEMONT, J.-D., and Leduc, N. (2008). Light controls shoot meristem organogenic activity and leaf primordia growth during bud burst in Rosa sp. Plant Cell Environ. *31*, 1534–1544.

Granier, C., and Tardieu, F. (1999). Leaf expansion and cell division are affected by reducing absorbed light before but not after the decline in cell division rate in the sunflower leaf. Plant Cell Environ. *22*, 1365–1376.

Kebrom, T.H., Chandler, P.M., Swain, S.M., King, R.W., Richards, R.A., and Spielmeyer, W. (2012). Inhibition of Tiller Bud Outgrowth in the tin Mutant of Wheat Is Associated with Precocious Internode Development. Plant Physiol. *160*, 308–318.

Lafarge, T., Seassau, C., Martin, M., Bueno, C., Clément-Vidal, A., Schreck, E., and Luquet, D. (2010). Regulation and recovery of sink strength in rice plants grown under changes in light intensity. Funct. Plant Biol. *37*, 413–428.

Li-Marchetti, C., Le Bras, C., Relion, D., Citerne, S., Huché-Thélier, L., Sakr, S., Morel, P., and Crespel, L. (2015). Genotypic differences in architectural and physiological responses to water restriction in rose bush. Front. Plant Sci. *6*, 355.

Lin, Y.-H., Lin, M.-H., Gresshoff, P.M., and Ferguson, B.J. (2011). An efficient petiole-feeding bioassay for introducing aqueous solutions into dicotyledonous plants. Nat. Protoc. *6*, 36.

Mason, M.G., Ross, J.J., Babst, B.A., Wienclaw, B.N., and Beveridge, C.A. (2014). Sugar demand, not auxin, is the initial regulator of apical dominance. Proc. Natl. Acad. Sci. *111*, 6092–6097.

Roman, H., Girault, T., Barbier, F., Péron, T., Brouard, N., Pěnčík, A., Novák, O., Vian, A., Sakr, S.,
Lothier, J., et al. (2016). Cytokinins are initial targets of light in the control of bud outgrowth. Plant Physiol. *172*, 489–509.

Simon, S., Morel, K., Durand, E., Brevalle, G., Girard, T., and Lauri, P.-É. (2012). Aphids at crossroads: when branch architecture alters aphid infestation patterns in the apple tree. Trees *26*, 273–282.

Whiting, M.D., Lang, G., and Ophardt, D. (2005). Rootstock and training system affect sweet cherry growth, yield, and fruit quality. HortScience *40*, 582–586.

APPENDIX 2 – SCRIPTS DES SIMULATIONS DU CHAPITRE 2

Annexe : scripts - calcul du bilan carboné pour LH et HH (chapitre 1)

In [1]:
```
import csv
import numpy as np
import math
import matplotlib.pyplot as plt
from array import *
from pylab import*
```

In [2]:
```
####### Definition of constants

#PAR interception
k1 = 0.747 #ok
k2 = 0.554 #ok

#carbon assimilation
alpha = 7.35e-2 #OK : fitté aux données clhro et photo
Pmin = 0.7867 #OK: fitté aux données clhro et photo
Pmax = 3963.17 # photosynthèse max. OK. D'après la littérature, photosynthèse sa
turante entre 15 et 20 µmol de Co2/m²/s
K_chloro = 7419.83
corr_chloro = 1.20 #parametre de correction des teneurs en chlorophylle entre 20
18 et 2011

photoperiod = 16 #hours/day

#respiration
k_respi_maint = 0.0
k_respi_growth = 0.0

#time
dt = 1
duration = 11 ## on peut faire moins si on veut, mais les données de 2011 permet
tent d'aller plus loin que 2008

# Param flower allometry
Param_Flower = np.array([5e-4, 3.3e-3, 1e-2])

#Param roots allometry
Param_Roots = np.array([5.6e-3,2.337e-1])

#conversions
Conv_carbon_struc = 0.45 #en g de C par g de matière structurale
                        # d'après la composition chimique de la cellulose
Conv_carbon_sugars = 0.4 #en g de carbone par g d'équivalent glucose. OK

Conv_carbon_prot = 0.2 #en g de carbone par g de proteines (quelle compo moyenn
e?): à vérifier dans littérature


# Inputs : I0, gradients de chlorophylle, dimensions des feuilles de rangs 1, 2
et 3 à BFV (basal leaf areas, lengths),
#          flux de carbone vers la masse structurale des racines et le bouton fl
oral, flux de carbone vers les proteines

# Number of leaves along the primary stem : dépend du traitement lumineux
NB_HH = 9
NB_LH = 8

# à modifier pour avoir les entrées de 2011
t_app_HH = np.loadtxt('Dates_appearance_HH_2011.csv', delimiter=';')
Param_chloro_gradient_HH = np.loadtxt('Param_chloro_HH_2011_v2.csv', delimiter=
';')
Param_IN_Exp_HH = np.loadtxt('Param_IN_Exp_HH_2011.csv', delimiter=';')
Param_IN_Diam_HH = np.loadtxt('Param_Diameter_HH_2011.csv', delimiter=';')
Param_IN_Density_HH = np.loadtxt('Param_density_HH_2011.csv', delimiter=';')
Param_Leaf_Exp_HH = np.loadtxt('Param_Leaf_Exp_HH_2011.csv', delimiter=';')
Param_LMA_struc_HH = np.loadtxt('Param_LMA_struc_HH_2011_v2.csv', delimiter=';')

t_app_LH = np.loadtxt('Dates_appearance_LH_2011.csv', delimiter=';')
Param_chloro_gradient_LH = np.loadtxt('Param_chloro_LH_2011_v2.csv', delimiter=
';')
Param_IN_Exp_LH = np.loadtxt('Param_IN_Exp_LH_2011.csv', delimiter=';')
Param_IN_Diam_LH = np.loadtxt('Param_Diameter_LH_2011.csv', delimiter=';')
Param_IN_Density_LH = np.loadtxt('Param_density_LH_2011.csv', delimiter=';')
Param_Leaf_Exp_LH = np.loadtxt('Param_Leaf_Exp_LH_2011.csv', delimiter=';')
Param_LMA_struc_LH = np.loadtxt('Param_LMA_struc_LH_2011_v2.csv', delimiter=';')
```

Computation of organ dimensions, light gradient, photosynthesis and carbon used for minimal structural material, as determined at FBV stage by parameters and inputs of the model

Internode expansion

In [3]:
```
def IN_expansion (t, Param_IN_Exp_j):

    L = Param_IN_Exp_j[0] /(1 + math.exp(4 * Param_IN_Exp_j[2] *(Param_IN_Exp_j
[1] - t)))

    return L
```

In [4]:
```
IN_exp_HH = np.array([[IN_expansion (t, Param_IN_Exp_HH[j]) for t in range (0,du
ration)] for j in range (0,NB_HH)])
IN_exp_LH = np.array([[IN_expansion (t, Param_IN_Exp_LH[j]) for t in range (0,du
ration)] for j in range (0,NB_LH)])
```

In [5]:
```
def IN_expansion_speed (t, Param_IN_Exp_j):

    dL_dt = 4* Param_IN_Exp_j[2] * Param_IN_Exp_j[0] * math.exp(4 * Param_IN_Exp
_j[2] *(Param_IN_Exp_j[1] - t))/(1 + math.exp(4 * Param_IN_Exp_j[2] *(Param_IN_E
xp_j[1] - t)))**2

    return dL_dt
```

In [6]:
```
IN_exp_speed_HH = np.array([[IN_expansion_speed (t, Param_IN_Exp_HH[j]) for t in
range (0,duration)] for j in range (0,NB_HH)])
IN_exp_speed_LH = np.array([[IN_expansion_speed (t, Param_IN_Exp_LH[j]) for t in
range (0,duration)] for j in range (0,NB_LH)])
```

In [7]:
```
#définition des couleurs
c = np.array(['orange','teal','grey','r','c','y',"m",'g',"blue"])

x=range(0,duration)
#internode length
plt.subplot(1,2,1)
for j in range (0,4):
    y = IN_exp_HH[j,0:duration]
    plt.plot(x,y,"-",color = c[j], label = j+1)
for j in range (0,4):
    y = IN_exp_LH[j,0:duration]
    plt.plot(x,y,"--",color = c[j], label = j+1)

plt.title('Lower ranks')
plt.ylim(0,5)
plt.xlabel('Time after FBV stage (days)')
xticks(arange(0,duration,2))
plt.ylabel('Internode length (cm)')
plt.legend(loc='lower left', bbox_to_anchor=(2.3, 0.2))

plt.subplot(1,2,2)
for j in range (4,NB_HH):
    y = IN_exp_HH[j,0:duration]
    plt.plot(x,y,"-",color = c[j], label = j+1)
for j in range (4,NB_LH):
    y = IN_exp_LH[j,0:duration]
    plt.plot(x,y,"--",color = c[j], label = j+1)

plt.title('Upper ranks')
plt.ylim(0,5)
plt.xlabel('Time after FBV stage (days)')
xticks(arange(0,duration,2))
#plt.ylabel('IN length (cm)')
plt.legend(loc='lower left', bbox_to_anchor=(1.5, 0.2))
plt.savefig('simu_IN_length.jpg')
plt.savefig('simu_IN_length.pdf')
```

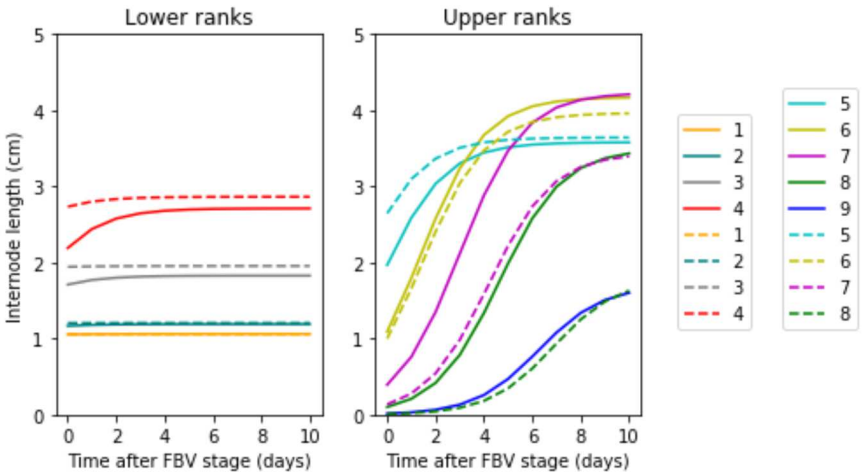

In [8]:
```
#définition des couleurs
c = np.array(['orange','teal','grey','r','c','y',"m",'g',"blue"])

x=range(0,duration)
#internode length speed
plt.subplot(1,2,1)
for j in range (0,4):
    y = IN_exp_speed_HH[j,0:duration]
    plt.plot(x,y,"-",color = c[j], label = j+1)
for j in range (0,4):
    y = IN_exp_speed_LH[j,0:duration]
    plt.plot(x,y,"--",color = c[j], label = j+1)

plt.title('Lower ranks')
plt.ylim(0,1)
plt.xlabel('Time after FBV stage (days)')
xticks(arange(0,duration,2))
plt.ylabel('Internode length increase rate (cm/d)')
plt.legend(loc='lower left', bbox_to_anchor=(2.3, 0.2))

plt.subplot(1,2,2)
for j in range (4,NB_HH):
    y = IN_exp_speed_HH[j,0:duration]
    plt.plot(x,y,"-",color = c[j], label = j+1)
for j in range (4,NB_LH):
    y = IN_exp_speed_LH[j,0:duration]
    plt.plot(x,y,"--",color = c[j], label = j+1)

plt.title('Upper ranks')
plt.ylim(0,1)
plt.xlabel('Time after FBV stage (days)')
xticks(arange(0,duration,2))
#plt.ylabel('IN length (cm)')
plt.legend(loc='lower left', bbox_to_anchor=(1.5, 0.2))
plt.savefig('simu_IN_length_speed.jpg')
plt.savefig('simu_IN_length_speed.pdf')
```

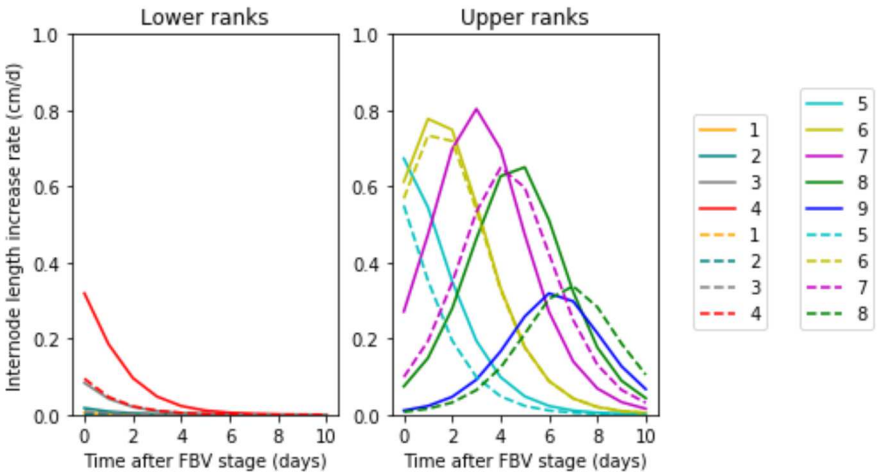

Internode thickening

In [9]:
```
def IN_diameter (t, Param_IN_Diam_j, t_app_j):

    diam = Param_IN_Diam_j[0] + Param_IN_Diam_j[2] * (t - t_app_j) + (math.exp(-
Param_IN_Diam_j[3] * (t-t_app_j)) - 1) * (Param_IN_Diam_j[2] - Param_IN_Diam_j
[1])/Param_IN_Diam_j[3]

    return diam
```

In [10]:
```
IN_diam_HH = np.array([[IN_diameter (t, Param_IN_Diam_HH[j], t_app_HH[j]) for t
in range (0,duration)] for j in range (0,NB_HH)])
IN_diam_LH = np.array([[IN_diameter (t, Param_IN_Diam_LH[j], t_app_LH[j]) for t
in range (0,duration)] for j in range (0,NB_LH)])
```

In [11]:
```
def IN_diameter_speed (t, Param_IN_Diam_j, t_app_j):

    ddiam_dt = Param_IN_Diam_j[2] - (math.exp(-Param_IN_Diam_j[3] * (t-t_app_
j))) * (Param_IN_Diam_j[2] - Param_IN_Diam_j[1])

    return ddiam_dt
```

In [12]:
```
IN_diam_speed_HH = np.array([[IN_diameter_speed (t, Param_IN_Diam_HH[j], t_app_H
H[j]) for t in range (0,duration)] for j in range (0,NB_HH)])
IN_diam_speed_LH = np.array([[IN_diameter_speed (t, Param_IN_Diam_LH[j], t_app_L
H[j]) for t in range (0,duration)] for j in range (0,NB_LH)])
```

In [13]:
```
x=range(0,duration)
#internode diameter
plt.subplot(1,2,1)
for j in range (0,4):
    y = IN_diam_HH[j,0:duration]
    plt.plot(x,y,"-",color = c[j], label = j+1)
for j in range (0,4):
    y = IN_diam_LH[j,0:duration]
    plt.plot(x,y,"--",color = c[j], label = j+1)

plt.title('Lower ranks')
plt.ylim(0,0.5)
plt.xlabel('Time after FBV stage (days)')
xticks(arange(0,duration,2))
plt.ylabel('Internode diameter (cm)')
plt.legend(loc='lower left', bbox_to_anchor=(2.3, 0.2))

plt.subplot(1,2,2)
for j in range (4,NB_HH):
    y = IN_diam_HH[j,0:duration]
    plt.plot(x,y,"-",color = c[j], label = j+1)
for j in range (4,NB_LH):
    y = IN_diam_LH[j,0:duration]
    plt.plot(x,y,"--",color = c[j], label = j+1)

plt.title('Upper ranks')
plt.ylim(0,0.5)
plt.xlabel('Time after FBV stage (days)')
xticks(arange(0,duration,2))
plt.legend(loc='lower left', bbox_to_anchor=(1.5, 0.2))
plt.savefig('simu_IN_diam.jpg')
plt.savefig('simu_IN_diam.pdf')
```

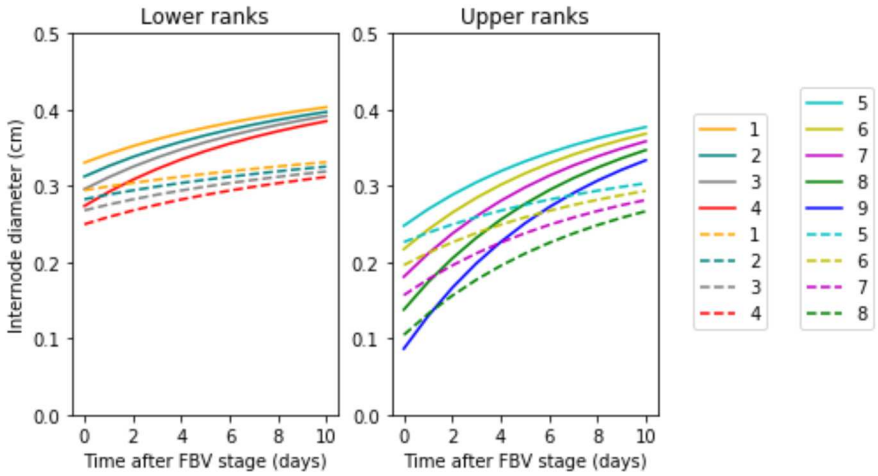

In [14]:
```
x=range(0,duration)
#internode diameter speed
plt.subplot(1,2,1)
for j in range (0,4):
    y = IN_diam_speed_HH[j,0:duration]
    plt.plot(x,y,"-",color = c[j], label = j+1)
for j in range (0,4):
    y = IN_diam_speed_LH[j,0:duration]
    plt.plot(x,y,"--",color = c[j], label = j+1)

plt.title('Lower ranks')
plt.ylim(0,0.05)
plt.xlabel('Time after FBV stage (days)')
xticks(arange(0,duration,2))
plt.ylabel('Internode diameter increse rate (cm/d)')
plt.legend(loc='lower left', bbox_to_anchor=(2.3, 0.2))

plt.subplot(1,2,2)
for j in range (4,NB_HH):
    y = IN_diam_speed_HH[j,0:duration]
    plt.plot(x,y,"-",color = c[j], label = j+1)
for j in range (4,NB_LH):
    y = IN_diam_speed_LH[j,0:duration]
    plt.plot(x,y,"--",color = c[j], label = j+1)

plt.title('Upper ranks')
plt.ylim(0,0.05)
plt.xlabel('Time after FBV stage (days)')
xticks(arange(0,duration,2))
plt.legend(loc='lower left', bbox_to_anchor=(1.5, 0.2))
plt.savefig('simu_IN_diam_speed.jpg')
plt.savefig('simu_IN_diam_speed.pdf')
```

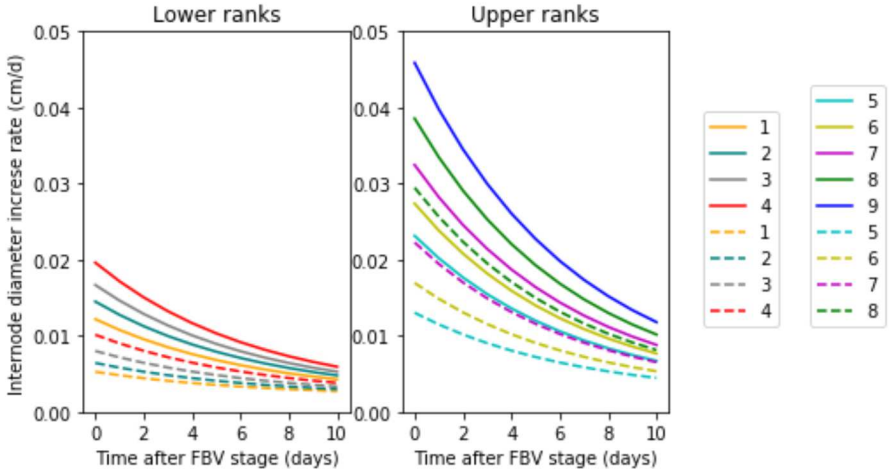

Leaf expansion

Code pour calculer l'expansion d'une feuille j (longueur et surafce à chaque pas de temps):

In [15]:
```
# Surfacic leaf expansion function :
    # imputs : leaf rank from the base, date, parameters of lsurfcic leaf expans
ion (Smax, t1/2, w)
    # outputs : length increase during dt, leaf length at t+dt, area increase du
ring dt, leaf area at t+dt
def leaf_expansion (t, Param_Leaf_Exp_j):

    S = Param_Leaf_Exp_j[0] /(1 + math.exp(4 * Param_Leaf_Exp_j[2] *(Param_Leaf_
Exp_j[1] - t)))**2

    return S
```

In [16]:
```
leaf_exp_HH = np.array([[leaf_expansion (t, Param_Leaf_Exp_HH[j]) for t in range
(0,duration)] for j in range (0,NB_HH)])
leaf_exp_LH = np.array([[leaf_expansion (t, Param_Leaf_Exp_LH[j]) for t in range
(0,duration)] for j in range (0,NB_LH)])
```

In [17]:
```
# Surfacic leaf expansion increase rate function :
    # imputs : leaf rank from the base, date, parameters of lsurfcic leaf expans
ion (Smax, t1/2, w)
    # outputs : length increase during dt, leaf length at t+dt, area increase du
ring dt, leaf area at t+dt
def leaf_expansion_speed (t, Param_Leaf_Exp_j):

    dS_dt = 8 * Param_Leaf_Exp_j[0] * Param_Leaf_Exp_j[2] * math.exp(4 * Param_L
eaf_Exp_j[2] *(Param_Leaf_Exp_j[1] - t))/(1 + math.exp(4 * Param_Leaf_Exp_j[2] *
(Param_Leaf_Exp_j[1] - t)))**3

    return dS_dt
```

In [18]:
```
leaf_exp_speed_HH = np.array([[leaf_expansion_speed (t, Param_Leaf_Exp_HH[j]) fo
r t in range (0,duration)] for j in range (0,NB_HH)])
leaf_exp_speed_LH = np.array([[leaf_expansion_speed (t, Param_Leaf_Exp_LH[j]) fo
r t in range (0,duration)] for j in range (0,NB_LH)])
```

In [19]:
```
x=range(0,duration)
#leaf areas
plt.subplot(1,2,1)
for j in range (0,4):
    y = leaf_exp_HH[j,0:duration]
    plt.plot(x,y,"-",color = c[j], label = j+1)
for j in range (0,4):
    y = leaf_exp_LH[j,0:duration]
    plt.plot(x,y,"--",color = c[j], label = j+1)

plt.title('Lower ranks')
plt.ylim(0,80)
plt.xlabel('Time after FBV stage (days)')
xticks(arange(0,duration,2))
plt.ylabel('Leaf area (cm2)')
plt.legend(loc='lower left', bbox_to_anchor=(2.3, 0.2))

plt.subplot(1,2,2)
for j in range (4,NB_HH):
    y = leaf_exp_HH[j,0:duration]
    plt.plot(x,y,"-",color = c[j], label = j+1)
for j in range (4,NB_LH):
    y = leaf_exp_LH[j,0:duration]
    plt.plot(x,y,"--",color = c[j], label = j+1)

plt.title('Upper ranks')
plt.ylim(0,80)
plt.xlabel('Time after FBV stage (days)')
xticks(arange(0,duration,2))
plt.legend(loc='lower left', bbox_to_anchor=(1.5, 0.2))
plt.savefig('simu_leaf_areas.pdf')
plt.savefig('simu_leaf_areas.jpg')
```

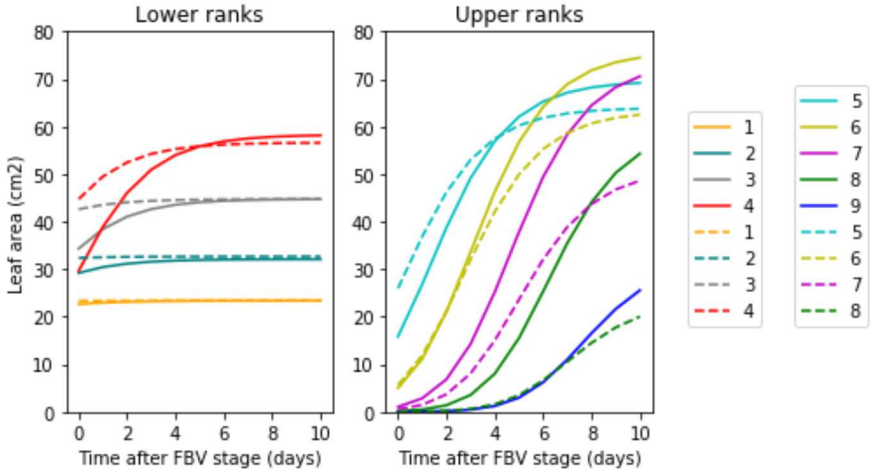

In [20]:
```
x=range(0,duration)
#leaf areas increase rate
plt.subplot(1,2,1)
for j in range (0,4):
    y = leaf_exp_speed_HH[j,0:duration]
    plt.plot(x,y,"-",color = c[j], label = j+1)
for j in range (0,4):
    y = leaf_exp_speed_LH[j,0:duration]
    plt.plot(x,y,"--",color = c[j], label = j+1)

plt.title('Lower ranks')
plt.ylim(0,15)
plt.xlabel('Time after FBV stage (days)')
xticks(arange(0,duration,2))
plt.ylabel('Leaf area increae rate(cm2/d)')
plt.legend(loc='lower left', bbox_to_anchor=(2.3, 0.2))

plt.subplot(1,2,2)
for j in range (4,NB_HH):
    y = leaf_exp_speed_HH[j,0:duration]
    plt.plot(x,y,"-",color = c[j], label = j+1)
for j in range (4,NB_LH):
    y = leaf_exp_speed_LH[j,0:duration]
    plt.plot(x,y,"--",color = c[j], label = j+1)

plt.title('Upper ranks')
plt.ylim(0,15)
plt.xlabel('Time after FBV stage (days)')
xticks(arange(0,duration,2))
plt.legend(loc='lower left', bbox_to_anchor=(1.5, 0.2))
plt.savefig('simu_leaf_areas_speed.pdf')
plt.savefig('simu_leaf_areas_speed.jpg')
```

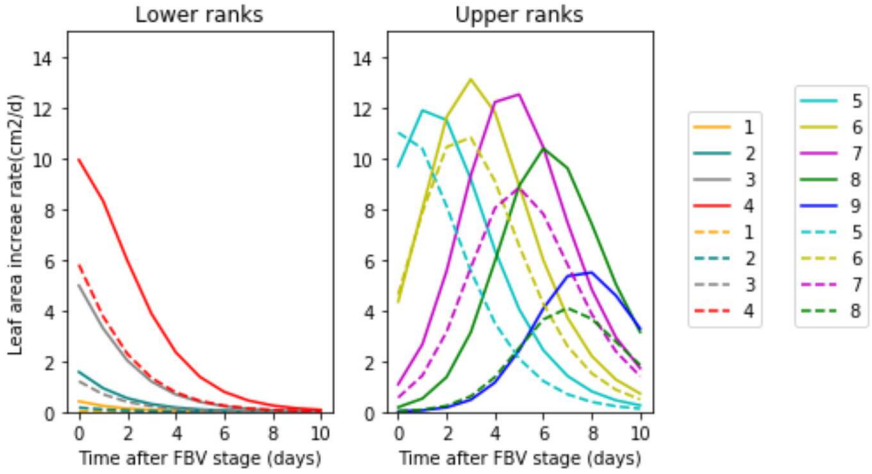

Structural growth

Internodes

In [21]:
```
def density(t, Param_IN_Density_j, t_app_j ):

    rho = Param_IN_Density_j[0] + Param_IN_Density_j[1] * (t - t_app_j)

    return rho
```

In [22]:
```
rho_HH = np.array([[density (t, Param_IN_Density_HH[j], t_app_HH[j]) for t in ra
nge (0,duration)] for j in range (0,NB_HH)])
rho_LH = np.array([[density (t, Param_IN_Density_LH[j], t_app_LH[j]) for t in ra
nge (0,duration)] for j in range (0,NB_LH)])
```

In [24]:
```
#density internode
x=range(0,duration)
#IN denisty
plt.subplot(1,2,1)
for j in range (0,4):
    y = rho_HH[j,0:duration]
    plt.plot(x,y,"-",color = c[j], label = j+1)
for j in range (0,4):
    y = rho_LH[j,0:duration]
    plt.plot(x,y,"--",color = c[j], label = j+1)

plt.title('Lower ranks')
plt.ylim(0,0.5)
plt.xlabel('Time after FBV stage (days)')
xticks(arange(0,duration,2))
plt.ylabel('Internode structural density (g/cm3)')
plt.legend(loc='lower left', bbox_to_anchor=(2.3, 0.2))

plt.subplot(1,2,2)
for j in range (4,NB_HH):
    y = rho_HH[j,0:duration]
    plt.plot(x,y,"-",color = c[j], label = j+1)
for j in range (4,NB_LH):
    y = rho_LH[j,0:duration]
    plt.plot(x,y,"--",color = c[j], label = j+1)

plt.title('Upper ranks')
plt.ylim(0,0.5)
plt.xlabel('Time after FBV stage (days)')
xticks(arange(0,duration,2))
plt.legend(loc='lower left', bbox_to_anchor=(1.5, 0.2))
plt.savefig('simu_IN_rho.jpg')
plt.savefig('simu_IN_rho.pdf')
```

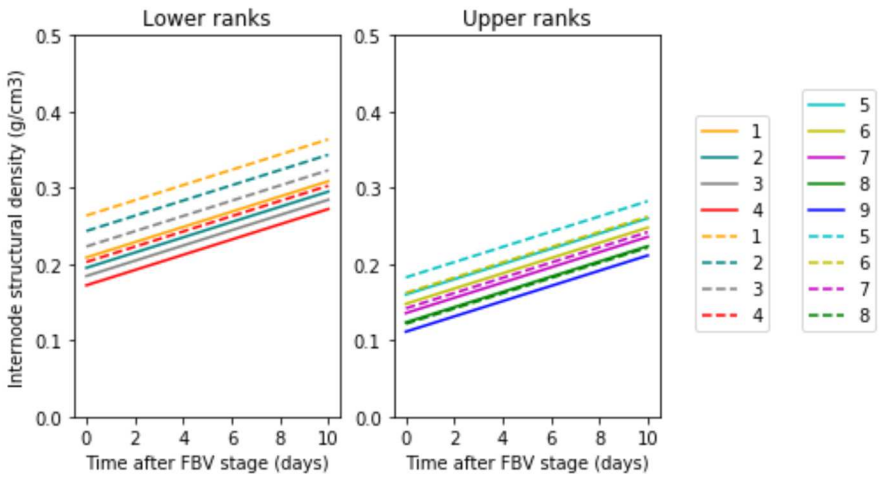

In [25]:
```
def IN_mass_struc (t, L_jt, diam_jt, rho_jt ):

    IN_mass = 1e3 *(math.pi/4) * L_jt * rho_jt * diam_jt**2

    return IN_mass
```

In [26]:
```
IN_mass_HH = np.array([[IN_mass_struc (t, IN_exp_HH[j,t], IN_diam_HH[j,t], rho_H
H[j,t]) for t in range (0,duration)] for j in range (0,NB_HH)])
IN_mass_LH = np.array([[IN_mass_struc (t, IN_exp_LH[j,t], IN_diam_LH[j,t], rho_L
H[j,t]) for t in range (0,duration)] for j in range (0,NB_LH)])
```

In [27]:
```
def IN_mass_struc_speed (t, L_jt, diam_jt, rho_jt, dL_dt_jt, ddiam_dt_dj, drho_dt_jt):

    dIN_mass_dt = (math.pi/4) *1e3* (dL_dt_jt * rho_jt * diam_jt**2 + drho_dt_jt * L_jt * diam_jt**2 + 2 *ddiam_dt_dj *rho_jt *L_jt * diam_jt)

    return dIN_mass_dt
```

In [28]:
```
IN_mass_speed_HH = np.array([[IN_mass_struc_speed (t, IN_exp_HH[j,t], IN_diam_HH[j,t], rho_HH[j,t], IN_exp_speed_HH[j,t], IN_diam_speed_HH[j,t], Param_IN_Densit y_HH[j,1]) for t in range (0,duration)] for j in range (0,NB_HH)])
IN_mass_speed_LH = np.array([[IN_mass_struc_speed (t, IN_exp_LH[j,t], IN_diam_LH[j,t], rho_LH[j,t], IN_exp_speed_LH[j,t], IN_diam_speed_LH[j,t], Param_IN_Densit y_LH[j,1]) for t in range (0,duration)] for j in range (0,NB_LH)])
```

In [29]:
```
#masse structurale internode
x=range(0,duration)
#IN mass
plt.subplot(1,2,1)
for j in range (0,4):
    y = IN_mass_HH[j,0:duration]
    plt.plot(x,y,"-",color = c[j], label = j+1)
for j in range (0,4):
    y = IN_mass_LH[j,0:duration]
    plt.plot(x,y,"--",color = c[j], label = j+1)

plt.title('Lower ranks')
plt.ylim(0,120)
plt.xlabel('Time after FBV stage (days)')
xticks(arange(0,duration,2))
plt.ylabel('Internode structural mass (mg)')
plt.legend(loc='lower left', bbox_to_anchor=(2.3, 0.2))

plt.subplot(1,2,2)
for j in range (4,NB_HH):
    y = IN_mass_HH[j,0:duration]
    plt.plot(x,y,"-",color = c[j], label = j+1)
for j in range (4,NB_LH):
    y = IN_mass_LH[j,0:duration]
    plt.plot(x,y,"--",color = c[j], label = j+1)

plt.title('Upper ranks')
plt.ylim(0,120)
plt.xlabel('Time after FBV stage (days)')
xticks(arange(0,duration,2))
plt.legend(loc='lower left', bbox_to_anchor=(1.5, 0.2))
plt.savefig('simu_IN_mass.jpg')
plt.savefig('simu_IN_mass.pdf')
```

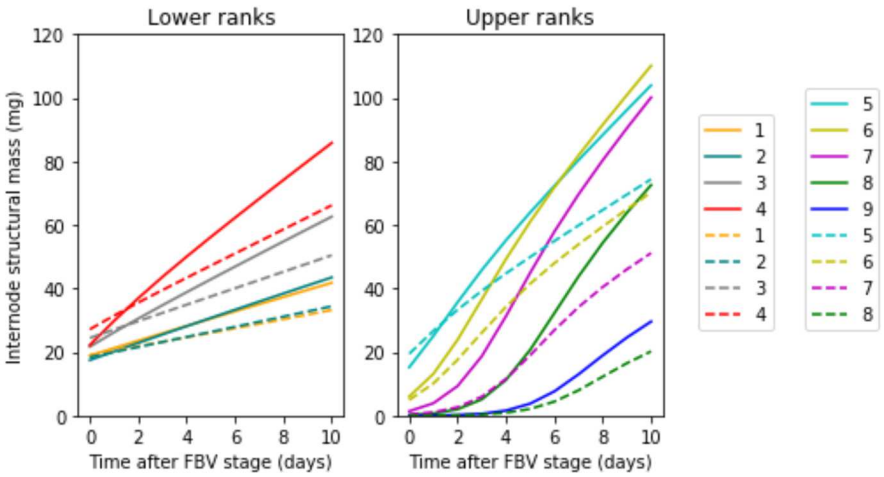

In [30]:
```
#masse structurale internode
x=range(0,duration)
#IN mass
plt.subplot(1,2,1)
for j in range (0,4):
    y = IN_mass_speed_HH[j,0:duration]
    plt.plot(x,y,"-",color = c[j], label = j+1)
for j in range (0,4):
    y = IN_mass_speed_LH[j,0:duration]
    plt.plot(x,y,"--",color = c[j], label = j+1)

plt.title('Lower ranks')
plt.ylim(0,15)
plt.xlabel('Time after FBV stage (days)')
xticks(arange(0,duration,2))
plt.ylabel('Internode structural mass increase rate (mg/d)')
plt.legend(loc='lower left', bbox_to_anchor=(2.3, 0.2))

plt.subplot(1,2,2)
for j in range (4,NB_HH):
    y = IN_mass_speed_HH[j,0:duration]
    plt.plot(x,y,"-",color = c[j], label = j+1)
for j in range (4,NB_LH):
    y = IN_mass_speed_LH[j,0:duration]
    plt.plot(x,y,"--",color = c[j], label = j+1)

plt.title('Basal ranks')
plt.ylim(0,15)
plt.xlabel('Time after FBV stage (days)')
xticks(arange(0,duration,2))
plt.legend(loc='lower left', bbox_to_anchor=(1.5, 0.2))
plt.savefig('simu_IN_mass_speed.jpg')
plt.savefig('simu_IN_mass_speed.pdf')
```

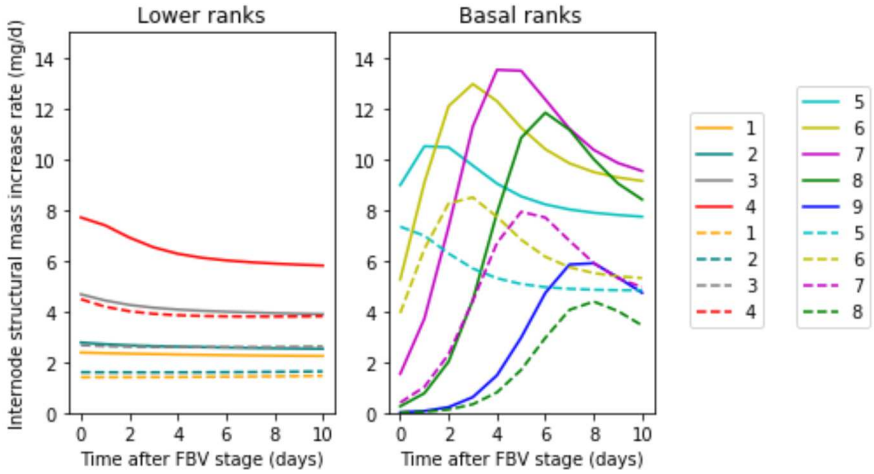

Leaves

In [31]:
```
def LMA_struc_HH(t, tapp, r, LMA_struc_juv, LMA_struc_max):

    LMA = LMA_struc_max - (LMA_struc_max - LMA_struc_juv) * math.exp(-r * (t-tap
p))

    return LMA
```

In [32]:
```
def LMA_struc_LH(t, tapp, r, LMA_struc_juv, LMA_struc_max_LL,LMA_struc_max_LH):

    LMA_struc_zero = LMA_struc_max_LL - (LMA_struc_max_LL - LMA_struc_juv) * mat
h.exp(-r * (0-tapp))
    LMA = LMA_struc_max_LH - (LMA_struc_max_LH - LMA_struc_zero) * math.exp(-r *
(t))

    return LMA
```

In [33]:
```
leaf_LMA_struc_HH = np.array([[LMA_struc_HH (t, Param_LMA_struc_HH[j,0],Param_LM
A_struc_HH[j,1],Param_LMA_struc_HH[j,2], Param_LMA_struc_HH[j,3]) for t in range
(0,duration)] for j in range (0,NB_HH)])
leaf_LMA_struc_LH = np.array([[LMA_struc_LH (t, Param_LMA_struc_LH[j,0],Param_LM
A_struc_LH[j,1],Param_LMA_struc_LH[j,2], Param_LMA_struc_LH[j,3],Param_LMA_struc
_LH[j,4]) for t in range (0,duration)] for j in range (0,NB_LH)])
```

In [34]:
```
def LMA_struc_speed_HH(t, tapp, r, LMA_struc_juv, LMA_struc_max):

    dLMA_dt = r * (LMA_struc_max - LMA_struc_juv) * math.exp(-r * (t-tapp))

    return dLMA_dt
```

In [35]:
```
def LMA_struc_speed_LH(t, tapp, r, LMA_struc_juv, LMA_struc_max_LL,LMA_struc_max
_LH):

    LMA_struc_zero = LMA_struc_max_LL - (LMA_struc_max_LL - LMA_struc_juv) * mat
h.exp(-r * (0-tapp))
    dLMA_dt = r* (LMA_struc_max_LH - LMA_struc_zero) * math.exp(-r * (t))

    return dLMA_dt
```

In [36]:
```
leaf_LMA_struc_speed_HH = np.array([[LMA_struc_speed_HH (t, Param_LMA_struc_HH
[j,0],Param_LMA_struc_HH[j,1],Param_LMA_struc_HH[j,2], Param_LMA_struc_HH[j,3])
for t in range (0,duration)] for j in range (0,NB_HH)])
leaf_LMA_struc_speed_LH = np.array([[LMA_struc_speed_LH (t, Param_LMA_struc_LH
[j,0],Param_LMA_struc_LH[j,1],Param_LMA_struc_LH[j,2], Param_LMA_struc_LH[j,3],P
aram_LMA_struc_LH[j,4]) for t in range (0,duration)] for j in range (0,NB_LH)])
```

In [37]:
```
#LMA
x=range(0,duration)

plt.subplot(1,2,1)
for j in range (0,4):
    y = leaf_LMA_struc_HH[j,0:duration]
    plt.plot(x,y,"-",color = c[j], label = j+1)
for j in range (0,4):
    y = leaf_LMA_struc_LH[j,0:duration]
    plt.plot(x,y,"--",color = c[j], label = j+1)

plt.title('Lower ranks')
plt.ylim(0,6)
xticks(arange(0,duration,2))
plt.xlabel('Time after FBV stage (days)')
plt.ylabel('Leaf mass per area (mg/cm2)')
plt.legend(loc='lower left', bbox_to_anchor=(2.3, 0.2))

plt.subplot(1,2,2)
for j in range (4,NB_HH):
    y = leaf_LMA_struc_HH[j,0:duration]
    plt.plot(x,y,"-",color = c[j], label = j+1)
for j in range (4,NB_LH):
    y = leaf_LMA_struc_LH[j,0:duration]
    plt.plot(x,y,"--",color = c[j], label = j+1)

plt.title('Upper ranks')
plt.ylim(0,6)
xticks(arange(0,duration,2))
plt.xlabel('Time after FBV stage (days)')
plt.legend(loc='lower left', bbox_to_anchor=(1.5, 0.2))
plt.savefig('simu_LMA.jpg')
plt.savefig('simu_LMA.pdf')
```

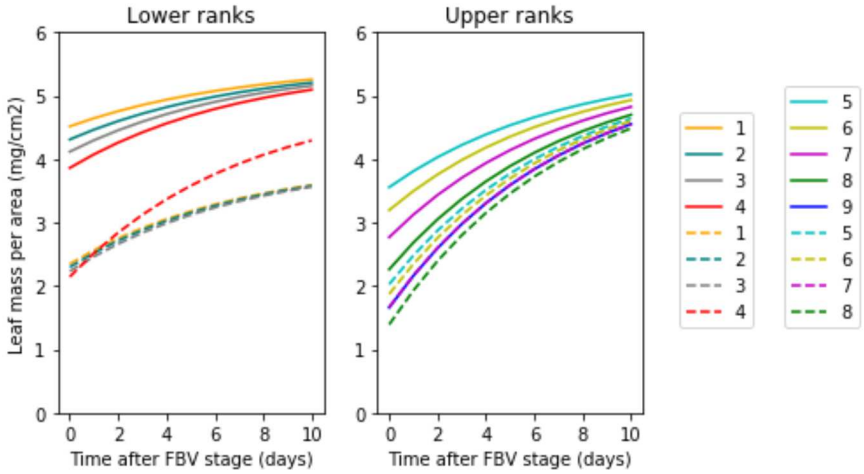

In [38]:
```
def leaf_mass_struc (t, S, LMA_struc):

    leaf_mass = S * LMA_struc

    return leaf_mass
```

In [39]:
```
def leaf_mass_struc_speed (t, S, LMA_struc, dS_dt, dLMA_struc_dt):

    dleaf_mass_dt = S * dLMA_struc_dt + dS_dt * LMA_struc

    return dleaf_mass_dt
```

In [40]:
```
leaf_mass_HH = np.array([[leaf_mass_struc (t, leaf_exp_HH[j,t], leaf_LMA_struc_H
H[j,t]) for t in range (0,duration)] for j in range (0,NB_HH)])
leaf_mass_LH = np.array([[leaf_mass_struc (t, leaf_exp_LH[j,t], leaf_LMA_struc_L
H[j,t]) for t in range (0,duration)] for j in range (0,NB_LH)])
```

In [41]:
```
leaf_mass_speed_HH = np.array([[leaf_mass_struc_speed (t, leaf_exp_HH[j,t], leaf
_LMA_struc_HH[j,t], leaf_exp_speed_HH[j,t], leaf_LMA_struc_speed_HH[j,t]) for t
in range (0,duration)] for j in range (0,NB_HH)])
leaf_mass_speed_LH = np.array([[leaf_mass_struc_speed (t, leaf_exp_LH[j,t], leaf
_LMA_struc_LH[j,t], leaf_exp_speed_LH[j,t], leaf_LMA_struc_speed_LH[j,t]) for t
in range (0,duration)] for j in range (0,NB_LH)])
```

In [42]:
```
#leaf mass
x=range(0,duration)

plt.subplot(1,2,1)
for j in range (0,4):
    y = leaf_mass_HH[j,0:duration]
    plt.plot(x,y,"-",color = c[j], label = j+1)
for j in range (0,4):
    y = leaf_mass_LH[j,0:duration]
    plt.plot(x,y,"--",color = c[j], label = j+1)

plt.title('Lower ranks')
plt.ylim(0,400)
plt.xlabel('Time after FBV stage (days)')
xticks(arange(0,duration,2))
plt.ylabel('Leaf structural mass (mg)')
plt.legend(loc='lower left', bbox_to_anchor=(2.3, 0.2))

plt.subplot(1,2,2)
for j in range (4,NB_HH):
    y = leaf_mass_HH[j,0:duration]
    plt.plot(x,y,"-",color = c[j], label = j+1)
for j in range (4,NB_LH):
    y = leaf_mass_LH[j,0:duration]
    plt.plot(x,y,"--",color = c[j], label = j+1)

plt.title('Upper ranks')
plt.ylim(0,400)
plt.xlabel('Time after FBV stage (days)')
xticks(arange(0,duration,2))
plt.legend(loc='lower left', bbox_to_anchor=(1.5, 0.2))
plt.savefig('simu_leaf_mass.jpg')
plt.savefig('simu_leaf_mass.pdf')
```

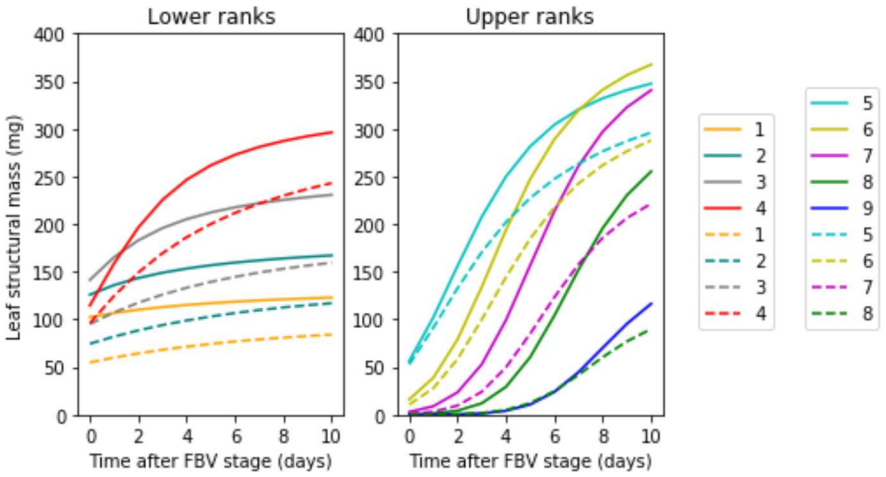

In [43]:
```
#leaf structural mass speed
x=range(0,duration)

plt.subplot(1,2,1)
for j in range (0,4):
    y = leaf_mass_speed_HH[j,0:duration]
    plt.plot(x,y,"-",color = c[j], label = j+1)
for j in range (0,4):
    y = leaf_mass_speed_LH[j,0:duration]
    plt.plot(x,y,"--",color = c[j], label = j+1)

plt.title('Lower ranks')
plt.ylim(0,100)
plt.xlabel('Time after FBV stage (days)')
xticks(arange(0,duration,2))
plt.ylabel('Leaf structural mass increase rate (mg/d)')
plt.legend(loc='lower left', bbox_to_anchor=(2.3, 0.2))

plt.subplot(1,2,2)
for j in range (4,NB_HH):
    y = leaf_mass_speed_HH[j,0:duration]
    plt.plot(x,y,"-",color = c[j], label = j+1)
for j in range (4,NB_LH):
    y = leaf_mass_speed_LH[j,0:duration]
    plt.plot(x,y,"--",color = c[j], label = j+1)

plt.title('Upper ranks')
plt.ylim(0,100)
plt.xlabel('Time after FBV stage (days)')
xticks(arange(0,duration,2))
plt.legend(loc='lower left', bbox_to_anchor=(1.5, 0.2))
plt.savefig('simu_leaf_mass_speed.jpg')
plt.savefig('simu_leaf_mass_speed.pdf')
```

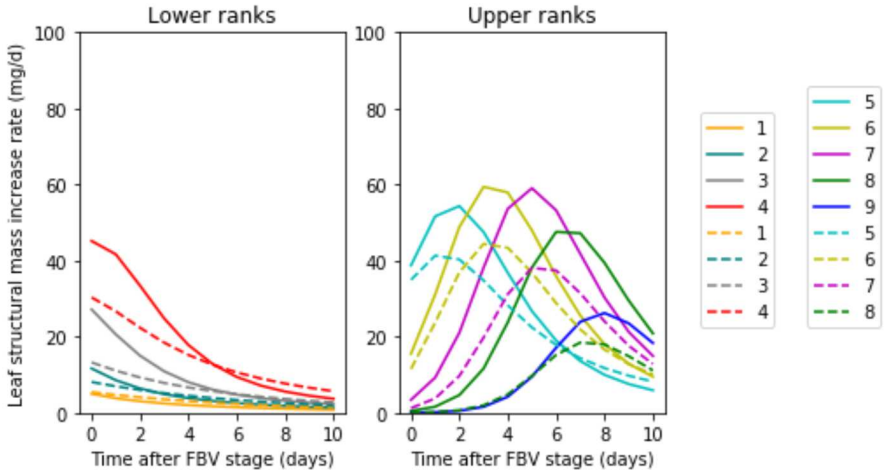

Flower

Structural flower mass (+ peduncle) grows folowing a determined allometry function with total leaf mass.

In [44]:
```
total_leaf_mass_HH = np.sum(leaf_mass_HH,axis=0)
total_leaf_mass_LH = np.sum(leaf_mass_LH,axis=0)

total_IN_mass_HH = np.sum(IN_mass_HH,axis=0)
total_IN_mass_LH = np.sum(IN_mass_LH,axis=0)

flower_mass_struc_HH = total_leaf_mass_HH  *(Param_Flower[0] * t**2 + Param_Flow
er[1] * t + Param_Flower[2])
flower_mass_struc_LH = total_leaf_mass_LH *(Param_Flower[0] * t**2 + Param_Flowe
r[1] * t + Param_Flower[2])
```

Roots

In [45]:
```
roots_mass_struc_HH = total_leaf_mass_HH * (Param_Roots[0] * t + Param_Roots[1])
roots_mass_struc_LH = total_leaf_mass_LH * (Param_Roots[0] * t + Param_Roots[1])
```

In [46]:
```
#Total organs masses
x=range(0,duration)

y1_HH = total_leaf_mass_HH[0:duration]
y2_HH = total_IN_mass_HH[0:duration]
y3_HH = flower_mass_struc_HH[0:duration]
y4_HH = roots_mass_struc_HH[0:duration]

plt.plot(x, y1_HH, "-", color = c[0], label = 'Leaves')
plt.plot(x, y2_HH, "-", color = c[1], label = 'Internodes')
plt.plot(x, y3_HH, "-", color = c[4], label = 'Flower')
plt.plot(x, y4_HH, "-", color = c[6], label = 'Roots')

y1_LH = total_leaf_mass_LH[0:duration]
y2_LH = total_IN_mass_LH[0:duration]
y3_LH = flower_mass_struc_LH[0:duration]
y4_LH = roots_mass_struc_LH[0:duration]

plt.plot(x, y1_LH, "--", color = c[0], label = 'Leaves')
plt.plot(x, y2_LH, "--", color = c[1], label = 'Internodes')
plt.plot(x, y3_LH, "--", color = c[4], label = 'Flower')
plt.plot(x, y4_LH, "--", color = c[6], label = 'Roots')


plt.xlabel('Time after FBV stage (days)')
plt.ylabel('Structural mass (mg)')
plt.legend(loc='lower left', bbox_to_anchor=(1, 0.2))


plt.savefig('simu_mass.jpg')
plt.savefig('simu_mass.pdf')
```

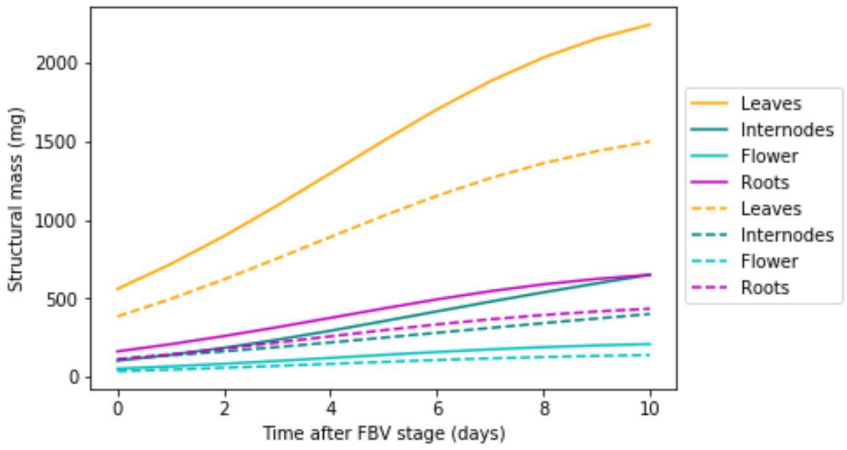

Plant

Masse structurale totale de la plante à chaque pas de temps, à partir de la somme des structures des différents organes

In [47]:
```
plant_struc_HH = total_IN_mass_HH + total_leaf_mass_HH  + flower_mass_struc_HH +
roots_mass_struc_HH
plant_struc_LH = total_IN_mass_LH + total_leaf_mass_LH  + flower_mass_struc_LH +
roots_mass_struc_LH
```

Derivative structural growth

Strucutral mass difference between t and $t+1$

In [48]:
```
deriv_plant_struc_HH = np.array([plant_struc_HH[t]-plant_struc_HH[t-1] for t in
range (1,duration)])
deriv_plant_struc_LH = np.array([plant_struc_LH[t]-plant_struc_LH[t-1] for t in
range (1,duration)])
```

PAR gradient function

Fonction qui calcule le PAR perçu par une feuille de rang j, connaissant le LAI des feuilles supérieures et l'intensité lumineuse au sommet du couvert

In [49]:
```
## LAI array for every rank at any time of the simulation
LAI_HH = np.zeros((NB_HH,duration))

for j in reversed(range (0, NB_HH-1)):
    LAI_HH[j] = LAI_HH[j+1] + leaf_exp_HH[j+1]/(100)

light_gradient_HH = k1* np.tile(I0,[NB_HH,1])*  np.exp(-k2*LAI_HH)


LAI_LH = np.zeros((NB_LH,duration))

for j in reversed(range (0, NB_LH-1)):
    LAI_LH[j] = LAI_LH[j+1] + leaf_exp_LH[j+1]/(100)

light_gradient_LH = k1* np.tile(I0,[NB_LH,1])*  np.exp(-k2*LAI_LH)
```

Remarque : d'après l'équation, le light_gradient quand le LAI=0 n'est as égal au I0, est-ce que c'est bon quand même?

In [50]:
```
#LAI gradient
x = range (0,duration)
for j in range(0,NB_HH):
    y = LAI_HH[j,0:duration]
    plt.plot(x,y, label = j+1)

plt.title('LAI')
plt.xlabel('Time after FBV stage (days)')
plt.ylabel('LAI ')
plt.legend()
plt.show()
```

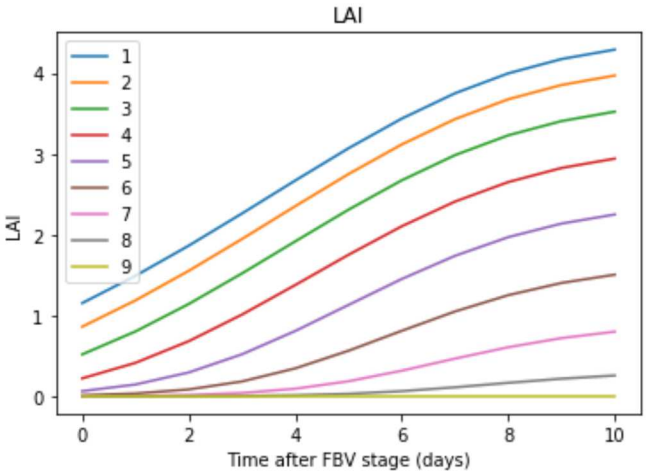

In [51]:
```
#light gradient
x = range (0,duration)
for j in range(0,NB_HH):
    y = light_gradient_HH[j,0:duration]
    plt.plot(x,y, label = j+1)

#for j in range (0,3):
 #   y = data_expe_PAR[j,:]
  #  plt.scatter([3,7],y, c='grey')


plt.title('light gradient')
plt.xlabel('Time after FBV stage (days)')
plt.ylabel('light gradient ')
plt.ylim(0,450)
plt.legend()
plt.show()
```

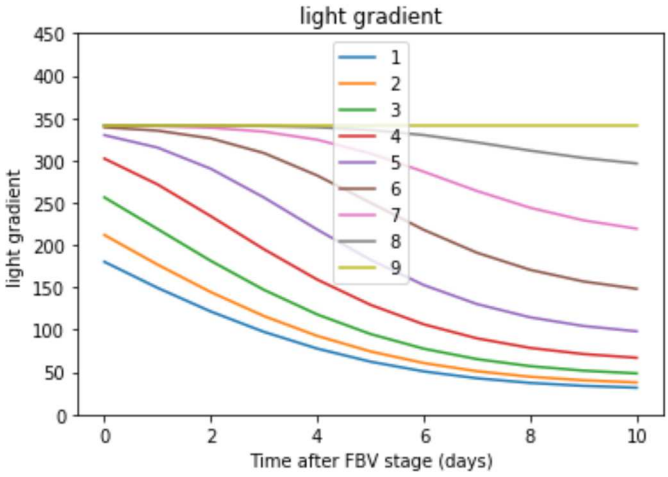

In [52]:
```
#leaf structural mass speed
x=range(0,duration)

plt.subplot(1,2,1)
for j in range (0,4):
    y = light_gradient_HH[j,0:duration]
    plt.plot(x,y,"-",color = c[j], label = j+1)
for j in range (0,4):
    y = light_gradient_LH[j,0:duration]
    plt.plot(x,y,"--",color = c[j], label = j+1)

plt.title('Lower ranks')
plt.ylim(0,450)
plt.xlabel('Time after FBV stage (days)')
xticks(arange(0,duration,2))
plt.ylabel('Ambient PAR light intensity (umol/m2/s)')
plt.legend(loc='lower left', bbox_to_anchor=(2.3, 0.2))

plt.subplot(1,2,2)
for j in range (4,NB_HH):
    y = light_gradient_HH[j,0:duration]
    plt.plot(x,y,"-",color = c[j], label = j+1)
for j in range (4,NB_LH):
    y = light_gradient_LH[j,0:duration]
    plt.plot(x,y,"--",color = c[j], label = j+1)

plt.title('Upper ranks')
plt.ylim(0,450)
plt.xlabel('Time after FBV stage (days)')
xticks(arange(0,duration,2))
plt.legend(loc='lower left', bbox_to_anchor=(1.5, 0.2))
plt.savefig('simu_leaf_PAR.jpg')
plt.savefig('simu_leaf_PAR.pdf')
```

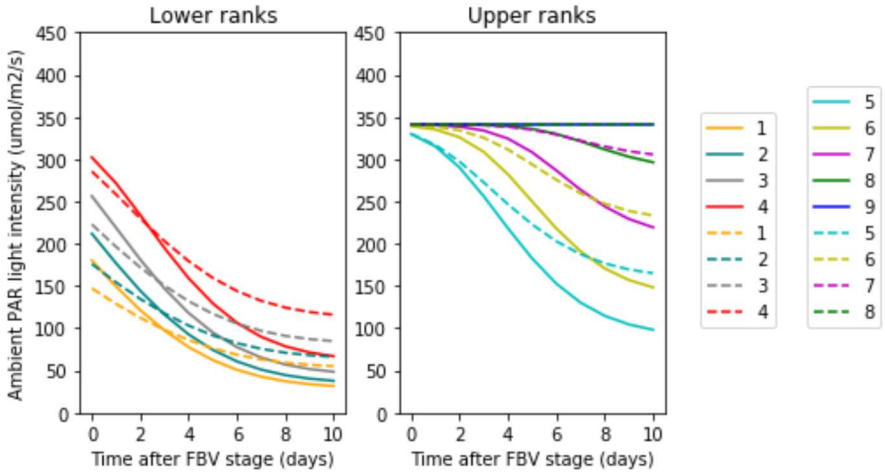

In [226]:
```
#light gradient
y_HH = range (1,NB_HH+1)
x_HH = light_gradient_HH[:,10]
plt.plot(x_HH, y_HH, color = 'orange', label='HH')

y_LH = range (1,NB_LH+1)
x_LH = light_gradient_LH[:,10]
plt.plot(x_LH, y_LH, "--", color = 'orange', label='LH')



plt.title('light gradient')
plt.ylabel('Phytomer rank')
yticks(arange(NB_HH+1))
plt.xlabel('PAR')
plt.ylim(0,10)
plt.legend()

plt.savefig('light_gradient.jpg')
plt.savefig('light_gradient.pdf')
```

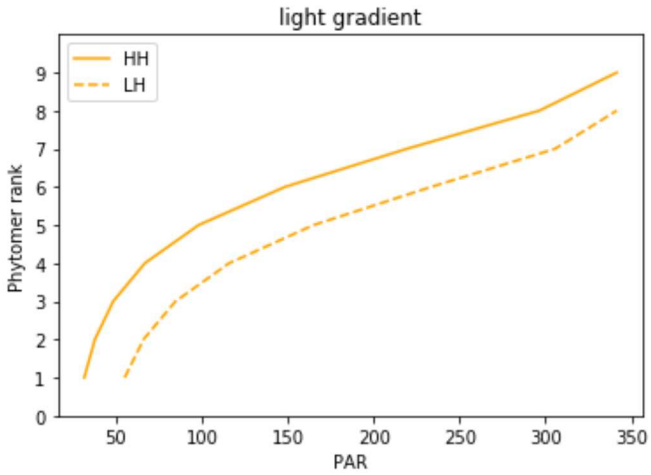

In [227]:
```
x_HH = light_gradient_HH[:,10]
x_HH
```

Out[227]:
```
array([ 31.69572239,  37.86315408,  48.50633204,  66.93814337,
        98.19980938, 148.36111823, 219.31338209, 296.28486275,
       341.379     ])
```

Function for carbon assimilation by photosynthesis

Fonction qui calcule le carbone produit par la photosynthèse au temps t pour une feuille j, étant donné sa teneur surfacique en chlorophylles

In [53]:
```
#chlorophylle gradient
def chloro(t, tapp, r_chloro, chloro_juv, chloro_max):

    chloro_surf = corr_chloro * (chloro_max - (chloro_max - chloro_juv) * math.e
xp(-r_chloro * (t-tapp)))

    return chloro_surf
```

In [54]:
```
#chlorophyll gradient computation
chloro_gradient_HH = np.array([[chloro (t, Param_chloro_gradient_HH[j,0], Param_
chloro_gradient_HH[j,1], Param_chloro_gradient_HH[j,2], Param_chloro_gradient_HH
[j,3]) for t in range (0,duration)] for j in range (0,NB_HH)])
chloro_gradient_LH = np.array([[chloro (t, Param_chloro_gradient_LH[j,0], Param_
chloro_gradient_LH[j,1], Param_chloro_gradient_LH[j,2], Param_chloro_gradient_LH
[j,3]) for t in range (0,duration)] for j in range (0,NB_LH)])
```

In [56]:
```
#surfacic chloro_gradient

x=range(0,duration)

plt.subplot(1,2,1)
for j in range (0,4):
    y = chloro_gradient_HH[j,0:duration]
    plt.plot(x,y,"-",color = c[j], label = j+1)
for j in range (0,4):
    y = chloro_gradient_LH[j,0:duration]
    plt.plot(x,y,"--",color = c[j], label = j+1)

plt.title('Lower ranks')
plt.ylim(0,50)
plt.xlabel('Time after FBV stage (days)')
xticks(arange(0,duration,2))
plt.ylabel('Surfacic chlorophyll index)')
plt.legend(loc='lower left', bbox_to_anchor=(2.3, 0.2))

plt.subplot(1,2,2)
for j in range (4,NB_HH):
    y = chloro_gradient_HH[j,0:duration]
    plt.plot(x,y,"-",color = c[j], label = j+1)
for j in range (4,NB_LH):
    y = chloro_gradient_LH[j,0:duration]
    plt.plot(x,y,"--",color = c[j], label = j+1)

plt.title('Upper ranks')
plt.ylim(0,50)
plt.xlabel('Time after FBV stage (days)')
xticks(arange(0,duration,2))
plt.legend(loc='lower left', bbox_to_anchor=(1.5, 0.2))

plt.savefig('simu_chloro.jpg')
plt.savefig('simu_chloro.pdf')
```

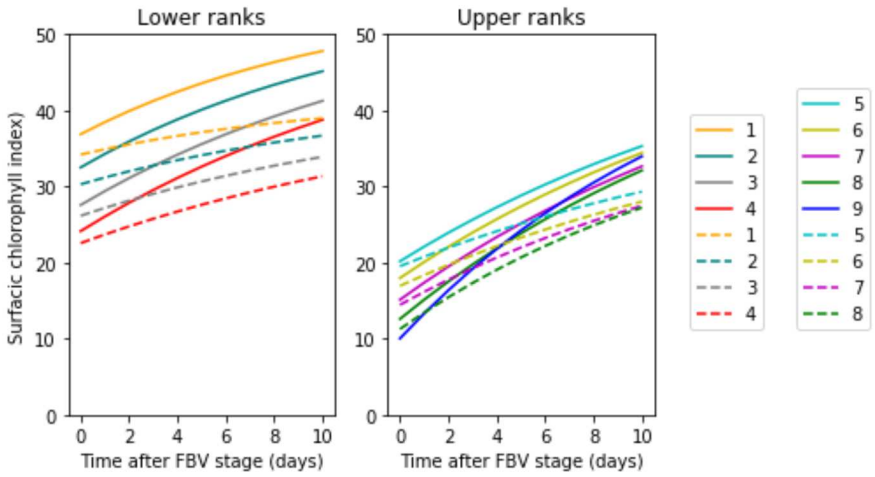

In [57]:
```
#photosynthesis per leaf per second
#HH
Popt_HH = Pmin + (Pmax * chloro_gradient_HH)/(chloro_gradient_HH + K_chloro)

surfacic_photosynthesis_HH = (alpha * light_gradient_HH * Popt_HH[0:NB_HH+1,0:du
ration])/(alpha * light_gradient_HH +Popt_HH[0:NB_HH+1,0:duration] )

carbon_photosynthesis_HH = leaf_exp_HH * 1e-4 * surfacic_photosynthesis_HH

#LH
Popt_LH = Pmin + (Pmax * chloro_gradient_LH)/(chloro_gradient_LH + K_chloro)

surfacic_photosynthesis_LH = (alpha * light_gradient_LH * Popt_LH[0:NB_LH+1,0:du
ration])/(alpha * light_gradient_LH +Popt_LH[0:NB_LH+1,0:duration] )

carbon_photosynthesis_LH = leaf_exp_LH * 1e-4 * surfacic_photosynthesis_LH
```

In [58]:
```
#surfacic photosynthesis : en µmol de CO2 par m2 par seconde

x=range(0,duration)

plt.subplot(1,2,1)
for j in range (0,4):
    y = surfacic_photosynthesis_HH[j,0:duration]
    plt.plot(x,y,"-",color = c[j], label = j+1)
for j in range (0,4):
    y = surfacic_photosynthesis_LH[j,0:duration]
    plt.plot(x,y,"--",color = c[j], label = j+1)

plt.title('Lower ranks')
plt.ylim(0,12)
plt.xlabel('Time after FBV stage (days)')
xticks(arange(0,duration,2))
plt.ylabel('Surfacic photosynthesis)')
plt.legend(loc='lower left', bbox_to_anchor=(2.3, 0.2))

plt.subplot(1,2,2)
for j in range (4,NB_HH):
    y = surfacic_photosynthesis_HH[j,0:duration]
    plt.plot(x,y,"-",color = c[j], label = j+1)
for j in range (4,NB_LH):
    y = surfacic_photosynthesis_LH[j,0:duration]
    plt.plot(x,y,"--",color = c[j], label = j+1)

plt.title('Upper ranks')
plt.ylim(0,12)
plt.xlabel('Time after FBV stage (days)')
xticks(arange(0,duration,2))
plt.legend(loc='lower left', bbox_to_anchor=(1.5, 0.2))

plt.savefig('simu_surf_photosynthesis.jpg')
plt.savefig('simu_surf_photosynthesis.pdf')
```

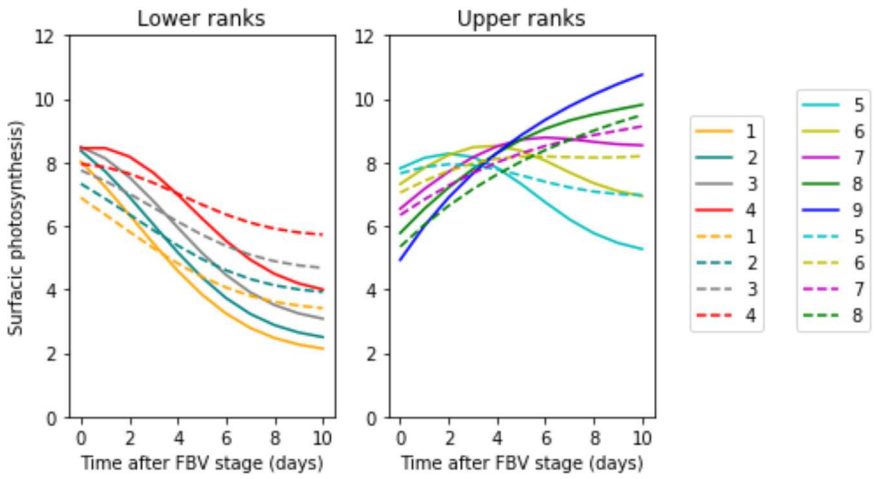

Computation of the carbon produced by the whole plant

In [59]:
```
# computation of the carbon photoassimilated during one day by summing all the l
eaves
#qté de C en mg fixé par jour par la plante

plant_carbon_photosynthesis_HH = photoperiod * 3600 * 12e-6* dt * np.sum(carbon_
photosynthesis_HH,axis=0)*1e3
plant_carbon_photosynthesis_LH = photoperiod * 3600 * 12e-6* dt * np.sum(carbon_
photosynthesis_LH,axis=0)*1e3
```

In [60]:
```
#plant photosynthesis et utilisation pour structure
x = range (0,duration-1)
y = plant_carbon_photosynthesis_HH[0:duration-1]
plt.plot(x,y,color ='green', label ='photosynthesis')
y = deriv_plant_struc_HH[0:duration-1]* Conv_carbon_struc
plt.plot(x,y, color='orange', label ='Structural growth')

y = plant_carbon_photosynthesis_LH[0:duration-1]
plt.plot(x,y,'--',color ='green', label ='photosynthesis')
y = deriv_plant_struc_LH[0:duration-1]* Conv_carbon_struc
plt.plot(x,y,'--',color='orange', label ='Structural growth')

plt.xlabel('Time after FBV stage (days)')
plt.ylabel('Daily carbon use and product (g/d) ')
plt.ylim(0,200)
plt.legend()
plt.legend(loc='lower left', bbox_to_anchor=(1.1, 0.2))


plt.savefig('simu_balance.jpg')
plt.savefig('simu_balance.pdf')
```

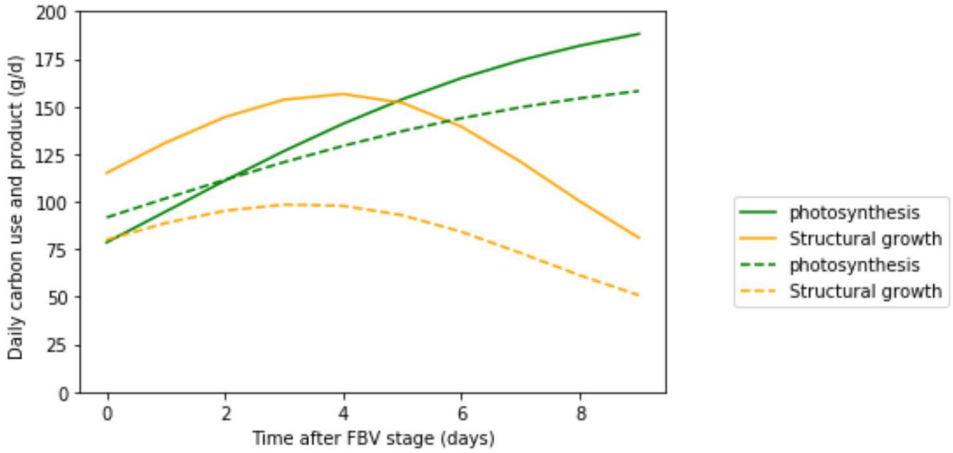

In [61]:
```
#bilan global
balance_HH = plant_carbon_photosynthesis_HH[0:duration-1] - deriv_plant_struc_HH
[0:duration-1]* Conv_carbon_struc
balance_LH = plant_carbon_photosynthesis_LH[0:duration-1] - deriv_plant_struc_LH
[0:duration-1]* Conv_carbon_struc

x = range (0,duration-1)
y = balance_HH[0:duration-1]
plt.plot(x,y,color ='green', label ='HH')
y = balance_LH[0:duration-1]
plt.plot(x,y,'--',color ='green', label ='LH')
plt.title('Carbon balance')
plt.xlabel('Time after FBV stage (days)')
plt.ylabel('carbon balance (mgC/d) ')
plt.legend()
plt.ylim(-50,120)
plt.show()
```

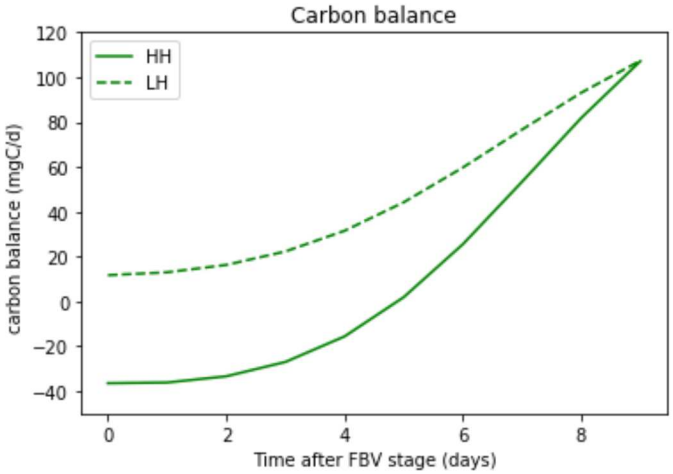

In [ ]:

computation of plant mass, and sugar contents

In [62]:
```
soluble_sugars_HH = [vinit_soluble_sugars_conc_HH * (plant_struc_HH - roots_mass
_struc_HH - flower_mass_struc_HH)[0]]
#Respiration = plant_struc[0] * k_respi_maint
#N_plant_mass[0] * k_respi_maint + d_struc_carbon[0] * k_respi_growth

#/!\ attention aux conversions de quantité de Co2 fixé, en masse de carbone qui
participe à la masse

for t in range (1,duration ):

    current_sugars_HH = soluble_sugars_HH[t-1] + (plant_carbon_photosynthesis_HH
[t-1] - deriv_plant_struc_HH[t-1]*Conv_carbon_struc)* Conv_carbon_sugars

    #Respi = plant_struc[t] * k_respi_maint + deriv_plant_struc[t-1] * k_respi_g
rowth
    #N_plant_mass[t] * k_respi_maint + d_struc_carbon[t] * k_respi_growth

    #current_sugars = current_sugars - Respi * Conv_carbon_sugars

    soluble_sugars_HH = np.append(soluble_sugars_HH,[current_sugars_HH])

    #Respiration = np.append(Respiration,[Respi])
```

In [63]:
```
soluble_sugars_conc_HH = soluble_sugars_HH/(plant_struc_HH - roots_mass_struc_HH
- flower_mass_struc_HH)
```

In [64]:
```
soluble_sugars_LH = [vinit_soluble_sugars_conc_LH * (plant_struc_LH - roots_mass
_struc_LH - flower_mass_struc_LH)[0]]

for t in range (1,duration ):

    current_sugars_LH = soluble_sugars_LH[t-1] + (plant_carbon_photosynthesis_LH
[t-1] - deriv_plant_struc_LH[t-1]*Conv_carbon_struc)* Conv_carbon_sugars

    soluble_sugars_LH = np.append(soluble_sugars_LH,[current_sugars_LH])
```

In [65]:
```
soluble_sugars_conc_LH = soluble_sugars_LH/(plant_struc_LH - roots_mass_struc_LH
- flower_mass_struc_LH)
```

In [68]:
```
#soluble sugars
x = range (0,duration)

y = soluble_sugars_HH[0:duration]
plt.plot(x,y,color ='green', label ='HH')
y = soluble_sugars_LH[0:duration]
plt.plot(x,y,'--',color ='green', label ='LH')
plt.title('Common pool of sugars')
plt.xlabel('Time after FBV stage (days)')
plt.ylabel('Sugars (mgC/d) ')
plt.legend()
plt.ylim(100,300)

plt.savefig('simu_sugars.jpg')
plt.savefig('simu_sugars.pdf')
```

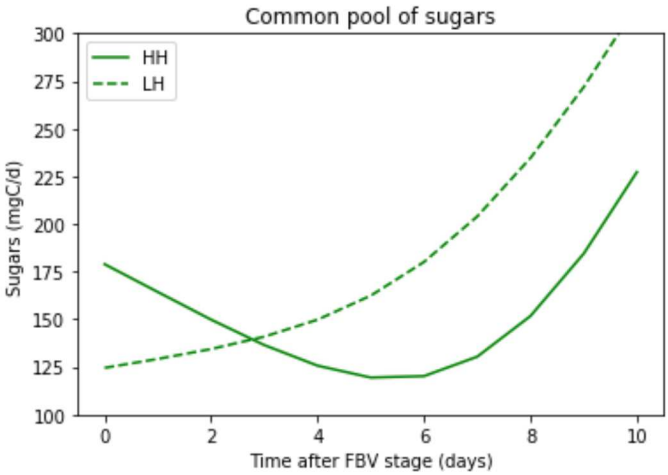

Titre : Etude du rôle des sucres, en interaction avec les hormones, dans la régulation du débourrement par l'intensité lumineuse. Une démarche alliant expériences et modélisation.

Mots clés : Amidon, cytokinines, intensité lumineuse, débourrement, ramification, modélisation

Résumé : La ramification est une variable du rendement des cultures dont la sensibilité aux conditions environnementales et dont le contrôle revêt un intérêt agronomique majeur. Nous nous intéressons ici à la régulation du débourrement des bourgeons axillaires par l'intensité lumineuse chez le rosier buisson. Plusieurs études ont souligné la sensibilité de cette phase à l'intensité de la lumière expérimentée par la plante avant ou pendant la période habituelle de débourrement. Récemment, le rôle des CKs dans la réponse du débourrement à l'intensité lumineuse perçue pendant la phase de ramification a été démontré. Cependant, le rôle des sucres dans la stimulation du débourrement par l'intensité lumineuse n'est pas bien défini. Dans ce travail, nous avons exploré le rôle que jouaient les sucres, en interactions avec les hormones régulatrices du débourrement, dans la réponse du bourgeon à différents traitements d'intensité lumineuse. Par la quantification du statut en sucres des plantes soumises à une restriction temporaire de lumière appliquée avant la période de débourrement, nous avons montré que la diminution de la compétition pour les sucres expliquait la stimulation du débourrement dans ce cas. Nous avons ensuite montré, *in vitro* et *in planta*, que la réponse du débourrement à l'intensité lumineuse pouvait être expliquée par une modulation de l'équilibre quantitatif en hormones (auxine, cytokinines, strigolactones) et en sucres au voisinage du bourgeon. Ces résultats ouvrent la voie pour la conception d'un modèle générique de débourrement à l'échelle de la plante en réponse à l'intensité lumineuse.

Title: Study of the role of sugars, in interaction with hormones, in light intensity modulation of bud outgrowth. An approach combining experiments and modelling.

Keywords: Starch, cytokinins, light intensity, bud outgrowth, branching, modelling

Abstract: Branching is a crop yield variable whose sensitivity to environmental conditions is of major agronomic interest. We are interested here in the regulation of axillary bud outgrowth by light intensity in bush roses. Several studies have highlighted the sensitivity of this phase to the light intensity experienced by the plant before or during the usual bud outgrowth period. Recently, the role of CKs in the response of bud outgrowth to the light intensity perceived during the branching phase has been demonstrated. However, the role of sugars in stimulating bud outgrowth by light intensity is still unclear. In this work, we explored the role of sugars, in interaction with hormones, in the bud outgrowth response to different light intensity treatments. By quantifying the sugar status of plants subjected to a temporary light restriction applied before the bud outgrowth period, we demonstrated that a lower competition for sugars explained the stimulation of bud outgrowth in this case. We then showed, for *in vitro* and *in planta* bud bearing nodes, that the response of bud outgrowth to light intensity is explained by a modulation of the quantitative equilibrium in hormones (auxin, cytokinins, strigolactones) and sugars contents in the vicinity of the bud. These results pave the way for the design of a generic model of bud outgrowth at the plant scale in response to light intensity.